6848 ANL-6848

6848 ANL-6848
6848 ANL-6848
6848 ANL-6848
6848 ANL-6848
6848 ANL-6848
6848 ANL-6848
6848 ANL-6848
6848 ANL-6848
6848 ANL-6848

*LEGAL NOTICE*

*This report was prepared as an account of Government sponsored work. Neither the United States, nor the Commission, nor any person acting on behalf of the Commission:*

*A. Makes any warranty or representation, expressed or implied, with respect to the accuracy, completeness, or usefulness of the information contained in this report, or that the use of any information, apparatus, method, or process disclosed in this report may not infringe privately owned rights; or*

*B. Assumes any liabilities with respect to the use of, or for damages resulting from the use of any information, apparatus, method, or process disclosed in this report.*

*As used in the above, "person acting on behalf of the Commission" includes any employee or contractor of the Commission, or employee of such contractor, to the extent that such employee or contractor of the Commission, or employee of such contractor prepares, disseminates, or provides access to, any information pursuant to his employment or contract with the Commission, or his employment with such contractor.*

*Price* $3.00 . *Available from the Office of Technical Services, Department of Commerce, Washington 25, D.C.*

ANL-6848
Physics
(TID-4500, 26th Ed.)
AEC Research and
Development Report

ARGONNE NATIONAL LABORATORY
9700 South Cass Avenue
Argonne, Illinois 60440

# NUCLEAR SPECTROSCOPY WITH DIRECT REACTIONS

## I. CONTRIBUTED PAPERS

Edited by
F. E. Throw

March 1964

Organizing Committee:
J. B. French
D. Kurath
L. L. Lee, Jr.
M. H. Macfarlane
J. P. Schiffer
R. Sherr
F. E. Throw

Operated by The University of Chicago
under
Contract W-31-109-eng-38
with the
U. S. Atomic Energy Commission

# FOREWORD

This volume of Contributed Papers represents one of the two major components of the Symposium on Nuclear Spectroscopy with Direct Reactions. Its function is to present a representative cross section of the current work in this field, and at the same time it avoids the necessity of crowding the actual meetings with a large number of too-short papers. Only a very few will be presented orally; this volume is intended as a basis for numerous informal conversations. The six sessions of the Symposium will be devoted almost entirely to the invited papers and open discussions of them. These will be reported in a volume of proceedings, to be compiled and issued as soon as possible after the Symposium (hopefully by about 1 June 1964).

The Symposium is sponsored by Argonne National Laboratory and has been accepted as a topical conference of the American Physical Society. It is being held on 9—11 March 1964 at the Center for Continuing Education, University of Chicago, 1307 East 60 St., Chicago, Illinois.

In preparing the papers for this volume, editorial dabbling was kept to a minimum. However, in the interest of a uniform format, some minor changes were made; and the pressure of time prevented checking these with the authors. If any meanings have been distorted thereby, the editor offers his apologies. Any corrections brought promptly to his attention will be listed on a sheet of errata in the Proceedings.

For their diligent efforts in preparing this volume in the short time allowed, thanks are due to the Physics Division secretaries: Miss Barbara Baldwin, Miss Jo Miller, Mrs. Judy Miller, Mrs. Kay Pemble, Mrs. Jeanette Vendel, and Mrs. Cay Yack. We are also

Session B PAGE

B-1. A STUDY OF THE REACTION $U^{238}(d,p)U^{239}$

B. E. F. Macefield and R. Middleton . . . . . 52

B-2. DISTORTED-WAVE ANALYSIS OF THE $Cr^{52}(d,p)Cr^{53}$ REACTION USING MEASURED OPTICAL-MODEL PARAMETERS

J. C. Legg, H. D. Scott, and M. K. Mehta . . . 63

B-3. A STUDY OF STRIPPING AND PICKUP REACTIONS ON $C^{12}$, $C^{13}$, and $C^{14}$

R. N. Glover and A. D. W. Jones . . . . . 70

B-4. LOW-LYING LEVELS IN $Ti^{48}$ OBSERVED IN THE (d,p) REACTION

P. D. Barnes, C. K. Bockelman, O Hansen, and A. Sperduto . . . . . 79

B-5. A HIGH-RESOLUTION STUDY OF (d,p) REACTIONS ON TARGETS OF $W^{182}$, $W^{184}$, AND $W^{186}$

John R. Erskine . . . . . 86

B-6. A STUDY OF (d,n) REACTIONS ON $Fe^{54}$ and $Ni^{58}$

D. S. Gemmell, L. L. Lee, Jr., J. P. Schiffer, and A. B. Smith . . . . . 98

B-7. A NOTE ON THE REACTIONS $Mg^{26}(d,p)Mg^{27}$ AND $Mg^{26}(t,d)Mg^{27}$

R. N. Glover . . . . . 104

Session C PAGE

C-1. PARTICLE-HOLE CALCULATION OF $Ca^{40}(\alpha,\alpha')$

Nathan S. Wall . . . . . 108

C-2. ANALYSIS OF ELASTIC SCATTERING OF 17-MEV PROTONS FROM HEAVY NUCLEI

F. G. Perey . . . . . 114

C-3. THE PARITY RULE FOR INELASTIC SCATTERING AT SMALL ANGLES

I. E. McCarthy . . . . . 118

C-4. THE DEUTERON GAMMA ANGULAR CORRELATION IN THE REACTION $Mg^{24}(d,d'\gamma)Mg^{24}+(1.37\ MEV)$ AT 11.8 MEV

V. Jung and U. Schmidt-Rohr . . . . . 123

C-5. EXCITATION OF $T = T_z + 2$ STATES

G. T. Garvey and B. F. Bayman . . . . . 125

C-6. ANALYSIS OF ELASTIC AND INELASTIC SCATTERING OF 40-MEV PROTONS

Martin P. Fricke . . . . . 130

C-7. SPECTROSCOPIC DATA DEDUCED FROM INELASTIC SCATTERING OF 44-MEV $\gamma$ PARTICLES IN MEDIUM-WEIGHT NUCLEI

H. Faraggi and J. Saudinos . . . . . 137

C-8. ISOBARIC ANALOGUE STATES AND INTERMEDIATE RESONANCES IN NUCLEI

S. Fallieros . . . . . 143

PAGE

C-9. ANGULAR MOMENTUM SELECTION AND ANGULAR CORRELATIONS IN DIRECT REACTIONS WITH STRONGLY ABSORBED PARTICLES

J. G. Wills and J. G. Cramer, Jr. . . . . 147

C-10. ANGULAR-CORRELATION STUDIES OF THE INELASTIC SCATTERING OF ALPHA PARTICLES FROM $C^{12}$, $Mg^{24}$, $Si^{28}$, AND $Fe^{56}$

J. G. Cramer, Jr., W. W. Eidson, and D. E. Blatchley . . . . . 153

Session D

D-1. NEUTRON REDUCED WIDTHS DETERMINED BY THE $N^{14}(N^{14},N^{13})N^{15}$ TRANSFER REACTION

J. A. McIntyre . . . . . 160

D-2. SELECTION RULES IN ${}_{22}Ti^{48}_{26}$ (p,p') INELASTIC SCATTERING

G. T. Garvey, G. M. Crawley, H. O. Funsten, N. R. Roberson, and L. Zamick . . . . . 168

D-3. DIRECT-REACTION STUDY OF THE $Ca^{41}$ AND $Ca^{49}$ SHELL-MODEL LEVELS

T. A. Belote, E. Kashy, A. Sperduto, H. A. Enge, and W. W. Buechner . . . . . 172

D-4. NUCLEON CAPTURE REACTIONS NEAR A = 40

J. L. Yntema and G. R. Satchler . . . . . 177

Session E PAGE

E-1. THE SINGLET DI-NUCLEON STATE IN NUCLEAR REACTIONS

G. M. Temmer . . . . . 180

E-2. THE FORMATION OF STRONGLY POPULATED LEVELS OF $(d_{5/2})^2_5$ AND $(f_{7/2})^2_7$ CONFIGURATION IN THE $(\alpha,d)$ REACTION

B. G. Harvey, E. Rivet, J. Cerny, R. H. Pehl, and J. Haag . . . . . 182

E-3. ANALYSIS OF TWO-NUCLEON STRIPPING REACTIONS

Norman K. Glendenning . . . . . 188

E-4. THE STUDY OF $(He^3,n)$ REACTIONS

G. U. Din, J. L. Weil, and G. C. Phillips . . . 199

E 5. THE (p,t) $(p,He^3)$, and $(p,\alpha)$ REACTIONS ON $O^{16}$ INDUCED BY 43.7-MEV PROTONS

Joseph Cerny and Richard H. Pehl . . . . . 208

E-6. A STUDY OF THE NUCLEAR REACTIONS $Mg^{26}(p,t)Mg^{24}$ AND $Mg^{26}(He^4,He^6)Mg^{24}$

M. E. Rickey, H. E. Wegner, K. W. Jones, B. M. Bardin, C. Hoot, and M. Kondo . . . . . 217

E-7. ANALYSIS OF THE $C^{13}(\alpha,n)O^{16}$ REACTION AT INTERMEDIATE ENERGIES

J. W. McRary and J. Y. Park, G. D. Thaxton and E. Merzbacher . . . . . 226

Session F PAGE

F-1. DIRECT REACTION CONTRIBUTIONS TO FLUCTUATING REACTION CROSS SECTIONS

G. M. Temmer, B. Teitelman, and F. G. Fender 228

F-2. MULTI-PARTICLE EXCITATIONS IN THE INTERMEDIATE COMPOUND STATE

A. Lande and B. Block . . . . . 230

F-3. AN ESTIMATION OF PION NUCLEAR ELASTIC CHARGE EXCHANGE SCATTERING

A. K. Kerman and R. K. Logan . . . . . 236

F-4. EXCITATION OF $C^{12}$ BY HIGH-ENERGY PROTONS

R. Haybron and H. McManus . . . . . 240

F-5. THEORY OF INTERMEDIATE STRUCTURE

J. E. Young . . . . . 241

# SESSION A

MONDAY MORNING

9 MARCH 1964

# A-1. THE VALIDITY OF THE WKB APPROXIMATION FOR HIGH-ENERGY DISTORTED-WAVE CALCULATIONS*

Daphne F. Jackson

Department of Physics, University of Washington, Seattle, Washington

The WKB approximation for distorted waves has been used in a large number of caluclations in which the energy of the bombarding particle exceeds about 90 MeV. However, the WKB approximation is essentially a small-angle approximation which uses straight-line paths and is valid only if reflection and refraction effects are relatively unimportant. Thus the use of this approximation may lead to (i) misleading conclusions about the localization of the reaction, (ii) errors in the location of the maxima and minima in the angular distributions, and (iii) incorrect values for the magnitude of the differential cross section — all of which will affect the accuracy of the information on nuclear structure to be drawn from the analyses of the reaction.

Recently, partial-wave methods for obtaining the distorted waves have been developed and applied to inelastic scattering[1] and stripping reactions[2] at low and medium energies. Comparison of the results obtained from partial-wave and WKB calculations have now

---

* Supported in part by the U. S. Atomic Energy Commission.

[1] N. K. Glendenning, Phys. Rev. 114, 1297 (1959); E. Rost and N. Austern, Phys. Rev. 120, 1375 (1960); R. H. Bassel, G. R. Satchler, R. M. Drisko, and E. Rost, Phys. Rev. 128, 2693 (1962).

[2] W. Tobocman, Phys. Rev. 115, 98 (1959); B. Buck and P. E. Hodgson, Phil. Mag. 6, 1371 (1961).

been made for the (p, p'),[3] (p, d),[4] and (p, 2p)[5] reactions for incident-proton energies in the range 90 – 200 MeV. Each pair of calculations was carried out in conventional zero-range DWBA, the only difference being in the method of obtaining the distorted waves.

(p, p'). The results of a comparison of partial-wave and WKB calculations for inelastic proton scattering from nuclei with A = 6 and A = 58 have already been reported.[3] If energy loss can be neglected, it is possible to take some account of refraction in the WKB calculation by taking the integration path along $\vec{k}_i + \vec{k}_f$, where $\vec{k}_i$ and $\vec{k}_f$ are the momenta of the incoming and outgoing proton, respectively.[6] The cross section obtained from the partial-wave calculation falls off more rapidly at large angles than in WKB approximation and the maxima are shifted to slightly smaller angles and are generally slightly increased in magnitude. For incident proton energies above 70 MeV the discrepancies between the two calculations are small.

(p, d). Calculations using the partial-wave method have been carried out for the $C^{12}(p, d)C^{11}$ reaction at 95 MeV and 145 MeV[4] in order to compare with earlier calculations which used the WKB approximation.[7] As in the case of the (p, p') reaction, the partial-wave results

---

[3] L. R. B. Elton, Proceedings of the Conference on Direct Interactions and Nuclear Reaction Mechanisms, Padua, 1962, (Gordon and Breach Science Publishers, New York, 1963), p. 1093; D. F. Jackson and L. R. B. Elton, Nucl. Phys. 43, 136 (1963).

[4] D. F. Jackson, Nucl. Phys. (to be published).

[5] T. Berggren and D. F. Jackson (to be published).

[6] R. J. Glauber, Lectures on Theoretical Physics (Interscience Publishers, Inc., New York, 1959), Vol. 1, p. 315.

[7] P. A. Benioff, Phys. Rev. 128, 740 (1962).

are larger than the WKB results at small angles and fall off much more rapidly at large angles, but the disagreement in magnitude is more serious for this reaction. Also, for the pickup of a p-shell neutron whose angular distribution is represented by $Y_1^m$, the WKB results indicate a very small contribution from m = 0, i.e., a localization of the reaction in the equatorial region of the nucleus, but this conclusion is not supported by the partial-wave results.[4] The reason for these discrepancies is that in the WKB treatment the product of the distortion functions for the incoming and outgoing particles has been approximated by a single integral along a straight-line path in the forward direction. While this procedure is reasonably successful for inelastic proton scattering with small energy loss, it is apparently not valid when the incoming and outgoing particles are different and are subject to very different distortion effects, and when the energy loss is not small.[8] Thus it appears thatthe additional approximations are mainly responsible for the breakdown of the WKB approximation in this case.

(p, 2p). Several calculations on the (p, 2p) reaction have used the WKB approximation for the distorted waves.[9] In this case, the two outgoing protons have less than half the energy of the incoming proton so that distortion effects for the incoming and outgoing protons are very different, and the distortion functions must of necessity be calculated separately and without further approximation. Since accurate results at scattering angles around $45^{\circ}$ are particularly important, the forward-scattering approximation is not used. Thus better agreement between the WKB and partial-wave calculations can be expected for the

---

[8] The Q value for the reaction $C^{12}(p, d)C^{11}$ is -16.5 MeV.

[9] T. Berggren and G. Jacob, Phys. Letters 1, 258 (1962); Nucl. Phys. 47, 481 (1963); A. Johannson and Y. Sakamoto, Nucl. Phys. 42, 625 (1963).

(p, 2p) reaction than for the (p, d) reaction; but as there are now three distorted waves, the small discrepancies seen in the comparison of the (p, p') calculations will be enhanced. This prediction is confirmed by a comparison made for the $Li^6$(p, 2p) reaction at 185 MeV[5] in which the two calculations differ by about 15% at the maxima and are in close agreement at large and small angles. (In the WKB approximation it is straightforward to use relativistic or nonrelativistic kinematics as appropriate, whereas the partial-wave method has been developed only for the non relativistic case; but the difference in kinematics introduces only a small displacement in the angular distribution.[5,10])

It will be seen that the validity of the WKB approximation has been tested so far in reactions on light nuclei in which the absorption of the nucleons is not strong. The reflection coefficients $|\exp(2i\delta_\ell)|$, where $\delta_\ell$ is the phase shift due to the distorting potential for the $\ell$ th partial wave, are given in Table I for two of these reactions. Except in the case of the outgoing deuteron from the (p, d) reaction, the reflection coefficients are not small, even for the low partial waves. Thus the fact that the WKB approximation is reasonably satisfactory for the (p, p') and (p, 2p) reactions seems to indicate that interpretations of these reactions which are based on localization effects due to reflection and refraction produced by the distorting potential[11] are not relevant at energies above 90 MeV, and confirms the conclusion that discrepancies between theory and experiment are mainly due to inadequate nuclear wave functions.[3,9] A similar conclusion for the (p, 2p) reaction has now been reached by McCarthy and Lim[10] as a result of a partial-wave calculation. For the

---

[10] I. E. McCarthy and K. L. Lim (preprint).

[11] See, for example, I. E. McCarthy, Proceedings of the Conference on Direct Interactions and Nuclear Reaction Mechanisms, Padua, 1962, (Gordon and Breach Science Publishers, New York, 1963), p. 94 and subsequent discussion; McCarthy and Lim, ibid., p. 180.

TABLE I. Reflection coefficients for the reactions $C^{12}$(p, d) and $Li^6$ (p, 2p). The energy of each particle in the center-of-mass system is given in MeV.

| | $C^{12}$(p, d) | | $Li^6$(p, 2p) | |
|---|---|---|---|---|
| $\ell$ | Proton $E_{c.m.} = 87.6$ | Deuteron $E_{c.m.} = 71.1$ | Proton $E_{c.m.} = 158.8$ | Proton $E_{c.m.} = 77.2$ |
| 0 | 0.394 | 0.046 | 0.733 | 0.570 |
| 2 | 0.424 | 0.051 | 0.759 | 0.635 |
| 4 | 0.520 | 0.070 | 0.810 | 0.765 |
| 6 | 0.745 | 0.141 | 0.870 | 0.897 |
| 8 | 0.939 | 0.437 | 0.925 | 0.967 |
| 10 | 0.987 | 0.790 | 0.966 | 0.992 |
| 12 | 0.998 | 0.948 | 0.986 | 0.998 |

(p, d) reaction alone, there is some evidence for localization in momentum space which may be a result of the strong absorption of the deuteron.[12] The contributions to the differential cross section at various angles corresponding to the $\ell$ th partial wave for the incident proton are given in Table II. The contributions from the appropriate partial waves for the deuteron, which are $\ell \pm 1$ for the pickup of a p-shell neutron, have been summed to give the figures in the table. It can be seen that for small angles ($\lesssim 20^\circ$) there is a fairly sharp localization in momentum space.

[12] N. Austern, Ann. Phys. 15, 299 (1961).

TABLE II. The contribution (in arbitrary units) to the differential cross section for $C^{12}(p, d)$ from different partial waves. Here m is the azimuthal quantum number of the p-shell neutron which is picked up, and the contribution labeled $|m| = 1$ is the sum for m = 1 and m = -1.

| $\ell$ | $5^\circ$ | | $15^\circ$ | | $25^\circ$ | |
|---|---|---|---|---|---|---|
| | m = 0 | $\|m\| = 1$ | m = 0 | $\|m\| = 1$ | m = 0 | $\|m\| = 1$ |
| 0 | 0.03 | . . . | 0.02 | . . . | 0.01 | . . . |
| 1 | 0.29 | . . . | 0.26 | 0.02 | 0.20 | 0.05 |
| 2 | 1.18 | 0.01 | 0.93 | 0.11 | 0.55 | 0.23 |
| 3 | 2.86 | 0.06 | 1.87 | 0.38 | 0.68 | 0.59 |
| 4 | 5.38 | 0.18 | 2.68 | 1.05 | 0.32 | 1.15 |
| 5 | 8.14 | 0.46 | 2.74 | 2.38 | -0.15 | 1.66 |
| 6 | 9.34 | 0.96 | 1.74 | 4.08 | -0.05 | 1.50 |
| 7 | 7.58 | 1.45 | 0.47 | 5.05 | 0.44 | 0.61 |
| 8 | 4.16 | 1.63 | -0.12 | 4.54 | 0.48 | -0.22 |
| 9 | 1.47 | 1.42 | -0.12 | 3.11 | 0.14 | -0.49 |
| 10 | 0.26 | 1.01 | -0.02 | 1.69 | -0.08 | -0.40 |
| 11 | -0.05 | 0.61 | 0.01 | 0.75 | -0.10 | -0.24 |
| 12 | -0.07 | 0.33 | 0.01 | 0.26 | -0.06 | -0.11 |

# A-2. STUDIES OF THE $O^{16}(He^3,\alpha)O^{15}$ AND $O^{16}(He^3,He^3)O^{16}$ REACTIONS*

W. P. Alford, L. M. Blau, and D. Cline

University of Rochester, Rochester, New York

The $(He^3,\alpha)$ reaction is the analogue of the (p,d) or (d,t) reactions, and existing measurements indicate that this reaction proceeds to a large extent by a direct mode of interaction. In order to investigate the usefulness of the $(He^3,\alpha)$ reaction as a spectroscopic probe, a careful study has been made of the $O^{16}(He^3,\alpha)O^{15}$ reaction leading to the ground state of $O^{15}$, and the results have been analyzed using the distorted-wave Born approximation program SALLY[1] of the Oak Ridge group.[2] The elastic scattering of $He^3$ from $O^{16}$ has been studied over the same energy range in order to establish the optical-model potentials for the DWBA calculation.

All measurements were made using the $He^3$ beam from the University of Rochester variable-energy cyclotron. For the reaction data a target of 0.60-mg/cm$^2$ Mylar was used, while a target of 0.35-mg/cm$^2$ NiO was used to measure the elastic scattering. Solid-state detectors were used to record data at angles greater than 30°. At smaller angles, a broad-range spectrograph with a position-indicating surface-barrier counter in the focal plane was used. At angles less than

*Work performed under the auspices of the U.S. Atomic Energy Commission.

[1] R. H. Bassel, R. M. Drisko, and G. R. Satchler, "The Distorted-Wave Theory of Direct Nuclear Reactions.I: 'Zero-Range' Formalism without Spin-Orbit Coupling and the Code SALLY," ORNL-3240 (unpublished).

[2] We would like to acknowledge the extensive assistance of R. H. Bassel and G. R. Satchler in carrying out the calculations.

$15^{\circ}$, the elastic groups from nickel and oxygen could not be resolved and a subtraction procedure was used to extract the oxygen group, resulting in rather large errors for the elastic cross section at small angles. In each angular distribution, data points were normalized relative to the count in a fixed monitor counter. Absolute cross sections were determined using a shielded Faraday cup to integrate the beam current during measurements of the excitation functions, and are subject to an uncertainty of about 20%.

The measured pickup reaction cross sections are shown in Fig. 1. The general shape of the angular distribution does not change markedly as the energy is varied, but the magnitude of the peak cross section varies by a factor of about two between 8.5 and 9.5 MeV. Excitation functions measured at three different angles are shown in Fig. 2, and exhibit rather large changes as the energy is varied. By contrast, the excitation functions for the elastic scattering (Fig. 3) show little energy variation except for the $E^{-2}$ dependence expected for Rutherford scattering. Angular distributions of the elastic scattering were measured at energies of 8.5 and 9.42 MeV, and are shown as the data points in Fig. 4.

Optical-model parameters for the incoming $He^3 + O^{16}$ channel were extracted from the elastic-scattering data using the least-squares search program HUNTER of the Oak Ridge group. Both real and imaginary parts of the potential were chosen to have the Saxon-Woods shape. In order to sample as much of parameter space as possible, searches were made from a large number of different starting points, but the same final set of parameters was always obtained. It was soon determined that no choice of parameters provided a satisfactory fit to the entire angular range; in the final searches, data points beyond $120^{\circ}$ were given zero weight in the search program. It was also found that the

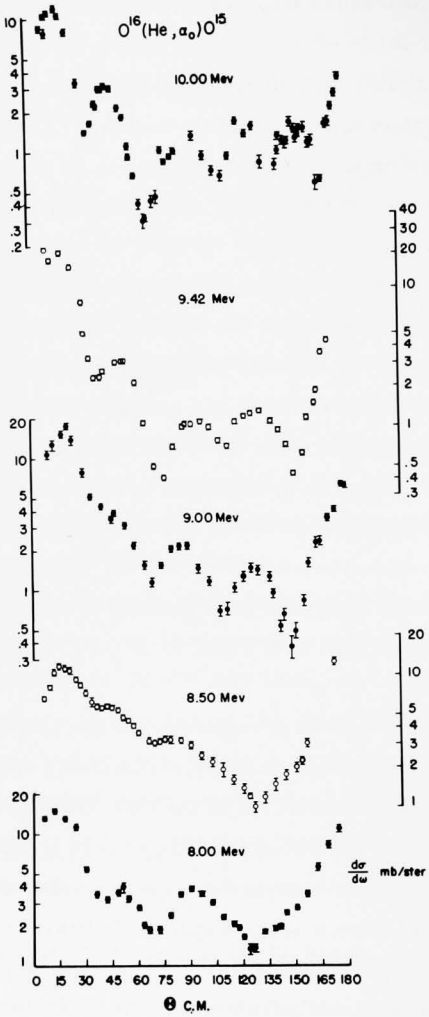


Fig. 1. Angular distributions of the $O^{16}(He^3, \alpha)O^{15}$ ground-state reaction between 8 and 10 MeV. The indicated errors are statistical, and absolute cross sections are accurate to 20%.

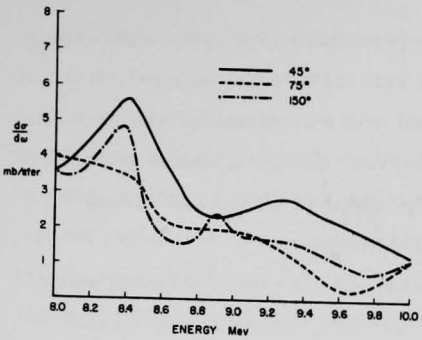


Fig. 2. Excitation functions for the $O^{16}(He^3, \alpha)O^{15}$ ground-state reaction at three angles.

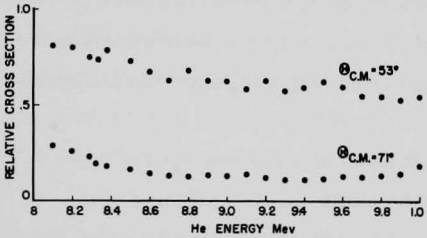


Fig. 3. Excitation functions for the elastic scattering of $He^3$ from $O^{16}$ at two angles.

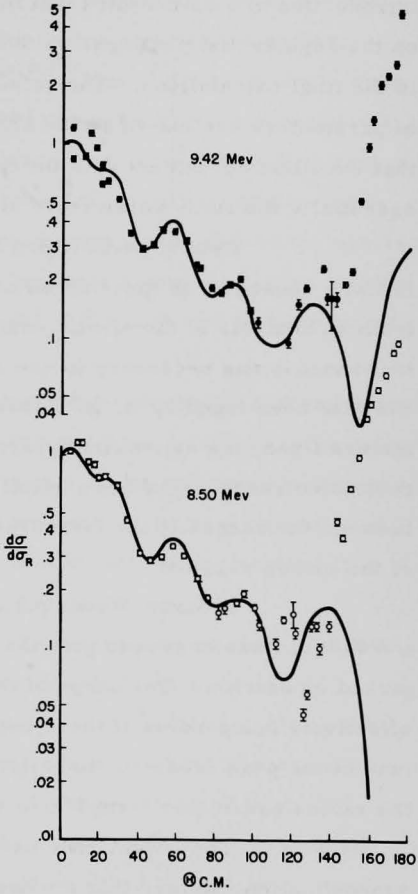


Fig. 4. Cross section relative to Rutherford for the elastic scattering of $He^3$ from $O^{16}$. The measured points are shown with experimental errors, and the solid curves show the results of the optical-model calculation for a Saxon-Woods potential with the following parameters.

8.50 MeV: $V = -104.2$ MeV; $W = 21.53$ MeV; $r_0 = 1.513$ fm; $a = 0.681$ fm.

9.42 MeV: $V = -104.9$ MeV; $W = 21.20$ MeV; $r_0 = 1.568$ fm; $a = 0.640$ fm.

$r_0 = 1.30$ fm for both energies.

introduction of a spin-orbit term in the potential had only a small effect on the angular distributions, so that no spin-orbit term was included in the final calculations. The calculated cross sections for the best set of parameters are shown as the solid curves in Fig. 4, and it is seen that excellent agreement with the data is obtained out to $140^{\circ}$ using essentially the same parameters at each energy.

Optical parameters for the exit $He^4 + O^{15}$ channel were initially chosen to be those obtained by Carter, Mitchell, and Davis[3] from an analysis of the elastic scattering of $He^4$ from $C^{12}$ and $O^{16}$. They found that it was necessary to use a real well depth of about 100 MeV, as has also been found by R. H. Bassel.[4] With the entrance-channel parameters fixed, the exit-channel parameters were then varied over a restricted range about these initial values to obtain the best agreement between the shapes of the measured and calculated angular distributions of the pickup reaction.

A Saxon-Woods potential with parameters $r_0 = 1.2$ fm, $a = 0.65$ fm was chosen to give the bound-state wave function for the picked up neutron. The shape of the angular distributions was found to be effectively independent of these parameters although the absolute magnitude of the peak cross section altered by a factor of two on increasing the radius parameter from 1.2 to 1.4 fm.

The DWBA code used, which employs the zero-range approximation, showed that the nuclear interior contributed strongly to the reaction. However, it is generally believed that the effect of the nuclear interior should be considerably damped out in a more exact calculation including such effects as a finite range. It is thus felt that

[3] E. B. Carter, G. E. Mitchell, and R. H. Davis (private communication, to be published).

[4] R. H. Bassel (private communication).

it was more physically reasonable to presume that the dominant contribution to the interaction occurred in the region close to the nuclear surface. It was found from the calculations that in order to obtain even qualitative agreement with the measured cross section a radial cut-off of about a fermi inside the nuclear surface was necessary. With such a cut-off radius, it was found that the shape and magnitude of the calculated cross section at forward angles was quite insensitive to the precise value of the radius. The calculations for large angles do show a marked dependence on cutoff, but this may be due to the fact that a sharp cutoff was used.

Quite reasonable agreement between theory and experiment was found for the shape of the angular distributions at all energies except 8.5 MeV, using a constant cutoff radius of 4.92 fm and making only small changes in the exit-channel optical parameters. The parameters used for best fit are given in Table I, and the calculated cross section at 9.42 MeV is compared with the data in Fig. 5.

To provide some idea of the usefulness of such calculations for the extraction of $\ell$ values and spectroscopic factors, it should be noted that the shape of the forward peak was substantially unchanged by variations of about ±5% in any of the exit-channel optical parameters or in the cutoff radius. The spectroscopic factors estimated from the analysis of these data were uncertain by a factor of about ±30% except for the data at 8.50 MeV which could only be fitted using a much smaller cut-off radius, giving a spectroscopic factor only about one-fifth as large as was found at other energies.

It may be that these discrepancies could be explained by introducing a small compound-nucleus contribution to the cross section and further calculations are in progress to try to separate the reaction into direct-interaction and compound-nucleus contributions. In spite of

TABLE I. Optical-model parameters for the best agreement between DWBA calculations and the measured $O^{16}(He^3, \alpha)O^{15}$ cross section.

| $E_{He^3}$ | Entrance channel | | | | Exit channel | | | | $r_{cutoff}$ | Quality of fit |
|---|---|---|---|---|---|---|---|---|---|---|
| | V | W | $r_0$ | a | V | W | $r_0$ | a | | |
| 8.00 | 104.0 | 21.50 | 1.500 | 0.700 | 110.0 | 5.0 | 1.400 | 0.750 | 4.92 | Good |
| 8.50 | 104.2 | 21.50 | 1.513 | 0.6813 | 100.0 | 5.0 | 1.400 | 0.699 | 3.10 | Poor |
| 9.00 | 104.5 | 21.35 | 1.525 | 0.650 | 125.0 | 3.5 | 1.300 | 0.550 | 4.92 | Good |
| 9.42 | 104.9 | 21.20 | 1.568 | 0.640 | 110.0 | 8.0 | 1.400 | 0.600 | 4.92 | Good |
| 10.00 | 105.0 | 20.50 | 1.575 | 0.636 | 100.0 | 10.0 | 1.500 | 0.650 | 4.92 | Good |

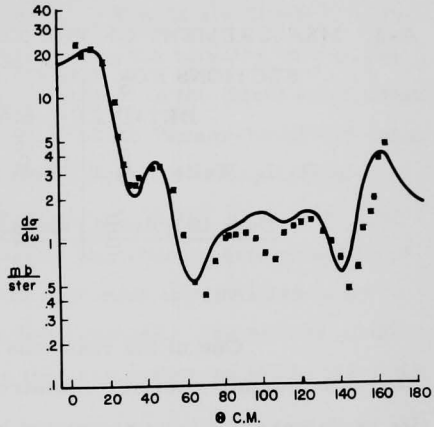


Fig. 5. Comparison of the DWBA calculation with experiment at 9.42 MeV. The parameters used in the calculation are listed in Table I, along with parameters for best fit at other energies.

this difficulty, it appears that DWBA calculations will be useful in interpreting the angular distributions of ($He^3$, α) reactions, and that these reactions will be able to yield reliable spectroscopic information even at relatively low energies such as were used here.

# A-3. MEASUREMENT OF THE NEUTRON POLARIZATION AND CROSS SECTIONS FOR THE $C^{12}(d,n)N^{13}$ REACTION BETWEEN 2.8 AND 4 MEV*

R. L. Walter, J. R. Sawers, and F. O. Purser

Duke University, Durham, North Carolina

One of the reactions that has been suggested as a possible source of partially polarized neutron beams is $C^{12}(d,n)N^{13}$. In the past its usefulness has been restricted because of the limited information available concerning the variation of the neutron polarization with energy and angle. The original intent of the present experiment was to investigate the polarization of these neutrons in order to supply this information. However, after an initial survey of the polarization, it was recognized that a complete study of both the cross section and the polarization would be useful in the attempts to separate the compound-nucleus effects from the direct-interaction contribution in this reaction. Thus, a thorough study of the $C^{12}(d,n)$ reaction was undertaken over a wide angular range for deuteron energies from 2.8 to 4.0 MeV.

A $5^{\circ}$ neutron-yield curve was measured with time-of-flight techniques and a pulsed deuteron beam from the Duke electrostatic accelerator. This technique allowed easy separation of $C^{12}(d,n)N^{13}$ neutrons from the neutrons that left $N^{13}$ in the first excited state and also from neutrons that arose from deuteron bombardment of the 1.1% abundant $C^{13}$ in the target. The relative efficiency of the (proton-recoil) liquid scintillator which was used in the time-of-flight system was

*Work supported by the U. S. Atomic Energy Commission.

calculated from the standard relation given by Swartz and Owen.[1] This calculated efficiency was checked by comparing the counting rate of the monoenergetic neutrons from the T(p,n) reaction in the liquid scintillator with the counting rate in a detector similar to the Hanson-McKibben long counter whose efficiency is known.[2] The two sets of values agreed to within 5%. Self-supporting carbon targets about 30 keV thick were employed. Use of such targets made possible an accurate determination of the amount of background from drive-in deuterons accumulated in the beam stop by counting with the carbon foil removed. The results of the yield curve are shown in Fig. 1 where they are compared to the previous

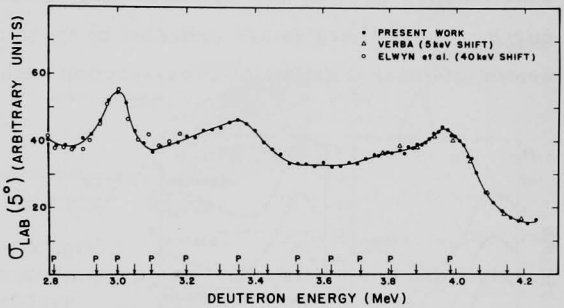


Fig. 1. Yield curve for the $C^{12}(d,n)$ reaction. The data of Elwyn et al. were obtained at 0°. The other data correspond to a 5° reaction angle.

work of Elwyn et al.[3] and Verba.[4] These earlier results were normalized to fit the data of the present measurement. Adjustments of the

[1] C. D. Swartz and G. E. Owen, in Fast Neutron Physics, Part I (Interscience Publishers, New York, 1959), Chap. II, B.

[2] W. D. Allen, in Fast Neutron Physics, Part I (Interscience Publishers, Inc., New York, 1959), Chap. II, A.

[3] A. Elwyn, J. V. Kane, S. Ofer, and D. H. Wilkinson, Phys. Rev. 116, 1490 (1959).

[4] J. W. Verba, A Study of the Resonant Contribution to the $C^{12}(d,n)N^{13}$ Reaction Near 4.00 MeV, Thesis, University of Rochester, Rochester, New York, 1962.

energy scales as indicated in the inset were applied. Neither of these shifts was outside of the energy calibrations given in the papers. Absolute determinations of the laboratory cross sections have been reported by Verba to be about 21 mb/sr at 3.93 MeV and Benenson, Jones, and McEllistrem[5] to be the same at 3.26 MeV. The ratio of these values is in excellent agreement with the ratio calculated from our values shown in Fig. 1. An absolute measurement was not carried out in the present experiment.

Angular distributions were measured at those energies where it was expected that compound-nucleus effects would be most evident and also at every 100 keV in the region between peaks in the yield curve. These energies are indicated by the arrows in Fig. 1. The center-of-mass differential-cross-section results are given in Fig. 2.

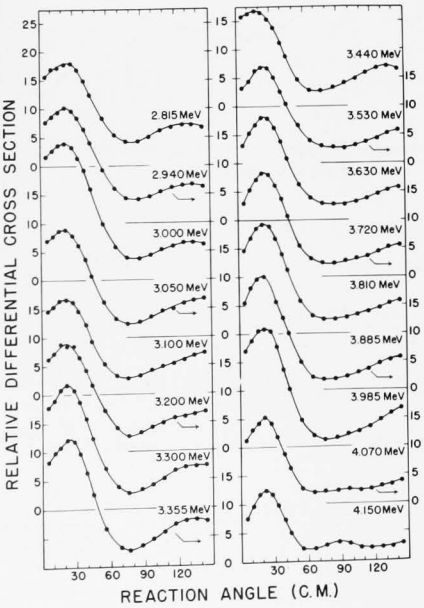


Fig. 2. Relative differential cross section in the center-of-mass system for the $C^{12}(d,n)$ reaction. The values at $5^{o}$ were normalized to center-of-mass values obtained from the curve in Fig. 1.

[5] R. E. Benenson, K. W. Jones, and M. T. McEllistrem, Phys. Rev. 101, 308 (1956).

The same time-of-flight apparatus, efficiency calculations, and 30-keV target were employed in these determinations. The 2.8- and 3.0-MeV distributions are in excellent agreement with the earlier work of Elwyn et al.[3] However, the present work is not entirely consistent with the differential cross sections reported by Verba[4] for the 3.8- and 4.1-MeV region. In general, relative to the forward maxima, we observe lower yields at the smallest angles, lower minima around 80°, and less backward peaking than were seen by Verba.

The method for measuring the neutron polarization is illustrated in Fig. 3. Deuterons were incident on self-supporting targets,

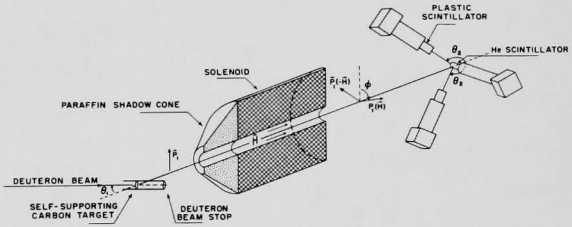


Fig. 3. Experimental arrangement for polarization determinations.

either 30 or 100 keV thick, and were stopped in a silver end cap 5 cm beyond the carbon foil. Neutrons emitted at the reaction angle $\theta_1$ were collimated to a 3° cone and were incident on helium gas contained in a thin-walled scintillation cell. Neutrons scattered from helium through an angle $\theta_2 = 132°$ (c.m.) were detected with plastic scintillators. Before counts were registered, coincidence and pulse-height requirements had to be satisfied. With this method, we were able to eliminate most of the counts arising from neutrons other than the monoenergetic (ground-state) neutrons of interest. The remaining background contribution to the data, including chance coincidences, was generally less than 5% of the total counts. A solenoid, which also served as a neutron shield and collimator, was used to rotate the polarization vector of the neutrons. This technique, in addition to employing two neutron detectors, minimized

the instrumental asymmetries inherent in polarization measurements. The helium analyzing power was calculated from the Dodder-Gammel-Seagrave phase shifts[6] and ranged from 0.60 to 0.95 over the neutron energies involved.

A preliminary check on the variation of the polarization with energy was conducted around the 3.0-MeV resonance by use of a 30-keV target. The results for reaction angles of 20°, 30°, and 40° (lab) are displayed in Fig. 4 where they are compared with the values obtained

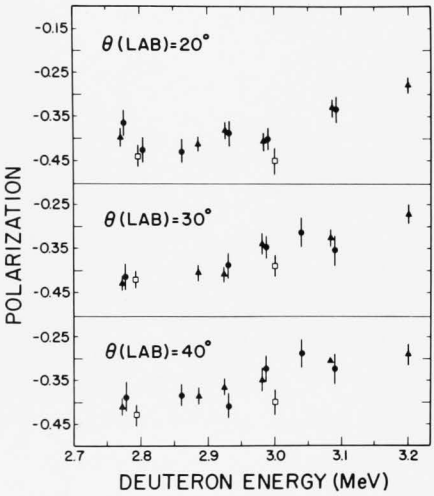


Fig. 4. Neutron polarization of the $C^{12}(d,n)$ reaction as a function of deuteron energy at several angles. The values represented by the circles and triangles are for targets 30 keV and 100 keV thick, respectively. The data of Haeberli and Rolland are represented by the squares.

with a 100-keV-thick target. Some earlier data obtained by Haeberli and Rolland,[7] which are also shown in this figure, agree well with the present work. Since the 30-keV data were consistent with the 100-keV results over this energy region where the narrowest structure in the yield curve

[6] J. D. Seagrave, Phys. Rev. 92, 1222 (1953).

[7] W. Haeberli, in Proceedings of the International Symposium on Polarization Phenomena of Nucleons, Helv. Phys. Acta, Supplementum VI, 157 (1961); also see W. Haeberli and W. W. Rolland, Bull. Am. Phys. Soc. 2, 234 (1957).

was observed, the 100-keV target was believed to be suitable for all the polarization measurements from 2.8 to 4.0 MeV.

Eleven angular distributions of the polarization were obtained. The energies selected for these measurements correspond to some of the energies where differential cross sections were measured; they are indicated in Fig. 1 by the arrows labeled with the letter P. Figure 5 is a graph of the results. The sign convention is in accord with

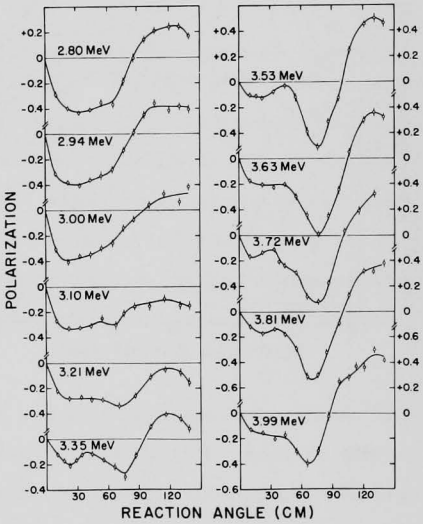


Fig. 5. Neutron polarization of the $C^{12}(d,n)$ reaction as a function of reaction angle for the deuteron energies shown.

that adopted at the Basel symposium. Standard deviations associated with the counting statistics are represented by the error bars. The only known uncertainty that perhaps should have been included in these errors is that associated with the analyzing power of helium. For our particular choice of analyzing angle ($132^{\circ}$ c.m.) this uncertainty could alter the back-angle data by as much as ±0.04. For forward angles, where the neutron energy is greater than 2 MeV, it is estimated that this uncertainty would not change the polarization by more than ±0.02 where the magnitude

of the polarization is large and by a proportionately smaller amount elsewhere, the amount obviously going to zero where the polarization passes through zero.

All of the data from Fig. 5 have been combined to form the contour plot of the polarization shown in Fig. 6. The importance of

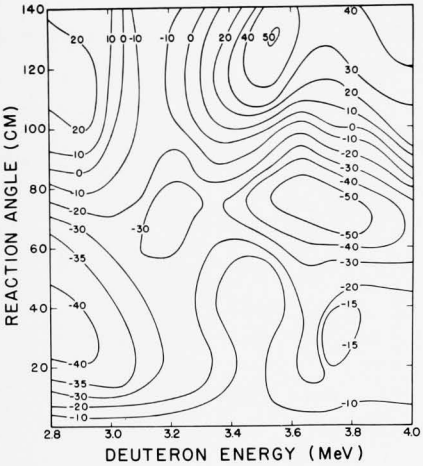


Fig. 6. Contour plot of the neutron polarization for the $C^{12}(d,n)$ reaction. The map was constructed by use of values read from the curves in Fig. 5. The numbers given for the contour lines are the percent of polarization.

the resonances is generally more apparent when the data are presented in this fashion. Recall that if the direct interaction predominates, one expects the contour lines to be nearly horizontal, as is the tendency here above 3.6 MeV.

The polarization distributions can be separated into three sets: a 2.8—3.0-MeV group, a 3.6—4.0-MeV group, and an intermediate group. We have replotted the higher energy group in Fig. 7 where we compare the data with the 12-MeV $C^{12}(d,n)$ data of Levintov and Trostin.[8] Also shown is a dashed curve which represents the trend of the 6—15-MeV $C^{12}(d,p)$ polarization results[9] of many research groups. The similarity

[8] I. I. Levintov and I. S. Trostin, J. Exptl. Theoret. Phys. 40, 1570 (1961); Soviet Phys.—JETP 13, 102 (1962).

[9] E. Boschitz, in Direct Interactions and Nuclear Reaction Mechanisms (Gordon and Breach, Science Publishers, New York, 1963), p. 640.

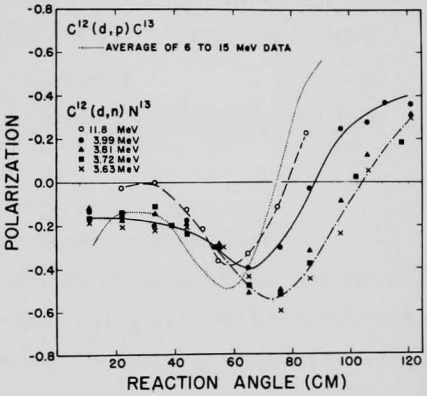


Fig. 7. Comparison of $C^{12}(d,n)$ neutron polarization with the $C^{12}(d,p)$ proton polarization. The dotted curve is taken from the paper by Boschitz. The 11.8-MeV neutron data were obtained by Levintov and Trostin. The curves through the neutron data were drawn only to aid in visualization.

indicates that the same mechanism that produces the neutron polarization near a deuteron energy of 4 MeV probably is responsible for the higher energy neutron and proton polarizations. One should be able to separate out the resonant effects in the present data, as is being attempted for the 3.9-MeV region,[10] and end up with a determination of the contribution to both the cross section and the polarization produced by the direct component of the interaction.

---

[10] D. P. Saylor (private communication). See also Ref. 4.

# A-4. ANALYSIS OF THE SCATTERING OF PROTONS BY $Ho^{165}$ IN TERMS OF THE COUPLED-CHANNEL CALCULATION

Taro Tamura*

Oak Ridge National Laboratory, Oak Ridge, Tennessee

Interest has been increased recently in analyzing the data of the elastic and inelastic scattering of α particles and nucleons by nuclei, by using the idea of the coupled-channel calculation. Thus Buck[1] made a systematic analysis of the excitation of the first $2^+$ state by nucleons and the first $2^+$ and $4^+$ states by α particles, while the present author[2] prepared a code so as to consider the excitation of the first $2^+$ and the $0^+$, $2^+$, $4^+$ two-phonon triad states at the same time and an analysis was made for the scattering of protons by Ni isotopes.[3] The purpose of the present article is to report on the extension of the previous work[2] so that the cases in which odd-A nuclei are used as target could also be treated. An actual numerical calculation has been made so far on the scattering of protons by $Ho^{165}$ and, as is seen in Fig. 1, fairly satisfactory agreement with experiment[4] has been obtained.

Although our code could be used both for spin-0 and spin-$\frac{1}{2}$ projectiles, we explain here our formulation for the spin-$\frac{1}{2}$ case. Let the spins of the states of the target nucleus which are strongly coupled

---

*On leave from the Tokyo University of Education, Tokyo, Japan.

[1] B. Buck, Phys. Rev. 127, 940 (1962).

[2] T. Tamura (to be published).

[3] J. K. Dickens, F. G. Perey, R. J. Silva, and T. Tamura, Phys. Letters 6, 53 (1963).

[4] A. Lieber and C. A. Whitten, Phys. Rev. 132, 2582 (1963).

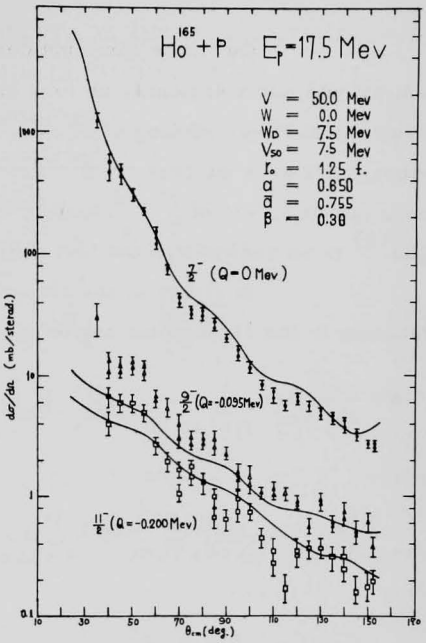


Fig. 1. Comparison of the differential cross sections of the elastic and inelastic scattering of 17.5-MeV protons by $Ho^{165}$.

together be $I_1, I_2, \cdots, I_N$, the state 1 being the ground state, and let the energy of the nucleons corresponding to the excitation of the nth state be $E_n$, $n = 1 \approx N$. Next define a quantum number J by

$$\vec{J} = \vec{I}_1 + \vec{j}_1. \tag{1}$$

Then for a fixed value of J there are several partial waves with quantum number $j_n$ for each energy $E_n$ which satisfy the selection rule

$$\vec{J} = \vec{I}_n + \vec{j}_n. \tag{2}$$

All these $j_n$ waves are coupled together, and when J becomes sufficiently large, the total number $N_c$ of such coupled waves becomes

$$N_c = \sum_n (2I_n + 1). \tag{3}$$

Our code can consider any nuclei, even or odd A and vibrational and rotational, so long as $N_c \leq 30$. Thus, for example, we can consider the coupling of $0^+$, $2^+$, $0^+$, $2^+$, $4^+$, and $3^-$ states in a vibrational even nucleus, of $0^+$, $2^+$, $4^+$, and $6^+$ states in a rotational even nucleus, and of $\frac{7}{2}^{\pm}$, $\frac{9}{2}^{\pm}$, and $\frac{11}{2}^{\pm}$ states of an odd-A deformed nucleus. ($Ho^{165}$ is an example of the last case.)

In either of the above-mentioned cases, the total wave function in the asymptotic region may be described as

$$\Psi = \frac{\sqrt{4\pi}}{rk_1\sqrt{v_1}} \sum_{(ii')m_s M_1} a^{(i)}_{m_s} b^{(i')}_{M_1} \sum_{j\ell J} (\ell\tfrac{1}{2}0m_s|jm_s)(jI_1m_sM_1|JM)$$

$$\times\left\{\hat{\ell}\, i^{\ell} \exp(i\sigma^1_{\ell}) \frac{1}{2i}\left[\exp(i\textstyle\sum^1_{\ell}) - \exp(-i\textstyle\sum^1_{\ell})\right] (\mathcal{Y}_{\ell j} \otimes \Phi_{I_1})_{JM} \right. \tag{4}$$

$$\left. - \sum_{n\ell'j'} (k_1/k_n)^{3/2}\, \hat{\ell}'\, i^{\ell'} \exp(i\sigma^n_{\ell'} + i\textstyle\sum^n_{\ell'})\, C^J_{\ell j;n\ell'j'} (\mathcal{Y}_{\ell'j'} \otimes \Phi_{I_n})_{JM}\right\}.$$

In Eq. (4), $\hat{\ell} = (2\ell + 1)^{\frac{1}{2}}$, $\sigma^n_{\ell}$ is the Coulomb phase shift for energy $E_n$, $\sum^n_{\ell} = (k_n r - \eta_n \ell_n(2k_n r) - \frac{1}{2}\ell\pi + \sigma^n_{\ell})$, $\Phi_{I_n}$ is the wave function of the $\underline{n}$th state, and $\mathcal{Y}_{\ell j m_j} = (\chi_{\frac{1}{2}} \otimes Y_{\ell})_{jm_j}$, with $\otimes$ denoting the vector coupling. $a^{(i)}_{m_s}$ and $b^{(i')}_{M_1}$ are amplitudes of magnetic substates belonging to respective ensembles i and i'.

The interaction assumed is

$$H = -(V + iW)\, f(r,\theta,\phi;\, a, R_0) - 4\, i\, W_D\, g(r,\theta,\phi;\, \bar{a}, R_0)$$

$$- (\hbar/\mu_{\pi}C)^2 (V_{SO}/ar)(\vec{\sigma}\cdot\vec{\ell})\, g(r,\theta,\phi;\, a R_0) + V_{Coulomb}(r,\theta,\phi;\, a R_0), \tag{5}$$

with

$$f(r,\theta,\phi;\, a R_0) = 1/\left\{1 + \exp\left(\left[r - R(\theta,\phi)\right]/a\right)\right\} ,$$

$$g(r,\theta,\phi;\, a R_0) = \exp\left(\left[r - R(\theta,\phi)\right]/a\right)\Big/\left\{1 + \exp\left(\left[r - R(\theta,\phi)\right]/a\right)\right\}^2 . \quad (6)$$

Other notations in Eq. (5) would be obvious.

The quantity $R(\theta,\phi)$ in Eq. (6) is expressed as

$$R(\theta,\phi) = R_0 \left[1 + \sum_{\lambda\mu} \alpha_{\lambda\mu} Y_{\lambda\mu}(\theta,\phi)\right] \quad (7)$$

for vibrational targets, while for rotational targets

$$R(\theta,\phi) = R_0 \left[1 + \sum_{\lambda} \beta_\lambda P_\lambda(\cos\theta)\right] \quad (7')$$

in the intrinsic coordinate system. When Eq. (7) or (7') is inserted in (5), the latter may be rewritten as

$$H = V_{diag} + V_{couple}, \quad (8)$$

where $V_{diag}$ means the part of H that is diagonal with respect to $\vec{j}$ and $\vec{I}_n$.

Corresponding to Eq. (1), the total wave function in the interior region may be written as

$$\Psi = (1/r) \sum_{jI_n\ell j} R^{(n)}_{JI_n\ell j}(r)\, (\mathcal{Y}_{\ell j} \otimes \Phi_{I_n})_{JM}, \quad (9)$$

and with the interaction (8), the coupled equation is given as

$$\left\{- d^2/d\rho_n^{\,2} + \ell(\ell+1)/\rho_n^{\,2} + V_{diag}/E_n - 1\right\} R^{(n)}_{JI_n\ell j}(r)$$

$$+ \sum_{I_n'\ell' j'} (1/E_n) \langle (\mathcal{Y}_{\ell j} \otimes \Phi_{I_n})_{JM} | V_{couple} | (\mathcal{Y}_{\ell' j'} \otimes \Phi_{I_n'})_{JM} \rangle R^{(n')}_{JI_n'\ell' j'}(r) = 0. \quad (10)$$

If Eq. (10) is solved numerically and the solution is matched to the asymptotic form given by (1), the scattering amplitudes $C^J_{\ell j;\ell' j' n'}$ are obtained and the cross sections are computed accordingly.

In the scattering of protons by $Ho^{165}$, the number $N_c$ of Eq. (3) becomes just 30 if all the $\frac{7}{2}^-$, $\frac{9}{2}^-$, $\frac{11}{2}^-$ are coupled together and Eq. (10) becomes a second-order differential equation where thirty functions are coupled together. Thus it takes about 7 hr on the CDC-1604 computer at Oak Ridge in computing the three differential cross sections for a given set of optical parameters.

Because of the length of the calculational time, it was thought necessary to fix the parametric values to those which are known from other analyses. Recently Perey[5] made a detailed analysis of the elastic scattering of protons by various nuclei in the mass region $A \approx 200$ and gave a good set of optical parameters; those values are used in our calculation. (See the inset of Fig. 1). On the other hand, the quadrupole moment and the splitting of the dipole resonance of $Ho^{165}$ indicates[6] $\beta = 0.30$ and this value is used in our calculation.

The result of the calculation is compared with experiment[4] in Fig. 1, and the agreement with experiment is very good.[7] One thing which is to be emphasized is that the experimental fact that $d\sigma(\rightarrow \frac{9}{2}^-)/d\sigma(\rightarrow \frac{1}{2}^-) \approx 2.0$ is explained naturally in our calculation, which is predicted to be equal to $35/9 \approx 4.0$, if a naive idea of the splitting of the quadrupole strength is applied.[4] This fact would mean that the present type of

---

[5] F. G. Perey (private communication).

[6] See, for example, M. Damos and W. Greiner (to be published).

[7] The disagreement of the differential inelastic cross sections at forward angles may be due to an insufficient unfolding of the contribution of the tail of the elastic scattering in the analysis of the experimental data (cf. Ref. 4).

calculation, albeit complicated, is worthwhile to be made for other cases too, and accumulation of experimental data is highly hoped.

The author expresses his sincere thanks to Drs. G. R. Satchler and F. G. Perey for a number of helpful and stimulating discussions.

# A-5. DISTORTED-WAVE ANALYSIS OF THE $Zr^{90}(d,p)Zr^{91}$ STRIPPING REACTION

William R. Smith

Oak Ridge National Laboratory, Oak Ridge, Tennessee*

## I. Introduction

Because of the ambiguities present in choosing elastic-scattering parameters, we attempt to estimate the sensitivity of the spectroscopic factors $S_\ell$ to different choices of acceptable elastic parameters and also to determine if the stripping data favor certain parameters over others. To assist in the latter study, the polarization of the (d,p) protons is also investigated.

The 10.85-MeV $Zr^{90}(d,p)Zr^{91}$ reactions[1] leading to the $d_{5/2}$ ground state, the $s_{1/2}$ 1.22-MeV state, and the $g_{7/2}$ 2.19-MeV state were chosen for several reasons. A previous investigation[2] indicated that the data could be fitted by the DWBA by use of elastic-scattering parameters; this nucleus has a closed neutron shell and a closed proton subshell so that the low-lying states of $Zr^{91}$ should be nearly single-particle states and the spectroscopic factors should have values near unity; data exist for elastic scattering of 11.8-MeV deuterons on zirconium[3]

---

*Operated by Union Carbide Corporation for the U. S. Atomic Energy Commission.

[1] R. L. Preston, H. J. Martin, and M. B. Sampson, Phys. Rev. 121, 1741 (1961).

[2] W. R. Smith and E. V. Ivash, Phys. Rev. 128, 1175 (1962). This work and the references contained therein form a background for the present work.

[3] G. Igo, W. Lorenz, and U. Schmidt-Rohr, Phys. Rev. 124, 832 (1961).

and for 16.2-MeV protons on niobium[4]; and proton polarization data for the $Sr^{88}(d,p)Sr^{89}$ reaction to the $\ell=0$ first excited state has been obtained[5] for $E_d = 10.85$ MeV.

## II. Procedure

The optical potentials are composed of a Woods-Saxon real potential form factor with radius $R_R A^{1/3}$ and diffuseness $a_R$, an imaginary potential with parameters $R_I A^{1/3}$ and $a_I$ of either the volume Woods-Saxon form or of the derivative Woods-Saxon form with surface peak unity, and the real and imaginary potential depths V and W. When a spin-orbit term is included, it is of the Thomas form using the pion mass and with a potential depth $V_{so}$. A homogeneous charge distribution with radius $R_R$ is included.

Deuteron parameters were obtained by varying $a_R$, V, and W with an automatic search code. This was done for a grid of $R_R$, $R_I$, and $a_I$ values spaced by intervals of 0.2 fm. The cross-section deviation at each angle is weighted by the reciprocal of the experimental cross section, and the square root of the sum over angles of the squares of the weighted deviations, divided by the number of experimental points, is denoted by X and is used as the fit criterion. The best fits over-all and those best for different $R_R$ have their parameters listed in Table I. In all, 88 sets of parameters were obtained.

For the protons, the starting parameters for the search involving $R_R = 1.25$ fm had values obtained from an empirical prescription.[6]

---

[4] C. B. Fulmer, Phys. Rev. 125, 631 (1962).

[5] E. J. Ludwig and D. W. Miller, Bull. Am. Phys. Soc. 8, 60 (1963).

[6] F. Perey, Phys. Rev. 131, 745 (1963).

TABLE I. Parameters and spectroscopic factors.

| Set | $R_R$ (fm) | $a_R$ (fm) | $R_I$ (fm) | $a_I$ (fm) | Volume or surface | V (MeV) | W (MeV) | 100X | $S_0$ | $S_2$ | $S_4$ | $S_0/S_2$ | $S_4/S_2$ |
|---|---|---|---|---|---|---|---|---|---|---|---|---|---|
| | | | | | | | Deuteron[a] | | | | | | |
| A | 1.3 | 0.567 | 1.1 | 1.0 | V | 85.0 | 17.4 | 0.702 | 0.389 | 0.484 | 0.302 | 0.805 | 0.625 |
| B | 1.3 | 0.567 | 1.3 | 1.0 | V | 83.9 | 12.7 | 0.601 | 0.411 | 0.522 | 0.348 | 0.787 | 0.666 |
| C | 1.3 | 0.599 | 1.3 | 0.8 | V | 83.9 | 14.1 | 0.692 | 0.368 | 0.521 | 0.307 | 0.706 | 0.590 |
| D | 1.3 | 0.572 | 0.9 | 1.0 | S | 84.6 | 15.5 | 0.601 | 0.397 | 0.535 | 0.338 | 0.742 | 0.631 |
| E | 1.3 | 0.577 | 1.1 | 1.0 | S | 82.5 | 12.5 | 0.510 | 0.524 | 0.627 | 0.398 | 0.835 | 0.635 |
| F | 1.3 | 0.533 | 1.3 | 1.0 | S | 80.7 | 9.36 | 0.653 | 0.470 | 0.636 | 0.473 | 0.739 | 0.744 |
| G | 1.3 | 0.618 | 1.1 | 0.8 | S | 82.8 | 17.6 | 0.520 | 0.407 | 0.530 | 0.330 | 0.768 | 0.622 |
| H | 1.1 | 0.775 | 1.3 | 0.8 | S | 105.2 | 12.8 | 0.616 | 0.625 | 0.660 | 0.362 | 0.946 | 0.548 |
| I | 1.3 | 0.677 | 1.3 | 0.8 | S | 78.5 | 13.5 | 0.694 | 0.420 | 0.651 | 0.405 | 0.645 | 0.622 |
| J | 1.5 | 0.522 | 1.1 | 0.4 | S | 62.3 | 44.5 | 0.840 | 0.387 | 0.672 | 0.443 | 0.575 | 0.659 |
| | | | | | | | Proton[a] | | | | | | |
| A | 1.25 | 0.678 | 1.25 | 0.47 | S | 50.6 | 14.1 | 0.840 | | | | | |
| B | 1.20 | 0.723 | 1.25 | 0.47 | S | 54.6 | 14.8 | 0.872 | 0.455 | 0.698 | 0.473 | 0.651 | 0.677 |
| C | 1.15 | 0.768 | 1.25 | 0.47 | S | 59.0 | 15.2 | 1.15 | 0.465 | 0.783 | 0.547 | 0.594 | 0.699 |

[a]In the stripping calculations, set (A) of the proton parameters was used with each set of deuteron parameters; and set (E) of the deuteron parameters was used with each set of proton parameters.

Two other radii were considered and the results are presented in Table I. The calculation included a spin-orbit potential $V_{so}$ = 8 MeV. Sample fits to the proton and deuteron elastic-scattering data are shown in Fig. 1.

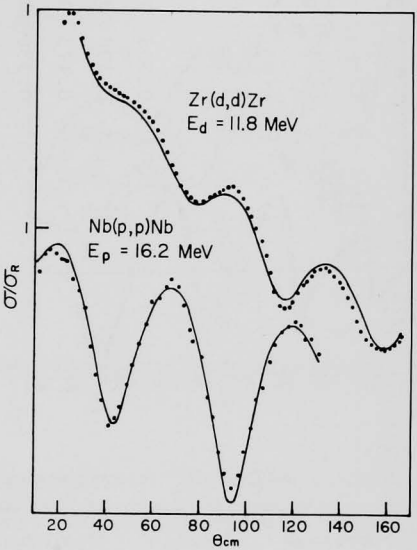


Fig. 1. Ratio of calculated to Rutherford differential cross sections for (top) the elastic scattering of deuterons on zirconium for parameter set G of Table I and (bottom) the elastic scattering of protons on niobium for parameter set A of Table I.

The parameters in Table I were used to calculate $Zr^{90}(d,p)Zr^{91}$ stripping angular distributions with neutron-capture angular momenta $\ell = 0$, 2, and 4. Representative stripping calculations are shown in Fig. 2. The neutron potential form factor is identical to the proton form factor in each case. These distributions were normalized to the $\ell$=0 and $\ell$=2 data, the former to the peak at 33° and the latter in an average way to the first and second peaks. The $\ell$=4 data are not shown and the experimental cross section is assumed to have a value of 0.7 mb/sr at the peak angle of the theoretical curves. With the above normalization, the cross-section ratios $S_\ell$ were extracted and are listed in Table I, along with their ratios to $S_2$. Table II lists the average of

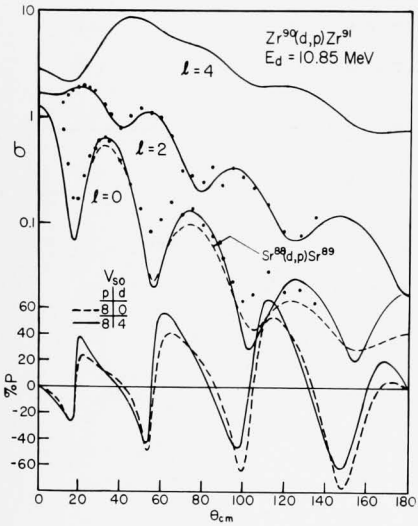


Fig. 2. Top three curves: $Zr^{90}(d,p)Zr^{91}$ angular distributions corresponding (from top to bottom) to $\ell=4$, 2, and 0. Dashed curve and bottom curves: Angular distribution and polarizations for the $E_d=11$ MeV $Sr^{88}(d,p)Sr^{89}$ $\ell=0$ reaction with $(V_{so})_p = 8$ MeV and $(V_{so})_d = 4$ MeV. One of the polarizations corresponds to $(V_{so})_d = 0$. The proton and deuteron parameters in all cases refer, respectively, to the proton set A and the deuteron set G in Table I.

TABLE II. Average spectroscopic factors.

| | Average $S_\ell$ | Average deviation (%) | Maximum deviation (%) | Average $S_\ell/S_2$ | Average deviation (%) | Maximum deviation (%) |
|---|---|---|---|---|---|---|
| 0 | 0.443 | 12.3 | 41.0 | 0.726 | 11.3 | 29.4 |
| 2 | 0.610 | 11.6 | 28.4 | | | |
| 4 | 0.394 | 15.9 | 38.8 | 0.645 | 5.95 | 15.5 |

these quantities along with the average absolute deviation and the maximum deviation.

The parameters in Table III represent the optimum fits obtained from widely varying regions of the parameter space and, together with the cases presented in Table I, have been used to calculate

TABLE III. Additional deuteron parameters.

| $R_R$ (fm) | $a_R$ (fm) | $R_I$ (fm) | $a_I$ (fm) | Volume or surface | V (MeV) | W (MeV) | 100X |
|---|---|---|---|---|---|---|---|
| 1.3 | 0.561 | 0.9 | 0.4 | V | 85.9 | 26.5 | 0.951 |
| 1.3 | 0.565 | 0.9 | 1.0 | V | 85.7 | 24.2 | 0.808 |
| 1.3 | 0.560 | 1.3 | 0.4 | V | 86.9 | 15.8 | 0.970 |
| 1.3 | 0.497 | 1.3 | 1.2 | V | 85.7 | 11.5 | 0.775 |
| 1.3 | 0.644 | 1.7 | 0.8 | V | 77.9 | 8.26 | 0.820 |
| 1.3 | 0.548 | 0.3 | 0.8 | S | 87.5 | 47.0 | 1.03 |
| 1.3 | 0.550 | 0.7 | 0.4 | S | 86.1 | 46.5 | 1.02 |
| 1.3 | 0.540 | 0.7 | 1.2 | S | 86.5 | 15.2 | 0.794 |

$\ell=0$ stripping polarizations employing deuteron and proton spin-orbit potentials of 4 and 8 MeV, respectively. Sample polarizations for the $\ell=0$ $Sr^{88}(d,p)Sr^{89*}$ reaction are exhibited in Fig. 2 for calculations with and without a deuteron spin-orbit potential.

## III. Results and Discussion

Initial efforts in studying the deuteron elastic scattering gave small values for X only with $R_R$ = 1.3 fm; therefore the majority of the calculations used this radius. There appears to be no sharp lower limit to $R_I$, but its upper limit is 1.9 fm for volume absorption and 1.5 fm for surface absorption. Similarly, $a_I$ is limited below at 0.4 fm but does not appear to have a sharp upper limit. The values $R_I$ = 1.3 and 1.1 fm give the lowest X for volume and surface absorption, respectively.

All the stripping curves corresponding to deuteron parameters with $X \lesssim 0.0062$ are roughly similar except the ones corresponding to $R_R = 1.1$ fm. In fact, the stripping angular distributions are strongly dependent on $R_R$ for both the proton and the deuteron. Furthermore, by extrapolation, the best fit to the $\ell=0$ data seems to be around $R_R$ (deuteron) $= 1.0$ fm and for the $\ell=2$ data around $R_R = 1.3$ fm. Since the $\ell=0$ case is more strongly affected, the smaller $R_R$ is preferable overall.

The polarizations calculated with the parameters of Tables I and III are all very similar, differing mainly in peak heights. An apparent correlation between polarization and differential cross section may be expressed as

$$\frac{dP}{d\theta} = N \frac{d^2\sigma}{d\theta^2} ,$$

where P, $\sigma$, N, and $\theta$ are, respectively, polarization, differential cross section, normalization, and angle. An estimate of what to expect when other spin-orbit potentials are used may be gained by noting that the polarization is approximately linearly dependent on the $V_{so}$. Thus the predicted polarization is not ambiguous and any serious disagreement with experiment would indicate a defect in the theory.

The spectroscopic factors listed in Table I may be used to estimate the reliability one might expect when these quantities are deduced in other cases. $S_2$ should be near unity and $S_0$ and $S_4$ perhaps less because of configuration mixing with higher states. This latter behavior is exhibited in Table II, but the fact that the $S_\ell$ appear to be generally too small indicates that their absolute magnitudes are not reliable. The average deviations may be taken as an indication of the average reliability of the spectroscopic-factor ratios; this is of the order of $\pm 10\%$, with maximum deviations of the order of $\pm 25\%$.

## Acknowledgments

I would like to thank Ray Satchler for discussions of this work and for showing me his results of a similar nature.

# A-6. EXACT EXPRESSIONS FOR COULOMB-WAVE STRIPPING AMPLITUDES*

Fernanco B. Morinigo

California Institute of Technology, Pasadena, California

## I. Introduction

In this paper we deal with one possible exact treatment of pure Coulomb distortions in stripping reactions; we present analytic expressions for first-order stripping amplitudes, calculated on the assumption that the relative motions of the nuclear fragments in both initial and final states are describable as pure Coulomb waves. The aim has been to develop formulae which are nearly as convenient as plane-wave expressions for the preliminary evaluation of experimental results, yet have the enormous advantage of taking into account the Coulomb distortions. For application among the light nuclei, our expressions should be at least as good as those of the simplest plane-wave theories in describing the angular distributions of stripping reactions.

The amplitudes also contain a factor which represents a general descrease in the magnitude of the cross sections because of the Coulomb repulsions in both incident and exit channels; this means that the reduced widths extracted from experimental data by use of our formulae will be considerably larger than those extracted by use of a plane-wave theory, in the direction of better agreement with theoretical

*Supported by the Office of Naval Research.

estimates of reduced widths. The true importance of these results may reside in the fact that Coulomb waves should be an excellent representation of the scattering states in the incident and exit channels at bombarding energies well below the Coulomb barrier, except in the vicinity of a resonance. Thus, information is in principle available about the nuclear structure of the product from experiments at low bombarding energies; also, the theory makes predictions for rates of nonresonant reactions proceeding by a stripping mechanism at low bombarding energies.

In previous papers[1-3] we have presented results appropriate in various special cases, either restricting the distortion to one channel only or restricting the orbital angular momentum of the captured orbit to L = 0. These papers discuss the details of the various assumptions and approximations which lead to our particular analytic expressions; they also contain a full description of techniques for handling the hypergeometric function. The projectile is assumed to have L = 0 and to be purely asymptotic, having a wave function $e^{-\alpha r}/r$; the final state is assumed to have a wave function $Y_L^M(\theta,\emptyset) \cdot r^{L-1} e^{-\beta r}$. The reasons for choosing this form, and its suitability, are fully discussed in Ref. 3 .

## II. Differential Cross Sections in Coulomb-Wave and Plane-Wave Theories

With the assumptions of our treatment, for experiments measuring no spin polarizations, the plane-wave approximation (PWBA)

---

[1] F. B. Morinigo, Phys. Rev. 133, B65 (1964).

[2] F. B. Morinigo, Nucl. Phys. 50, 136 (1964).

[3] F. B. Morinigo, Phys. Rev. (submitted Nov. 1963).

yields

$$(d\sigma/d\Omega)_{PWBA} = W_0 \left[Q^L/(Q^2 + \beta^2)^{L+1}\right]^2, \qquad (2.1)$$

where $W_0$ is a constant containing kinematic factors and the reduced widths, $\beta$ is the decay parameter of our final-state wave function, and Q is a vector representing the change in linear momentum of the target particle. In the Coulomb-wave approximation (CWBA) we find, after manipulations similar to those of Ref. 3, using standard techniques

$$(d\sigma/d\Omega)_{CWBA} = (d\sigma/d\Omega)_{PWBA}\, D(n,k,K') \cdot D(n',K',k) \cdot R_0, \qquad (2.2)$$

where $D(n,k,K')$ and $D(n',K',k)$ are factors independent of angles which describe an over-all reduction in magnitude due to the Coulomb repulsion, i.e.,

$$D(n,k,K') = \left[2\pi n/(e^{2\pi n}-1)\right] \exp\left\{2n \arctan\left[2\beta k/(K'^2 - k^2 + \beta^2)\right]\right\}, \qquad (2.3)$$

where $\underline{n}, \underline{n}'$ are Coulomb parameters, and $\vec{k}$, $\vec{K}'$ are wave vectors.[3]

The factor $R_0$ contains the new angular dependence. It is quite formidable to write out explicitly, although the form here is not necessarily the simplest. It is convenient to define it as a chain of symbols:

$$R_0 = [4\pi/(2L+1)]\, \left|\Gamma(L+in')/\Gamma(-in)\Gamma(1+in)\Gamma(1+in')\Gamma(L)\right|^2 \sum_M \left|A_{LM} + B_{LM}\right|^2, \qquad (2.4a)$$

$$A_{LM} = [(L+in')/L]\, [1 - \tfrac{1}{2}\{1-(-1)^{L+M}\}(k^2/\vec{k}\cdot\vec{Q})]$$

$$\times \sum_{\mu=0}^{L} \binom{L}{\mu} W^{\mu} [\Gamma(\mu-in)\Gamma(1+in)/\Gamma(\mu+1)]\, F(-in', \mu-in, \mu+1, Z), \qquad (2.4b)$$

$$W = -G/(1+G), \qquad (2.4c)$$

$$Z = (GG' - E)/(1 + G)(1 + G'), \tag{2.4d}$$

$$G = (-2i\beta k - 2\vec{k} \cdot \vec{Q}) / (Q^2 + \beta^2), \tag{2.4e}$$

$$G' = (-2i\beta K' + 2\vec{K}' \cdot \vec{Q})/(Q^2 + \beta^2), \tag{2.4f}$$

$$E = (-2kK' - 2\vec{k} \cdot \vec{K}')/(Q^2 + \beta^2), \tag{2.4g}$$

$$B_{LM} = \tfrac{1}{2}\{1-(-1)^{L+M}\}(k^2/\vec{k}\cdot\vec{Q})(1+G)^{-1}(1+G')^{-1}\sum_{\mu=0}^{L-1}\binom{L-1}{\mu} W^{\mu} \cdot X, \tag{2.4h}$$

$$X = Y_1 [\Gamma(\mu-in)\Gamma(in+2)/\Gamma(\mu+2)]\, F(-in'+1, \mu-in, \mu+2, Z)$$
$$+ Y_2 [\Gamma(\mu-in+1)\Gamma(in+2)/\Gamma(\mu+3)]\, F(-in'+1, \mu-in+1, \mu+3, Z), \tag{2.4i}$$

$$Y_1 = (1+G)[1+G'(L+in')/L], \tag{2.4j}$$

$$Y_2 = (E-GG')(L+in')/L, \tag{2.4k}$$

## III. Discussion

Our results (2.1)—(2.4) form the essential part of our theory; we have arrived at analytic expressions for first-order stripping amplitudes which include the effects of pure Coulomb distortions. For the special cases L = 0 or n = 0 or n' = 0, these expressions reduce to those derived in earlier papers.[1—4] Other authors[5,6] have made comparisons with experiment of approximate expressions containing some

---

[4] K. A. Ter-Martjrosian, Soviet Phys.—JETP 2, 620 (1956).

[5] A. Dar, A. de-Shalit, and A. B. Reiner, Phys. Rev. 131, 1732 (1963).

[6] L. C. Biedenharn, K. Boyer, and M. Goldstein, Phys. Rev. 104, 382 (1956).

of the features of our answer. To the extent that we have a suitable description of the bound states, our answer corresponds to a limit to which all stripping amplitudes must tend at very low bombarding energies not in the immediate vicinity of a resonance.

It may be that for many cases of interest the form of the bound-state wave function assumed in this paper will be a poor approximation. In this case, it may be possible to resort to linear combinations of terms of the same form as a suitable description; unfortunately, in this way new parameters are introduced which could not really be experimentally determined with any substantial certainty. A detailed comparison of the predictions of our formula with a variety of experimental data will be made in a paper now in preparation.

## Acknowledgments

The author is grateful for the many valuable comments and criticism received from Dr. Jorg Eichler, and for the prodding of Professor W. A. Fowler to come up with such results.

# A-7. EFFECT OF FINITE-RANGE n-p POTENTIAL IN COULOMB STRIPPING REACTIONS*

Arthur K. Kerman, Massachusetts Institute of Technology, Cambridge, Massachusetts

and

Faison P. Gibson, Oak Ridge Institute of Nuclear Studies, Oak Ridge, Tennessee

## Introduction

In recent years there have been a number of differential cross-section calculations[1—4] for (d,p) stripping reactions by use of DWBA methods. With rare exceptions[5,6] these methods include an assumption of zero range for the neutron-proton potential and disregard the possibility of deuteron stretching during the stripping process. The present work is an attempt to remove these deficiencies for the particular case of Coulomb stripping, i.e., for those situations in which the deuteron and proton energies are below the Coulomb barrier. This energy region permits certain convenient approximations and allows one to obtain fairly accurate estimates of experimental reduced widths

*Work is supported in part through AEC Contract AT(30-1)-2098.

[1] W. Tobocman, Phys. Rev. 115, 98 (1959).

[2] R. H. Bassel, R. M. Drisko, and G. R. Satchler, AEC Report ORNL-3240 (1962).

[3] B. Buck and P. E. Hodgson, Phil. Mag. 6, 1371 (1961).

[4] W. R. Smith, Phys. Rev. 131, 304 (1963).

[5] A. Dar, A. de Shalit, and A. S. Reiner, Phys. Rev. 131, 1732 (1963).

[6] N. Austern, R. M. Drisko, E. C. Halbert, and G. R. Satchler, Phys. Rev. (to be published).

which do not rely strongly upon any assumptions regarding wave functions and potentials in and close to the target. This comes about from the circumstance that the major contribution to the integral of the stripping matrix element comes from the region near the classical turning points while only a rather negligible contribution comes from the region within the target nucleus.

The Tobocman zero-range DWBA program has been modified to incorporate finite-range and polarization effects and a series of runs has been made for the differential cross sections on a $Bi^{209}$ target for a variety of incident energies, Q's, and $\ell$ values of the captured neutron. These cross sections have been compared with those from the unmodified program. We note that the unmodified program has been rather successfully used by Erskine et al.[7] to fit the shape of experimental angular distributions in this region.

## Approach

The DWBA stripping matrix element employed is

$$T = \langle F_p^{(-)}(\vec{r}_p)\, u(\vec{r}_n, \vec{\xi}_n)\, |V_{np}(r)|\, \psi_d^{(+)}(\vec{r}_p, \vec{r}_n)\, v(\vec{\xi})\rangle$$

$$= \langle F_p^{(-)}(\vec{r}_p)\, G_n(\vec{r}_n)\, |V_{np}(r)|\, \psi_d^{(+)}(\vec{r}_p, \vec{r}_n)\rangle$$

$$= \langle F_p^{(-)}(\vec{R} + \tfrac{1}{2}\vec{r})\, G_n(\vec{R} - \tfrac{1}{2}\vec{r})\, |V_{np}(\vec{r})|\, \psi_d^{(+)}(\vec{R}, r_n)\rangle \ ,$$

where $\vec{r}_p$ is the radius vector from target to proton, $\vec{r}_n$ is the radius vector from target to neutron, $\vec{\xi}$ is the collection of coordinates for the target nucleons, $\vec{r} = \vec{r}_p - \vec{r}_n$, $\vec{R} = \frac{1}{2}(\vec{r}_p + \vec{r}_n)$, $F_p^{(-)}$ is the scattering function

[7] J. R. Erskine, W. W. Buechner, and H. A. Enge, Phys. Rev. 128, 720 (1962).

for a proton, $\psi_d^{(+)}$ is the scattering function for a deuteron, $V_{np}$ is the neutron-proton potential, u is the internal wave function of the target, v is the internal wave function of the residual nucleus, $G_n = \int d\vec{\xi}\, u^* v$ is the "wave function of the captured neutron" (taken as a harmonic-oscillator function within the target and a Hankel function times a spherical harmonic without), and $\psi_d^{(+)}$ is an eigenfunction of the Hamiltonian $H_D = H_R + H_r + V_s$, where

$$H_R = T_R + \frac{Ze^2}{R} + V_{opt}(R),$$

$$H_r = T_r + V_{np}(r),$$

$$V_{opt}(R) = (V + iW) \Big/ \left[1 + \exp\left(\frac{R - R_0}{A}\right)\right]$$

$$= \text{Saxon-well optical potential},$$

$$V_s = V_{cp} + V_{op} = \text{polarizing potential},$$

$$V_{cp} = Ze^2\left(\frac{1}{\left|\vec{R} + \frac{1}{2}\vec{r}\right|} - \frac{1}{R}\right) = \text{Coulomb polarizing potential},$$

$$V_{op} = V_{opt}\left(\left|\vec{R} + \frac{1}{2}\vec{r}\right|\right) - V_{opt}(R) = \text{optical polarizing potential}.$$

We neglect $V_{op}$ but allow $V_{opt}(R)$, already present in the Tobocman program, to remain.

The eigenfunction $\psi_d^{(+)}(\vec{R}, \vec{r})$ is handled by the adiabatic approximation. Thus

$$\psi_d^{(+)}(\vec{R}, \vec{r}) = F_{ds}^{(+)}(\vec{R})\ \phi_d(\vec{r}, \vec{R}),$$

where

$$(H_r + V_{cp})\phi_d = [\epsilon_0 + \epsilon_2(R)]\,\phi_d,$$

$$[H_R + \epsilon_2(R)]\,F_{ds} = E_d F_{ds},$$

$E_d$ being the external energy of the incident deuteron, $\epsilon_0$ the negative of the deuteron binding energy, and $\epsilon_2(R)$ the perturbation to $\epsilon_0$ due to Coulomb polarization.

To calculate $\phi_d$ and $\epsilon_2(R)$ we use perturbation theory, assuming the excited states of the deuteron to be free-particle states. Then

$$\phi_d(\vec{r},\vec{R}) = \phi_0(r) + \phi_1(\vec{r},\vec{R}) + \phi_2(\vec{r},\vec{R}),$$

where $\phi_0$ is the Hulthen wave function and $\phi_1$ and $\phi_2$ are the first- and second-order perturbations due to $V_{cp}$ which is approximated by its dipole component cut off by a step function for $r < 2R$. The function $\phi_2(R)$ is approximated by the second-order energy perturbation due to the dipole. In the latter case, the branch of the dipole expression valid for $r < 2R$ is used for all values of r; but a cutoff is imposed for $R < R_0$, where $R_0$ is the nuclear radius. For Coulomb stripping these approximations appear reasonable since the significant region of integration of the T matrix is that for $r \ll 2R$ and $R > R_0$.

$F_{ds}(R)$ is calculated numerically by entering the subroutine of the Tobocman program which calculates $F_d(R)$, the eigenfunction of $H_R$, and inserting the additional potential $\epsilon_2(R)$.

The wave functions on the left-hand side of the matrix elements are calculated to second order by Taylor series in $\vec{r}$ about $\vec{R}$.

For $V_{np}$ we assume the Hulthen potential.

Calculating to second order, we can now express the T matrix as the sum of the following nonzero elements:[8]

$$T_1 = \langle F_p^{(-)}(\vec{R})\, G_n(\vec{R})\, |\, V_{np}(r)\, |\, F_{ds}^{(+)}(\vec{R})\phi_0(r)\rangle,$$

$$T_2 = \langle [\tfrac{1}{2}\vec{r}\cdot\vec{\nabla}_p F_p^{(-)}(\vec{R})]\; G_n(\vec{R})\, |\, V_{np}(r)\, |\, F_{ds}^{(+)}(\vec{R})\,\phi_1(\vec{r},\vec{R})\rangle,$$

$$T_3 = -\langle F_p^{(-)}(\vec{R})[\tfrac{1}{2}\vec{r}\cdot\vec{\nabla}_n]G_n(\vec{R})\,|\, V_{np}(r)\,|\, F_{ds}^{(+)}(\vec{R})\,\phi_1(\vec{r},\vec{R})\rangle\,,$$

$$T_4 = \tfrac{1}{2}\langle [\tfrac{1}{2}\vec{r}\cdot(\vec{\nabla}_p - \vec{\nabla}_n)]^2 F_p^{(-)}(\vec{R})G_n(\vec{R})\,|\, V_{np}(r)\,|\, F_{ds}^{(+)}(\vec{R})\phi_0(\vec{r},\vec{R})\rangle,$$

$$T_5 = \langle F_p^{(-)}(\vec{R})\, G_n(\vec{R})\, |\, V_{np}(r)\, |\, F_{ds}^{(+)}(\vec{R})\,\phi_{20}(\vec{r},\vec{R})\rangle,$$

where $\vec{\nabla}_p$ acts only on $F_p^{(-)}$, $\vec{\nabla}_n$ acts only on $G_n$, and $\phi_{20}$ is the $\ell=0$ component of $\phi_2$.

Except for the inclusion of $\epsilon_2$ in computing $F_{ds}$, $T_1$ would be the matrix element normally computed by Tobocman's zero-range program.

After the Tobocman program was modified to include all of these elements, the series of computer runs for a $Bi^{209}$ target was conducted. The shape of the proton angular distribution was only very slightly affected by the modifications while the change in peak magnitude ranged up to about 16%. The distributions were plotted on the picture tube of the MIT IBM-7090 and photographed; a typical plot appears in Fig. 1. A summary of peak deviations obtained is shown in Table I. The Coulomb region was somewhat arbitrarily delimited by the barrier heights determined from reasonable optical potentials. Note that

---

[8] Other apparent elements vanish because of angular-momentum or parity considerations.

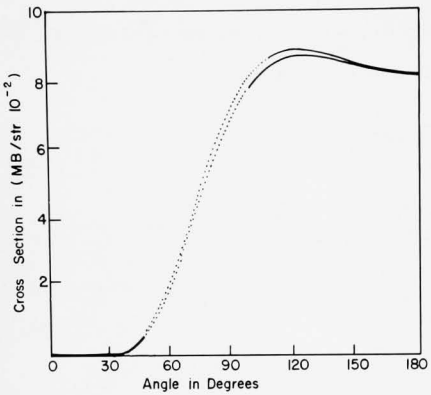


Fig. 1. Typical display on the picture tube of the MIT IBM-7090. It compares the differential cross sections from the modified program with that from the unmodified program. This is the case of $Bi^{209}$ with $\ell=0$, $E_d = 10$ MeV, and $\phi = 0.2$ MeV. The upper curve is the result of the modified program.

numerical explorations were conducted beyond the Coulomb stripping region although our approximations are no longer trustworthy there; but no unusual behavior was noted in that region.

The expression for reduced width as computed by the Tobocman program is

$$\gamma = \frac{\hbar^2}{2\mu_{IN}} R_0 \, u_\ell^2(R_0),$$

where $\gamma$ is the reduced width, $\hbar$ is Planck's constant divided by $2\pi$, $\mu_{IN}$ is the reduced mass of the target and captured neutron, $R_0$ is the nuclear radius, and $u_\ell$ is the radial portion of the neutron wave function.

Outside the target radius, the true neutron wave function and the Tobocman one differ only by a constant factor. Thus for Coulomb stripping the "true reduced width" may be estimated by

$$\gamma_e = \gamma_c \left[ \frac{d\sigma_e}{d\Omega} \Big/ \frac{d\sigma_c}{d\Omega} \right],$$

where the subscript "c" refers to numbers computed by the program and "e" to experimental results. The effect of the program modifications on $\gamma_e$ will thus be inverse to the effect on $d\sigma_e/d\Omega$ (since $\gamma_c$ is not changed).

TABLE I. Percent deviation of peak of modified differential cross section from the peak of the Tobocman cross section. The region above the dashed line in each section of the table is the Coulomb stripping region (see text).

| $\ell$ | $E_d$ (MeV) | Q (MeV) -1.8 | -0.203 | +2.0 | +4.0 | +6.0 | +8.0 | +14.0 | +20.0 |
|---|---|---|---|---|---|---|---|---|---|
| 0 | 6 | | 6.4 | 10.5 | 13.9 | 16.2 | 17.1 | | |
| | 8 | 1.1 | 6.7 | 11.4 | 14.3 | 16.9 | 19.2 | 69.8 | 101.8 |
| | 10 | -4.8 | 2.0 | 7.2 | 9.8 | 23.0 | 34.9 | | |
| | 12 | -6.2 | -1.1 | 2.6 | 10.5 | 14.5 | 22.8 | | |
| | 14 | -6.2 | -3.6 | 3.7 | 9.3 | 14.1 | 18.2 | | |
| | 16 | | -3.7 | | 9.2 | | | | |
| | 18 | | 0.5 | | | | | | |
| 2 | 6 | | 6.6 | | 13.8 | 16.0 | 17.4 | | |
| | 8 | 2.3 | 7.2 | 11.7 | 14.3 | 17.0 | 19.2 | | |
| | 10 | | 2.3 | 7.2 | 10.3 | | | | |
| | 12 | -2.0 | 0.8 | | 11.3 | | 31.0 | | |
| | 14 | | | | | | | | |
| 4 | 6 | | 7.1 | | | | | | |
| | 8 | | 8.2 | | 14.8 | | 18.6 | | |
| | 10 | | | | 9.6 | | | | |
| | 12 | | 2.7 | | 5.5[a] | | | | |

[a] The angular distribution is twin peaked. The deviation for the other peak is 14.1%.

Thus, for example, for 8-MeV deuterons, $\gamma_e \approx 0.16$ MeV for the 2.57-MeV level of $Bi^{210}$ as obtained from the zero-range program and Erskine's[7] data. The modified program reduces this about 6.7%.

## Conclusions

One concludes that in the Coulomb stripping region for a $Bi^{209}$ target the finite-range and polarization effects usually increase the differential cross section and reduce the estimate of the physical reduced width by a variable amount of not more than about 16%. This is, of course, evidence that the zero-range approximation is a rather good one in this region. These conclusions are based on employment of a Hulthen potential and wave function. Other deuteron potentials and wave functions will be tried in future work.

# SESSION B

MONDAY AFTERNOON

9 MARCH 1964

# B-1. A STUDY OF THE REACTION $U^{238}(d, p)U^{239}$

B. E. F. Macefield

Nuclear Physics Department, University of Oxford, England

and

R. Middleton*

Atomic Weapons Research Establishment, Aldermaston, England

Information on the level structure of the uranium isotopes has come almost completely from neutron capture and inelastic scattering, Coulomb excitation, and α- and β-decay data. Reaction studies such as (d, p) or (t, p) are either nonexistent or have insufficient resolution to obtain detailed level positions.[1-3] A study of the uranium isotopes is of interest since they are highly distorted nuclei and a systematic study of stripping reactions on such nuclei has not been attempted. The correlation of the experimental results with the Nilsson model[4] and the work of Satchler[5] should indicate any inadequacies in Nilsson's description of the odd-mass uranium isotopes. Little was known of the level scheme of $U^{239}$ before the

---

* Present address: Department of Physics, University of Pennsylvania, Philadelphia, Pennsylvania.

[1] G. B. Holm, J. R. Burwell, and D. W. Miller, Phys. Rev. 122, 1260 (1961).

[2] J. A. Harvey, Phys. Rev. 81, 353 (1951).

[3] G. B. Holm, J. R. Burwell, and D. W. Miller, Phys. Rev. 118, 1247 (1960).

[4] S. G. Nilsson, Kgl. Danske Videnskab. Selskab., Mat.-fys. Medd. 29, 16 (1955).

[5] G. R. Satchler, Ann. Phys. (N.Y.) 3, 275 (1958).

present work.[6] A comparison with $Pu^{241}$ indicates that the ground-state spin of $U^{239}$ should be 5/2 with positive parity since the only difference between the two nuclei is a pair of coupled protons. The $Pu^{241}$ ground state has also been identified with the [622] state of the Nilsson model.

The reaction under study was examined with the Aldermaston tandem generator and multigap spectrograph.[7] The target consisted of natural $U^{238}$. The $U^{238}$ target was of thickness 600 $\mu g/cm^2$. The total thickness of the target was known to $\pm 10\%$ but the uniformity was not determined. It is estimated to be not worse than $\pm 30\%$. A bombarding energy of 12 MeV was used for the reaction.

Figure 1 shows a typical proton spectrum obtained from the $U^{238}(d, p)$ reaction. The various proton groups have been labeled according to the levels in the final nucleus as determined in this work. Twenty-four groups have definitely been assigned to the above reaction. The energy

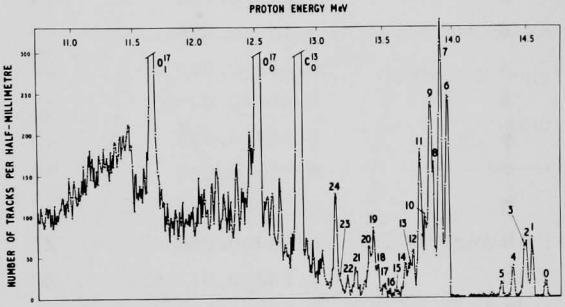


Fig. 1. Typical proton energy spectrum from the $U^{238}(d,p)U^{239}$ reaction; $E_d = 12.03$ MeV, $\theta = 72\frac{1}{2}^{\circ}$.

---

[6] Landolt-Börnstein, 1961.

[7] R. Middleton and S. Hinds, Nucl. Phys. 34, 404 (1962).

resolution width is approximately 25 keV, mostly due to target thickness. Three strong groups due to light-mass impurities are also to be seen on the spectrum. The angular distributions for the ground state and first eleven excited states are shown in Fig. 2. The error bars represent the uncertainties due to counting statistics and resolution uncertainties. The significance of the curves shown in Fig. 2 will be discussed below. The ground-state Q value for the $U^{238}(d,p)U^{239}$ reaction was determined to be $2.588 \pm 0.020$ MeV, which compares with the value $2.537 \pm 0.100$ MeV obtained from the mass tables of Everling et al.[8] Table I shows the corresponding excitations

TABLE I. Level excitations for states in $U^{239}$ obtained from the reaction $U^{238}(d,p)U^{239}$.

| Group number | Excitation (MeV) | Group number | Excitation (MeV) |
|---|---|---|---|
| 0 | 0 | | |
| 1 | $0.092 \pm 0.005$ | 13 | $0.96 \pm 0.015$ |
| 2 | $0.131 \pm 0.005$ | 14 | $0.99 \pm 0.015$ |
| 3 | $0.138 \pm 0.005$ | 15 | $1.06 \pm 0.015$ |
| 4 | $0.222 \pm 0.005$ | 16 | $1.11 \pm 0.015$ |
| 5 | $0.301 \pm 0.005$ | 17 | $1.15 \pm 0.015$ |
| 6 | $0.688 \pm 0.005$ | 18 | $1.19 \pm 0.015$ |
| 7 | $0.738 \pm 0.010$ | 19 | $1.22 \pm 0.015$ |
| 8 | $0.789 \pm 0.010$ | 20 | $1.25 \pm 0.015$ |
| 9 | $0.809 \pm 0.010$ | 21 | $1.36 \pm 0.015$ |
| 10 | $0.848 \pm 0.010$ | 22 | $0.43 \pm 0.015$ |
| 11 | $0.883 \pm 0.010$ | 23 | $1.49 \pm 0.015$ |
| 12 | $0.933 \pm 0.010$ | 24 | $1.52 \pm 0.015$ |

[8] F. Everling, L. A. König, J. H. E. Mattauch, and A. H. Wapstra, Nucl. Phys. 18, 529 (1960).

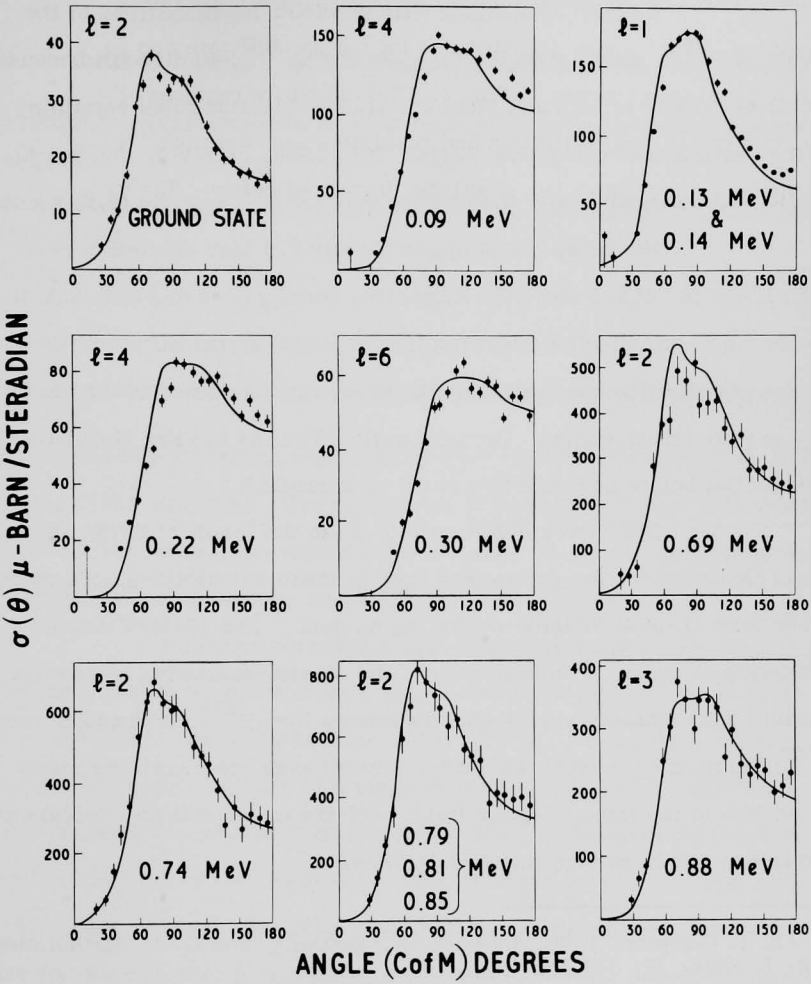


Fig. 2. Angular distributions of the first twelve observed proton groups from the $U^{238}(d,p)U^{239}$ reaction; $E_d$ = 12.03 MeV. The curves are the result of DWBA calculations (see text).

for the 24 groups labeled in Fig. 1.

A direct comparison with previous determinations of the levels in $U^{239}$, mainly from the (n, γ) reactions,[9,10] is difficult because the level density is high and there are strong selection rules pertaining to the excitation of collective states. It is clear, however, that the (n, γ) results are compatible with the present interpretations of the (d, p) spectra.

No states above approximately 1.5 MeV excitation have been listed in Table I since the increasing density of states and lack of resolution makes positive identification of single states difficult. Attempts to determine band structure or the energy separation of the various groups were unsuccessful. The information from the angular distributions was needed before any structure could be identified.

The curves shown in Fig. 2 are the result of DWBA stripping calculations. The parameters used in these calculations were determined from 11-MeV deuteron scattering on gold[11] and 17-MeV proton scattering on gold.[12] In principle,[13] the elastic-scattering parameters should be determined by scattering deuterons from $U^{238}$ and protons from $U^{239}$; but at the energies used in the present work the overriding effect is one due to the large Coulomb field, with the result that the optical-model parameters would be very poorly determined.

---

[9] P. J. Campion, J. W. Knowles, G. Manning, and G. A. Bartholomew, Can. J. Phys. 37, 377 (1959).

[10] N. F. Fiebiger (private communication).

[11] M. A. Melkanoff, T. Sawada, and N. Cindro, Phys. Letters 2, 98 (1962).

[12] M. A. Melkanoff, J. S. Nodvik, D. S. Saxon, and R. D. Woods, Phys. Rev. 106, 793 (1957).

[13] B. E. F. Macefield, R. Middleton, and D. J. Pullen, Nucl. Phys. 44, 309 (1963).

The parameters used in the initial trial are shown in Table II.

TABLE II. Optical-model parameters used in DWBA calculations.

| Parameter | -U (MeV) | -W (MeV) | r (fm) | a (fm) |
|---|---|---|---|---|
| Particle | | | | |
| Deuteron | 60 | 15 | 1.5 | 0.6 |
| Proton | 48 | 8 | 1.33 | 0.5 |
| Proton (II) | 57 | 8 | 1.3 | 0.5 |

A Saxon-Wood distribution was used for both the real and imaginary components of the potential. The second set of proton parameters (labeled II) were modified values that were found necessary to get an improved fit to the ground-state transition, assumed to be an $\ell = 2$ capture.

Using the parameters that fitted the ground state transition, calculations were made for other $\ell$ values and attempts were made to fit the remaining angular distributions. This procedure has been previously used by the present authors in a study of the $Se^{76}(d, p)Se^{77}$ reaction.[13] It was immediately obvious that the shape of the calculated curves was fairly insensitive to the value of $\ell$. This is shown in Fig. 3. The curves in Fig. 3 are shown on the correct relative scale for a reduced width of unity for each curve. It is evident that transitions with angular momentum exchanges as high as $\ell = 8$ should be observable in stripping reactions on heavy nuclei if these states have an appreciable reduced width.

In Fig. 4 we show a plot of the ratio of the peak calculated cross section to that calculated for 180° as a function of $\ell$. This ratio is

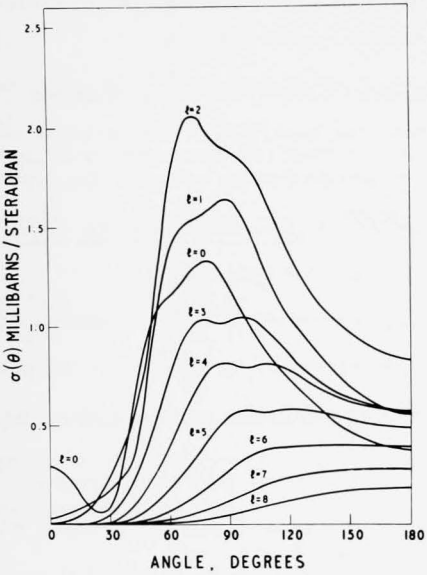


Fig. 3. DWBA angular distributions for the reaction $U^{238}(d,p)U^{239}$; $E_d$ = 12.0 MeV, Q = 2.59 MeV. A reduced width of unity was assumed for each transition.

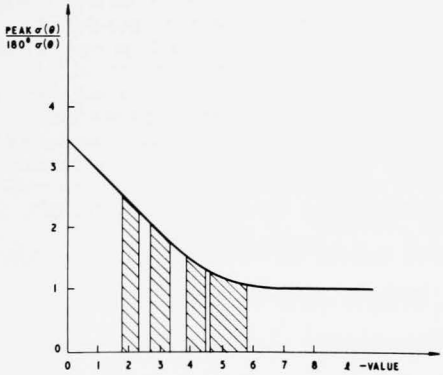


Fig. 4. A comparison of the theoretical (smooth curve) and experimental values (hatched areas) for the ratio of peak cross section to 180° cross section as a function of $\ell$.

B-1 59
B-1 59
B-1 59
B-1 59
B-1 59
B-1 59
B-1 59
B-1 59
B-1 59

including the spectroscopic and DWBA factors, for transitions to the ground-state rotational band of $U^{239}$. They are shown for two different values of the distortion parameters which bracket the uranium nuclei. It is obvious that only the ground state and 92-keV state can be expected to show any reasonable transition strength. The experimental peak cross sections are also indicated. Only transitions involving angular momentum exchanges up to $\ell = 6$ are shown since the momentum exchange must be less than or equal to the principal quantum number of the orbit. This requirement holds provided that the expansion of the collective state in terms of single-particle states from one shell is valid.

The states at 222 keV and 301 keV excitation can be identified with the 9/2 and 11/2 members of the [624] Nilsson band. Table IV shows the excitation strengths expected from the Nilsson model for the

TABLE IV. Comparison of experimental and theoretical cross sections for the reaction on $U^{238}(d, p)U^{239}$.

| Excitation (keV) | L | J | $\sigma(\theta)^a$ (μb) | $\sigma(\theta)^b$ (μb) | $\sigma(\theta)^c$ (μb) |
|---|---|---|---|---|---|
| (160) | 4 | 7/2 | 5 | 8 | . . . |
| 222 | 4 | 9/2 | 17 | 12 | 65 |
| 301 | 6 | 11/2 | 39 | 41 | 40 |
| (395) | 6 | 13/2 | 1.2 | 2.4 | . . . |

[a] Predicted peak differential cross section, $\eta=4$. See Ref. 4.

[b] Predicted peak differential cross section, $\eta=6$. See Ref. 4.

[c] Experimental value from present work.

[624] band. In Tables III and IV the excitation energies in brackets are those deduced from an [I(I+1) = K(K+1)] dependence by use of the states definitely identified in the band. A comparison of Tables III and IV shows that the unresolved group at 135 keV (Fig. 1) contains components of the [622] and [624] bands. The combined angular distribution of the groups at 135 keV can be fitted with an $\ell=1$ distribution, but little significance can be attached to this until the angular distributions of the separate states have been obtained. A summary of the spins and band structure determined in the present work is found in Table V.

TABLE V. Characteristics of states in $U^{239}$ determined from present work.

| Excitation (keV) | $J^{\pi}$ | K | [N $\ell$ $\Lambda$] |
|---|---|---|---|
| 0 | $5/2^+$ | 5/2 | 622 |
| 92 | $9/2^+$ | 5/2 | 622 |
| 222 | $9/2^+$ | 7/2 | 642 |
| 301 | $11/2^+$ | 7/2 | 642 |

The pronounced gap observed in the spectra between 300 keV and 650 keV excitation in $U^{239}$ is probably due to two causes. The first is the angular-momentum cutoff in each band and the second is the semi-magic number at 152 neutrons indicated by the Nilsson model.

No attempt to analyze the states above 650 keV excitation into rotational bands was made since the resolution is inadequate.

It can be seen that the combination of the Nilsson model and a DWBA calculation predicts angular distributions and absolute intensities which are in fair agreement with experiment; probably to within a factor of 3. We can infer from this that the Nilsson configurations are a realistic estimate of the single-particle character of the collective state of the nuclei under consideration. This is particularly pleasing since for these heavy-mass nuclei the predictions of the model are not a sensitive function of the model parameters.

The data on the [622] and [624] bands of $U^{239}$ indicate that the selection rules imposed by the Nilsson wave functions hold and in consequence there is no evidence for any shell mixing.

# B-2. DISTORTED-WAVE ANALYSIS OF THE $Cr^{52}(d, p)Cr^{53}$ REACTION USING MEASURED OPTICAL-MODEL PARAMETERS*

J. C. Legg, H. D. Scott, and M. K. Mehta

Rice University, Houston, Texas

In recent years, the use of fast large-memory computers has made it possible to develop a distorted-wave (DW) theory of deuteron stripping and use it in the analysis of the results of stripping experiments. There has been, in general, some difficulty in determining the optical-model potentials which distort the incoming deuteron wave and the outgoing proton wave. The fact that deuteron elastic scattering may be fitted by a large number of different optical-model potentials which give different results when used in DW calculations has further complicated the analysis of stripping experiments.

We have performed a series of experiments studying the $Cr^{52}(d, p)Cr^{53}$ reaction to test the success of the DW theory in predicting the results of a stripping experiment when one uses optical-model potentials which fit the elastic-scattering angular distributions. This paper presents a few of the results of these experiments.

Angular distributions for the elastic scattering of deuterons from $Cr^{52}$ and for the proton groups resulting from the $Cr^{52}(d, p)Cr^{53}$ reaction were obtained at several deuteron bombarding energies. Also, corresponding

* Work supported in part by the U.S. Atomic Energy Commission.

angular distributions for the elastic scattering of protons from $Cr^{53}$ were obtained at $E_p(c.m.) = E_d(c.m.) + 5.714$ MeV, in which the 5.714 MeV is the ground-state Q value for the $Cr^{52}(d,p)Cr^{53}$ reaction.

The targets used were chromium enriched to 99.9% isotopic abundance of the desired isotope evaporated onto thin carbon backings. Particles were detected by solid-state detectors capable of stopping the most energetic proton observed. Cross sections were determined by comparison with Rutherford scattering at 3, 3.5, and 4 MeV. The probable error due to counting statistics was less than 2% at all angles for the elastically scattered particles and less than 4% at all angles for the ground-state protons from the (d, p) reaction.

Optical-model fits were obtained for the elastic scatterings by use of the ABACUS-2 code. Saxon-Woods potentials of the form $V(r) = V_c(r) - (V + iW)\{1 + \exp[(r - r_0 A^{1/3})/a]\}^{-1}$ were used to fit both proton and deuteron scattering. Here $V_c(r)$ is the Coulomb potential due to a uniform charged sphere of radius $1.25\ A^{1/3}$ fm, A is the atomic weight of the target nucleus, $r_0$ was set equal to 1.25 fm, and V, W, and a were varied to produce the best fit to the experimental data. The values of V, W, and a which produced the best fits are listed in Table I.

The deuteron elastic-scattering angular distributions and their optical-model fits are shown in Fig. 1. Since the angular distributions exhibit very little structure, the optical-model potentials obtained are not as uniquely determined by the criterion of best fit as one would like. Two sets of potentials were studied: Type A with a real well depth of approximately 50 MeV, and Type B with a real well depth of approximately 90 MeV.

TABLE I. Optical-model potentials.

| Deuteron energy | Type A | | | Type B | | | Proton energy | | | |
|---|---|---|---|---|---|---|---|---|---|---|
| | V(MeV) | W(MeV) | a(fm) | V(MeV) | W(MeV) | a(fm) | | V(MeV) | W(MeV) | a(fm) |
| 4.39 | 53.99 | 8.02 | 0.548 | 89.91 | 15.05 | 0.518 | 10.13 | 54.23 | 9.16 | 0.541 |
| 4.93 | 53.69 | 8.10 | 0.520 | 90.10 | 15.06 | 0.518 | 10.66 | 54.32 | 9.16 | 0.484 |
| 5.41 | 56.99 | 8.17 | 0.523 | 90.27 | 15.01 | 0.546 | 11.13 | 50.83 | 8.87 | 0.553 |
| 5.72 | 51.23 | 8.39 | 0.447 | 87.75 | 15.66 | 0.430 | 11.40 | 50.71 | 9.01 | 0.547 |

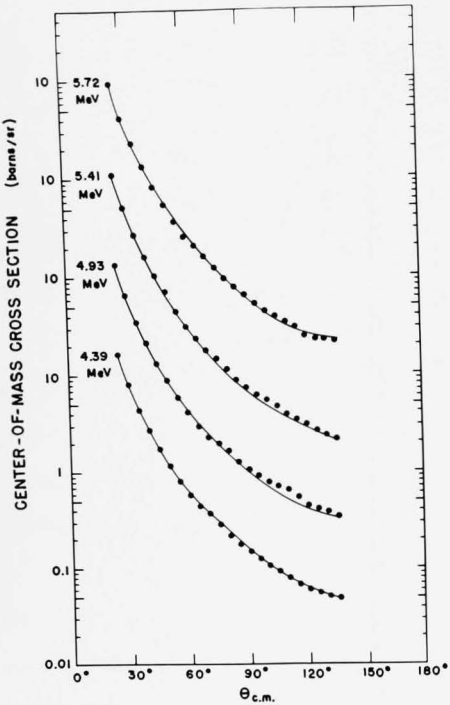


Fig. 1. Angular distributions for the elastic scattering of deuterons from $Cr^{52}$. The solid curves are optical-model fits to the data. The parameters of the optical potentials used are listed in Table I.

The optical-model fits using these potentials are indistinguishable on a graph such as Fig. 1.

The corresponding elastic proton angular distributions and their optical-model fits are shown in Fig. 2. These angular distributions do have enough structure to uniquely determine the optical potentials. These fits are only slightly better than those obtained by use of the potential formula of Perey.[1] However, since the DW code used in this work accepted only an optical potential of the form shown above, these potentials

[1] F. Perey, Phys. Rev. 131, 745 (1963).

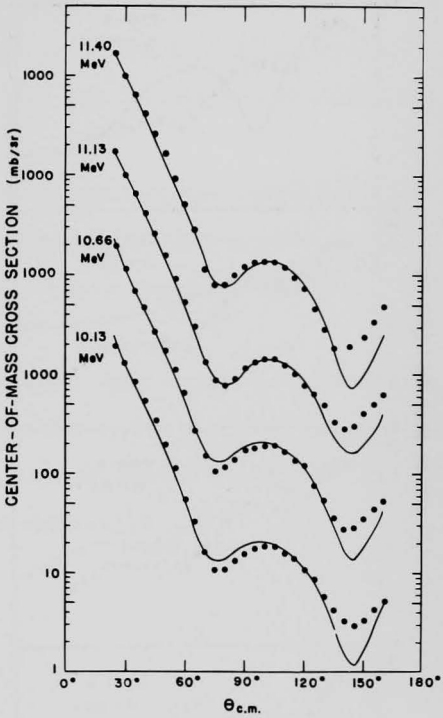


Fig. 2. Angular distribution for the elastic scattering of protons from $Cr^{53}$. The solid curves are optical-model fits to the data. The parameters of the optical potentials used are listed in Table I.

were obtained and used in the DW calculations.

The DW calculations for the (d, p) reaction were then performed with the potentials obtained from fitting the associated elastic scatterings. These calculations were performed with the DW code of Tobocman and Gibbs. As shown in Fig. 3, calculations using Type A and Type B deuteron potentials and integrating from the origin yielded curves which differed appreciably from each other and the experimental results. Using a radial cutoff of 7.6 fm in the integration improved the agreement between the DW curves and the experimental results considerably. The

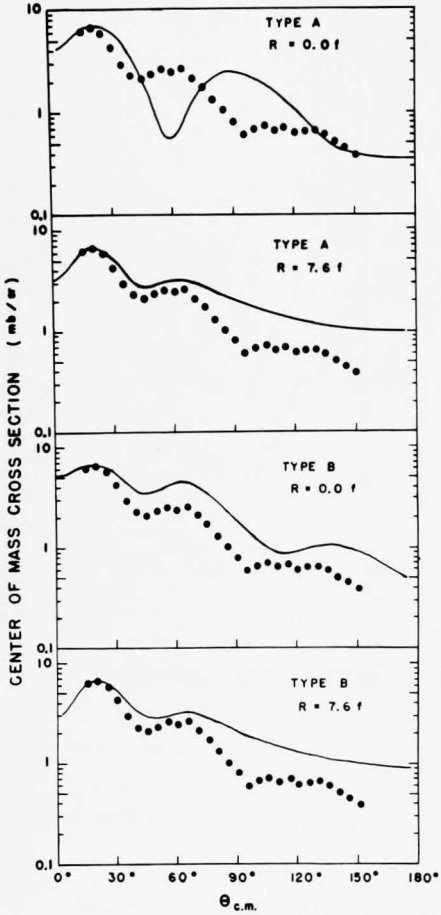


Fig. 3. DW fits to the angular distribution of ground-state protons from $Cr^{52}(d,p)Cr^{53}$ at $E_d = 5.72$ MeV, obtained by use of measured optical-model parameters. Fits are shown for Type A and Type B optical-model parameters and for no radial cutoff on integration and 7.6 fm radial cutoff. All curves are arbitrarily normalized to the maximum experimental cross section.

7.6-fm cutoff was chosen because this was approximately the radius at which Perey and Perey found that the tails of different deuteron optical-model absorption potentials coincided for copper.[2] The radial cutoff calculations placed the first minimum in the angular distribution correctly at

[2] C. M. Perey and F. G. Perey, Phys. Rev. 132, 755 (1963).

all energies. However, the over-all agreement between calculated and experimental angular distributions improved as the deuteron bombarding energy was increased to 5.72 MeV. Thus Fig. 3 is the best fit obtained at the energies we are discussing.

The DW calculations with Type A or Type B potentials and with or without a radial cutoff on the integration reproduce quite nicely the variation of the experimental (d, p) maximum cross sections as a function of deuteron bombarding energy.

These results indicate that a radial cutoff in the integration is a necessary part of a DW calculation if one uses the proper optical-model potentials. If one uses a radial cutoff, the DW calculation is then in acceptable agreement with experimental results.

# B-3. A STUDY OF STRIPPING AND PICKUP REACTIONS ON $C^{12}$, $C^{13}$, AND $C^{14}$

R. N. Glover, A. W. R. E., Aldermaston

and

A. D. W. Jones, Nuclear Physics Laboratory, University of Oxford

The data reported here on stripping and pickup reactions linking the carbon isotopes is part of a more general program being carried out on the Aldermaston tandem Van de Graaff. Briefly, the equipment consists of a solid-state counter telescope in a 16-in. scattering chamber with pulse addition to preserve resolution and pulse multiplication to provide particle identification and to route an RIDL kicksorter. Up to four reactions can be studied simultaneously with a consequent saving in time and improvement in accuracy of relative cross-section measurements.

The following reactions were studied:

(1) $C^{12}$(d,p) at 8 and 12 MeV,

(2) $C^{13}$(d,p) and (d,t) at 8 and 12 MeV,

(3) $C^{13}$(p,d) at 8 and 12 MeV,

(4) $C^{14}$(d,p) and (d,t) at 12 MeV,

(5) $C^{14}$(p,d) at 12 MeV,

(6) $C^{12}$(t,d) at 12 MeV.

Reduced widths were extracted using plane-wave theory in the manner described by Macfarlane and French.[1] Table I contains the

[1] M. H. Macfarlane and J. B. French, Rev. Mod. Phys. 32, 567 (1960).

results. Some comment is needed on our results for certain reactions in relation to earlier data.

## 1. $C^{12}(d,p)C^{13}$

All our results are based on our measured value of 13 mb for the $C^{12}(d,p)C^{13}$ ground-state transition at 12 MeV. This value and our value at 8 MeV agree with the absolute cross-section curve given by the results of Zaika *et al.*[2] and Morita *et al.*[3] Hamburger's[4] results lie parallel to this curve but 50% higher. Consequently for strict comparison with our data all the Pittsburgh cross sections and reduced widths based on a $C^{12}(d,p_0)$ cross section of 15.5 mb at 14.8 MeV values should be reduced by one third. Then our results at 8 and 12 MeV, those of Green and Middleton[5] (reduced as above) at 9 MeV, and the 14.8-MeV data of McGruer *et al.*[6] are in reasonable agreement.

## 2. $C^{13}(d,p)C^{14}$

The data of McGruer *et al.*[6] at 14.8 MeV are in fair agreement with our 12-MeV data. Their reduced widths appear to be larger than ours by a constant ratio. At 8 MeV our $C^{13}(d,p_0)$ cross

---

[2] N. I. Zaika *et al.*, Soviet Phys. JETP 12, 1 (1960).

[3] S. Morita *et al.*, J. Phys. Soc. Japan 15, 550 (1960).

[4] E. W. Hamburger, University of Pittsburgh, Ph.D. Thesis, NP-7531 (1959).

[5] T. S. Green and R. Middleton, Proc. Phys. Soc. (London) 69A, 28 (1956).

[6] J. N. McGruer, E. K. Warburton, and R. S. Bender, Phys. Rev. 100, 235 (1956).

TABLE I. Results of (d,p), (p,d), (d,t), and (t,d) reactions on carbon isotopes.

| Reaction | $E_x$ | $E_{beam}$ (MeV) | Q (MeV) | $J_0^{\pi}$ | $J_f^{\pi}$ | $\ell$ | $r_0$ | Relative $\theta^2$ or $\lambda\theta^2$ | Absolute $\theta^2$ or $\lambda\theta^2$ | $\lambda$ | $\theta^2$ or $\lambda\theta^2$ from previous data[a] | $\sigma_{exp}$[b] (mb/sr) |
|---|---|---|---|---|---|---|---|---|---|---|---|---|
| $C^{12}(d,p)C^{13}$ | 0 | 8 | +2.72 | $0^+$ | 1/2- | 1 | 4.5 | 1 | 0.036 | | 0.042 | 19.5 |
| | 3.09 | | | | 1/2+ | 0 | 5.0 | 3.3 | 0.12 | | 0.19 | 112 * |
| | 3.68 | | | | 3/2- | 1 | | | | | 0.013 | |
| | 3.85 | | | | 5/2+ | 2 | 5.5 | 1.2 | 0.043 | | 0.073 | 64 |
| $C^{12}(d,p)C^{13}$ | 0 | 12 | +2.72 | $0^+$ | 1/2- | 1 | 4.5 | 1 | 0.026 | | 0.031 | 13 |
| | 3.09 | | | | 1/2+ | 0 | 4.5 | 5.4 | 0.14 | | 0.15 | 58 * |
| | 3.68 | | | | 3/2- | 1 | 4.5 | 0.3 | 0.007 | | 0.006 | 12 * |
| | 3.85 | | | | 5/2+ | 2 | 5.0 | 1.8 | 0.047 | | 0.071 | 55 |
| $C^{13}(d,p)C^{14}$ | 0 | 8 | +5.94 | 1/2- | $0^+$ | 1 | 5.5 | 1 | 0.013 | | | 1.4 |
| | 6.09 | | | | $1^-$ | 0 | 5.0 | 4.4 | 0.057 | | | 46 * |
| | 6.72 | | | | $3^-$ | 2 | 5.5 | 1.7 | 0.022 | | | 15 |
| | 7.35 | | | | $2^-$ | 2 | 5.5 | 2.1 | 0.027 | | | 14 |
| $C^{13}(d,p)C^{14}$ | 0 | 12 | +5.94 | 1/2- | $0^+$ | 1 | 5.0 | 1 | 0.028 | | 0.063 | 2.7 |
| | 6.09 | | | | $1^-$ | 0 | 4.5 | 2.9 | 0.082 | | 0.20 | 29 * |
| | 6.72 | | | | $3^-$ | 2 | 5.5 | 1.0 | 0.027 | | 0.07 | 19 |
| | 7.35 | | | | $2^-$ | 2 | 5.5 | 1.1 | 0.032 | | 0.06 | 17 |
| $C^{14}(d,p)C^{15}$ | 0 | 12 | -1.01 | $0^+$ | 1/2+ | 0 | 4.5 | 1 | 0.11 | | 0.093 | 25 * |
| | 0.66 | | | | 5/2+ | 2 | 5.5 | 0.4 | 0.043 | | 0.032 | 61 * |

| | | | | | | | | | | | | |
|---|---|---|---|---|---|---|---|---|---|---|---|---|
| $C^{13}(p,d)C^{12}$ | 0 | 8 | -2.72 | 1/2- | $0^+$ | 1 | 5.5 | | 0.012 | | | 8.9 |
| $C^{13}(p,d)C^{12}$ | 0 | 12 | -2.72 | 1/2- | $0^+$ | 1 | 4.5 | 1 | 0.025 | | | 14.7 |
| | 4.43 | | | | $2^+$ | 1 | 4.5 | 0.9 | 0.022 | | | 4.4 |
| $C^{14}(p,d)C^{13}$ | 0 | 12 | -5.94 | $0^+$ | 1/2- | 1 | 5.5 | | 0.026 | | | 9.3 |
| $C^{13}(d,t)C^{12}$ | 0 | 8 | +1.31 | $1/2^-$ | $0^+$ | 1 | 5.5 | 1 | 3.68 | 307[c] | | 17.7 |
| | 4.43 | | | | $2^+$ | 1 | 7.5 | 0.8 | 2.88 | 102[c] | | 7.3 |
| $C^{13}(d,t)C^{12}$ | 0 | 12 | +1.31 | 1/2- | $0^+$ | 1 | 5.5 | 1 | 4.05 | 162 | 5.89 | 12.6* |
| | 4.43 | | | | $2^+$ | 1 | 5.5 | 0.8 | 3.25 | 148 | 4.47 | 5.6 |
| $C^{14}(d,t)C^{13}$ | 0 | 12 | -1.91 | $0^+$ | 1/2- | 1 | 5.5 | 1 | 9.90 | 396 | 6.20 | 29 |
| | 3.09 | | | | 1/2+ | 0 | 5.5 | 0.03 | 0.30 | | 0.17 | 1.7* |
| | 3.68 | | | | 3/2- | 1 | 5.5 | 0.4 | 3.94 | | 4.2 | 5.7 |
| | 3.85 | | | | 5/2+ | 2 | | | d | | 0.11 | 0.9 |
| $C^{12}(t,d)C^{13}$ | 0 | 12 | -1.31 | $0^+$ | 1/2- | 1 | 4.0 | 1 | 5.23 | 201 | | 36 * |
| | 3.09 | | | | 1/2+ | 0 | 4.0 | 13.9 | 72.6 | (520) | | 12.3* |
| | 3.68 | | | | 3/2- | 1 | 5.5 | 1.1 | 5.63 | (800) | | 8.3* |
| | 3.85 | | | | 5/2+ | 2 | 5.0 | 0.9 | 4.46 | 95 | | 39 |

[a] See Macfarlane and French (Ref. 1). All 14.8-MeV data are from the Pittsburgh group, except $C^{12}(d,p)$ at 8 MeV.

[b] Experimental cross section at peak, or at $10^{\circ}$ (lab) if still increasing. The latter points are denoted by *.

[c] Alternative values depend on whether the $C^{13}(p,d_0)$ or the $C^{12}(d,p)$ reduced width at 8 MeV was used.

[d] Angular distribution shows no stripping peak.

section of 1.4 mb is in reasonable agreement with the value of 2 mb at 6 MeV from the excitation function of Lisle *et al.*[7]

### 3. $C^{13}(d,t)C^{12}$

The reduced widths $\lambda\theta^2$ agree well with the work of Mayo and Hamburger[8] when related to the same $C^{12}(d,p)$ ground-state cross section.

### 4. $C^{14}(d,p)C^{15}$

The reduced widths agree with those reported by Moore[9] *without* reduction to normalize cross sections.

### 5. $C^{15}(d,t)C^{13}$

The values of $\lambda\theta^2$ given by Macfarlane and French[1] are based on the cross sections of Moore *et al.*[10] adjusted to the value of 15.5 mb for the $C^{12}(d,p_0)$ cross section at 14.8 MeV. In his thesis, Moore[9] further reduces these cross sections—apparently

---

[7] J. C. Lisle *et al.*, Nucl. Phys. 47, 56 (1963).

[8] S. Mayo and A. I. Hamburger, Phys. Rev. 117, 832 (1960).

[9] W. E. Moore, University of Pittsburgh, Ph.D. Thesis, NP-7570 (1959).

[10] W. E. Moore, J. N. McGruer, and A. I. Hamburger, Phys. Rev. Letters 1, 29 (1958).

due to an amended figure for the $C^{14}$ enrichment. The $\lambda\theta^2$ values in Table I are smaller than our values if taken from Moore's thesis or similar if the amended enrichment figure is not used, but not larger by the expected amount. There is therefore some discrepancy between our $C^{14}$ data and those of the Pittsburgh group.

It is of interest (Table I) that the reduced widths derived from (d,p) and (p,d) reactions at the same bombarding energy of 12 MeV are in agreement. The exception is the 8-MeV results linking the $C^{12}$ and $C^{13}$ ground states. It has been suggested by other authors that compound-nucleus effects may be important in the $C^{12}$(d,p) reaction.

Figure 1 presents plots of reduced widths versus bombarding energy for (d,p) and (t,d) reactions linking the $C^{12}$ - $C^{13}$ and $C^{13}$ - $C^{14}$ ground states. Pickup-reaction data have been plotted at the equivalent energy for the inverse reaction.

<u>$C^{12}$(d,p)$C^{13}$ g.s.</u> The two curves agree very well when normalized to the same $C^{12}(d,p_0)$ absolute cross section and confirm the increased reduced width around 8 MeV.

<u>$C^{13}$(d,p)$C^{14}$ g.s.</u> The value at 4 MeV is derived from the angular distributions of Deshpande,[11] the upper and lower limits being obtained by use of the cross sections of Deshpande and of Lisle <u>et al.</u>,[7] respectively. The reduced widths seem to cluster in the range 0.02—0.03. The value of McGruer <u>et al.</u>[6] seems significantly higher (0.042) even if renormalized.

From these two graphs, $\theta^2$ would appear to be equal for the

---

[11] V. K. Deshpande, Nucl. Phys. <u>47</u>, 257 (1963).

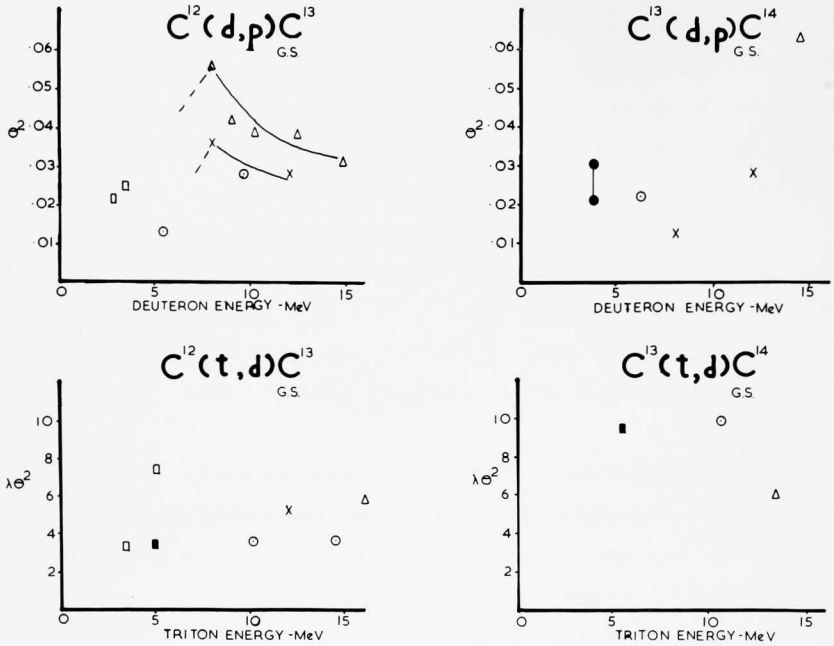


Fig. 1. $\theta^2$ and $\lambda\theta^2$ vs bombarding energy for (d,p) and (t,d) reactions linking the $C^{12}$-$C^{13}$ and $C^{13}$-$C^{14}$ ground states. Pickup reaction data have been plotted at the equivalent energy for the inverse reaction. The symbols denote:

- × Present experiments (stripping).
- ⊙ Present experiments (pickup).
- △ Pittsburgh group, except $C^{12}$(d,p) at 8 and 9 MeV (see Ref. 1).
- □ Other data (see Ref. 1).
- ▮ Barros et al. (Ref. 12).
- ● Deshpande (Ref. 11) and Lisle et al. (Ref. 7).

two reactions. Since we may presume $\theta_0^{\,2}(1p)$ is constant, this suggests that the spectroscopic factor S is the same for both reactions. However, in jj coupling we expect S = 1 and 2 for $C^{12}(d,p_0)$ and $C^{13}(d,p_0)$, respectively. Theoretical calculation of the variation of spectroscopic factor with the spin-orbit parameter for these two reactions would be of interest,

especially since there is now some evidence for $a/K \approx 3$.

$\underline{C^{12}(t,d)C^{13}}$. The values of $\lambda\theta^2$ seem independent of energy, although there are no data near 8 MeV, and suggest $\lambda \approx 4/0.025 \approx 160$.

$\underline{C^{13}(t,d)C^{14}}$. Our $\lambda\theta^2$ and that of Barros *et al.*[12] agree. As discussed earlier, there is some doubt about the Pittsburgh value. From these two graphs, $\lambda\theta^2$ would appear to be in the ratio 2.5: 1 which is either consistent with $S \approx 2$ for the $C^{13}$ - $C^{14}$ ground-state transition and inconsistent with the (d,p) data, or else implies that $\lambda$ varies by a factor of 2.5 for the two reactions, or else that $\theta_0^2$ does not have the same value for (d,p) and (d,t) reactions (or their inverse reactions). None of these explanations is particularly attractive.

Study of the $C^{12}(d,p)$ and $C^{12}(t,d)$ reactions should enable values of $\lambda$ to be extracted for transitions to excited states. There are few measurements of this nature, partly due to the adverse Q values of the inverse reactions. Values of $\lambda\theta^2$ for the (t,d) and (d,t) transitions linking the $C^{12}$ - $C^{13}$ ground states are in reasonable agreement. Values from the $C^{12}(t,d)$ reaction for $C^{13}$ states at 3.68 and 3.85 MeV agree with the ground-state $\lambda\theta^2$ value. The theoretical angular distributions for the $\ell = 0$ transition to the 3.09-MeV $C^{13}$ level (Q = -4.4 MeV) is a very poor fit, behaving similarly to certain (d,n) transitions wherein the binding energy of the captured proton is close to zero (see Macfarlane and French[1]). This suggests that Coulomb effects may be important in (t,d) reactions. The $\ell = 1$ fit for the transition to the 3.68-MeV

---

[12] F. de S. Barros, P. D. Forsyth, A. A. Jaffe, and I. J. Taylor, Proc. Phys. Soc. (London) 77A, 853 (1961).

state Q = -5.0 MeV has a secondary maximum several times greater than the experimental points. Values of $\lambda\theta^2$ for these two transitions are therefore unreliable, particularly so in the $\ell = 0$ case. Comparing values of $\lambda\theta^2$ and $\theta^2$ for transitions to the ground state and to the 3.86-MeV state at 12 MeV incident energy, we obtain values of $\lambda$ differing by a factor 2. For the various (d,t) and (t,d) reactions listed in Table I, $\lambda\theta^2$ seems more constant than $\lambda$ itself. Clearly more data are required.

# B-4. LOW-LYING LEVELS IN $Ti^{48}$ OBSERVED IN THE (d,p) REACTION*

P. D. Barnes and C. K. Bockelman,
Yale University, New Haven, Connecticut,

O. Hansen, University Institute for Theoretical Physics,
Copenhagen, Denmark,

and

A. Sperduto, Massachusetts Institute of
Technology, Cambridge, Massachusetts

## I. Introduction

An investigation of the level structure of the isotopes $Ti^{47-51}$ is presently in progress. The following is a preliminary report on the analysis of the reaction $Ti^{47}(d,p)Ti^{48}$ and is restricted to the low-lying levels.

## II. Experimental Method

Deuterons accelerated to 6 MeV in the M.I.T.-O.N.R. Van de Graaff accelerator were focussed into an area 0.5 mm × 1 mm on a stationary target mounted in the M.I.T. 24-gap broad-range spectrograph.[1] The target, prepared in the magnetic isotope separator at the Institute for Theoretical Physics in Copenhagen, consisted of a deposit of separated $Ti^{47}$ (99%) on a carbon backing 50 $\mu$ gm/cm$^2$ thick. Its chief contaminants were $C^{12}$, $C^{13}$, $N^{14}$, $O^{16}$, and trace amounts of $Si^{28}$ and $S^{32}$.

---

* Work supported in part by the U. S. Atomic Energy Commission.

[1] H. A. Enge and W. W. Buechner, Rev. Sci. Instr. 34, 155 (1963).

The reaction products were momentum analyzed in the spectrograph and detected in Kodak NTA 50-micron nuclear emulsions. Track distributions were obtained by scanning with a microscope across the developed plates in $\frac{1}{2}$-mm strips. Proton tracks were selected according to their lengths, direction, and grain density. The observed peaks in the track distributions had full widths at half maximum corresponding to 15 keV. This resulted from a 10-keV spread in the deuteron beam energy, a 4-keV contribution to the proton energy spread due to target thickness, and an instrumental line-width contribution of 10 keV because the target was not a line source.

Thus energy spectra were obtained at 23 angles ($7.5^{\circ}$–$172.5^{\circ}$). The residual mass associated with the various particle groups was assigned by observing the shift in group energy with angle. The angular distribution of each titanium level was obtained by determining the area under the appropriate peak at each angle and making corrections for contributions from background, contaminants, and variations in solid angle along the plate. The magnitude of the corrections for contaminant peaks was obtained by normalizing to the angular-distribution data in the literature for reactions at similar beam energies.

This particular experiment was made under conditions such that iron in the spectrograph could not be properly cycled to remove hysteresis and as a result a systematic variation in Q values of the order of 50 keV was observed as a function of angle.[2] These fluctuations in the data were removed by assigning to each of the twenty-four spectrograph gaps an effective magnetic field which, in conjunction with the original $Po^{210}$ alpha-particle calibration and the beam energy, would

---

[2] These problems have been discussed by A. Sperduto and W. W. Buechner in a paper entitled "Q Value Measurements at M.I.T.," presented at the Second International Conference on Nuclidic Masses, Vienna, Austria, 1963.

give Q values equal to those reported in the literature for several easily recognized contaminant reactions. Although this process may not give accurate absolute Q values, it is capable of giving excitation energies with good precision.

## III. Results and Analysis

The proton angular-distribution data obtained in this series of titanium experiments are being analyzed in terms of distorted-wave Born-approximation calculations made by Dr. G. R. Satchler at the Oak Ridge National Laboratory. Deuteron elastic-scattering cross-section data on Ti isotopes obtained by the authors at 6 MeV and by other experimenters at different energies[3] have been fitted by an optical potential of the Wood-Saxon type, viz.

$$V(r) = -\frac{V}{e^{x}+1} + 4i\,W\frac{d}{dx'}\frac{1}{e^{x'}+1}$$

plus a Coulomb term representing the interaction with a uniformly charged sphere of radius 1.3 fm. Here $x = (r - r_0 A^{1/3})/a$ and $x' = (r' - r_0' A^{1/3})/a'$.

Table I lists the set of parameters that were used for the deuteron and proton optical potentials. In the DWBA calculation, the neutron was considered to be bound in a Saxon well with binding energy $B = Q + 2.23$ MeV, $r_0 = 1.25$ fm and diffuseness $a = 0.65$ fm. A zero lower cutoff was used on the radial integrals as well as a zero-range interaction. The fits to the angular-distribution data were not very sensitive to the magnitude of the lower cutoff. Figures 1 and 2 show

---

[3] See Table II in C. M. Perey and F. G. Perey, Phys. Rev. 132, 755 (1963) for a survey of the available elastic deuteron scattering data at energies greater than 10 MeV.

TABLE I. Optical-model parameters.

| Parameter | Deuteron | Proton |
|---|---|---|
| V | 103 MeV | 52 MeV |
| $r_0$ | 1.0 fm | 1.25 fm |
| a | 0.9 fm | 0.65 fm |
| $r_0'$ | 1.41 fm | 1.25 fm |
| a' | 0.65 fm | 0.47 fm |
| W | 100 MeV | 48 MeV |
| $r_c$ | 1.3 fm | 1.25 fm |

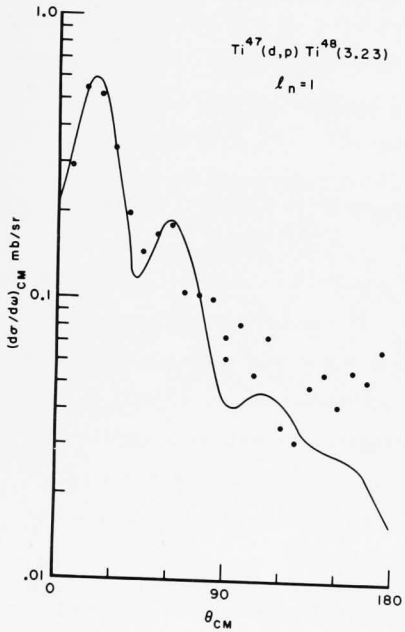


Fig. 1. Angular distribution of the $Ti^{47}(d,p)Ti^{48}(3.23)$ reaction. The points are experimental data and the smooth curve is the fit of the normalized DWBA calculation.

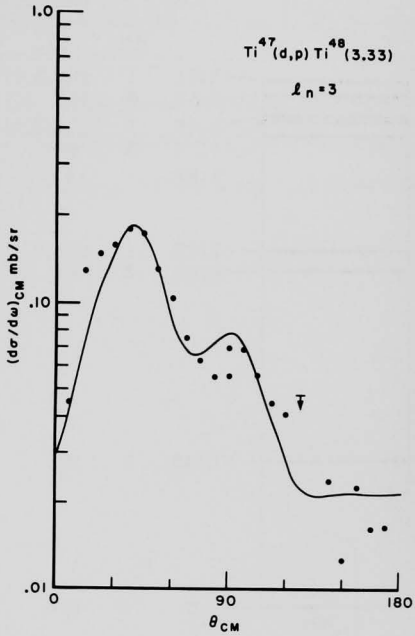


Fig. 2. Angular distribution of the $Ti^{47}(d,p)Ti^{48}(3.33)$ reaction. The points are experimental data and the smooth curve is the fit of the normalized DWBA calculation.

typical $\ell_n = 1$ and $\ell_n = 3$ angular distributions, respectively, together with the predictions of the DWBA calculations.

Levels in $Ti^{48}$ were observed up to 8 MeV in excitation. However, this very preliminary report will be restricted to the first eight excited states. The observed level scheme is shown in Fig. 3 together with the value of the orbital angular momentum $\ell_n$ of the captured neutron, suggested by the DWBA analysis. Since the target has a $\frac{5}{2}^-$ character, spins of $1^+$ through $4^+$ may be reached with $\ell_n = 1$ or 3; in the present preliminary fits, only the dominant contributions have been indicated. The ground-state-to-ground-state transition, $Ti^{47}(d,p)Ti^{48}(0.0)$, was only weakly observed and it is estimated that

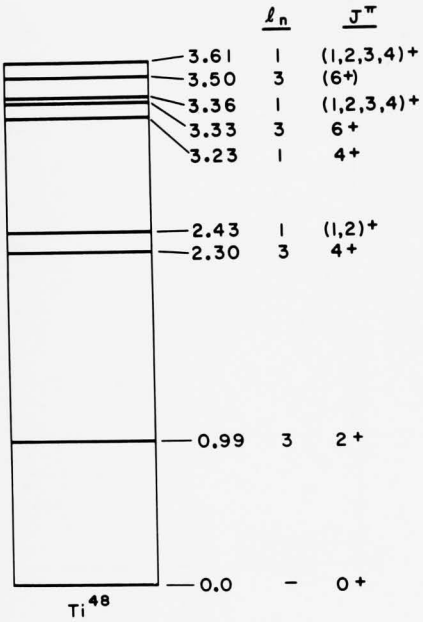


Fig. 3. The level scheme of the $Ti^{48}$ nucleus. The values of $\ell_n$ are those suggested by the DWBA calculation. The values of $J^+$ are those listed in the N. D. S. which are consistent with the observed $\ell_n$ values.

$$\frac{\sigma\,[\,Ti^{47}(d,p)Ti^{48}(0.0)]}{\sigma\,[\,Ti^{47}(d,p)Ti^{48}(0.99)]} < 0.03.$$

The spins and parities of the $Ti^{48}$ levels have been studied in a variety of experiments[4] and are listed in the third column of Fig. 3. The spin of the 3.50-MeV level has been limited by the work of Hillman,[5] and Kashy et al.[6] to 5, 6, 7. The present work eliminates the possibility of J = 7 and supports the tentative assignment of $J = 6^+$. The $\ell_n = 1$ assignment

---

[4] Nuclear Data Project, National Research Council.

[5] M. Hillman, Phys. Rev. 129, 2227 (1963).

[6] E. Kashy and T. W. Condon (to be published).

to the 3.36-MeV and the 3.61-MeV levels limits the spin to 1, 2, 3, 4 and positive parity.

It should be noted that the assignment of odd values of $\ell_n$ to the states observed precludes their identification with the $3^-$ octupole states cited by McDaniels et al.[7] at 3.5 MeV or by Matsuda[8] at 3.36 MeV.

---

[7] D. K. McDaniels, J. S. Blair, S. W. Chen, and G. W. Farwell, Nucl. Phys. 17, 614 (1960).

[8] K. Matsuda, Nucl. Phys. 33, 536 (1962).

# B-5. A HIGH-RESOLUTION STUDY OF (d,p) REACTIONS ON TARGETS OF $W^{182}$, $W^{184}$, AND $W^{186}$†

John R. Erskine

Argonne National Laboratory, Argonne, Illinois

## Introduction

The lower excited states of $W^{183}$ are known to be well described by the model of a rotator plus an odd nucleon. Kerman[1] was able to fit the excitation energies with a high degree of accuracy by use of this model. The levels of $W^{185}$ and $W^{187}$ should also be described by this same model. However, certain refinements provided by the quasi-particle picture are needed to understand the changes in the intrinsic states between $W^{183}$, $W^{185}$, and $W^{187}$. The (d,p) reaction provides a tool for exciting the energy levels in the odd-A tungsten isotopes. However, the high resolution of a magnetic spectrograph is needed to observe the various states individually.

The energy levels in $W^{183}$ have been studied experimentally by Murray et al.,[2] who used a bent-crystal spectrometer. Their information, together with the theoretical analysis by Kerman, provides a check on the present $W^{182}(d,p)W^{183}$ reaction. Some incomplete information is available[3] in the energy levels of $W^{185}$ but nothing has previously been reported on the level structure of $W^{187}$.

---

†Work performed under the auspices of the U. S. Atomic Energy Commission.

[1] A. K. Kerman, Kgl. Danske Videnskab. Selskab, Mat.-fys. Medd. 30, No. 15 (1956).

[2] J. J. Murray, F. Boehm, P. Marmier, and J. W. M. DuMond, Phys. Rev. 97, 1007 (1955).

[3] Nuclear Data Sheets, National Academy of Sciences, National Research Council, 1962 (U.S. Government Printing Office, Washington, D.C.).

Theoretical calculations of the proton spectra from the three reactions were made by use of a computer code[4] which calculates the differential cross sections and excitation energies of the final-state nucleus. This code uses the model of a rotator plus an odd nucleon and includes the effects of band mixing. Input parameters are the moments of inertia, quantum numbers, and wave functions of the various intrinsic states, as well as the relative position of the intrinsic states, the mixing coefficient $\langle J_- \rangle$, and the decoupling parameter a. The differential cross sections are obtained by means of an expression for the reduced-width amplitudes given by Satchler[5] and a set of intrinsic single-particle differential cross sections.

The Hamiltonian matrix used by the computer to calculate the energies and wave functions was

$$H_{ii} = \begin{cases} A_i[J(J+1) - K_i(K_i+1) + \delta_{K_i \frac{1}{2}} a_i (J+\frac{1}{2})(-1)^{J+\frac{1}{2}}] + E_i^0 & \text{for } J \geq K_i, \\ 0 & \text{for } J < K_i, \end{cases}$$

$$H_{ij} = H_{ji} = \begin{cases} -\frac{1}{2}(A_i + A_j)[(J+K_i)(J-K_i+1)]^{\frac{1}{2}} \langle J_- \rangle_{ij} & \text{for } J \geq K_i \text{ and } K_i = K_j + 1, \\ 0 & \text{for } J < K_i,\ J < K_j, \text{ or } |K_i - K_j| \neq 1, \end{cases}$$

where $A_i = \hbar^2/2\mathcal{I}$ is the unit of rotational energy, J is the total angular momentum of the state, $K_i$ is the projection of J on the symmetry axis, $a_i$ is the decoupling coefficient, $E_i^0$ is the position of the intrinsic state,

[4] J. R. Erskine and W. W. Buechner, Phys. Rev. 133, B370 (1964).

[5] G. R. Satchler, Ann. Phys. (N. Y.) 3, 275 (1958).

and $\langle J_- \rangle_{ij}$ is a parameter which determines the strength of the band mixing.

The level structure of $W^{183}$, $W^{185}$, and $W^{187}$ is somewhat complicated by the band mixing between the $[510\ \frac{1}{2}^-]$ and $[512\ \frac{3}{2}^-]$ intrinsic states. This band mixing, however, is also helpful since the relative differential cross sections in the (d,p) reaction leading to the two levels which mix are greatly altered by this band mixing and, consequently, the proper calculation of the relative cross section provides a fairly sensitive test of the choice of parameters used in the calculation.

## Experimental Procedure and Results

The data were recorded with a broad-range magnetic spectrograph in conjunction with the Argonne tandem accelerator. A bombarding energy of 12.0 MeV was used. Angular-distribution data were taken at scattering angles from $7.5^\circ$ to $90^\circ$. The targets were prepared by evaporating the separated isotopes of tungsten, in the form of $WO_3$, on self-supporting carbon backings.

Proton spectra recorded with targets of $W^{182}$, $W^{184}$, and $W^{186}$ are shown in Fig. 1. Excitation energies and Q values observed for the lower excited states of $W^{183}$, $W^{185}$, and $W^{187}$ are listed in Table I. Also included are assignments of $\ell$ for the levels near the ground state, which are based on the angular distribution data. The $\ell$ values of transitions leading to levels in $W^{183}$ are inferred from the known spins. The $\ell$ values assigned to the transitions which lead to levels in $W^{185}$ and $W^{187}$ were obtained by comparing the measured angular distribution of these levels with the angular distributions of the known levels in the $W^{182}(d,p)W^{183}$ reaction. In addition, Table I includes values of J and K assigned in accordance with the theoretical calculations described below.

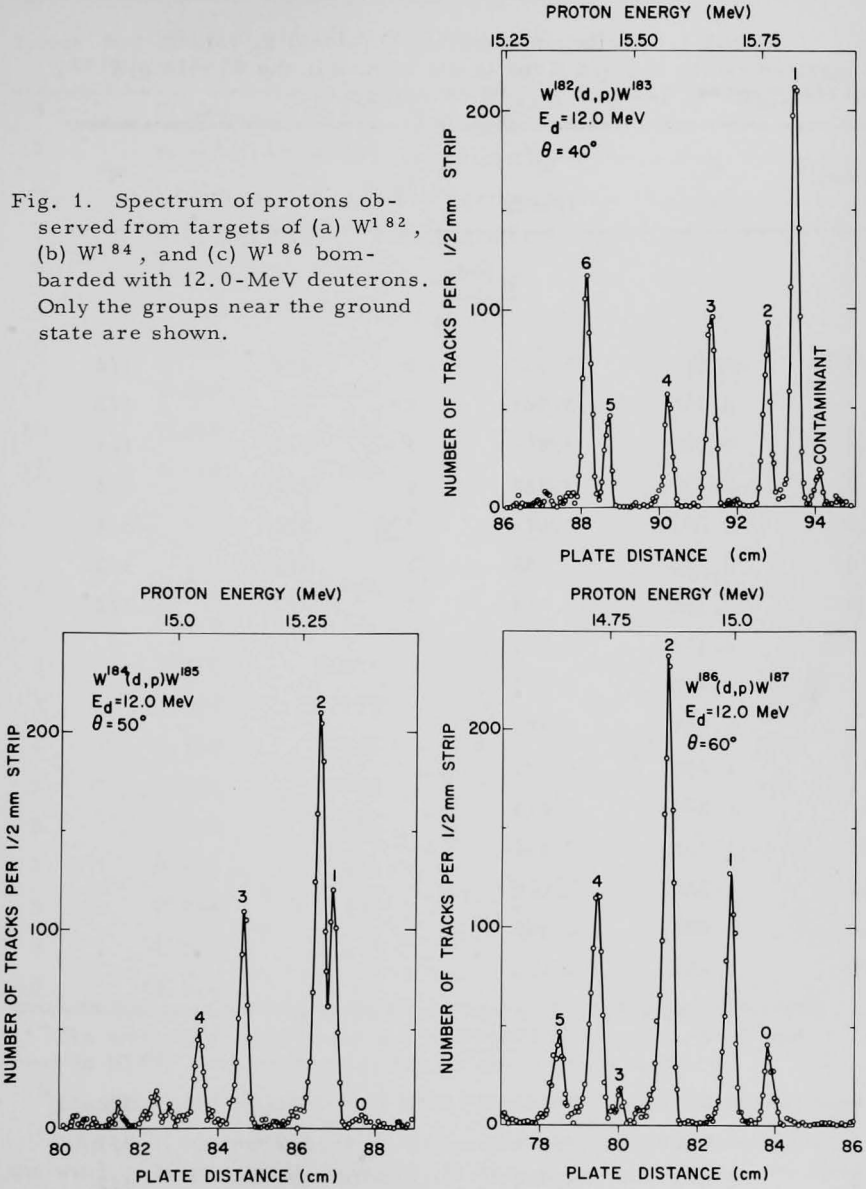


Fig. 1. Spectrum of protons observed from targets of (a) $W^{182}$, (b) $W^{184}$, and (c) $W^{186}$ bombarded with 12.0-MeV deuterons. Only the groups near the ground state are shown.

TABLE I. Excitation energies, Q values, $\ell_n$ values, and suggested values of J and K for levels formed in the $W^{182}(d,p)W^{183}$, $W^{184}(d,p)W^{185}$, and $W^{186}(d,p)W^{187}$ reactions.

| Level | $E_x$ [a] (MeV) | Q [b] (MeV) | $\ell_n$ | J | K |
|---|---|---|---|---|---|
| | | $W^{183}$ | | | |
| 0 [c] | (0.0) | (3.967) | 1 | 1/2 | 1/2 |
| 1 | 0.046 | 3.921 | 1 | 3/2 | 1/2 |
| 2 | 0.100 | 3.867 | 3 | 5/2 | 1/2 |
| 3 | 0.209 | 3.758 | 1 | 3/2 | 3/2 |
| 4 | 0.293 | 3.674 | 3 | 5/2 | 3/2 |
| 5 | 0.412 | 3.555 | 3 | 7/2 | 3/2 |
| 6 | 0.453 | 3.514 | 3 | 7/2 | 7/2 |
| 7 | 1.156 | 2.811 | | | |
| 8 | 1.474 | 1.493 | | | |
| 9 | 1.558 | 2.409 | | | |
| 10 | 1.636 | 2.331 | | | |
| 11 | 1.689 | 2.278 | | | |
| 12 | 1.731 | 2.236 | | | |
| 13 | 1.789 | 2.178 | | | |
| 14 | 1.820 | 2.147 | | | |
| 15 | 1.851 | 2.116 | | | |
| | | W185 | | | |
| 0 | 0.0 | 3.524 | (1) | 3/2 | 3/2 |
| 1 | 0.060 | 3.464 | 3 | 5/2 | 3/2 |
| 2 | 0.085 | 3.439 | 1 | 3/2 | 1/2 |
| 3 | 0.235 | 3.289 | 3 | 7/2 | 7/2 |

TABLE I (cont'd.)

| Level | $E_x$ [a] (MeV) | $Q$ [b] (MeV) | $\ell_n$ | J | K |
|---|---|---|---|---|---|
| 4 | 0.327 | 3.197 | 3 | 7/2 | 1/2 |
| 5 | 0.657 | 2.867 | | | |
| 6 | 0.721 | 2.803 | | | |
| 7 | 0.996 | 2.528 | | | |
| 8 | 1.102 | 2.422 | | | |
| 9 | 1.136 | 2.388 | | | |
| 10 | 1.174 | 2.350 | | | |
| 11 | 1.210 | 2.314 | | | |
| 12 | 1.279 | 2.245 | | | |
| 13 | 1.418 | 2.106 | | | |
| | | $W^{187}$ | | | |
| 0 | 0.0 | 3.236 | 1 | 3/2 | 3/2 |
| 1 | 0.079 | 3.157 | 3 | 5/2 | 3/2 |
| 2 | 0.205 | 3.031 | 1 | 3/2 | 1/2 |
| 3 | 0.304 | 2.932 | 3 | 5/2 | 1/2 |
| 4 | 0.351 | 2.885 | 3 | 7/2 | 7/2 |
| 5 | 0.434 | 2.802 | 3 | 7/2 | 1/2 |
| 6 | 0.782 | 2.454 | | | |
| 7 | 0.813 | 2.423 | | | |
| 8 | 0.844 | 2.392 | | | |
| 9 | 0.889 | 2.347 | | | |
| 10 | 0.974 | 2.262 | | | |

[a] The estimated uncertainty is 3 keV for levels 1—6 in $W^{183}$ and 1—5 in $W^{187}$. The uncertainty for all other levels is 5 keV.

[b] The estimated uncertainty is 5 keV for the ground-state transitions.

[c] This level was not observed. However, its position is known from the work of Murray et al. who give 46.48 keV as the energy of the first excited state in $W^{183}$.

## Discussion

Calculated spectra for the three different reactions are shown in Fig. 2. For $W^{183}$, the exact parameters given by Kerman[1] were used. For this nucleus as well as for the other two, the Nilsson wave functions for a deformation $\eta = 4$ were adopted since the final results are not sensitive to the deformation. As can be seen in Fig. 2, the experimental and theoretical spectra for the $W^{182}(d,p)W^{183}$ reactions are in fairly close agreement. The ground-state group in $W^{183}$ is predicted to have only 1% of the intensity of the group leading to the first excited state. This ground-state group was not observed in any of the data. All the other groups which arise from the $[510\ \frac{1}{2}^-]$, $[512\ \frac{3}{2}^-]$, and $[503\ \frac{7}{2}^-]$ intrinsic states are observed and are in good agreement in cross section and in excitation energy. This agreement confirms Kerman's calculations and suggests that the present method should be able to identify the various energy levels in $W^{185}$ and $W^{187}$.

The excitation energies of the observed levels in $W^{185}$ and $W^{187}$ were fitted as well as possible by adjusting the various parameters of the same three intrinsic states required for $W^{183}$. No explicit use of the quasi-particle picture was made at this point beyond recognizing that filled particle states became hole states. Since there are fewer observed levels than parameters, a constraint was imposed on the parameters by keeping the moments of inertia for the $K = \frac{1}{2}$ and $K = \frac{3}{2}$ states in the same proportion as Kerman had found for $W^{183}$. The fitting is not as reliable for $W^{185}$ as for $W^{187}$ since the number of states observed is one less in $W^{185}$. The missing state, presumably the $J = 5/2$, $K = 1/2$ state, probably is too weak to have been observed. As a consequence, the moments of inertia and decoupling parameter for $W^{185}$ could not be accurately determined. The adopted values of these quantities are the

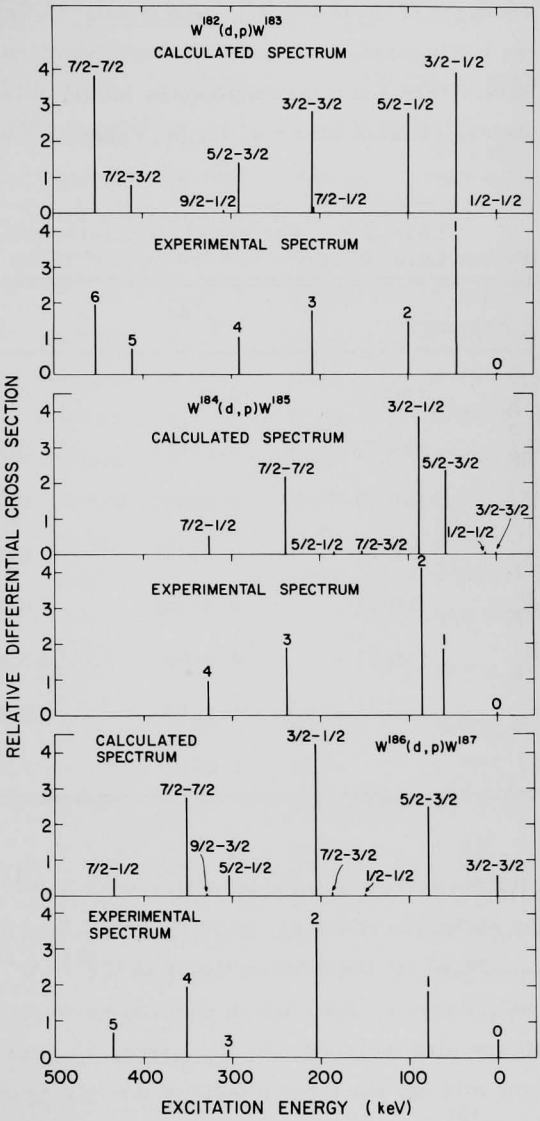


Fig. 2. A comparison between the calculated and observed spectra of protons from the $W^{182}(d,p)W^{183}$, $W^{184}(d,p)W^{185}$, and $W^{186}(d,p)W^{187}$ reactions. Each calculated state is labeled with a symbol J-K which specifies the total angular momentum J and the projection of J on the symmetry axis.

averages of those for $W^{183}$ and $W^{187}$. However, the relative position of the intrinsic states and the mixing coefficient $\langle J_- \rangle$ were left as free parameters and were empirically adjusted for the best fit. The parameters of these best fits for $W^{185}$ and $W^{187}$ are given in Table II along

TABLE II. The principal parameters used in the calculation of the excitation energies and differential cross sections.

| Parameter | $W^{183}$ | $W^{185}$ | $W^{187}$ |
|---|---|---|---|
| $E^0_{K=1/2}$ (MeV) | 0.0 | 0.0 | 0.146 |
| $E^0_{K=3/2}$ (MeV) | 0.19676 | 0.003 | 0.0 |
| $E^0_{K=7/2}$ (MeV) | 0.45041 | 0.227 | 0.3505 |
| $A_{K=1/2}$ (MeV) | 0.01585 | 0.01713 | 0.01842 |
| $A_{K=3/2}$ (MeV) | 0.01405 | 0.01518 | 0.01632 |
| $A_{K=7/2}$ (MeV) | 0.0150 | 0.01621 | 0.01742 |
| $a_{K=1/2}$ | 0.1684 | 0.0717 | -0.025 |
| $\langle J_- \rangle$ | 1.4537 | 1.25 | 0.75 |

with the parameters found by Kerman for $W^{183}$. In Table III are listed the excitation energies, wave functions, and differential cross sections calculated for the various levels in $W^{183}$, $W^{185}$, and $W^{187}$. The differential cross sections which one obtains when the band mixing is turned off are also included. By comparing the cross sections with and without band mixing, the large effects of the mixing can be seen, particularly for $W^{185}$.

TABLE III. Excitation energies and wave functions calculated for $W^{183}$, $W^{185}$, and $W^{187}$ together with the expected differential cross sections for exciting these levels in the present (d,p) reactions.

| J | K | E (keV) | Wave function $a_{K=1/2}$ | $a_{K=3/2}$ | $a_{K=7/2}$ | Relative $d\sigma/d\Omega$ With mixing | Without mixing |
|---|---|---|---|---|---|---|---|
| | | | | $W^{183}$ | | | |
| 1/2 | 1/2 | 0.0 | 1.00 | 0.0 | 0.0 | 0.006 | 0.006 |
| 3/2 | 1/2 | 46.31 | 0.971 | 0.239 | 0.0 | 0.56 | 0.78 |
| 3/2 | 3/2 | 208.68 | 0.239 | -0.971 | 0.0 | 0.41 | 0.19 |
| 5/2 | 1/2 | 99.30 | 0.941 | 0.339 | 0.0 | 0.40 | 0.19 |
| 5/2 | 3/2 | 291.86 | 0.339 | -0.941 | 0.0 | 0.20 | 0.41 |
| 7/2 | 1/2 | 207.11 | 0.886 | 0.464 | 0.0 | 0.02 | 0.08 |
| 7/2 | 3/2 | 412.06 | 0.464 | -0.886 | 0.0 | 0.11 | 0.05 |
| 7/2 | 7/2 | 453.08 | 0.0 | 0.0 | 1.0 | 0.55 | 0.55 |
| | | | | $W^{185}$ | | | |
| 1/2 | 1/2 | 13.6 | 1.00 | 0.0 | 0.0 | 0.006 | 0.006 |
| 3/2 | 1/2 | 86.5 | 0.891 | -0.454 | 0.0 | 0.97 | 0.78 |
| 3/2 | 3/2 | 0.0 | 0.454 | 0.891 | 0.0 | 0.00005 | 0.19 |
| 5/2 | 1/2 | 184.2 | 0.846 | -0.534 | 0.0 | 0.001 | 0.19 |
| 5/2 | 3/2 | 57.7 | 0.534 | 0.846 | 0.0 | 0.60 | 0.41 |
| 7/2 | 1/2 | 325.4 | 0.849 | -0.529 | 0.0 | 0.13 | 0.08 |
| 7/2 | 3/2 | 151.2 | 0.529 | 0.849 | 0.0 | 0.002 | 0.05 |
| 7/2 | 7/2 | 235.0 | 0.0 | 0.0 | 1.0 | 0.55 | 0.55 |

TABLE III (cont'd.)

| J | K | E (keV) | Wave function $a_{K=1/2}$ | $a_{K=3/2}$ | $a_{K=7/2}$ | Relative $d\sigma/d\Omega$ With mixing | Without mixing |
|---|---|---|---|---|---|---|---|
| | | | | $W^{187}$ | | | |
| 1/2 | 1/2 | 149.0 | 1.0 | 0.0 | 0.0 | 0.006 | 0.006 |
| 3/2 | 1/2 | 205.4 | 0.994 | -0.110 | 0.0 | 0.85 | 0.78 |
| 3/2 | 3/2 | 0.0 | 0.110 | 0.994 | 0.0 | 0.12 | 0.19 |
| 5/2 | 1/2 | 303.4 | 0.986 | -0.165 | 0.0 | 0.11 | 0.19 |
| 5/2 | 3/2 | 77.9 | 0.166 | 0.986 | 0.0 | 0.49 | 0.41 |
| 7/2 | 1/2 | 433.8 | 0.978 | -0.209 | 0.0 | 0.11 | 0.08 |
| 7/2 | 3/2 | 187.5 | 0.209 | 0.978 | 0.0 | 0.03 | 0.05 |
| 7/2 | 7/2 | 351.0 | 0.0 | 0.0 | 1.0 | 0.55 | 0.55 |

These fits to $W^{185}$ and $W^{187}$ have been achieved by fitting the observed excitation energies without using the differential-cross-section data. If now the theoretical and experimental cross sections are compared, one has a test of the spin and orbital assignments. The agreement between the calculated and experimental spectra for the $W^{184}(d,p)W^{185}$ and $W^{186}(d,p)W^{187}$ reactions is quite good, as can be seen in Fig. 2. This is a strong indication that the spins and intrinsic states have been correctly identified and that the simple rotator-plus-odd-nucleon model is a reasonably valid description of the low-lying states of $W^{185}$ and $W^{187}$.

One interesting feature of the level structure of $W^{185}$ and $W^{187}$ is the behavior of the $J = 5/2$, $K = 1/2$ and $J = 3/2$, $K = 3/2$ states as the degree of band mixing is increased. These states appear with a

smaller intensity in the calculated spectrum of the $W^{184}(d,p)W^{185}$ reaction than in the calculated spectrum of the $W^{186}(d,p)W^{187}$ reaction. (See Fig. 2.) This intensity difference is produced by the greater amount of band mixing in $W^{185}$ compared with $W^{187}$. The strength of the weakened states is given to the J = 5/2, K = 3/2 and J = 3/2, K = 1/2 states with which they admix. This behavior is apparent in the observed spectra (Fig. 1) where levels 0 and 3 in the $W^{186}(d,p)W^{187}$ reaction spectra have counterparts in the $W^{184}(d,p)W^{185}$ reaction spectra which are very weak or not observable.

Some attempt was made to compare the results of the present analysis and interpretation with the quasi-particle calculation for low-lying levels of $W^{183}$, $W^{185}$, and $W^{187}$ made by Yoshida as reported by Isoya.[6] For $W^{185}$ the relative positions of the $[510\ \frac{1}{2}^-]$, $[512\ \frac{3}{2}^-]$, and $[503\ \frac{7}{2}^-]$ intrinsic states are in agreement with Yoshida's predictions, but not for $W^{187}$. For the latter isotope, the $[503\ \frac{7}{2}^-]$ state is found to be at a much higher excitation than Yoshida's calculation predicts.

---

[6] A. Isoya, Phys. Rev. 130, 234 (1963).

# B-6. A STUDY OF (d,n) REACTIONS ON $Fe^{54}$ AND $Ni^{58}$†

D. S. Gemmell, L. L. Lee, Jr., J. P. Schiffer, and A. B. Smith

Argonne National Laboratory, Argonne, Illinois

## Introduction

Over the years a great deal of very useful nuclear-structure information has been obtained from (d,p) reactions on light and medium-weight nuclei. The difficulties in detection and energy measurement for neutrons has thus far inhibited similar exploitation of the (d,n) reaction. Except for the very light nuclei, which can be successfully studied with low-energy pulsed accelerators, almost no data exist. We have therefore started a study, using the pulsed deuteron beam from the Argonne tandem Van de Graaff, of (d,n) reactions on targets for which $40 \leq A \leq 64$. The present paper reports preliminary results from this program.

The (d,n) reaction can, of course, be treated in exactly the same manner as the (d,p) reaction, with the proton and neutron interchanging roles. One may expect to extract proton reduced widths in the same manner as neutron widths are extracted from (d,p) data. In addition, one may expect to observe effects of isobaric-spin splitting in the states of the final nucleus.[1]

---

† Work performed under the auspices of the U. S. Atomic Energy Commission.

[1] J. B. French and M. H. Macfarlane, Nucl. Phys. 26, 168 (1961).

## Experiment

The beam-pulsing technique[2] on the Argonne tandem is similar to that described by Lefevre, Borchers, and Poppe.[3] The beam is bunched before acceleration and chopped at a frequency of 3.75 Mc/sec after acceleration. Average currents of about 0.05 μA are easily achieved with a pulse width of less than 2 nsec. Fast neutrons from the target are detected in a NE 213 liquid scintillator, 8 in. in diameter by 4 in. thick, mounted on a 58 AVP 5-in. photomultiplier. The neutron flight time is converted into pulse height in a conventional converter[4] and fed into a multichannel analyzer. Pulse-shape discrimination is employed to eliminate pulses due to gamma rays in the scintillator, and a high bias level is maintained on the neutron counter so that only the high-energy neutrons of interest are counted. With these detectors, it is possible to get usable counting rates with flight paths of about 10 m. These path lengths can be used over an angular range from $5^{\circ}$ to about $135^{\circ}$, although only measurements at angles less than $60^{\circ}$ have thus far been made.

Thin self-supporting isotopically enriched foils of $Fe^{54}$ and $Ni^{58}$ were bombarded with 7-MeV deuterons. After passing through the target, the beam was stopped in a lead backing. This was found to produce fewer background neutrons than other available materials. In our early measurements we have been troubled by carbon contamination of the targets and beam stopper; a strong peak from $C^{12}(d,n)N^{13}_{g.s.}$ was present in all of our spectra. Fortunately, this peak can easily be

---

[2] F. J. Lynch, Argonne National Laboratory Report ANL-6720 (1963), p. 39.

[3] H. W. Lefevre, R. R. Borchers, and C. H. Poppe, Rev. Sci. Instr. 33, 1231 (1962).

[4] Designed by the Argonne Electronics Division.

distinguished from the peaks of interest by virtue of the more pronounced energy change as a function of angle of observation.

## Results

The spectrum of neutrons at 14.5° from bombardment of the $Fe^{54}$ target is shown in Fig. 1. The peaks marked by asterisks were

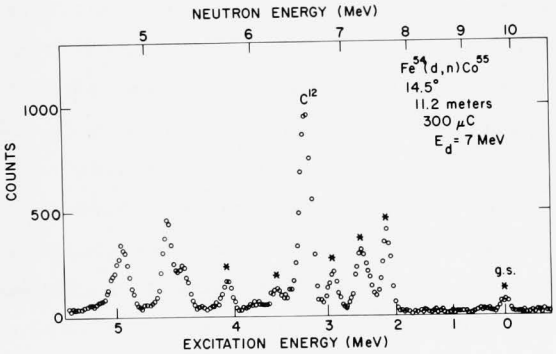


Fig. 1. Neutron spectrum from the $Fe^{54}(d,n)$ reaction.

definitely assigned to the $Fe^{54}(d,n)Co^{55}$ reaction and angular distributions were obtained for these neutron groups. These angular distributions are shown in Fig. 2. Comparison with calculated DWBA angular distributions[5] indicates $\ell_p=1$ assignments for the states at excitation energies of 2.15 MeV and 2.55 MeV and probably for the states at 2.92 MeV and 4.15 MeV excitations, although better data are certainly desirable. The angular distribution for the neutrons from the ground state of $Co^{55}$ is consistent with the expected $\ell_p=3$.

Two of the angular distributions taken with the $Ni^{58}$ target are shown in Fig. 3. Neutrons to the ground state and to the state at

---

[5] The authors are indebted to G. R. Satchler for performing these calculations.

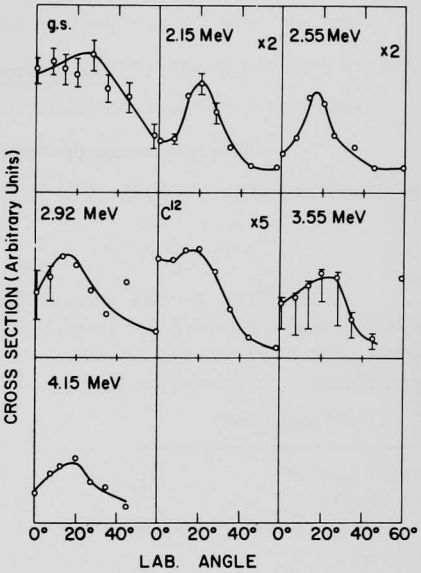


Fig. 2. Angular distributions for the neutron groups from the reaction $Fe^{54}(d,n)$.

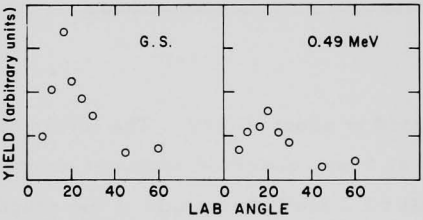


Fig. 3. Angular distributions for neutrons emitted to the ground state and first excited state of $Cu^{59}$ in the reaction $Ni^{58}(d,n)Cu^{59}$.

0.49 MeV excitation show the $\ell_p$=1 angular distribution expected from simple shell-model considerations.

## Discussion

Our preliminary results on the levels observed in $Co^{55}$ and $Cu^{59}$ are listed in Table I. The uncertainty in the excitation energies

TABLE I. Levels observed in the $Fe^{54}(d,n)$ and $Ni^{58}(d,n)$ reactions, together with the probable values of the orbital angular momentum $\ell_p$ for the captured protons.

| $Fe^{54}(d,n)Co^{55}$ | | $Ni^{58}(d,n)Cu^{59}$ | |
|---|---|---|---|
| Level in $Co^{55}$ (MeV) | $\ell_p$ | Level in $Cu^{59}$ (MeV) | $\ell_p$ |
| 0.0 | 3 | 0.0 | 1 |
| 2.15 | 1 | 0.49 | 1 |
| 2.55 | 1 | | |
| 2.92 | (1) | | |
| 3.55 | (3) | | |
| 4.15 | (1) | | |

listed is about 50 keV. The levels of $Co^{55}$ have been studied by Kumabe et al.[6] who observed states at excitations of 1.8, 2.2, and 2.45 MeV (all ±0.2 MeV) in a study of the reaction $Ni^{58}(p,\alpha)Co^{55}$. Of these, we do

[6] S. Kumabe, H. Ogata, T. Kamatuzaki, N. Inoue, S. Tomita, Y. Yamada, T. Yamaki, and S. Matsumoto, Nucl. Phys. 46, 437 (1963).

not observe the level at 1.8 MeV excitation which may be weakly excited in the (d,n) reaction. Our results for $Cu^{59}$ are consistent with the results of Butler and Gossett[7] who studied the reaction $Ni^{58}(p,\gamma)Cu^{59}$. It must be emphasized that our results are preliminary and more work is necessary before we can fully understand the spectra and angular distributions observed.

---

[7] J. W. Butler and C. R. Gossett, Phys. Rev. 108, 1473 (1957).

# B-7. A NOTE ON THE REACTIONS $Mg^{26}(d,p)Mg^{27}$ AND $Mg^{26}(t,d)Mg^{27}$

R. N. Glover

Atomic Weapons Research Establishment, Aldermaston, Berkshire

The various stripping and pickup reactions linking the magnesium isotopes are being studied at several energies. This note contains some preliminary data on the reactions $Mg^{26}(d,p)Mg^{27}$ and $Mg^{26}(t,d)Mg^{27}$ at 6 and 10 MeV bombarding energy with the aid of the Aldermaston multichannel spectrograph. Further experiment with the scattering chamber and counter telescopes will be done shortly. The interest in the present experiment lies in the extraction of values of $\lambda$, the mass-3 form factor. An alignment telescope was used to check that the beam hit the same spot on the $Mg^{26}$ target for all exposures.

The (d, p) experiment shows that, for the doublet at 3.76 and 3.78 MeV, the 3.78-MeV level (not the 3.76 MeV level) has spin $\left(\frac{3}{2}, \frac{5}{2}\right)^{+}$. The transition to the 3.76-MeV state agrees well with an $\ell = 3$ pattern. An advantage of studying the (t, d) reaction with the spectrograph is that the resolving power is doubled. The 3.47-3.48 MeV doublet was therefore separated and the $\ell = 0$ transition shown to belong to the 3.47-MeV level and not the 3.48-MeV level.

Table I shows values of $(2J + 1)\theta^2$ and $\lambda(2J + 1)\theta^2$ extracted from the(d, p) and (t, d) reactions, respectively, and the resultant values of $\lambda$. The values of $\lambda$ extracted for the ground-state rotational band (0-, 0.98-, and 1.69-MeV levels) seem reasonably consistent and agree with values obtained from the reactions $C^{13}(d, t_{0,1})$ and $(p, d_{0,1})$ and $C^{12}(t, d_0)$ and $(d, p_0)$ at 12 MeV. The value of $\lambda$ for states from 3—4 MeV excitation is about 100, in agreement with the values obtained from comparing the reactions $C^{12}(t, d)$ and (d, p) with the 3.85-MeV $C^{13}$ levels.

TABLE I. Comparison of $Mg^{26}$(d, p) and (t, d) reactions.

| Bombarding energy (MeV) | Level (MeV) | $\ell$ | (d, p) $r_0$ | (d, p) Relative $(2J + 1)\theta^2$ | (t, d) $r_0$ | (t, d) Relative $\lambda(2J + 1)\theta^2$ | $\lambda$ |
|---|---|---|---|---|---|---|---|
| 10 | 0 | 0 | 5.5 | 37.2 | 5.3 | 7977 | 214 |
| | 0.98 | 2 | 5.5 | 33.4 | 6.0 | 5020 | 150 |
| | 1.69 | 2 | 4.5 | 18.9 | 5.3 | 2527 | 134 |
| | 3.47 | 0 | 5.0 | 45.8 | 4.0 | 4241 | 93 |
| | 3.56 | 1 | | a | 5.3 | 6860 | |
| | 3.76 | 3 | 6.0 | 83.3 | 6.5 | 8370 | 100 |
| | 3.78 | 2 | 5.0 | 12.7 | 5.3 | 1199 | 94 |
| | 4.15 | 2 | 5.0 | 6.1 | | | |
| 6 | 0 | 0 | 6.0 | 21.6 | 6.0 | 4173 | 193 |
| | 0.98 | 2 | 5.5 | 25.2 | 5.5 | 2936 | 117 |
| | 1.69 | 2 | 5.5 | 11.6 | 5.5 | 1157 | 100 |

[a]Too strong to analyze.

For the ground-state rotational band, the 6-MeV data suggest smaller values of $\lambda$ tending towards the value of 100 observed at higher excitation at 10 MeV.

The data have been recently obtained so that as yet no serious thought has been given to their interpretation; but they do seem to suggest that plane-wave theory may not give a description of (t, d) and (d, t) reactions adequate for simple extraction of reduced widths.

# SESSION C

TUESDAY MORNING

10 MARCH 1964

# C-1. PARTICLE-HOLE CALCULATION OF $Ca^{40}(\alpha,\alpha')$†

Nathan S. Wall‡

Laboratory for Nuclear Science, Massachusetts Institute of Technology, Cambridge, Massachusetts

The usual distorted-wave analysis of inelastic scattering has been used to extract collective parameters of the particular excited state.[1] This parameter is usually expressed in terms of a surface-tension parameter $C_\ell$ or a deformation parameter $\beta_\ell$. It is generally the object of a microscopic theory of vibrational or rotational nuclei to deduce these parameters from an effective nucleon-nucleon interaction. For vibrational nuclei, one such description is G. E. Brown's[2] particle-hole interaction. V. Gillet,[3] in a very detailed analysis, has calculated the spectra of $C^{12}$, $O^{16}$, and $Ca^{40}$ on this basis. These and similar calculations have been rather widely used in the past year to interpret inelastic electron-scattering experiments[4–6] with quite some

†This work supported in part through funds provided by the Atomic Energy Commission Contract Number AT(30-1) 2098.

‡On leave from the Physics Department at the University of Maryland.

[1] Bassel *et al.*, Phys. Rev. 128, 2693 (1962).

[2] Brown, Castillejo, and Evans, Nucl. Phys. 22, 1 (1961).

[3] V. Gillet, Thesis, Paris, 1962.

[4] H. P. Jolly, Phys. Letters 5, 289 (1963).

[5] Lewis *et al.*, Phys. Rev. Letters 10, 493 (1963).

[6] V. Gillet and M. Melkanoff (to be published).

success. Prior to this Sanderson[7] and Sanderson and Wall[8] had attempted to analyze high-energy proton and inelastic alpha-particle scattering, respectively, in terms of particle-hole wave functions for the excited states. It is a more detailed analysis of this latter calculation which is described here. The earlier work of Ref. 8 had a number of shortcomings which necessitated a more correct description of the distortion of the incident and outgoing waves as well as the alpha-nucleon interaction. It is essentially these two modifications of the earlier calculation which have been built into the present calculation.

In what follows we use the development and notation of Bassel et al.[1] to describe the inelastic scattering. We have used a modified version (JULIE) of their DWBA code to calculate the inelastic scattering. In the DWBA the transition matrix can be written as

$$T_{fi} = \int d\vec{r}\; X_f^{(-)*}(k_f, r)\, \langle v_f | V | v_i \rangle\, X_i^{(+)}(k_i, r). \qquad (1)$$

The matrix element of the effective interaction $\langle v_f | V | v_i \rangle$ can be described in the second quantization formalism as

$$V_{fi} = \Sigma_{ph}\, a_{ph}\, \langle h\, k_f | V | p k_i \rangle\, a^+_{k_f}\, a_{k_i}\, a^+_{jl}(r_n)\, a_j(r_n). \qquad (2)$$

Here $\langle h\, k_f | V | p k_i \rangle$ is a single-particle matrix element for an incident alpha particle with wave number $k_i$ to scatter to $k_f$ and a nucleon in a state h to be excited to state p.

---

[7] E. Sanderson, Nucl. Phys. 35, 557 (1962).

[8] E. Sanderson and N. S. Wall, Phys. Letters 2, 173 (1962).

The effective single-particle interaction can be decomposed by the Wigner-Eckart theorem to a reduced matrix element which may be written as

$$\langle V_f \| V_\ell \| V_i \rangle = A_\ell F_\ell (r_\alpha)$$

in the notation of Ref. 2. Using a Gaussian interaction of strength $V_0$ and range b, with no spin or isotopic-spin dependence, the reduced matrix element can be written as

$$A_\ell F_\ell (r_\alpha) = (4\pi)^{\frac{1}{2}} V_0 \Sigma a_{ph} (-1)^{j_h + \ell_h + \frac{1}{2}} (\hat{j}_p \hat{j}_h \hat{\ell}_p \hat{\ell}_h \hat{\ell})^{\frac{1}{2}}$$
$$\times \begin{Bmatrix} \ell_h & \ell_p & \ell \\ j_p & j_h & \frac{1}{2} \end{Bmatrix} \begin{pmatrix} \ell_h & \ell & \ell_p \\ 0 & 0 & 0 \end{pmatrix} \tag{3}$$
$$\times \int dr_n \, u_p (r_n) \, u_h (r_n) \, j_\ell \left( \frac{2 i r_\alpha r_n}{b^2} \right).$$

In Eq. (3), $a_{ph}$ is the amplitude of the particular particle-hole configuration $\hat{x} = 2x + 1$, and $\ell$ and j are the oribital angular momentum and total spin of the appropriate single-particle state u. The curly bracket is a 6j symbol and the round bracket a 3j symbol. The quantity $j_\ell$ is the spherical Bessel function of order $\ell$, $r_\alpha$ is the alpha-particle coordinate, and $r_n$ the coordinate of the struck nucleon. The phase convention is that of Gillet and the amplitudes are those given by him.

For the reasons given in Ref. 8, we have used single-particle wave functions appropriate to a Saxon well. These wave functions were generated by the ABACUS[9] program, and a subsidiary

---

[9] We wish to thank E. Auerbach of Brookhaven National Laboratory for the use of this program.

program performed the integration of Eq. (3). Also, as in Ref. 8, we have used only the T=0 components of the excited-state wave functions.

Using the formalism described above, we have calculated the inelastic scattering to the various $3^-$ states of $Ca^{40}$. In Fig. 1 we

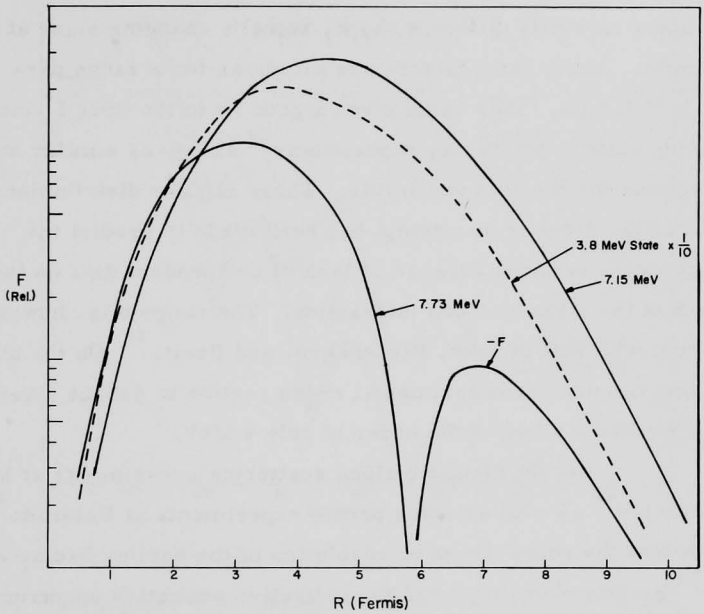


Fig. 1. The form factors F for Gillet's first three $3^-$ states of $Ca^{40}$ as a function of radius. The relative amplitudes of these three curves are to scale. Note the negative behavior of the 7.73-MeV state.

show the form factor for the first three $3^-$ states of $Ca^{40}$. Notice that the one corresponding to the first $3^-$ excited state has a form not too different from the usual derivative of the optical potential except that it is asymmetric toward large radii. Further, it should be noted that it peaks at a much smaller radius (about 4 fm) than would the usual type

of form factor rather than at something more like 5.4 fm. The form factor for the second excited state has much the same form but it is down in magnitude by a factor of about 7 and peaks at a slightly larger radius. The form factor for the third excited state given by Gillet has a radically different shape, actually changing signs at large radii. These form factors are all shown for a range parameter b of 2.3 fm. This value gives a good fit to the first $3^-$ inelastic-scattering state in the Saclay experiments[10] and gives similar angular distributions for the next two levels. These angular distributions are shown in Fig. 2 where no attempt has been made to predict the absolute cross sections because of lack of independent data on the strength of the alpha-nucleon interaction. The range b is, however, consistent with that of Sack, Biedenharn, and Breit.[11] On the other hand, one can use the experimental cross section to deduce a value for $V_0$; we find a value of the order of only 4 MeV.

Recent inelastic alpha scattering experiments at MIT[12] and Berkeley[13] as well as some proton experiments at Colorado[14] indicate that the relatively poor resolution of the earlier Saclay experiments[10] greatly oversimplified the collective excitation spectrum of $Ca^{40}$.

---

[10] Saudinos et al., Compt. Rend. 252, 260 (1961).

[11] Sack, Biedenharn, and Breit, Phys. Rev. 93, 321 (1954).

[12] Wall, Bauer, Bernstein, Heyman, and Lippincott (private communication).

[13] E. Rivet (private communication).

[14] W. S. Gray, R. A. Kenefick, and J. J. Kraushaar, Bull. Am. Phys. Soc. 9, 92 (1964).

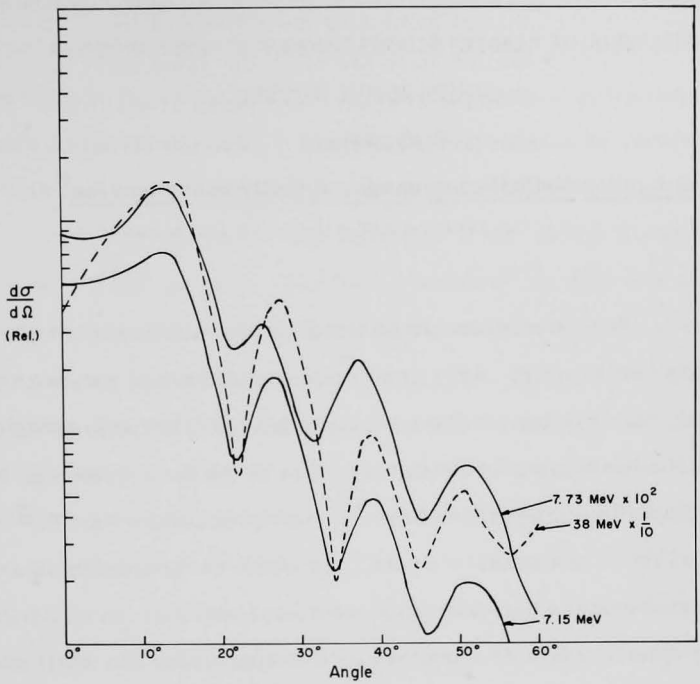


Fig. 2. The angular distributions in relative units as a function of the center-of-mass angle for the same states.

In the region of interest for comparison with Gillet's calculation of excited states, and therefore pertinent to the present calculations, at least four times the number of levels are seen. These newer experiments at MIT and Berkeley are presently being analyzed. Preliminary analysis of a state at about 6.3 MeV shows an intensity of 0.04 relative to the 3.73-MeV one that is to be identified as the T=0, $3^-$, giant-resonance one (3.84 MeV according to Gillet). This intensity is in very good agreement with that calculated for the second excited state of Gillet at 7.15 MeV.

# C-2. ANALYSIS OF ELASTIC SCATTERING OF 17-MEV PROTONS FROM HEAVY NUCLEI

F. G. Perey

Oak Ridge National Laboratory, Oak Ridge, Tennessee*

Recent experiments on the elastic scattering of 17-MeV protons from heavy nuclei[1] have shown that the diffraction patterns of differential cross sections for Ta and W are damped relative to those observed for the heavier nuclei Pb and Bi. Data at the same energy on Pt and Au show a situation intermediate between the above pairs of nuclei.[2] On the basis of the known behavior of the differential cross section as a function of optical-model parameters, this would suggest that the imaginary part of the optical potential decreases as one approaches the shell closure at Pb. It is the purpose of this paper to show that the data are consistent with a single set of optical-model parameters for all these nuclei, as determined by fitting the Pb and Bi angular distributions, provided one takes into account the permanent quadrupole deformations of the outer nuclei by means of a coupled-channel calculation.

A preliminary analysis of the data showed some disagreement between the normalization of the data and the optical-model curves

---

* Operated by Union Carbide Corporation, Nuclear Division, for the U.S. Atomic Energy Commission.

[1] G. Schrank and R. E. Pollock, Phys. Rev. 132, 2200 (1963).

[2] I. E. Dayton and G. Schrank, Phys. Rev. 101, 1358 (1956).

for Ta and W. The data were therefore renormalized for the analysis by 0.92 for Ta and 0.83 for W. In the case of W, this is larger than the estimated error on the normalization. It was also found that the data for Au and Pt could be renormalized by 0.9 to obtain a significant improvement in the fit. This had not been noticed in a previous analysis of these data.[3]

In this paper, the definition of the optical model and the notation of Ref. 3 will be used. The first analysis of the data was made by varying only the real and imaginary well depths but keeping the geometrical parameters as used in a recent survey[3] ($r_0$ = 1.25 F, $a_S$ = 0.65 F, and $a_D$ = 0.47 F). Satisfactory fits could not be obtained, particularly for Pb and Bi, until $a_D$ was increased to 0.76 F. It had already been noticed[3] that an increase in $a_D$ over the value used for medium-weight nuclei improved the fits for heavy nuclei at both 17 and 22.2 MeV. It must be concluded, therefore, that for heavy nuclei $a_D$ must be larger than for medium-weight nuclei. The real well depths which were obtained are in agreement with the known behavior[3] which includes a symmetry term and a Coulomb correction term. As expected from the variation of the diffraction pattern, the imaginary potential-well depth decreased as the mass of the target nucleus increased.

Since Pb and Bi are nearly doubly-closed shells, it is expected that they are spherically symmetric. This is not the case for the other nuclei studied. From Coulomb excitations,[4] it is known that nuclei in the region of Ta and W have quadrupole deformation parameters $\beta \approx 0.25$, whereas those in the region of Pt and Au have $\beta \approx 0.15$. Using the parameters

---

[3] F. G. Perey, Phys. Rev. 131, 745 (1963).

[4] P. H. Stelson (private communication).

determined from the fits on Pb and Bi ($V_S = 53.5$ MeV, $W_D = 7.5$ MeV) but allowing for the symmetry term and Coulomb correction term in $V_S$, a two-channel calculation was done using a program previously described[5] with the quadrupole deformation parameters given above. The results are shown in Fig. 1. The agreement is satisfactory and the damping of the diffraction pattern clearly reproduced. Inelastic scattering for the quadrupole excitation of these nuclei is not available for comparison. However, elastic and inelastic scattering of 17-MeV protons from $Ho^{165}$ are in agreement[6] with the parameters obtained in this study.

It should be concluded that the observed behavior of the elastic scattering of 17-MeV protons from heavy nuclei is consistent with their known quadrupole deformations and that the increase in the imaginary part of the potential as a function of A, obtained in a previous study,[3] is probably due to the effects of quadrupole deformation.

I wish to express my thanks to Dr. T. Tamura for helpful discussions and to Dr. B. Buck for use of his coupled-equation program.

---

[5] B. Buck, Phys. Rev. 130, 712 (1963).

[6] T. Tamura (private communication).

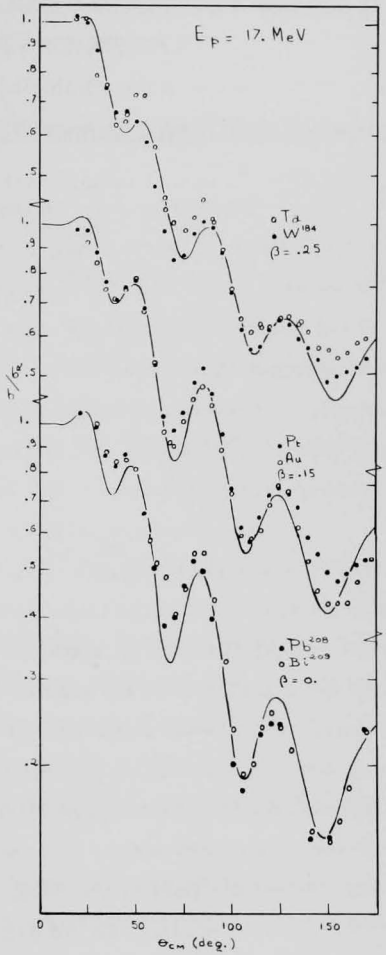


Fig. 1. Elastic differential cross sections of 17-MeV protons compared with coupled-channel calculations.

# C-3. THE PARITY RULE FOR INELASTIC SCATTERING AT SMALL ANGLES*

I. E. McCarthy

Department of Physics, University of California, Davis, California

The parity rule[1] states that for inelastic scattering in which the Q value is fairly small compared with the incident energy, the differential cross section decreases as the scattering angle approaches zero if the parity of the nuclear state is changed, and increases as the scattering angle approaches zero if the parity of the nuclear state is unchanged. If the angular-momentum transfer L is zero, the rule is slightly modified by saying that there is an energy for which the differential cross section increases with decreasing scattering angle.

The first part of the rule for odd L arises from a selection rule that is exact for forward scattering in the adiabatic limit, provided there is no space-exchange term in the direct-interaction potential. In realistic cases, the rule as stated is still true. The second part of the rule for even L is true if the elastic-scattering phase shifts obey certain conditions. The forward differential cross section arises from interference between different partial matrix elements $I^{M}_{L,\ell\ell'}$ in the distorted-wave Born approximation due to large differences in the phase shifts in each channel for successive values of $\ell$ near the surface value $\lambda$. The argument for the second part of the rule, while not involving a rigid selection rule, is roughly equivalent to the argument[2] for the Blair phase rule[3] for surface reactions.

*Supported by the U. S. Atomic Energy Commission.

[1] A. J. Kromminga and I. E. McCarthy, Phys. Rev. Letters 6, 62 (1961).

[2] See for example N. Austern, in Selected Topics in Nuclear Theory (International Atomic Energy Agency, Vienna, 1963), p. 39.

[3] J. S. Blair, in Proceedings of the International Conference on Nuclear Structure, Kingston, 1960 (University of Toronto Press, Toronto, 1960).

The differential cross section is given in the usual notation by

$$\frac{d\sigma}{d\Omega}(\theta) = (\mu/2\pi\hbar^2)^2 (k'/k)\Sigma_{av} |\mathcal{M}_L^M(\theta)|^2, \tag{1}$$

where, neglecting space exchange,

$$\mathcal{M}_L^M(\theta) = \Sigma_{\ell\ell'} I_{L,\ell\ell'}^M Y_{\ell'}^M(\theta,0). \tag{2}$$

We have the selection rule that $\ell + \ell' + L$ is even and $\ell$, $\ell'$, L obey triangle inequalities.

If the optical-model wave functions for the entrance and exit channels are identical, we have

$$I_{L,\ell\ell'}^M = (-1)^L I_{L,\ell'\ell}^M. \tag{3}$$

For a zero-range interaction in the case of a two-body collision mechanism, the space-exchange term vanishes; and it is quite small compared with the nonexchange term in a realistic case. For a collective excitation mechanism, the problem does not arise.

For odd L it is clear that $\mathcal{M}_L^M(0)$ vanishes if Eq. (3) is true.

For even $L \neq 0$, the forward cross section is zero if we approximate the optical-model wave functions by plane waves. For distorted waves, each partial wave has a phase which is approximately equal to the phase shift at values of the radius r where the wave function is large. (This phase is in addition to the phase $\ell\pi/2$ due to the factor $i^\ell$ in the partial-wave expansion.) For real potentials this is an exact result, well-known in potential-scattering theory.[4] The phase of $I_{L,\ell\ell'}^M$

---

[4] R. G. Newton, J. Math. Phys. 1, 319 (1960).

is therefore approximately $(\ell-\ell')\pi/2 + \delta_\ell + \delta_{\ell'}$. If the phase shifts for $\ell < \lambda$ are large, the terms in the sum (2) for $\ell, \ell' \lesssim \lambda$ do not cancel the terms for $\ell, \ell' \gtrsim \lambda$ as they do in the plane-wave case. In fact, the former terms (represented by vectors on an Argand diagram) are rotated by a large amount, thus reinforcing the latter terms.

The shape of the angular distribution at small angles can be understood as follows. Because of phase averaging for $\ell < \lambda$ and centrifugal repulsion for $\ell > \lambda$, only the terms with $\ell, \ell' \approx \lambda$ contribute appreciably to $\mathcal{M}_L^M$. The function $Y_{\ell'}^M(\theta,0)$ is proportional to the Mth derivative of $P_{\ell'}(\cos\theta)$ with respect to $\cos\theta$. For $M \neq 0$ it is very small at small angles and we need only consider $Y_{\ell'}^0(\theta,0)$ which is proportional to $P_{\ell'}(\cos\theta)$.

For L odd and $\cos\theta = 1$, the cross section is zero if Eq. (3) holds. It therefore increases as $1 - \cos\theta$ increases as long as the $P_{\ell'}(\cos\theta)$ for $\ell' \approx \lambda$ remain roughly in phase. For protons at about 20 MeV incident energy, the differential cross section usually increases up to about $40^\circ$, since $\lambda$ is about 4 or 5 for medium nuclei. For $\alpha$ particles of the same energy, $\lambda$ is about 8 to 10 and higher Legendre polynomials (which decrease more rapidly with increasing $\theta$) predominate. Hence the decrease of differential cross section can only be observed at small angles. This verifies the first part of the rule. For even $L \neq 0$, the main part of the forward cross section comes from $\ell' \approx \lambda$. It decreases like the average of $P_{\ell'}(\cos\theta)$ for $\ell' \approx \lambda$ as $\theta$ increases. Thus the second part of the parity rule is verified.

For L = 0 the forward cross section is large in the plane-wave approximation. For distorted waves it fluctuates with energy but there is always an energy for which it is large.

It is of great interest to do experiments at very small angles to see how well the parity rule is obeyed. Such experiments will throw a lot of light on the reaction mechanism.

However the present interest is to look at the importance of the parity rule in spectroscopy, where it is a very practical way of determining the parity of an excited state when that of the ground state is known.

It is interesting to compare the parity rule with the Blair phase rule which is another method of determining parities from inelastic scattering. The rules in fact give identical results at small angles for single-phonon excitations.

The phase rule is more easily applied to the inelastic scattering of heavier ions such as $\alpha$ particles because it requires the observation of several maxima and minima in the angular distribution and hence high surface values of $\ell$. On the other hand, the parity rule is more easily applied to the inelastic scattering of lighter ions such as protons because in this case one does not need to observe very small angles to see the increase or decrease of the cross section. Typical calculations for 44-MeV alpha-particle inelastic scattering with L = 2 or 4 show a decrease of cross section with decreasing angle down to $5^{\circ}$. The increase below $5^{\circ}$ is quite pronounced but difficult to observe in practice.

Two-phonon excitations have two main contributions. The direct two-phonon excitation term obeys the parity rule. The second-order Born-approximation term representing successive excitation of two one-phonon states obeys the parity rule only if the intermediate state can be regarded as adiabatic. However, it is such a strong rule that it appears to hold in these cases, at least in numerical calculations. It would be very interesting to see how well it holds in experiments.

The phase rule is not so easily applied to two-phonon excitations where interference between the two terms often results in a reversal of the phase of the angular distribution. For example a $4^{+}$ two-phonon excitation can have the same phase as a $3^{-}$ one-phonon excitation.

The parity rule can be used where the phase rule fails to distinguish these cases. It has been sucessfully applied, for example by Stoval and Hintz,[5] to the 3.16-MeV excited state of $Fe^{56}$ which it shows to be not a $3^-$ one-phonon excitation — although its angular distribution is in phase with the elastic scattering.

A detailed quantitative study of the range of Q values for which the parity rule gives useful results has not yet been made. However, in certain calculations for proton inelastic scattering with odd L, the cross section has been noticed to decrease with decreasing scattering angle for Q values at least as high as a quarter of the incident energy. This criterion might be useful as a rough guide. For even-L inelastic scattering of α particles, existing calculations show that the cross section increases as the scattering angle approaches zero if the Q value is not more than about 1/10 of the incident energy.

---

[5] T. Stovall and N. Hintz, University of Minnesota Linear Accelerator Laboratory Annual Progress Report, Nov. 1962 (unpublished), p. 37.

# C-4. THE DEUTERON-GAMMA ANGULAR CORRELATION IN THE REACTION $Mg^{24}(d, d'\gamma)Mg^{24+}$ (1.37 MeV) at 11.8 MeV

V. Jung and U. Schmidt-Rohr

Max-Planck-Institut für Kernphysik, Heidelberg, Germany

The angular distribution of inelastically scattered deuterons from the reaction $Mg^{24}(d, d'\gamma)Mg^{24}$ leading to the first excited state of $Mg^{24}$(1.37 MeV) was measured in coincidence with the $\gamma$ rays on the normal to the reaction plane. The collimating aperture of the $\gamma$ detector, a 3x3-in. NaI crystal, subtends an effective half angle of 20°, the deuteron detector a half angle of 2.8°. The deuteron detector was a 250-$\mu$-thick CsI crystal. The energy of the scattered deuterons was degraded by aluminum foils to the extent that the inelastic deuterons were just stopped in the crystal. The inelastic deuteron line appears in this way on the high-energy side of the pulse-height spectrum of the detector and the low-energy part of the pulses could be suppressed by cable clipping according to their longer rise time. The coincidence circuit was a usual fast-slow system.

The result, the ratio of inelastic deuterons in coincidence with 1.37-MeV $\gamma$ rays to noncoincident inelastic deuterons, is plotted in Fig. 1 as a function of the scattering angle. The plotted errors are relative standard deviations. The additional absolute scale error is $\pm$10%.

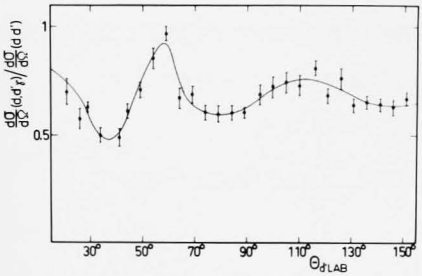


Fig. 1. Ratio of inelastic deuterons in coincidence with $\gamma$ rays on the normal to the reaction plane to noncoincident inelastic deuterons $\frac{d\sigma}{d\Omega}(d,d'\gamma)/\frac{d\sigma}{d\Omega}(d,d')$ normalized to the efficiency of the $\gamma$-ray detector. A ratio of unity would correspond to an isotropic $\gamma$ distribution.

The measured angular distribution shows a marked structure, in which the number and sharpness of the maxima are similar to distributions calculated by Satchler et al.[1] for the $p'\gamma$ correlation from inelastic scattering of 16-MeV protons on $Mg^{24}$. From a comparison of the distributions, it can be concluded that the probability for spin-flip in inelastic deuteron scattering is not very large.

---

[1] G. R. Satchler, R. M. Drisko, and R. H. Bassel, Bull. Am. Phys. Soc. 6, 66 (1961).

# C-5. EXCITATION OF $T = T_z + 2$ STATES*

G. T. Garvey and B. F. Bayman

Princeton University, Princeton, New Jersey

In view of the recent interest in isobaric-analogue states, it is pertinent to consider reactions that could lead to states with $T = T_z + 2$ units of isobaric spin. To our knowledge, such states have never been observed. In heavier nuclei where the purity of isobaric spin is expected to decrease, these states can still be considered simply as analogues to the low-lying states of the isobar with $T_z' = T_z + 2$.

Consider the (p, t) reaction in a case in which the $T_z$ of the target is greater than 1/2 and $T_i = T_z$. The isobaric spin of the ground state of the final nucleus will be $T_f = T_i - 1$. The 1/2 unit of isobaric spin both for the incoming proton and for the outgoing triton will allow us to reach final states of isobaric spins $T_f = T_i + 1$, $T_i$, $T_i - 1$. The states with $T_f = T_i + 1$ are the ones of interest. Equivalent isobaric-spin selection rules hold for the (p, n) reaction. However, if its mechanism is simple charge exchange (sending $\psi_{T_z}^{T_i}$ into $T_- \psi_{T_z}^{T_i}$), we only reach states with $T_f = T_i$. It appears to us that two-neutron pickup reactions are the only ones that will excite $T = T_z + 2$ states in a first-order process.

Although these states may be expected to lie at rather high excitation energy, as is shown in Table I, they will probably not be particle unstable. This is illustrated in Fig. 1 for mass 16. The isobaric-spin-allowed one-particle decays of the T=2 states must proceed through the T=3/2 states in $O^{15}$ or $N^{15}$, which apparently

---

*Work supported by the U. S. Atomic Energy Commision and the Higgins Scientific Trust Fund.

TABLE I. (p, t) Excitation of the lowest $T = T_z + 2$ in some even-even nuclei. Column 2 presents excitation energies derived from mass differences, corrected for Coulomb energy differences. Columns 3, 4, and 5 were calculated from the wave functions of J. D. McCullen, B. F. Bayman, and L. Zamick, Phys. Rev. (to be published). In column 4, $S_{gs}$ is the spectroscopic factor for the excitation of the ground state.

| (1) Final nucleus | (2) Energy of $T = T_z+2$ (MeV) (from Coulomb energy differences) | (3) Energy of $T = T_z+2$ (MeV) (from M. B. Z.) | (4) $S_{gs}$ | (5) $S_{T=T_z+2}$ |
|---|---|---|---|---|
| $O^{16}$ | 23.1 | | | |
| $Ne^{20}$ | 16.6 | | | |
| $Mg^{24}$ | 15.4 | | | |
| $Ti^{44}$ | 9.8 | 8.3 | 1.02 | 0.11 |
| $Ti^{46}$ | 14.02 | 12.9 | 1.16 | 0.06 |
| $Ti^{48}$ | 16.8 | 16.8 | 0.83 | 0.04 |
| $Cr^{50}$ | 13.0 | 12.9 | 0.68 | 0.10 |
| $Fe^{52}$ | 8.46 | 8.3 | 0.58 | 0.25 |

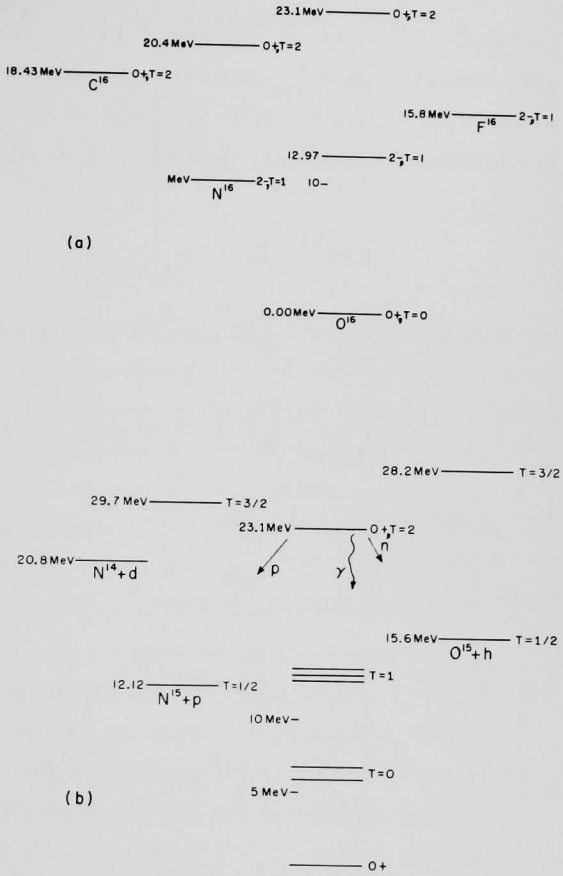


Fig. 1. (a) Lowest lying energy levels of specified T in the mass-16 system based on the energy of the ground state of the $T=T_Z$ member. (b) Lowest lying levels to be considered in the decay of the T=2 states of $O^{16}$. Note that all isotopic-spin-allowed modes of particle decay require more energy than the lowest lying T=2 level.

lie at high enough energies to make these modes of decay improbable. Alpha-particle decay is also forbidden and the energetics of 2-particle emission are also unfavorable.

If we wish to estimate the strengths of transitions to $T_f = T_i + 1$ states, we require the corresponding nuclear wave functions. We will consider the region $20 \leqslant Z, N \leqslant 28$, where wave functions have

calculated,[1,2] on the assumption that the nucleons outside the $Ca^{40}$ core remain in the $1f_{7/2}$ shell and interact via the two-nucleon force whose $1f_{7/2}$ matrix elements are given by the spectrum of $Sc^{42}$. On this picture, for example, the $Fe^{54}$ ground state has the wave function

$$\psi(Fe^{54}\ I=0) = \psi_{p_1 \ldots p_6}\left(\frac{7}{2}^{-2}\ J_p=0\right)\ \psi_{n_1 \ldots n_8}\left(\frac{7}{2}^{8}\ J_n=0\right),$$

whereas states in $Fe^{52}$ with angular momentum L have wave functions

$$\psi(Fe^{52}\ \alpha\ LM) = \sum_{J_p, J_n} C^{\alpha L}_{J_p J_n}\left[\psi_{p_1 \ldots p_6}\left(\frac{7}{2}^{-2}\ J_p\right)\ \psi_{n_1 \ldots n_6}\left(\frac{7}{2}^{-2}\ J_n\right)\right]^L_M .$$

Here $\alpha$ distinguishes the different $Fe^{52}$ states with total angular momentum L, and the $C^{\alpha L}_{J_p J_n}$ are the eigenvector components calculated by McCullen, Bayman and Zamick.[2] Then we can write

$$\begin{aligned}
\psi(Fe^{54}\ I=0) &= \psi_{p_1 \ldots p_6}\left(\frac{7}{2}^{-2}\ J_p=0\right)\ \psi_{n_1 \ldots n_6}\left(\frac{7}{2}^{8}\ J_n=0\right) \\
&= \sum_L \left(\frac{7}{2}^{-2}\ L; \frac{7}{2}^{-2}\ L\ |\}\ \frac{7}{2}^{8}\ 0\right)\left\{\left[\psi_{p_1 \ldots p_6}\left(\frac{7}{2}^{-2}\ J_p=0\right)\right.\right. \\
&\qquad \left.\left.\times\left(\psi_{n_1 \ldots n_6}\ \frac{7}{2}^{-2}\ L\right)\right]^L \psi_{n_7 n_8}\left(\frac{7}{2}^{2}\ L\right)\right\}^0_0 \\
&= \sum_L \left(\frac{7}{2}^{-2}\ L; \frac{7}{2}^{-2}\ L\ |\}\ \frac{7}{2}^{8}\ 0\right)\ C^{\alpha L}_{0L} \\
&\qquad \times\left\{\psi_{p_1 \ldots n_6}(Fe^{52}\ \alpha L)\ \psi_{n_7 n_8}\left(\frac{7}{2}^{2}\ L\right)\right\}^0_0 ,
\end{aligned}$$

---

[1] J. Ginocchio and J. B. French, Phys. Letters 7, 137 (1963).

[2] J. D. McCullen, B. F. Bayman, and L. Zamick, Phys. Rev. (to be published).

and the (p, t) spectroscopic factor for the excitation of $\psi(Fe^{52}\ \alpha\ I)$ is accordingly

$$S_{\alpha I} = \frac{8\cdot 7}{2}\left(\frac{7}{2}^{-2}\ I;\ \frac{7}{2}^{-2}\ I\ |\}\ \frac{7}{2}^{8}\ 0\right)^2 \left[C^{\alpha I}_{0I}\right]^2$$

$$= (2I+1)\left[C^{\alpha I}_{0I}\right]^2 .$$

For the ground state ($\alpha = 1$, $I = 0$) of $Fe^{52}$, $\left[C^{10}_{00}\right]^2 = 0.58$; for the $T = 2$ state ($\alpha = 3$, $L = 0$) that is the analogue of the $Cr^{52}$ ground state, $\left[C^{30}_{00}\right]^2 = 0.25$. Thus the spectroscopic factor for the excitation of the lowest T=2 state is almost half that for the excitation of the T=0 ground state. Table I summarizes our estimates of excitation energies and spectroscopic factors for the lowest $T = T_z + 2 = T_i + 1$ states in even-even nuclei. In all the cases we have considered, the spectroscopic factor for the $T = T_i + 1$ state is sufficiently greater than that of adjacent states so that the $T = T_i + 1$ state should be detectable.

A study of the electromagnetic decay of $T = T_i + 1$ states should provide information about their isobaric-spin purity. The $\Delta T = 0, \pm 1$ selection rule for electromagnetic transitions allows decay to the $T=T_i$ states, but forbids decay to the energetically favored $T = T_i - 1$ states. Thus the decays of the $T = T_i + 1$ states would be very sensitive to admixtures of components with lower isobaric spin.

# C-6. ANALYSIS OF ELASTIC AND INELASTIC SCATTERING OF 40-MeV PROTONS*

Martin P. Fricke

University of Minnesota, Minneapolis, Minnesota

Elastic-scattering angular distributions[1] of 40-MeV protons from $Fe^{54}$, $Fe^{56}$, $Ni^{58}$, $Ni^{60}$, and $Pb^{208}$, over the angular range from 10° to 100°, were analyzed in terms of an optical-model potential with the aid of an automatic parameter-search routine[2] using a least-squares criterion. Figure 1 shows a typical example of the fits obtained, and Table I lists the parameters for the potential

$$U = -V\left(\frac{1}{e^{x}+1}\right) - i\left(W - W'\frac{d}{dx'}\right)\left(\frac{1}{e^{x'}+1}\right)$$

$$- \left(\frac{\hbar}{m_{\pi}c}\right)^{2} (V_s + iW_s)\, \vec{\sigma}\cdot\vec{\ell}\, \frac{1}{r}\frac{d}{dr}\left(\frac{1}{e^{x}+1}\right)$$

$$+ \begin{cases} \dfrac{Ze^2}{r} & \text{for} \quad r > R_c, \\[2ex] \dfrac{Ze^2}{2R_c}\left(3 - \dfrac{r^2}{R_c^{\,2}}\right) & \text{for} \quad r \leq R_c, \end{cases}$$

$$x = \frac{r-R}{a}, \qquad x' = \frac{r-R'}{a'}, \qquad R = r_0 A^{1/3}, \qquad R' = r_0' A^{1/3},$$

---

* Research supported in part by the U.S. Atomic Energy Commission.

[1] M. K. Brussel and J. H. Williams, Phys. Rev. 114, 525 (1959).

[2] R. M. Drisko (unpublished).

TABLE I. Optical-model parameters and calculated reaction cross sections for elastic scattering of 40-MeV protons.

| Nucleus | V | W | W' | $V_s$ | $W_s$ | $r_0$ | $r_0'$ | $r_c$ | a | a' | $\sigma_R$(mb) |
|---|---|---|---|---|---|---|---|---|---|---|---|
| $Fe^{54}$ | 44.8 | 8.1 | 0 | 6.51 | 0 | 1.169 | 1.403 | 1.2 | 0.7553 | 0.4405 | 938 |
| $Fe^{54}$ | 45.9 | 0 | 34.9 | 7.40 | 0 | 1.164 | 1.043 | 1.2 | 0.6935 | 0.6947 | 940 |
| $Fe^{56}$ | 43.5 | 6.5 | 0 | 6.37 | 0 | 1.173 | 1.451 | 1.2 | 0.7361 | 0.7582 | 1055 |
| $Fe^{56}$ | 44.3 | 0 | 30.4 | 7.43 | 0 | 1.180 | 1.028 | 1.2 | 0.7026 | 0.8045 | 1015 |
| $Ni^{58}$ | 39.6 | 9.57 | 0 | 4.50 | 0 | 1.251 | 1.387 | 1.2 | 0.7604 | 0.2537 | 986 |
| $Ni^{58}$ | 44.5 | 0 | 43.2 | 10.3 | 0 | 1.165 | 1.027 | 1.2 | 0.7471 | 0.6035 | 957 |
| $Ni^{60}$ | 44.3 | 7.1 | 0 | 6.52 | 0 | 1.165 | 1.459 | 1.2 | 0.7545 | 0.5937 | 1067 |
| $Ni^{60}$ | 44.7 | 0 | 39.6 | 7.54 | 0 | 1.184 | 1.056 | 1.2 | 0.7074 | 0.6528 | 1021 |
| $Cu^{65}$ | 44.4 | 6.3 | 0 | 7.90 | 0 | 1.150 | 1.535 | 1.2 | 0.7765 | 0.7794 | . . . |
| $Cu^{65}$ | 44.9 | 0 | 39.6 | 7.52 | 0 | 1.163 | 0.973 | 1.2 | 0.8059 | 0.8184 | 1165 |
| $Pb^{208}$ | 51 | 8.0 | 0 | 6.6 | 0 | 1.20 | 1.428 | 1.2 | 0.65 | 0.704 | . . . |
| $Pb^{208}$ | 49 | 0 | 72.4 | 5.7 | 0 | 1.21 | 1.230 | 1.2 | 0.77 | 0.551 | . . . |

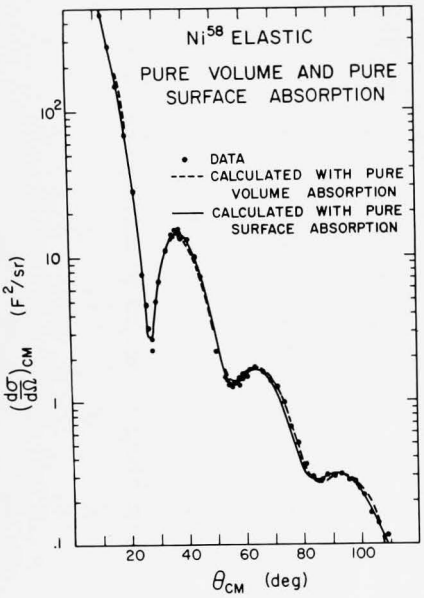


Fig. 1. Elastic scattering from $Ni^{58}$.

where all energies are in MeV and all lengths in fermis. The elastic scattering is best described using radii for the real potential whose average for these nuclei is $1.18 \times A^{1/3}$ fm, as opposed to the value of $1.25 \times A^{1/3}$ fm used at low energies.[3] Both surface and volume forms of the imaginary central potential are found to describe these data with equal success.

The inelastic scattering from these nuclei was then calculated in distorted-wave Born approximation assuming collective excitations to $2^+$ and $3^-$ states, and transition strengths were obtained by comparison

---

[3] F. G. Perey, Phys. Rev. 131, 745 (1963).

with the data.[4] The inelastic-scattering calculations also are not appreciably different for surface and volume forms of absorption in the distorting potential.

While the elastic-scattering calculations agree excellently with experiment, calculations of the inelastic scattering using a real interaction form factor based on the collective model[5] show significant deviations from experiment. Agreement was restored for $Fe^{54}$ and $Pb^{208}$ by using a complex interaction, obtained by also allowing the imaginary central part of the optical-model potential to be nonspherical (with equal deformabilities for the real and imaginary parts). Typical examples of the fits to quadrupole and octupole inelastic scattering obtained with the real interaction are shown in Figs. 2 and 3, and Table II lists the corresponding deformabilities $\beta_\ell$.[5] Figure 4 shows the improvement obtained in scattering from $Pb^{208}$ when the imaginary potential is also deformable.

In the case of $Ni^{58}$, polarization measurements are also available. In Fig. 5 these are compared with the predictions of the optical model obtained by fitting the elastic-cross-section data alone. Corrections for the experimentally unresolved inelastic polarization were made but found to be quite small.

Acknowledgments

The author wishes to express his thanks to Drs. G. R. Satchler, R. H. Bassel, and R. M. Drisko of the Oak Ridge National Laboratory for their considerable efforts and patient instruction in all phases of the analysis.

---

[4] T. Stovall, Ph.D. Thesis, University of Minnesota (1962); Proceedings of the Rutherford Jubilee International Conference, Manchester, 1961, edited by J. B. Birks (Heywood and Co., Ltd., London, 1961).

[5] R. H. Bassel, G. R. Satchler, R. M. Drisko, and E. Rost, Phys. Rev. 128, 2693 (1962).

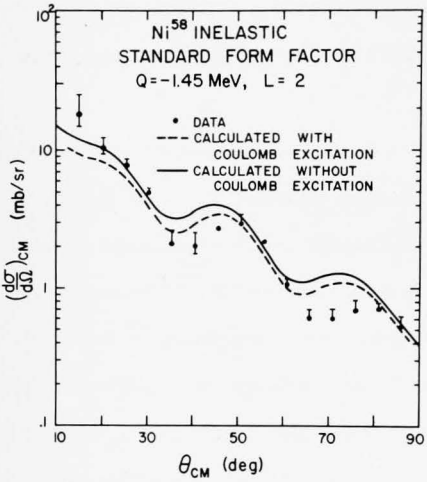


Fig. 2. Quadrupole inelastic scattering from $Ni^{58}$ using real interaction.

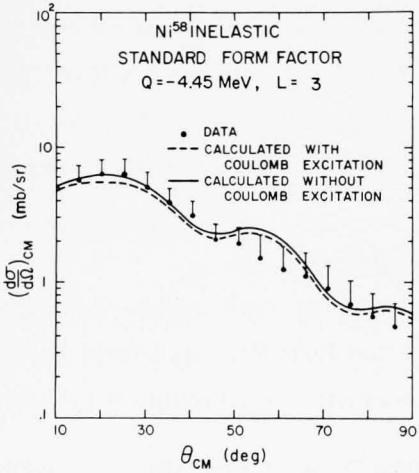


Fig. 3. Octupole inelastic scattering from $Ni^{58}$ using real interaction.

TABLE II. Angular momenta and deformabilities determined from inelastic scattering of 40-MeV protons.

| Nucleus | Q(MeV) | $\ell$ | $\beta_\ell$ |
|---|---|---|---|
| $Fe^{54}$ | -1.34 | 2 | 0.17 |
| $Fe^{54}$ | -2.97 | 2 | 0.17 |
| $Fe^{54}$ | -4.72 | 3 | 0.12 |
| $Fe^{54}$ | -6.40 | 3 | 0.17 |
| $Fe^{56}$ | -3.16 | 2 | 0.1 |
| $Fe^{56}$ | -4.66 | 3 | 0.2 |
| $Ni^{58}$ | -1.45 | 2 | 0.20 |
| $Ni^{58}$ | -4.45 | 3 | 0.20 |
| $Ni^{60}$ | -1.36 | 2 | 0.23 |
| $Ni^{60}$ | -2.55 | 3 or 4 | $\beta_3 = 0.09$ |
| | | | $\beta_4 = 0.07$ |
| $Ni^{60}$ | -4.05 | 3 | 0.18 |
| $Ni^{60}$ | -5.13 | 2 or 4 | $\beta_2 = 0.14$ |
| | | | $\beta_4 = 0.11$ |
| $Pb^{208}$ | -2.62 | 3 | 0.14 |

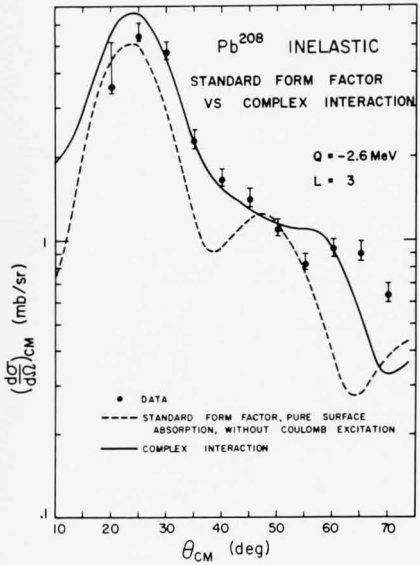


Fig. 4. Octupole inelastic scattering from $Pb^{208}$ using real and complex interactions.

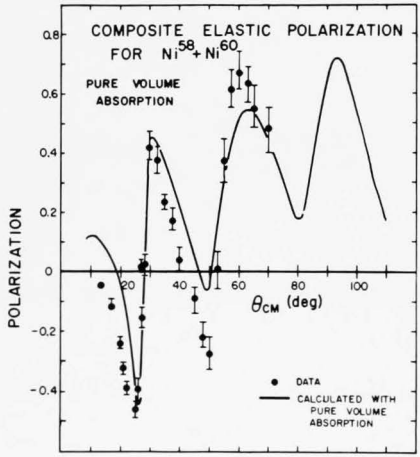


Fig. 5. Composite elastic polarization for natural nickel from calculations for $Ni^{58}$ and $Ni^{60}$.

# C-7. SPECTROSCOPIC DATA DEDUCED FROM INELASTIC SCATTERING OF 44-MEV ALPHA PARTICLES IN MEDIUM-WEIGHT NUCLEI

H. Faraggi and J. Saudinos

Centre d'Etudes Nucleaires de Saclay (Seine et Oise), France

In the last few years, our group in Saclay[1] has been accumulating experimental data on levels excited by ($\alpha, \alpha'$) reactions in several isotopes of iron (54, 56, 58), nickel (58, 60, 62, 64), and zinc (64, 66, 68).

Assuming the validity of the Drozdov-Blair-Sharp-Wilets[2] inelastic diffractional model, which fits the present results very well, it was possible to obtain the spins, parities, and reduced radiative width $B(E\ell)$ of excited states up to 6 MeV. Those data show strong nuclear regularities, especially as to the variation with mass number of the position and $B(E\ell)$ values, not only of the first quadrupole excitation, which is an already well known characteristic, but also of the first octupole state. However, the observed phase relationships of the second $2^+$ (2' states) and the first $4^+$ states exhibit some features difficult to understand in the two-phonon picture.

---

[1] G. Bruge, J. C. Faivre, M. Barloutaud, H. Faraggi, and J. Saudinos, Phys. Letters 7, 203 (1963); 6, 222 (1963); M. Barloutaud et al., Proceedings of the Conference on Direct Interactions and Nuclear Reaction Mechanisms, Padua, Italy, September 3-8, 1962 (Gordon and Breach Science Publishers, New York, 1963), p. 765.

[2] S. I. Drozdov, Soviet Phys. — JETP 36, 1875 (1959); J. S. Blair, Proceedings of the Conference on Direct Interactions and Nuclear Reaction Mechanisms, Padua, Italy, September 3-8, 1962 (Gordon and Breach Science Publishers, New York, 1963), p. 669; J. S. Blair, D. Sharp, and L. Wilets, Phys. Rev. 125, 1625 (1962).

Basic experimental facts and assumptions used in interpretation of the data are the following. The inelastic scattering of medium-energy α particles leads to the strong excitation of only a small number of levels in the explored range of energies (below 6 MeV). The measured angular distributions exhibit the characteristic diffraction pattern, with well defined phase relations, often called the Blair Phase Rule. In fact, there are two different "Blair Phase Rules": (a) for the most strongly excited states, Blair Phase Rule No. 1 (BPRI) is obeyed, i.e., the oscillations of their angular-distribution curves are in phase or out of phase with the elastic one depending on whether they have negative or positive parity; and (b) on the other hand, for weakly excited states, sometimes BPRI is obeyed and sometimes the reverse of this phase rule is observed. This reversal of the phase rule for the 2' and first $4^+$ state is obtained by Blair[3] as a consequence of a double excitation process. We shall call it BPRII; in principle it should be observed for all two-phonon states.

As a test of these assumptions, satisfactory agreement, within all approximations involved, is obtained between $B(E\ell)$ values deduced from this type of $(\alpha, \alpha')$ analysis and values obtained either by Coulomb excitation or inelastic electron scattering (see Table I).

The results so obtained are presented in Fig. 1. Positive-parity excited states (labeled by triangles) and negative-parity excited states (labeled by straight lines) follow BPRI. Positive-parity excited states labeled by straight lines follow BPRII. For states obeying BPRI the enhancement factor G of the $B(E\ell)$, in Weisskopf units, is given.

---

[3] J. S. Blair, Proceedings of the Rutherford Jubilee International Conference, Manchester, 1961, edited by J. B. Birks (Heywood and Co., Ltd., London, 1961), p. 475.

TABLE I. Comparison of the different values obtained for the "deformation parameter" $\beta_\ell \approx \sqrt{B(E\ell)}$ by several experimental approaches.

| | $J^\pi$ | E (MeV) | $(\alpha,\alpha')$[a] | (p,p') | (e,e') | C.E.[g] |
|---|---|---|---|---|---|---|
| $Fe^{54}$ | $2^+$ | 1.39 | 0.14 | 0.14 | 0.15 | |
| | 2' | 2.94 | 0.12 | 0.13[b] | 0.11[e] | |
| $Fe^{56}$ | $2^+$ | 0.83 | 0.27 | | 0.19 | 0.22 |
| | 2' | 2.57 | 0.07 | | 0.07[e] | |
| | $3^-$ | 4.37 | 0.11 | | 0.10 | |
| $Fe^{58}$ | $2^+$ | 0.806 | 0.25 | 0.17[c] | | |
| | 2' | 1.66 | 0.06 | | | |
| | $3^-$ | 3.8 | 0.07 | | | |
| | $3^-$ | 4.46 | 0.07 | | | |
| $Ni^{58}$ | $2^+$ | 1.45 | 0.31 | 0.15[c] | 0.16[f] | 0.187 |
| | 2' | 2.94 | 0.06 | | 0.09 | |
| | $3^-$ | 4.39 | 0.13 | | 0.21 | |
| $Ni^{60}$ | $2^+$ | 1.33 | 0.28 | | 0.17[f] | 0.204 |
| | $3^-$ | 4.1 | 0.13 | | 0.25 | |
| $Ni^{62}$ | $2^+$ | 1.17 | 0.19 | 0.28[d] | | 0.190 |
| $Ni^{64}$ | $2^+$ | 1.34 | 0.17 | 0.23[d] | | |
| $Zn^{64}$ | $2^+$ | 0.99 | 0.35 | | | 0.25 |
| | $3^-$ | 2.93 | 0.15 | | | |

[a] Reference 1.

[b] H. O. Funsten et al. (preprint).

[c] P. Darriulat et al., UCRL-11054.

[d] See Reference 5.

[e] J. Bellicard et al., Nucl. Phys. 36, 476 (1962).

[f] H. Crannell et al., Phys. Rev. 125, 923 (1961).

[g] P. H. Stelson and F. K. MacGowan, Nucl. Phys. 32, 652 (1962).

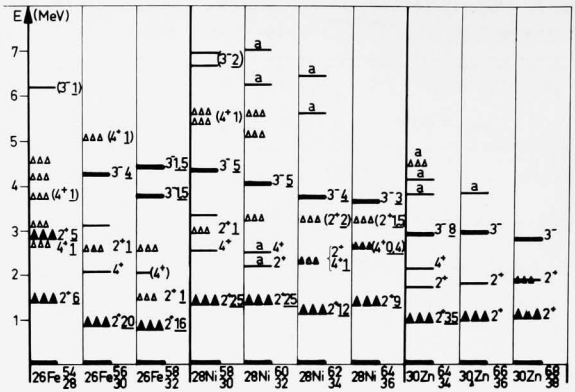


Fig. 1. Each excited level is placed at its excitation energy and is followed by its spin and parity (parentheses indicate $J^{\pi}$ values deduced only from the present analysis), and by the enhancement factor G in Weisskopf units. For each nucleus, strong lines and filled triangles indicate strongly excited levels. Straight lines are characteristic of angular-distribution oscillations in phase with that of the ground state; lines of triangles are characteristic of angular-distribution oscillations out of phase with it. The levels labeled (a) have been taken from Argonne experiments [H. W. Broek, Phys. Letters 3, 132 (1963); Phys. Rev. 130, 1914 (1963] and are included here to make this survey more complete.

The first $2^+$ and $3^-$ states exhibit large G values with smooth variation from nucleus to nucleus. In $Fe^{58}$, it should be noticed that the octupole excitation is shared equally between two neighboring states. In $Fe^{54}$, the first $2^+$ level is very weakly excited, while the 2' state is as strongly excited as the first one; also, in that nucleus, the $3^-$ state has not been observed in the expected energy region in our experiments, so that the excited level scheme of $Fe^{54}$ does not appear very similar to the others.

Between the first $2^+$ and the $3^-$ states, we usually found 3 levels less strongly excited, the behavior of which is particularly interesting because it appears somewhat like a puzzle in the framework of the

vibrational model. A detailed discussion of this intermediate region has already been given[1] and we shall summarize its features.

(1) The first $4^+$ state follows BPRI in $Fe^{54}$, $Ni^{62}$, and $Ni^{64}$ and follows BPRII in $Fe^{56}$, $Ni^{58}$, $Ni^{60}$, and $Zn^{64}$. In BPRII the cross section of the $4^+$ state is entirely determined by that of the first $2^+$ state. This is quite well verified by the present results. But it must also be concluded then that in $Fe^{54}$, $Ni^{62}$, and $Ni^{64}$, where BPRI applies, the single one-phonon excitation is strongly predominant.

(2) Looking now at the 2' levels, we see that BPRII is followed by $Ni^{60}$, $Zn^{64}$, and $Zn^{66}$, and that BPRI is followed by $Fe^{54}$, $Fe^{56}$, $Ni^{58}$, $Ni^{62}$, and $Ni^{64}$ (while in $Zn^{68}$ no strong oscillations are apparent). For these 2' states, an experimental correlation can be established between the two different observed phase rules and the experimentally measured ratios of cross-over to cascade for the de-excitation of these states; BPRII is observed when the cross-over is strongly forbidden (in accordance with the simplest harmonic-oscillator version of the vibrational picture), while BPRI is observed when the cross-over is not too strongly forbidden (for $Zn^{68}$, an intermediate value of the ratio is observed).

(3) The third observed state, if it is assumed to follow BPRI, is of negative parity in $Fe^{56}$ and $Ni^{58}$ and of positive parity (probably $2^+$) in all other nuclei. The G factor is of the order of unity.

Above the octupole level, a few states are also excited. If one assumes the validity of BPRI, there is some evidence for a systematic $4^+$ state around 5 MeV and of several $3^-$ states between 6 and 7 MeV, with G factors of the order of unity.

There is usually good agreement between $(\alpha, \alpha')$, $(e, e')$ and $(p, p')$ results except for the $3^-$ level[4] of $Fe^{54}$ and the interpretation of the mode of excitation of the 2' and $4^+$ states of $Ni^{62}$ and $Ni^{64}$.[5]

The present survey shows that the prediction of the two-phonon picture for the phase reversal is not verified overall. This may not be very surprising since the validity of the adiabatic approximation and of the vibrational model is not firmly established in that nuclear region. As a matter of fact, a model of interaction quasi-particles is able to reproduce the positions of the observed $2^+$, 2', and $4^+$ states.[6]

It seems of great interest to calculate cross sections and angular distributions by use of the more fundamental approach of the BCS and RPA theory.

---

[4] J. Bellicard and P. Barreau, Nucl. Phys. 36, 476 (1962).

[5] J. K. Dickens, F. G. Perey, R. J. Silva, and T. Tamura, Phys. Letters 6, 53 (1963).

[6] Arvieu and Veneroni, Phys. Letters (to be published).

# C-8. ISOBARIC ANALOGUE STATES AND INTERMEDIATE RESONANCES IN NUCLEI*

S. Fallieros†

Laboratory for Nuclear Science, Massachusetts Institute of Technology, Cambridge, Massachusetts

Elastic proton-scattering experiments, as well as measurements of the associated (p,n) reaction cross sections were recently performed by Fox et. al.[1] At incident-proton energies corresponding to the excitation of the isobaric-analogue states[2,3] in the compound system, characteristic resonance peaks were observed. A discussion of the mechanism responsible for the appearance of these resonances is the subject of this paper. The example of the analogue in $Y^{89}$ of the ground state of $Sr^{89}$ will be studied as an illustration. The simplified language of the pure shell model will be used in the following; complications due to additonal

---

*Supported by AEC Contract AT(30-1) - 2098.

†On leave from the Bartol Research Foundation, Swarthmore, Pennsylvania.

[1] J. D. Fox, C. F. Moore, and D. Robson, preprint. See also recent reports in Bull. Am. Phys. Soc. 9, 106 and 107 (1964).

[2] The existence and properties of the isobaric-analogue states were originally established in (p,n) reaction experiments by Anderson et. al. See for example, J. D. Anderson, C. Wong, and J. W. McClure, Phys. Rev. 120, 2170 (1962).

[3] Theoretical discussions on the properties of analogue states by Lane and Soper, French and Macfarlane, Ikeda, Fujii, and Fujita, and Pinkston are available in the literature.

correlations have been considered largely irrelevant for the validity of our arguments. Accordingly, the ground state of $Sr^{88}$ is assumed to contain filled proton and neutron levels up to and including the $p_{3/2}$ subshell, with the $p_{1/2}$ and $g_{9/2}$ levels occupied only by neutrons. The nucleus $Sr^{89}$ then contains an additional $d_{5/2}$ neutron bound by $\sim$ 6.5 MeV. The Q value for the excitation of the analogue state in $Y^{89}$ by a (p,n) reaction on $Sr^{89}$ is known[1,2] to be 11.8 MeV, corresponding[1] to an excitation energy in $Y^{89}$ of $\sim$ 12.5 MeV. In the elastic proton scattering experiment on $Sr^{88}$, Fox et al. observed a peak at an incident energy of 5.1 MeV. The following remarks are discussed.

1. A single-particle interpretation is incompatible both with the widths ($\sim$10 keV) and the positions of the observed resonances. Such an interpretation assumes that the difference in binding between the last neutron (the $d_{5/2}$ neutron is $Sr^{89}$) and a proton of the same configuration ($d_{5/2}$ proton in $Y^{89}$) is exactly equal to the Coulomb energy difference between the two neighboring nuclei. The single-proton level will then lie in the continuum and will be responsible for the observed resonance.

In general, however, since a proton and a neutron interact quite differently with the (N - Z) neutrons in a nucleus (e.g., the attractive triplet-even interaction is allowed for the proton but not for the neutron), one should expect the distance between corresponding proton and neutron levels to be smaller than the Coulomb energy difference. In $Y^{89}$, for example, the energy of the first excited state is 0.9 MeV and presumably characterizes the distance between the $p_{1/2}$ and $g_{9/2}$ subshells. The above assignment would then imply the $d_{5/2}$ level, which is the next single-particle level in order, lies more than 10 MeV higher. This is an unreasonably high energy, in particular

when compared with the difference in binding ($\sim$5 MeV) between a $g_{9/2}$ and a $d_{5/2}$ neutron in the same nucleus.

2. Already familiar properties of the analogue states[2,3] imply that the observed resonant states contain only a small and nonresonant single-particle (single-proton) component and consist mainly of three-quasiparticle configurations (one proton, one neutron, and one neutron hole, relative to the ground state of the target nucleus). This follows the assumed similarity in the symmetry properties (isotopic spin) between the analogue and the ground state of a pair of neighboring nuclei. Writing, for example, $|Sr^{88}\rangle = |T, T_3\rangle$ to represent the ground state of $Sr^{88}$ with $T = -T_3 = \frac{1}{2}(N - Z) = 6$ and $d_{5/2}(n)\ |Sr^{88}\rangle = |T + \frac{1}{2}, T_3 - \frac{1}{2}\rangle$ for the ground state of $Sr^{89}$, we obtain the analogue state in $Y^{89}$ by direct application of the isotopic-spin raising operator:

$$T_+\ |T + \tfrac{1}{2}, T_3 - \tfrac{1}{2}\rangle = \sqrt{2T + 1}\ |T + \tfrac{1}{2}, T_3 + \tfrac{1}{2}\rangle$$

$$= \{d_{5/2}(p) + \sqrt{10}\ [g_{9/2}(p)\ g^{-1}_{9/2}(n)]_0\ d_{5/2}(n)$$

$$+ \sqrt{2}\ [p_{1/2}(p)\ p^{-1}_{1/2}(n)]_0\ d_{5/2}(n)\ \}\ |Sr^{88}\rangle,$$

where, for example, $[g_{9/2}(p)\ g^{-1}_{9/2}(n)]_0$ denotes a $g_{9/2}$ proton and a $g_{9/2}$ neutron hole coupled to angular momentum zero. The amplitudes $\sqrt{10}$ and $\sqrt{2}$ represent the number of excess neutrons available in each subshell. It is worth emphasizing the large amplitudes favouring the three-quasiparticle components as well as the fact that the energy of the resulting state is now equal to the Coulomb energy difference as is required by the charge independance of the nuclear interactions. This is reflected in the above wave function by the particular coherent mixing of the various configurations and does not impose any similar

requirement on the single-particle energies of these configurations.

3. The three-quasiparticle interpretation of the analogue-state resonances appears to provide a particularly simple example of an intermediate type of resonance proposed recently by Kerman et al.[4,5] The three-quasiparticle states then correspond exactly to the doorway states suggested by Feshbach and Block.[6] It follows from arguments essentially identical to those given by the above mentioned authors that the widths for nucleon emission of the analogue states will be significantly narrower than the corresponding single-particle widths. On the other hand, the coupling of these states to more complicated compound states of the system[4,6] should, in our case, be considerably inhibited[3] since it can be caused only by the isotopic-spin-violating Coulomb interactions.

The author wishes to express his gratitude to Professor Arthur Kerman for several stimulating discussions. Thanks are also due to Dr. S. Shafroth for conversations on the properties of the analogue states as well as for providing a preprint of the work by Fox et al. Discussions with Professor H. Feshbach on the properties of doorway states are also gratefully acknowledged.

---

[4] A. K. Kerman, L. S. Rodberg, and J. E. Young, Phys. Rev. Letters 9, 422 (1963).

[5] A different description of intermediate resonances has been given by K. Izumo, Progr. Theoret. Phys. (Kyoto) 26, 807 (1961).

[6] B. Block and H. Feshbach, Ann. Phys. (N. Y.) 23, 47 (1963).

# C-9. ANGULAR MOMENTUM SELECTION AND ANGULAR CORRELATIONS IN DIRECT REACTIONS WITH STRONGLY ABSORBED PARTICLES*

J. G. Wills and J. G. Cramer, Jr.

Physics Department, Indiana University
Bloomington, Indiana

It is known that in the inelastic scattering of alpha particles from nuclei, only a few angular momentum values in the region $\ell \approx kR$, where k is the particle wave number and R is the nuclear radius, play an important role in determining the cross section.[1] This effect is due, in large part, to the strong absorption of alpha particles in the nucleus.

In the scattering of alpha particles from an even-even nucleus, the angular correlation between an inelastically scattered alpha particle which leaves the nucleus in a $2^+$ state and the successive de-excitation gamma ray is known[2] to have, in the plane of the reaction, the form

$$W(\phi) = A + B \cdot \sin^2 2(\phi - \phi_0), \qquad (1)$$

where $\phi$ is the angle of emission of the gamma ray and A, B, and $\phi_0$ are functions of the alpha-particle scattering angle $\phi_{\alpha'}$. (It is the quantity $-\phi_0$ that has usually been associated with some recoil direction

*Supported by the National Science Foundation.

[1] E. Rost, Phys. Rev. 128, 2708 (1962).

[2] J. G. Cramer, Jr., and W. W. Eidson, Nucl. Phys. (submitted for publication).

and plotted as a function of $\phi_{\alpha'}$.) Recent experiments have shown that the behavior of the symmetry angle $\phi_0$ behaves in a way which is qualitatively different from the predictions of plane-wave and adiabatic calculations.[3—5] The adiabatic approximation[6] predicts that $-\phi_0 = \frac{1}{2}(\pi - \phi_{\alpha'})$, a linear function that goes from $-\phi_0 = 90^\circ$ to $-\phi_0 = 0^\circ$ as $\phi_{\alpha'}$ varies from $0^\circ$ to $180^\circ$. The plane-wave prediction is very much like the adiabatic except at small angles.[6,7] In contrast, the experimental results show a $-\phi_0$ which goes repeatedly through $90^\circ$ sweeps as $\phi_{\alpha'}$ varies between $0^\circ$ and $180^\circ$.

It is interesting to see if one can correlate these two facts, the contribution of only a few $\ell$ values to the scattering amplitude and the "strange" behavior of the correlation symmetry angle $\phi_0$. We make the simplifying assumption that only one incoming angular momentum value L and only one outgoing angular momentum value $\ell$ participate in the inelastic scattering. Then the scattering amplitude to the $2^+$ state has the simple form

$$T_{2m} \propto C(\ell 2L;m,-m)\, Y_{\ell m}(\phi_{\alpha'},0) \qquad (2)$$

with the z axis along the beam direction. $C(\ell 2L;m,-m)$ is a Clebsch-Gordan coefficient, using the notation of Rose.[8] All factors which are

---

[3] K. K. McDaniels, D. L. Hendrie, R. H. Bassel, and G. R. Satchler, Phys. Letters 1, 295 (1962).

[4] W. W. Eidson, J. G. Cramer, Jr., D. E. Blatchley, and R. D. Bent, Nucl. Phys. (submitted for publication).

[5] J. G. Cramer, Jr., W. W. Eidson, and D. E. Blatchley, paper on p.153 of this volume.

[6] J. S. Blair and L. Wilets, Phys. Rev. 121, 1493 (1961).

[7] G. R. Satchler, Proc. Phys. Soc. (London) 68, 1306 (1955).

[8] M. E. Rose, Elementary Theory of Angular Momentum (John Wiley & Sons, Inc., New York, 1957).

the same for all values of m, and hence will not influence the angular correlation, have been ignored. In Eq. (2), angular momentum conservation implies that $|L - \ell| \leq 2 \leq L + \ell$ and parity conservation requires that $L - \ell$ be even only. Thus there are only three cases: $L = \ell$ and $L = \ell \pm 2$. With this simplification, the gamma-ray symmetry angle is given by

$$-\phi_0 = \tfrac{1}{2} \tan^{-1} \left[ 2T_{21}/(T_{22} - \sqrt{3/2}\ T_{20}) \right]. \tag{3}$$

First we examine the case where $\ell = L - 2$. This should be the case of interest in inelastic scattering since the outgoing particle has a smaller energy and will select a smaller $\ell$ value. Evaluating the Clebsch-Gordan coefficient, we have

$$-\phi_0 = \tfrac{1}{2} \tan^{-1} \frac{2[\sqrt{\ell(\ell+2)}\ Y_{\ell 1}(\phi_{a'}, 0)]}{\frac{1}{2}\sqrt{\ell(\ell-1)}\ Y_{22}(\phi_{a'}, 0) - \frac{3}{2}\sqrt{(\ell+1)(\ell+2)}\ Y_{\ell 0}(\phi_{a'}, 0)}. \tag{4}$$

Now if we assume that $\ell >> m$, the approximate formulas for spherical harmonics can be used[9] (for $\phi_{a'}$ not close to $0^\circ$ or $180^\circ$):

$$\begin{aligned} Y_{\ell 0}(\theta) &\approx -\cos\left[(2\ell+1)\frac{\theta}{2} - \frac{\pi}{4}\right], \\ Y_{\ell 1}(\theta) &\approx \sin\left[(2\ell+1)\frac{\theta}{2} - \frac{\pi}{4}\right], \\ Y_{\ell 2}(\theta) &\approx \cos\left[(2\ell+1)\frac{\theta}{2} - \frac{\pi}{4}\right]. \end{aligned} \tag{5}$$

Substituting these relations into Eq. (4), we have

$$-\phi_0 \approx +\tfrac{1}{2} \tan^{-1} \left\{\tan\left[(2\ell+1)\frac{\phi_{a'}}{2} - \frac{\pi}{4}\right]\right\}$$

or

$$-\phi_0 \approx \tfrac{1}{4}\left[(2\ell+1)\phi_{a'} - \frac{\pi}{2}\right]. \tag{6}$$

---

[9] E. Jahnke and F. Emde, Tables of Functions (Dover Publications, New York, 1945).

This result for $\ell = 9$ is shown as the top drawing in Fig. 1 and displays the same type of behavior as is seen experimentally. One therefore concludes that such behavior is a result of only a small number of contributing angular momenta. This behavior can be obtained by either a surface direct reaction or by an isolated-resonance compound-nucleus reaction in which the resonating level has a spin of 2 or more.

The case $\ell = L$ corresponds to the adiabatic approximation where the incoming and outgoing particles have the same energy and thus select the same $\ell$ value. Here we have

$$-\phi_0 = \tfrac{1}{2}\tan^{-1}\frac{2\,Y_{\ell 1}(\phi_{a'})}{\sqrt{\ell - 1)(\ell + 2)}\,Y_{\ell 2}(\phi_{a'}) + \sqrt{\ell(\ell + 1)}\,Y_{\ell 0}(\phi_{a'})}. \quad (7)$$

By using the recursion relation[9]

$$\sqrt{(\ell - 1)(\ell + 2)}\,Y_{\ell 2}(\theta,0) + \sqrt{\ell(\ell + 1)}\,Y_{\ell 0}(\theta,0) = -2\cot\theta\,Y_{\ell 1}(\theta,0), \quad (8)$$

we have $-\phi_0 = -\frac{1}{2}\phi_{a'}$, or $-\phi_0 = \frac{1}{2}\pi - \frac{1}{2}\phi_{a'}$, since any multiple of $\pi/2$ can be added, the correlation function having a period of $\pi/2$. This result agrees with the predictions of the adiabatic approximation and is shown in the middle drawing of Fig. 1.

The third case, $\ell = L + 2$, provides an interesting prediction. The selection of a higher outgoing $\ell$ value would only occur for a positive-Q reaction. In this case

$$-\phi_0 = \tfrac{1}{2}\tan^{-1}\frac{\sqrt{(\ell - 1)(\ell + 1)}\,Y_{\ell 1}(\phi_{a'})}{\frac{1}{2}\sqrt{(\ell + 1)(\ell + 2)}\,Y_{\ell 2}(\phi_{a'}) - \frac{3}{2}\sqrt{\ell(\ell - 1)}\,Y_{\ell 0}(\phi_{a'})}. \quad (9)$$

If we again use the approximate formulas (5), we obtain

$$-\phi_0 = -\tfrac{1}{2}\tan^{-1}\{\tan[(2\ell + 1)\frac{\phi_{a'}}{2} - \frac{\pi}{4}]\},$$

or

$$-\phi_0 = -\tfrac{1}{4}[(2\ell + 1)\phi_{a'} - \frac{\pi}{2}], \quad (10)$$

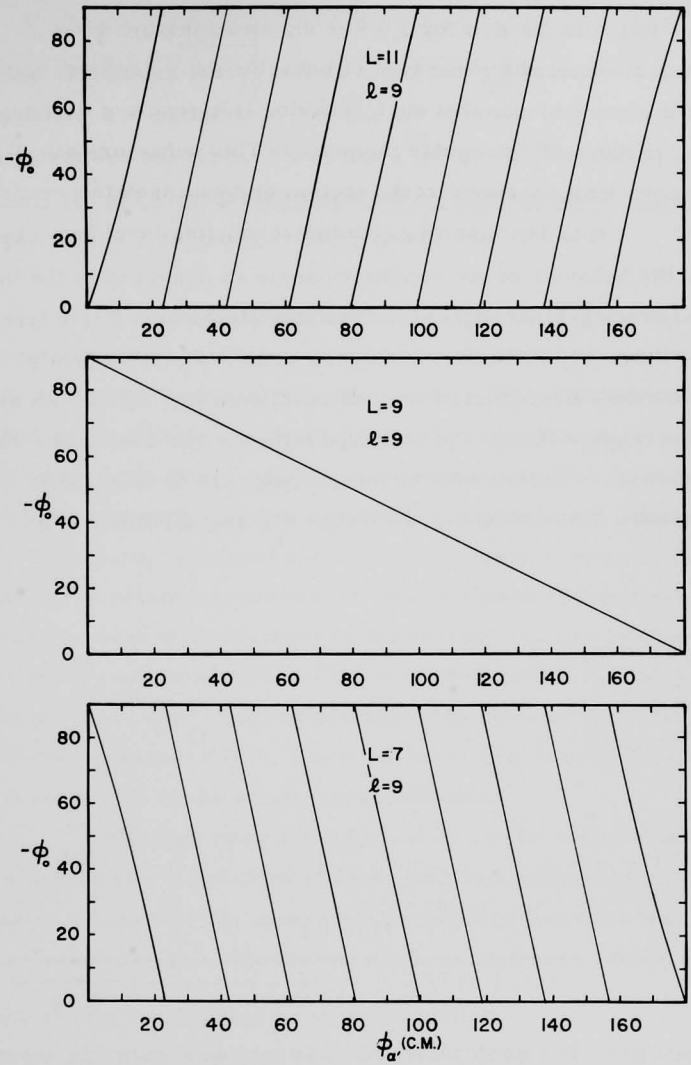


Fig. 1. The correlation symmetry angle $\phi_0$ as a function of the inelastic alpha-particle scattering angle $\phi_\alpha$, for the case where $\ell = 9$. Upper, middle, and lower sections show the cases where $\ell = L - 2$, $\ell = L$, and $\ell = L + 2$, respectively.

a result similar to the first case, $\ell = L - 2$, <u>except</u> that $-\phi_0$ is a decreasing function of $\phi_{\alpha'}$ instead of an increasing function as before. Thus, if one were to examine the angular correlation in a positive-Q reaction, perhaps $N^{14}(d,\alpha\gamma)C^{12}$, one would expect the symmetry angle to vary in the manner shown in the bottom drawing of Fig. 1.

It is felt that this calculation provides a simple explanation for the behavior of the symmetry angle as observed in the inelastic scattering of strongly absorbed particles where fairly large angular-momentum values are involved, as is the case in $(\alpha,\alpha'\gamma)$ reactions. As a final point, it can be seen from Eq. (6) that an experimental correlation function of this type tells one the dominant $\ell$ value of the reaction. Further work is now in progress to investigate effects arising from including more than one angular-momentum value.

# C-10. ANGULAR-CORRELATION STUDIES OF THE INELASTIC SCATTERING OF ALPHA PARTICLES FROM $C^{12}$, $Mg^{24}$, $Si^{28}$, AND $Fe^{56}$†

J. G. Cramer, Jr., W. W. Eidson, and D. E. Blatchley‡

Department of Physics, Indiana University, Bloomington, Indiana

When alpha particles are inelastically scattered from an even-even nucleus to excite a $J^{\pi} = 2^{+}$ state, all of the particles in the reaction except the final nucleus are spinless. When the excited state, which has been polarized by the nuclear reaction, gamma-decays directly back to the ground state, the angular correlation function of the reaction-plane gamma rays has a particularly simple and transparent form.[1] Therefore, it is possible through the measurement of angular correlations to obtain a great deal of information on the way in which the excited nucleus was polarized by the nuclear reaction, and thus on the relative phases and amplitudes of the scattering amplitudes of the reaction process. Such information cannot be obtained from differential-cross-section measurements, since the latter are determined only by the over-all magnitude of the scattering amplitudes.

Although complete information can be obtained on the relative phases and magnitudes of these scattering amplitudes, as has been shown elsewhere,[1] by measuring correlation functions both in and out of the reaction plane, the discussion presented here will be confined

†Supported by the National Science Foundation.

‡Present address: Department of Physics, State University of Iowa, Iowa City, Iowa.

[1] J. G. Cramer, Jr., and W. W. Eidson, Nucl. Phys. (submitted for publication).

to the behavior of $\phi_0$, the symmetry angle of the reaction-plane correlation function

$$W(\pi/2,\phi) = A + B\cdot\sin^2 2(\phi - \phi_0). \quad (1)$$

Here $\phi$ is the angle of gamma emission, and A and B are empirical parameters; all are functions of the alpha-particle scattering angle $\phi_{\alpha'}$.

Alpha-gamma angular correlations have been measured at many scattering angles for each of the reactions $C^{12}(\alpha,\alpha'\gamma)$, $Mg^{24}(\alpha,\alpha'\gamma_{1.37})$, $Si^{28}(\alpha,\alpha'\gamma_{1.77})$, and $Fe^{56}(\alpha,\alpha'\gamma_{0.84})$. The correlation functions were determined at each alpha-particle scattering angle by measuring the coincidence gamma-ray yield at eleven or more different gamma-ray detection angles. The functions thus measured were corrected for angular-resolution effects and least-squares fitted to Eq. (1) through the use of an IBM-709 computer.[2] However, the correlation results for $Fe^{56}$ are very recent and have not yet been analyzed in this manner but by rather superficial hand analysis. Therefore, they should be considered only as preliminary results which serve as a general indication of the behavior of the correlation function for $Fe^{56}(\alpha,\alpha'\gamma)$.

Targets of natural carbon, magnesium, silicon, and iron were bombarded with 22.5-MeV alpha particles from the Indiana University cyclotron. Scattered alpha particles were detected with a silicon surface-barrier detector and their energy spectrum displayed in one quadrant of a 1024-channel analyzer which was gated with fast ($2\tau$ = 20 $\mu$sec) coincidence circuitry. The coincidence electronics supplied a gating pulse only when a scattered alpha particle in the proper

---

[2] W. W. Eidson, J. G. Cramer, Jr., D. E. Blatchley, and R. D. Bent, Nucl. Phys. (submitted for publication).

energy range was in coincidence with a gamma ray (also of the proper energy) detected with a 3 × 3-in NaI(Tl) crystal located in the reaction plane.

In Fig. 1, the correlation-symmetry angle $-\phi_0$ as a function of scattering angle is shown for $C^{12}$ and $Mg^{24}$. The diagonal

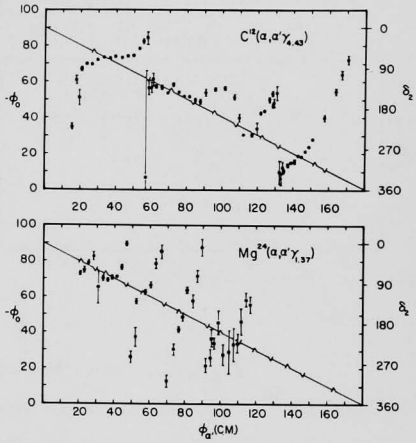


Fig. 1. Plot of the correlation symmetry angle $\phi_0$ as a function of the center-of-mass angle of the inelastically scattered alpha particles, for the reactions $C^{12}(\alpha,\alpha'\gamma)$ and $Mg^{24}(\alpha,\alpha'\gamma)$. Straight lines in both plots indicate the prediction of the adiabatic theory. Carets indicate maxima in the inelastic differential cross section, while inverted carets indicate minima.

lines in these drawings represent the prediction of the adiabatic approximation,[3] and the carets and inverted carets on these lines mark the respective positions of maxima and minima in the inelastic scattering cross section.[4] There is an excellent correlation between the minima of the cross section and the breaks in the correlation-symmetry angle. Somewhat less well correlated are the maxima of the cross section and the points at which the symmetry angle agrees with the adiabatic prediction.

---

[3] J. S. Blair and L. Wilets, Phys. Rev. 121, 1493 (1961).

[4] J. G. Cramer, Jr., and W. W. Eidson, Bull. Am. Phys. Soc. 8, 317 (1963).

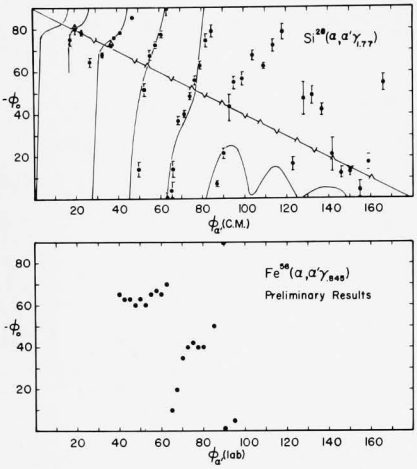


Fig. 2. Plot of the correlation symmetry angle $\phi_0$ as a function of the scattering angle of the inelastically scattered alpha particles, for the reactions $Si^{28}(\alpha,\alpha'\gamma)$ and $Fe^{56}(\alpha,\alpha'\gamma)$. In the $Si^{28}$ data, the straight line indicates the prediction of the adiabatic theory, carets indicate maxima in the inelastic differential cross section, and inverted carets indicate minima. The solid line represents the prediction of a DWBA fit to the data as described in the text. It must be noted that the results for $Fe^{56}$ are preliminary and the symmetry angle is plotted as a function of lab scattering angle.

Figure 2 shows the behavior of the symmetry angle for $Si^{28}$ and $Fe^{56}$. The silicon data behave much like those of magnesium, and again the correlation between the cross section minima and the sweeps of symmetry angle is apparent. The curve through the data points is the result of a DWBA calculation which will be discussed below. The $Fe^{56}$ results are, as stated above, only preliminary and serve principally to indicate that here too the striking sweeps of the symmetry angle are present, just as in the lighter nuclei.

Very recent work in the theory of angular correlations[5] indicates that the rapid variation of the symmetry angle with scattering angle, as illustrated in these data, is associated with the selection of a particular angular momentum value in the partial-wave expansion of the scattering amplitudes. These data, when interpreted in this way, indicate that the amplitudes have a strong component for which the incoming angular momentum L exceeds the outgoing angular momentum $\ell$ by 2

[5] J. G. Wills and J. G. Cramer, Jr., paper C-9 of this volume.

units, and $\ell \approx 6$ for carbon, $\ell \approx 8$ for magnesium, and $\ell \approx 9$ for silicon. The tendency of the symmetry angle $-\phi_0$ to follow the adiabatic prediction in the region between these sweeps is an indication that there is also a sizable $L = \ell$ contribution to the scattering amplitudes of the reaction.

Figure 3 shows the DWBA fits to the elastic and inelastic scattering differential cross sections[4] of $Si^{28}$ which give rise to the

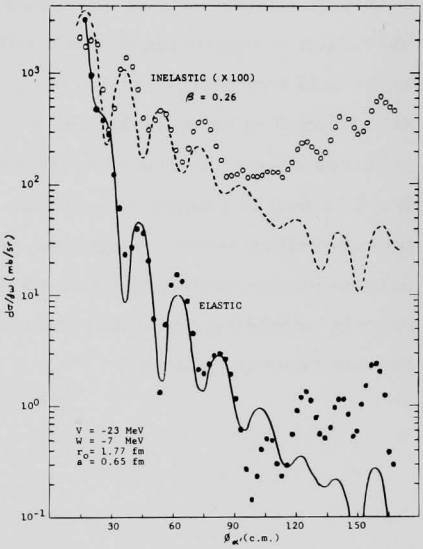


Fig. 3. Measured elastic and inelastic differential cross sections for the reaction $Si^{28} + \alpha$. The solid and dashed lines are the predicted cross sections obtained from a DWBA fit as described in the text.

symmetry-angle predictions shown in Fig. 2. This calculation was performed with the DWBA coupled-equations code of J. G. Wills, using a harmonic-vibrator model to describe the first excited state of $Si^{28}$. The optimum parameters for fitting the elastic cross section in this region were V = -23 MeV, W = -7 MeV, R = 1.77 fm $\times A^{1/3}$ and d = 0.65 fm, where V and W are the real and imaginary parts of a volume-absorption optical potential, R is the nuclear radius, and d is the Wood-Saxon diffuseness parameter. This was one of three fits which gave a reasonable approximation to the elastic and inelastic cross sections, but only

this set of parameters reproduced (with any degree of accuracy) the behavior of the correlation symmetry axis. Thus the simultaneous fitting of elastic, inelastic, and angular-correlation data[6] seems to be an effective way of resolving the ambiguities in the optical potential[7] which have recently been noted. Perhaps of more serious concern is the fact that no set of parameters could accurately predict the behavior simultaneously of all data sets at all angles, and coupled-equation fits showed no indication of improving this situation. This failure might be attributed to the fact that compound-nucleus and Coulomb-excitation effects were not included in the calculation, and to the fact that the excited state requires a more detailed description than that employed in the calculation. Work is now in progress to include these effects in such calculations as that described above. Experimental work recently completed will determine correlation functions both in and out of the reaction plane, thereby providing additional information about the scattering amplitudes and the reaction process.

---

[6] K. K. McDaniels, D. L. Hendrie, R. H. Bassel, and G. R. Satchler, Phys. Letters 1, 295 (1962).

[7] R. M. Drisko, G. R. Satchler, and R. H. Bassel, Phys. Letters 5, 347 (1963).

# SESSION D

TUESDAY AFTERNOON

10 MARCH 1964

# D-1. NEUTRON REDUCED WIDTHS DETERMINED BY THE $N^{14}(N^{14}, N^{13})N^{15}$ TRANSFER REACTION*

J. A. McIntyre

Physics Department, Texas A and M University, College Station, Texas

Since the initial work of Breit and Ebel,[1] it has been clear that neutron reduced widths might possibly be determined through the study of neutron-transfer reactions. The program outlined eight years ago by these authors has not been carried out, however, because of subsequent doubts[2] that the neutron-transfer "tunneling" mechanism studied in their paper was the correct one for describing the transfer process. The purpose of this report is to present data which show that for at least one reaction [the $N^{14}(N^{14}, N^{13})N^{15}$ reaction] the tunneling description is very likely the correct one. The experimental data and the tunneling theory will then be combined to yield a reduced width for nitrogen (on the assumption that the reduced widths for $N^{14}$ and $N^{15}$ are the same). Finally the reduced width obtained will be compared with reduced widths obtained from deuteron-stripping

*Supported by the U. S. Atomic Energy Commission.

[1] G. Breit and M. E. Ebel, Phys. Rev. 103, 679 (1956).

[2] A review of the difficulties encountered in analyzing the experimental data with the "tunneling" theory is given by G. Breit, in Handbuch der Physik, edited by S. Flügge (Springer-Verlag, Berlin, 1959), Vol. XLI, Part 1, Sect. 48.

cross sections[3] and shell-model calculations.[4]

The experimental angular distribution[5,6] of the $N^{13}$ nucleus in the $N^{14}(N^{14}, N^{13})N^{15}$ reaction at 6.15 MeV is shown in Fig. 1. The theoretical angular-distribution curve has been derived

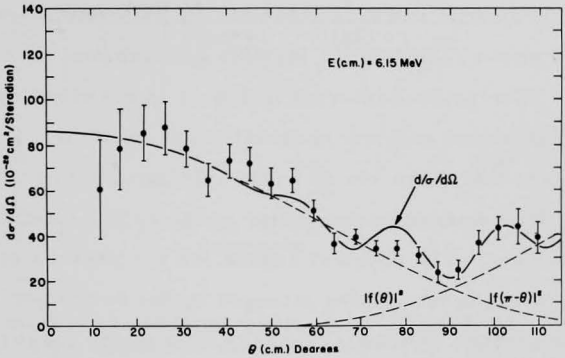


Fig. 1. Differential cross sections for neutron transfer at 6.15 MeV, plotted in the center-of-mass system. The experimental points are from Ref. 6, the $d\sigma/d\Omega$ solid curve is the tunneling calculation of Ref. 8. The two dashed curves show the values of the absolute squares of the scattering amplitudes of the projectile and recoil nuclei.

---

[3] M. H. Macfarlane and J. B. French, Rev. Mod. Phys. 32, 567 (1960).

[4] R. M. Drisko, R. H. Bassel, and E. C. Halbert (Oak Ridge JULIE Program).

[5] L. C. Becker, F. C. Jobes, and J. A. McIntyre, Third Conference on Reactions between Complex Nuclei, Asilomar, April 1963 (to be published).

[6] L. C. Becker, Yale University, Thesis (to be published).

independently by Breit and collaborators[7] and by Greider.[8] The small discrepancy between their results is not indicated on the curve. Also shown in the figure are the absolute-square values of the amplitudes for the projectile and recoil $N^{13}$ nuclei. Because of the identical nature of the projectile and target nuclei, the differential-cross-section curve shows interference maxima and minima.

The point of interest in Fig. 1 is the close agreement between the calculated and experimental cross sections. It is important to note here that there are no adjustable parameters in the calculation except for a normalization factor which can be used to determine the reduced widths. The physical reason for the absence of parameters, of course, is that the interacting nitrogen nuclei do not get close enough to one another to interact through the nuclear forces. For the 6.15-MeV situation studied here, the distance of closest approach R between the nitrogen nuclei is 11.5 F corresponding to $r_0 = 2.4$ F, where $R = r_0(A_1^{1/3} + A_2^{1/3})$. Thus, the motion of the nitrogen nuclei is determined only by the Coulomb field.

The reason for the failure of the tunneling theory at higher energies[2,9] (8.15 MeV) can be seen from Figs. 2 and 3 where the experimental[10] and theoretical[7,8] angular distributions for the reaction at 7.2 and 8.0 MeV are shown. At these higher energies

---

[7] G. Breit, K. W. Chun, and H. G. Wahsweiler (submitted to the Physical Review).

[8] K. R. Greider, Third Conference on Reactions between Complex Nuclei, Asilomar, April 1963 (to be published); K. R. Greider, "Nucleus Rearrangement Scattering I" (to be published).

[9] H. L. Reynolds and A. Zucker, Phys. Rev. 101, 166 (1956).

[10] J. C. Hiebert and J. A. McIntyre, Bull. Am. Phys. Soc. 9, 67 (1964).

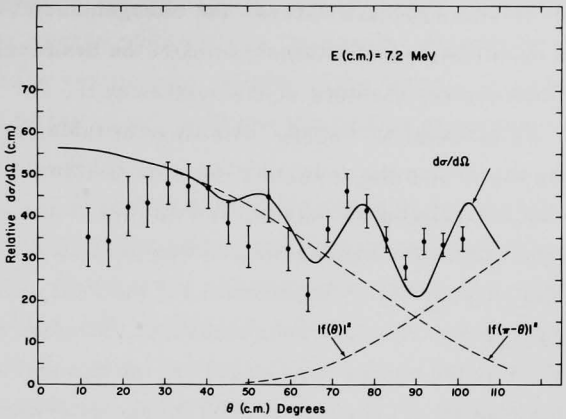


Fig. 2. Differential cross sections for neutron transfer at 7.2 MeV, plotted in the center-of-mass system. The experimental points are from Ref. 10, the $d\sigma/d\Omega$ curve is the tunneling calculation of Ref. 8.

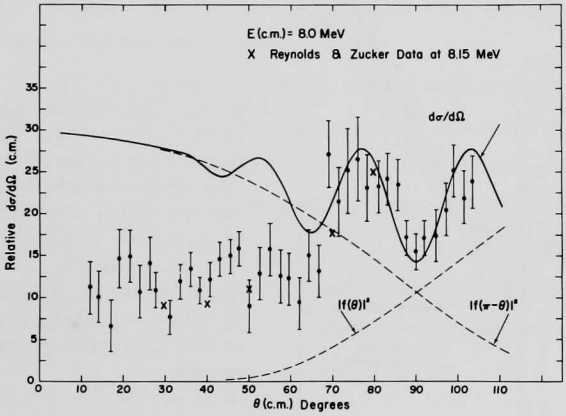


Fig. 3. Same as Fig. 2 except that the center-of-mass energy is 8.0 MeV. Earlier data of Reynolds and Zucker (Ref. 9) are also shown for comparison.

the distance of closest approach between the nitrogen nuclei is reduced and the recoil nuclei begin to be absorbed out of the beam beginning at $0^{\circ}$ where the internuclear distance is at a minimum.

As already mentioned, the only adjustable parameters in the tunneling theory are the reduced widths for the transferred neutron. These appear as normalizing factors in the differential and total cross sections. In addition to the angular-distribution prediction, the tunneling theory yields also an energy dependence for the total cross sections $\sigma(E)$. The total cross section has been measured therefore over a range of energies to verify the energy dependence for the transfer reaction and also to obtain an accurate cross section for the determination of the reduced widths. The experimental results[6] are shown in Fig. 4. For comparison, the tunneling theory of Breit, Chun, and

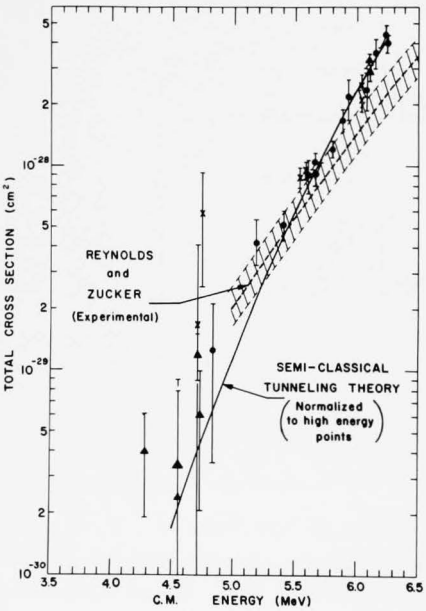


Fig. 4. Total cross sections for neutron transfer. The experimental points are from Ref. 6. The cross-hatched band represents earlier experimental data of Reynolds and Zucker (Ref. 9). The curve is the tunneling calculation of Breit, Chun, and Wahsweiler (Ref. 7) normalized to the high-energy experimental points.

and Wahsweiler[7] is also shown, normalized to the experimental data at the higher energy points where the angular-distribution measurements (Fig. 1) have verified the validity of the theory. Also included (as indicated by the broad band) are the earlier experimental results of Reynolds and Zucker.[9]

It is seen that in the range of energies between 5.5 and 6.5 MeV the tunneling theory and the experimental data are in good agreement. At the lower energies, the theory drops below the experimental values, but, as Breit has pointed out,[2] such an effect should occur at sufficiently low energies because of the virtual Coulomb excitation process. At energies above those covered in Fig. 4, it has already been shown that the tunneling theory no longer describes the transfer process (see Figs. 2 and 3). Thus, there is a relatively narrow energy range [at least for the $N^{14}(N^{14}, N^{13})N^{15}$ reaction] where the tunneling theory applies. However, if care is taken to work in this region, reliable values of the reduced width should be obtainable from the tunneling theory.

Finally then, the values of the reduced width are obtained from the total-cross-section measurement by using the normalization of the curve in Fig. 4, the product of the reduced widths $(1/\lambda_{14})(1/\lambda_{15})$ being obtained.[11] By asuming that these reduced widths are equal, which is not unreasonable,[3] $1/\lambda = 1/\lambda_{14} = 1/\lambda_{15}$ can be determined.

This value of the reduced width can be compared with the usual single-particle reduced width[3] in the following way. By definition,[1]

$$1/\lambda \equiv r^2 R^2(r),$$

---

[11] The equations used in this calculation are Eq. (25.2) in Ref. 1 and Eq. (4.3) in Ref. 7.

where R(r) is the radial wave function of the neutron. Also, by definition,[3] the single-particle reduced width $\theta_0^2$ can be expressed

$$\theta_0^2 \equiv r^3 R^2(r)/3.$$

Thus,

$$\theta_0^2 \equiv r/3\lambda. \qquad (1)$$

By inserting the value of $\lambda$ (as determined above from the transfer reaction) into Eq. (1), a value of $\theta_0^2 = 0.08 \pm 0.01$ has been found for $N^{14}$ and $N^{15}$. The uncertainty in the transfer-reaction value for $\theta_0^2$ quoted here is an experimental one only. However a comparable uncertainty should also be attached to the theoretical value[12] with which the experiment was compared. The transfer result is therefore quoted in Table I as 0.080 ± 0.015, the uncertainty being obtained by folding

TABLE I. Comparison of single-particle reduced widths $\theta_0^2$ (5F).

| Reference | $\theta_0^2$ |
|---|---|
| Macfarlane and French | 0.040 ± 0.010 |
| Oak Ridge (JULIE) | 0.052 ± 0.025 |
| Neutron transfer | 0.080 ± 0.015 |

[12] G. Breit (private communication).

together the experimental and theoretical values.

Values for $\theta_0^2$ have also been obtained by other methods and are listed in Table I. Using Butler stripping theory and a comprehensive analysis of (d,p) experimental results, Macfarlane and French[3] have found a value $\theta_0^2 = 0.040 \pm 0.010$. A value $\theta_0^2 = 0.052 \pm 0.025$ has also been obtained from a shell-model calculation at Oak Ridge.[4] Inspection of Table I indicates that the neutron-transfer value for $\theta_0^2$ is significantly larger than that obtained from the (d,p) analysis. The reason for this discrepancy is not known at the present time.

# D-2. SELECTION RULES IN $_{22}Ti^{48}_{26}$(p, p') INELASTIC SCATTERING*

G. T. Garvey, G. M. Crawley, H. O. Funsten,
N. R. Roberson, and L. Zamick

Palmer Physical Laboratory, Princeton University

We consider the nucleus $_{22}Ti^{48}_{26}$ in the limit of a pure shell-model configuration — a $Ca^{40}$ core plus 2 protons and 6 neutrons in the $f_{7/2}$ shell. Thus, $Ti^{48}$ has the unique property of having the same number of protons and neutron holes in the $f_{7/2}$ shell. Under the interchange of protons and neutron holes, $Ti^{48}$ goes into itself. Under this same operation the wave functions of $Ti^{48}$ either change sign (odd signature) or remain the same (even signature). This is now illustrated by writing down the wave functions for the first two spin-2 states in $Ti^{48}$ at 0.99 and 2.43 MeV, as calculated by McCullen, Bayman, and Zamick. Letting $L_P$ and $L_N^{-1}$ be the angular momenta of the 2 protons and 2 neutron holes, respectively, we have

$$E = 0.99 \text{ MeV}: \quad \psi \approx 0.69\ [L_P = 0,\ L_N^{-1} = 2]^{J=2}$$

$$- 0.69\ [L_P = 2,\ L_N^{-1} = 0]^{J=2} + 0\ [L_P = 2,\ L_N^{-1} = 2]^{J=2},$$

$$E = 2.43 \text{ MeV}: \quad \psi \approx 0.56\ [L_P = 0,\ L_N^{-1} = 2]^{J=2}$$

$$+ 0.56\ [L_P = 2,\ L_N^{-1} = 0]^{J=2} + 0.52\ [L_P = 2,\ L_N^{-1} = 2]^{J=2}.$$

The first state above has odd signature and the second state has even signature.

*Work supported by the U. S. Atomic Energy Commission and the Higgins Scientific Trust Fund.

This unique property of $Ti^{48}$ leads to some interesting selection rules. In particular, the matrix element of an even tensor operator between states of the same signature vanishes. This can be applied to the inelastic scattering from the J=0 state of $Ti^{48}$ to an excited state of J = 2, 4, or 6. We make the assumption that the inelastic scattering process proceeds by means of a direct reaction, and that the part of the interaction operator which excites the $Ti^{48}$ target to a state of angular momentum L(2, 4, or 6) is of the form $\sum_i g_L(r_i) Y_L(\Omega_i)$, where the sum extends over all the neutrons and protons in the $f_{7/2}$ shell.

The calculation of the authors mentioned above assigns the signatures shown in Table I to the various states of $Ti^{48}$. Thus, the excitation of the first spin-4 state, the second spin-2 state, and the second spin-6 state should be inhibited if the above assumptions are correct.

TABLE I. Signatures of the states of $Ti^{48}$.

| E | J | Signature |
|---|---|---|
| 0 | 0 | EVEN |
| 0.99 | 2 | ODD |
| 2.43 | 2 | EVEN |
| 2.30 | 4 | EVEN |
| 3.24 | 4 | ODD |
| 3.36[a] | 6 | ODD |
| 3.49[a] | 6 | EVEN |

[a] Theoretical.

To test these selection rules, inelastic scattering experiments (p, p') were performed with the Princeton cyclotron using 17.5-MeV protons. The experiments were performed first with an over-all resolution width of 80 keV and later with an improved resolution width of about 25 keV. Lithium-drifted junction counters were used to detect the scattered particles.

The experiments seem to verify the selection rules quite strikingly. The spin-2 state at 2.43 MeV is down in cross section by a factor of at least 15 from the state at 0.99 MeV. The spin-4 state at 2.30 MeV is down by a factor of 5 from the spin-4 state at 3.24 MeV. The spin-6 states have not yet been examined. Since the inhibited spin-4 state lies lower than the enhanced one, an allowance for Q-value dependence of the reaction will make the inhibition even greater.

Can the shell-model explanation of the inhibition be trusted? Although the shell model works well for many things, it is at its worst in trying to predict quadrupole moments or, more generally, matrix elements of operators $\sum_i r_i^L Y_i^L$. But the inelastic-scattering operator is just this type. In a vibrational picture, the spin-2 state at 0.99 MeV could be regarded as a one-quantum excitation whereas the second spin-2 at 2.43 MeV and the first spin-4 at 2.30 MeV (which are almost degenerate) would be 2-quantum excitations. (The spin-0 part of this triplet is missing.) Since, in a direct reaction, only one quantum can be excited by inelastic scattering, the latter two states could not be reached. The strongly excited spin-4 state at 3.24 MeV could be regarded as a hexadecapole vibration.

Methods of differentiating between the shell-model and the vibrational-model pictures have not yet been carried out, but some proposals are here presented. If $Ti^{48}$ is a vibrational nucleus, then certainly $Ti^{46}$ would also be vibrational — even more so than $Ti^{48}$ since

it lies closer to the middle of the open $f_{7/2}$ shell. Then the inhibitions would occur not only in $Ti^{48}$, as predicted in the shell model, but also in $Ti^{46}$. The experimental data on $Ti^{46}(p, p')$ have been taken but, at the time this paper was written, had not yet been analyzed. Another method of choosing between the two models would be to do a Coulomb-excitation experiment to the excited states of $Ti^{48}$. The Coulomb-excitation operator is very similar to the inelastic-scattering operator, differing only in the fact that the sum $\sum_i r_i^L Y_i^L$ extends only over the protons. On the shell-model picture, excitation of the spin-2 state at 2.43 MeV and the spin-4 state at 2.30 MeV would <u>not</u> be inhibited. On the vibrational model, the inhibition would still be present because, as before, it is not possible to excite two quanta in a direct reaction.

# D-3. DIRECT-REACTION STUDY OF THE $Ca^{41}$ AND $Ca^{49}$ SHELL-MODEL LEVELS*

T. A. Belote, E. Kashy,† A. Sperduto, H. A. Enge, and W. W. Buechner

Physics Department and Laboratory for Nuclear Science
Massachusetts Institute of Technology
Cambridge 39, Massachusetts

The deuteron-stripping $Ca^{40}(d,p)Ca^{41}$ reaction[1] and the $Ca^{48}(d,p)Ca^{49}$ reaction[2] have been used for an investigation of the shell-model levels of $Ca^{41}$ and $Ca^{49}$. The analysis of the stripping angular-distribution data allows one to determine the angular momentum of the captured neutron and to extract spectroscopic factors. In these experiments the DWBA direct-reaction code JULIE (originated by Satchler et al. at Oak Ridge National Laboratory) was used to extract this information from the angular-distribution measurements. The recent results of Lee and Schiffer,[3] who have found a J dependence in $\ell_n=1$ stripping angular distributions, allows one also to use these data to determine J values for the case of $\frac{1}{2}^-$ and $\frac{3}{2}^-$ states.

In the case of $Ca^{41}$, a $1f_{7/2}$ configuration is expected for the ground state, with the next two single-particle levels having the

*This work has been supported in part through an AEC contract, with funds provided by the U. S. Atomic Energy Commission, by the Office of Naval Research, and by the Air Force Office of Scientific Research.

†Now at Princeton University, Princeton, New Jersey.

[1] T. A. Belote, J. Rapaport, and W. W. Buechner, Bull. Am. Phys. Soc. 9, 79 (1964).

[2] E. Kashy, A. Sperduto, H. A. Enge, and W. W. Buechner (to be published).

[3] L. L. Lee and J. P. Schiffer, Phys. Rev. Letters 12, 108 (1964).

shell-model configurations $2p_{3/2}$ and $2p_{1/2}$; whereas in $Ca^{49}$ the ground state should be $2p_{3/2}$ with the next single-particle level $2p_{1/2}$. In $Ca^{41}$, there are two $\ell_n=1$ levels near $E_x$ = 2 MeV and a group of five levels with $\ell_n=1$ stripping angular distributions near $E_x$ = 4 MeV. The two levels near 2 MeV are the fragmented components of the $2p_{3/2}$ single-particle state, and the five levels near 4.0 MeV are the major fragments of the $2p_{1/2}$ single-particle state. The assignments of $J^\pi = \frac{3}{2}^-$ and $\frac{1}{2}^-$ for these levels are consistent with the results of Ref. 3. The ground state and first excited state ($E_x$ = 2.026 MeV) of $Ca^{49}$ have unambiguous assignments of $J^\pi = \frac{3}{2}^-$ and $\frac{1}{2}^-$, respectively. The centers of gravity and sums of spectroscopic factors for these states are given in Table I and are also shown in Fig. 1, where the ground state of $Ca^{49}$ is shown plotted at the center of gravity of the $2p_{3/2}$ single-particle state in $Ca^{41}$ at 2.08 MeV. Only the single-particle levels are shown in the figure. Below 6.825 MeV, a total of 120 levels was observed in $Ca^{41}$, and eleven levels were seen in $Ca^{49}$ below 6.1 MeV.

Using the observed value of 2.04 MeV for the splitting of the $2p_{3/2}$ and $2p_{1/2}$ levels in $Ca^{41}$, one expects the $1f_{5/2}$ single-particle level to be at 4.9 MeV in $Ca^{41}$. Three $\ell_n=3$ levels are seen in this region of excitation with a center of gravity at 5.50 MeV and $\sum S = 0.47$. In $Ca^{49}$, three $\ell_n=3$ levels are also seen with a center of gravity at 3.95 MeV and $\sum S = 0.89$. We have assumed that these levels have $J^\pi = \frac{5}{2}^-$ which would be the case if the ground-state wave functions of the target nuclei were described by the lowest possible shell-model orbitals.

A rather strong $\ell_n=4$ level is observed in $Ca^{49}$ at $E_x$ = 4.020 MeV with S = 0.31, and one $\ell_n=4$ level in $Ca^{41}$ is observed at $E_x$ = 4.977 MeV with S = 0.08. These levels are believed to be sizable fragments of the $1g_{9/2}$ single-particle states. Because of the high level density in $Ca^{41}$, many $\ell_n=4$ levels may be masked by nearby levels.

TABLE I. Summary of single-particle level positions and strengths in $Ca^{41}$ and $Ca^{49}$.

| Nuclei | Configuration | Excitation energy $E_x$ (MeV) | Number of levels | $\sum S$ | $\Delta E_x$ $Ca^{41}$ - $Ca^{49}$ (MeV) |
|---|---|---|---|---|---|
| $Ca^{41}$ | $1f_{7/2}$ | 0.0 | 1 | 1 | . . . |
| $Ca^{49}$ | . . . | . . . | . . . | . . . | . . . |
| $Ca^{41}$ | | 2.08 | 2 | 1.22 | |
| | $2p_{3/2}$ | | | | 2.08 |
| $Ca^{49}$ | | 0.0 | 1 | 1.03 | |
| $Ca^{41}$ | | 4.12 | 5 | 1.16 | |
| | $2p_{1/2}$ | | | | 2.09 |
| $Ca^{49}$ | | 2.03 | 1 | 1.33 | |
| $Ca^{41}$ | | 5.50 | 3 | 0.47 | |
| | $1f_{5/2}$ | | | | 1.55 |
| $Ca^{49}$ | | 3.95 | 3 | 0.89 | |
| $Ca^{41}$ | | 4.98 | 1 | 0.08 | |
| | $1g_{9/2}$ | | | | $>0.96$ |
| $Ca^{49}$ | | 4.02 | 1 | 0.31 | |

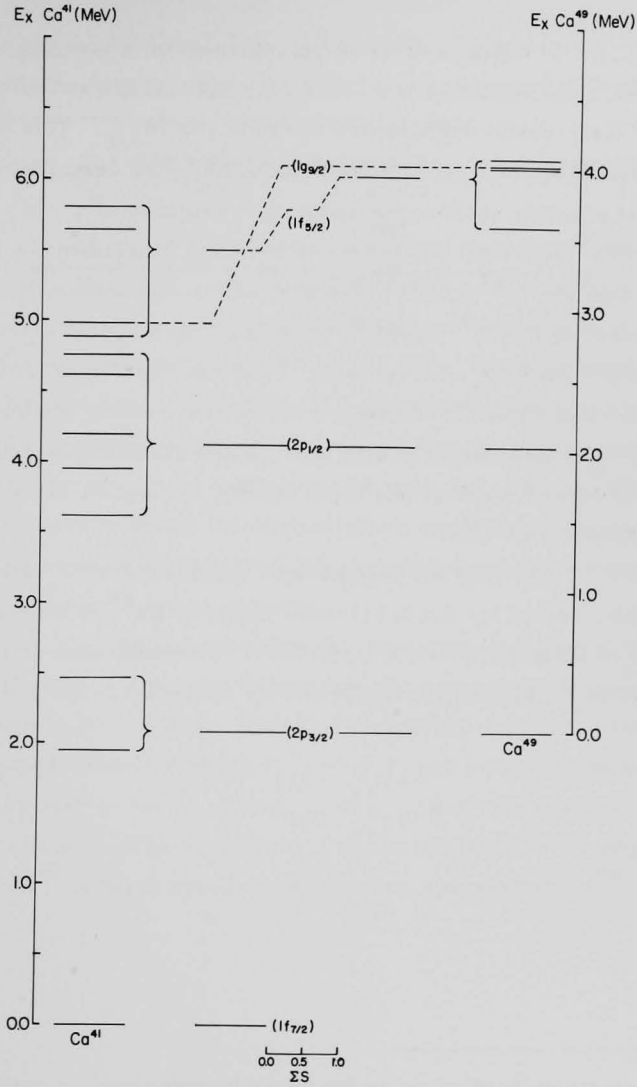


Fig. 1. The shell-model levels of $Ca^{41}$ and $Ca^{49}$ showing the presumed components of these levels, and sums of spectroscopic factors are shown with the $Ca^{49}$ ground state displaced to the center of gravity of the $2p_{3/2}$ level in $Ca^{41}$.

In addition to the stripping reaction where the neutron is left in a higher shell-model orbital, it is possible that the stripping takes place by lower shell-model orbitals—for example, by $1d_{3/2}$. This would be the case where the ground-state wave functions are not described as simply the lowest possible shell-model orbitals. Evidence of a $(1d_{3/2})^{-2}$ component in $Ti^{46}$ has been pointed out in a recent experiment by Kashy and Conlon[4] with the $Ti^{48}(p,d)Ti^{47}$ reaction and in conjunction with the results of Rapaport[5] on the $Ti^{46}(d,p)Ti^{47}$ reaction. Such appears to be the case for the 2.017-MeV, $\ell_n=2$ level in $Ca^{41}$ and has been discussed by Macfarlane and French.[6] In view of the recent results of Lee and Schiffer,[3] it is interesting to note that the angular distribution of this $\ell_n=2$ level differs considerably from other $\ell_n=2$ angular distributions for angles greater than $60^{\circ}$.

The sum of spectroscopic factors for all $\ell_n=2$ levels below 6.825 MeV, except for the 2.017-MeV level, in $Ca^{41}$ is 0.16 and is 0.08 for all $\ell_n=0$ levels also below 6.825 MeV. This indicates that both the $2d_{5/2}$ and $3s_{1/2}$ single-particle levels lie above 6.825 MeV in $Ca^{41}$.

---

[4] E. Kashy and T. W. Conlon (to be published).

[5] J. Rapaport, Ph.D. Thesis, M.I.T., June 1963; Phys. Rev. (to be published).

[6] M. H. Macfarlane and J. B. French, Rev. Mod. Phys. 32, 567 (1960).

# D-4. NUCLEON CAPTURE REACTIONS NEAR A = 40†

J. L. Yntema, Argonne National Laboratory, Argonne, Illinois

and

G. R. Satchler, Oak Ridge National Laboratory, Oak Ridge, Tennessee

The $(d,He^3)$ reaction on $Ca^{40}$ and isotopically enriched targets of $Ti^{46}$, $Ti^{47}$, $Ti^{48}$, $Ti^{49}$, and $Ti^{50}$ has been investigated. Absolute differential cross sections for a number of transitions were obtained over an angular range from $11^{\circ}$ to $33^{\circ}$. The angular distributions are compared with distorted-wave calculations which use the optical-model-potential parameters derived from the elastic scattering of 21-MeV deuterons on the same target materials. The $Ca^{40}(d,He^3)K^{39}$ reaction was used to obtain the normalization coefficients necessary to extract spectroscopic factors from the comparison of the measured and calculated differential cross sections.

The results show that the excitation energies of the $d_{3/2}$ and $s_{1/2}$ hole states are surprisingly low and increase with the number of $f_{7/2}$ neutrons in the nucleus. Results obtained from the (d,t) reaction on the Ca isotopes indicate that the $f_{7/2}$ — $d_{3/2}$ gap decreases to a minimum of about 0.96 MeV in $Ca^{45}$. The $d_{3/2}$ — $s_{1/2}$ gap appears to decrease from $Ca^{41}$ to $Ca^{47}$. The $d_{3/2}$ — $s_{1/2}$ gap in the $(d,He^3)$ reaction on $Ca^{42}$, $Ca^{43}$, and $Ca^{44}$ is much smaller than the one observed in $Ca^{40}$.

---

†Work performed under the auspices of the U. S. Atomic Energy Commission.

# SESSION E

WEDNESDAY MORNING

11 MARCH 1964

# E-1. THE SINGLET DI-NUCLEON STATE IN NUCLEAR REACTIONS*

G. M. Temmer

Rutgers, The State University

The final-state interaction of two neutrons, two protons, and neutron plus proton in the singlet state has been demonstrated previously, but most beautifully in the reaction $p + d \rightarrow p + p + n$.[1] The possibility of singlet-state deuteron pickup from nuclei is being investigated for the special case $C^{13}(p,d^*)C^{12*}$(4.43 MeV) at tandem energies, using coincidences. The production of these "resonances" will be strongly peaked forward, and in fact needs to be looked for near $0^\circ$. This is not possible for charged particles without a special magnet. However, the breakup neutrons which, like the protons, would carry approximately half the outgoing di-nucleon energy, could be detected at $0^\circ$. Dr. J. D. Anderson (Livermore) kindly sent us his time-of-flight spectra for $C^{13}(p,n)N^{13}$ at $0^\circ$ and $40^\circ$ which revealed an unexplained peak at 2.8 MeV (at $0^\circ$) which disappeared at $40^\circ$ (proton energy 10.6 MeV). We calculate the position of the half-energy neutron peak from singlet deuteron breakup to be 2.82 MeV. The observed width is about 500 keV and the cross section is about 3 mb/sterad. The "group" corresponding to the first excited state of $C^{12}$ lies energetically too low to be observable. Fortunately there are no

*Supported in part by the National Science Foundation.

[1] P. F. Donovan, J. V. Kane, et. al. (private communication).

states of $N^{13}$ in the crucial region, although the appropriate states were seen to shift properly with angle. The target was $C^{13}O_2$, and the background check with $C^{12}O_2$ revealed no peaks. We are encouraged to continue our search for the breakup protons. The general usefulness of reactions such as (p,d*), (p,2p), and (α,d*) in nuclear spectroscopy will be discussed.

# E-2. THE FORMATION OF STRONGLY POPULATED LEVELS OF $(d_{5/2})^2_5$ AND $(f_{7/2})^2_7$ CONFIGURATION IN THE (α, d) REACTION*

B. G. Harvey, E. Rivet, J. Cerny, R. H. Pehl, and J. Haag†

Department of Chemistry and Lawrence Radiation Laboratory
University of California, Berkeley, California

## Introduction

The preferential excitation of certain nuclear levels in (α, d) reactions was first observed by use of the 48-MeV helium ion beam of the 60-in. cyclotron. The spectra from the product nuclei $N^{14}$, $O^{16}$, $O^{17}$, and $F^{18}$ showed one or more very large peaks.

These strongly excited levels were reported[1] to be the J=5 levels of the $(d_{5/2})^2$ configuration. The target core is unchanged during the reaction while the captured proton and neutron each enter the $d_{5/2}$ shell. It was shown that in such cases the state of highest allowable total angular momentum will be preferentially populated. The investigation of these strongly excited $(d_{5/2})^2_5$ levels has been continued and a similar investigation has been started in the region where the $f_{7/2}$ shell should be populated.

---

* Work performed under the auspices of the U.S. Atomic Energy Commission.

† Permanent address: Purdue, Indianapolis, Indiana

[1] B. G. Harvey, J. Cerny, R. H. Pehl, and E. Rivet, Nucl. Phys. 39, 160 (1962).

## Experimental Results

The (α, d) reaction was observed from $C^{12}$, $Ne^{20}$, $Mg^{24}$, $Ar^{40}$, and $Ca^{40}$ target nuclei. The preparation of the carbon target has been described previously.[2] The natural magnesium target 2.6 mg/cm$^2$ thick was prepared by evaporation. Rolling chips of natural calcium in an inert atmosphere provided calcium foils about 1 mg/cm$^2$ thick. $Ar^{40}$ and $Ne^{20}$ gases were bombarded in a 3-in.-diameter gas holder equipped with 0.001-in.-thick Dural windows.

External beams of 45- or 50-MeV helium ions from the 88-in. cyclotron were used. The outgoing particles were identified by a semiconductor counter telescope feeding a pulse multiplier. Pulses from a 0.050-in.-thick lithium-drifted silicon transmission counter were added to the pulses from a 0.090-in. lithium-drifted stopping detector and the sum was analyzed by a 400-channel RIDL pulse-height analyzer. The experimental conditions allowed a deuteron energy resolution width of about 230 keV from a solid target.

## Results and Discussion

Energy spectra and angular distributions of deuterons were measured for the product nuclei $Na^{22}$, $Al^{26}$, $K^{42}$, and $Sc^{42}$. Figure 1 shows typical deuteron energy spectra for each reaction. The deuteron energy scale was established by measuring deuteron spectra from $C^{12}(\alpha, d)N^{14}$. Enough oxygen was present in the $Ca^{40}$ and $Mg^{24}$ targets to identify the strong deuteron line from $O^{16}(\alpha, d)F^{18}$ (1.1 MeV), thus providing an additional energy calibration point.

---

[2] R. H. Pehl, Studies in Nuclear Spectroscopy by Two-Nucleon Transfer Reactions, (Ph.D. thesis, Lawrence Radiation Laboratory Report UCRL-10993, August 1963 (unpublished).

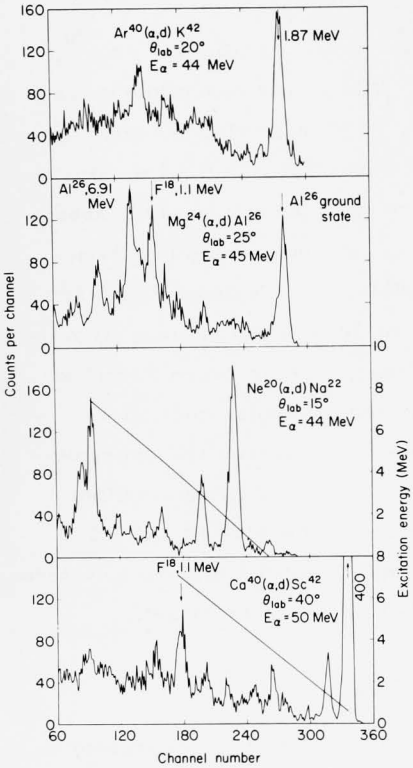


Fig. 1. Deuteron energy spectra from the $Ar^{40}(\alpha,d)K^{42}$, the $Mg^{24}(\alpha,d)Al^{26}$, the $Ne^{20}(\alpha,d)Na^{22}$, and the $Ca^{40}(\alpha,d)Sc^{42}$ reactions.

At least one, and in some cases two, levels of the product nucleus were very highly populated, as Fig. 1 shows. Several of the angular distributions of deuterons corresponding to the strong levels are shown in Fig. 2; they are all very similar to one another.

The Q values for the formation of the highly populated levels are shown in Table I. The results of previously reported experiments are also included. Figure 3 shows that the Q values for formation of the 1.53-MeV level of $Na^{22}$ and the ground state of $Al^{26}$ fall on a

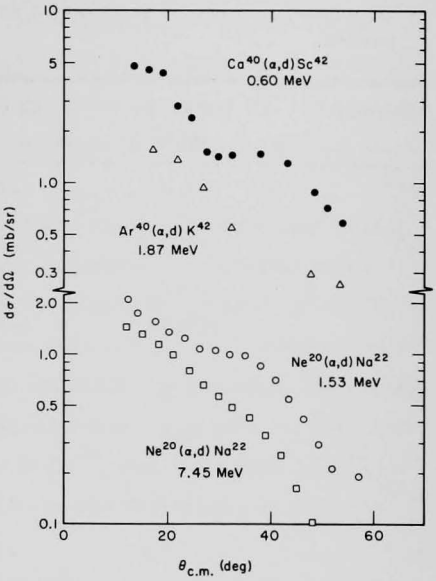


Fig. 2. Angular distribution of the strongly populated levels in the $K^{42}$, $Na^{22}$, and $Sc^{42}$ nuclei.

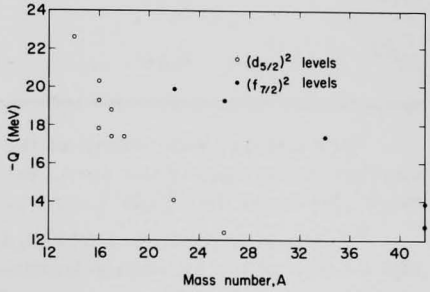


Fig. 3. Dependence of Q on mass number A for the (α, d) reaction to the $(d_{5/2})^2_5$ and $(f_{7/2})^2_7$ levels.

TABLE I. The Q values for the formation of the highly populated levels. The other information is from previous experiments.

| Nucleus | Energy level | Q values | $J\pi T$ | Configuration |
|---|---|---|---|---|
| $N^{14}$ | 9.0 | -22.6 | 5 + 0 | $(d_{5/2})^2$ |
| $O^{16}$ [a] | 14.7 | -17.8 | (4)+ 0 | $(d_{5/2})^2$ |
| | 16.2 | -19.3 | (5,6)+ 0 | $(d_{5/2})^2$ |
| | (17.2) | (-20.3) | (5,6)+ 0 | $(d_{5/2})^2$ |
| $O^{17}$ [a] | 7.6 | -17.4 | 11/2 - 0 | $(d_{5/2})^2$ |
| | 9.0 | -18.8 | 9/2 - 0 | $(d_{5/2})^2$ |
| $F^{18}$ | 1.1 | -17.4 | 5+ 0 | $(d_{5/2})^2$ |
| $Na^{22}$ | 1.53 | -14.1 | (5 +) 0 | $(d_{5/2})^2$ |
| $Al^{26}$ | 0.0 | -12.4 | 5+ 0 | $(d_{5/2})^2$ |
| $Na^{22}$ | 7.45 | -19.9 | (7 +) 0 | $(f_{7/2})^2$ |
| $Al^{26}$ | 6.91 | -19.3 | (7 +) 0 | $(f_{7/2})^2$ |
| $Cl^{34}$ [b] | 5.2 | -17.4 | (7 +)0 | $(f_{7/2})^2$ |
| $K^{42}$ | 1.87 | -12.7 | (7 +) 0 | $(f_{7/2})^2$ |
| $Sc^{42}$ | 0.60 | -13.9 | 7+ 0 | $(f_{7/2})^2$ |

[a] The angular momentum of the captured deuteron is coupled to the angular momentum of the core, producing multiple peaks in the case of the $1^+$ $N^{14}$ and the $\frac{1}{2}^-$ $N^{15}$ cores.

[b] From an unpublished $S^{32}(\alpha, d)Cl^{34}$ investigation using the 48-MeV alpha beam of the 60-in. cyclotron.

smooth line with the Q values for excitation of the previously reported $(d_{5/2})^2$ J=5 levels when plotted as a function of mass number. It is therefore very probable that these two levels have also the configuration $(d_{5/2})^2$ J=5. In fact, the spin of the ground state of $Al^{26}$ is already known to be $5^+$, and the strongly excited level is either the ground state or very close to the ground state.

The level of $Sc^{42}$ at 0.6 MeV must have high spin (since it is a long-lived isomeric state[3]). Since the selection rules forbid formation by (α, d) reactions of even-spin levels of a $(j)^2$ configuration, it is most likely that the level has spin and parity $7^+$ arising from the $(f_{7/2})^2$ configuration. Since the Q value for its formation falls on a smooth curve (as a function of mass number) with the level at 7.45 MeV in $Na^{22}$, 6.91 MeV in $Al^{26}$, 5.2 MeV in $Cl^{34}$, and 1.87 MeV in $K^{42}$, it is very probable that these levels also are the J=7 members of the $(f_{7/2})^2$ configuration.

Levels of $Sc^{42}$ at 0.60, 1.43, 2.25, 3.00, and 3.55 MeV were identified. The $(He^3, p)$ reaction, which can excite both odd-spin and even-spin members of the $(f_{7/2})^2$ configuration, excited levels of $Sc^{42}$ at 0, 0.617, 1.035, 1.509, 1.958, 2.248, and 2.998 MeV.[4] It is thus very likely that the 0-, 1.035-, and 1.958-MeV levels are states of even spin, since $(He^3, p)$ excites them but (α, d) does not.

---

[3] P. C. Rogers and G. E. Gordon, Phys. Rev. 129, 2653 (1963).

[4] J. McCullen and B. Bayman, Palmer Physical Laboratory, Princeton, New Jersey (private communication).

# E-3. ANALYSIS OF TWO-NUCLEON STRIPPING REACTIONS

Norman K. Glendenning

Lawrence Radiation Laboratory, University of California, Berkeley, California

In an earlier work, two-nucleon stripping reactions were formulated in such a way as to give a central role to the structure of the nuclear states involved.[1,2] The differential cross section was obtained in the form

$$\frac{d\sigma}{d\Omega} = \frac{m_i^* m_f^*}{(2\pi\hbar^2)^2} (fC)^2 \frac{k_f}{k_i} \frac{2J_f + 1}{2J_i + 1} \sum_{LSJM_L} \frac{b_S^2}{2S + 1} \left| \sum_N G_{NLSJ} B_{NL}^{M_L} \right|^2 , \quad (1)$$

where L, S, and J are the orbital, spin, and total angular momentum of the transferred pair. The amplitude $B_{NL}^{M}$ for the absorption of a pair of nucleons into the state whose center-of-mass motion is characterized by the indicated quantum numbers is entirely analogous to the similarly denoted quantity in the theory of (d, p) reactions.

The nuclear structure information is contained in the factor G which is a product of three overlap integrals:

$$G_{NLSJ} = \sum_\gamma \beta_{\gamma LSJ} \, \Omega_n \, \langle n0, NL; L | n_1\ell_1, n_2\ell_2; L \rangle . \quad (2)$$

---

[1] N. K. Glendenning, "Nuclear Stripping Reactions," in Annual Review of Nuclear Science, edited by E. Segré (Annual Reviews, Inc., Palo Alto, 1963), Vol. 13, p. 191.

[2] Similar developments have been suggested independently by J. Jänecke, Nucl. Phys. 48, 129 (1963); Ching liang Lin and S. Yoshida (preprint, Institute for Nuclear Study, Tokyo); E. M. Henley and D. U. L. Yu (preprint, University of Washington, Seattle).

The overlap $\beta$ measures the degree to which the final nucleus appears as the target plus two nucleons in the state $\gamma \equiv n_1\ell_1 n_2\ell_2 \cdots$ with orbital, spin, and total angular momenta L, S, and J. More precisely,

$$\beta_{\gamma LSJ} = \int \left[\Psi_{J_i}(A)\, \Phi_{\gamma LSJ}(r_1, r_2)\right]^*_{J_f} \Psi_{J_f}(A, r_1, r_2)\, dA\, d\bar{r}_1\, d\bar{r}_2. \tag{3}$$

The overlap integral $\Omega_n$ is taken with respect to the relative motion of the two captured nucleons between the final state in the nucleus and the initial state in the projectile. For reactions initiated by $He^4$,

$$\begin{aligned}\Omega_n &= 4\pi \int \phi_{n0}\left(\tfrac{1}{2}\nu r^2\right) \phi_{00}(4\eta^2 r^2)\, r^2 dr \\ &= \frac{[(2n-1)!]^2}{2^{n-1}(n-1)!} \left(\frac{4\eta\sqrt{2\nu}}{8\eta^2+\nu}\right)^{3/2} \left(1 - \frac{2\nu}{8\eta^2+\nu}\right)^n,\end{aligned} \tag{4}$$

where, for the $He^4$ nuclide,[3] we have assumed a Guassian wave function

$$\psi \approx \exp(-\eta^2 \Sigma r_{ij}^2), \quad \eta \approx 0.233\ F^{-1}; \tag{5}$$

and for the bound states we have assumed harmonic-oscillator wave functions $\phi_{n\ell}$ with parameter[4]

$$\nu \approx A^{-1/3} F^{-2}. \tag{6}$$

The bracket $\langle n0, NL; L | n_1\ell_1, n_2\ell_2; L\rangle$ is the amplitude for relative s motion for the state of the two nucleons when they occupy $n_1\ell_1$ and $n_2\ell_2$ and have total orbital angular momentum L. These transformation brackets have been tabulated.[5]

---

[3] For reactions initiated by $He^3$ or triton, replace $\eta^2$ by $\frac{3}{4}\eta^2$ in Eq. (4), where $\eta \approx 0.206$ and $0.242$, respectively.

[4] Our definition of $\nu$ is such that the single-particle harmonic-oscillator functions are proportional to $\exp(-\frac{1}{2}\nu r^2)$.

[5] T. A. Brody and M. Moskinsky, Tables of Transformation Brackets (Monografias del Inst. de Fis., Mexico, 1960).

When a specific model is assumed for the nuclear wave functions, the overlap factors $\beta$ can be computed. This has been done in some typical cases.[1] In particular, for even-even targets and final states with a nucleon in $j_1$ and $j_2$ and an undisturbed core, $\beta$ is just the recoupling coefficient for the LS-jj tranformation,[6] i.e.,

$$\beta_{\gamma LSJ} = [(2S+1)(2L+1)(2j_1+1)(2j_2+1)]^{1/2} \begin{Bmatrix} \ell_1 & 1/2 & j_1 \\ \ell_2 & 1/2 & j_2 \\ L & S & J \end{Bmatrix}. \quad (7)$$

As an example, we consider the $C^{12}(\alpha, d)N^{14}$ reaction, because of the existence of pertinent experimental[7] and theoretical[8] information. The energy spectrum of those states in $N^{14}$ that are assumed to be formed by an inert $C^{12}$ core plus two nucleons, have been computed by True.[8] We shall use his wave functions here. For the s and d orbits, he used an oscillator parameter $\nu = 0.27\ F^{-2}$ and for the p orbit, $\nu = 0.32\ F^{-2}$. We use the former value throughout.

For configuration-mixed states, the overlap $\beta_\gamma$ given by Eq. (7) is multiplied by $a_\gamma$, the admixture coefficient in the wave function.

For the pure configuration relevant to $N^{14}$, the structure factors G are shown in Table I while the appropriate linear combinations corresponding to wave functions of True[8] are shown in Table II.

A comparison of the structure factors in Table I for the dominant configurations of the T=0 states of $N^{14}$ (see Tables IV and V of Ref. 8) with the structure factors shown in Table II for the complete wave

---

[6] What is required are the space-symmetric coefficients. These are obtained from the usual ones by multiplying by the factor $\sqrt{2}$ whenever $\ell_1 \neq \ell_2$ and/or $j_1 \neq j_2$.

[7] B. G. Harvey, J. Cerny, R. H. Pehl, and E. Rivet, Nucl. Phys. 39, 160 (1962) and private communication.

[8] W. W. True, Phys. Rev. 130, 1530 (1963).

TABLE I. Structure factors for pure configurations of isospin T=0 in $N^{14}$.

| Configuration | J | L | $G_{NL1J}$ N = 1 | N = 2 | N = 3 |
|---|---|---|---|---|---|
| $p_{1/2}^2$ | 1 | 0 | 0.0373 | -0.130 | |
| | | 2 | -0.584 | | |
| $p_{1/2}2s_{1/2}$ | 0 | 1 | 0.0457 | 0.619 | |
| | 1 | 1 | 0.0373 | 0.505 | |
| $p_{1/2}d_{5/2}$ | 2 | 1 | -0.141 | 0.383 | |
| | | 3 | 0.146 | | |
| | 3 | 3 | 0.554 | | |
| $(2s_{1/2})^2$ | 1 | 0 | 0.0324 | 0.0457 | 0.438 |
| $(d_{5/2})^2$ | 1 | 0 | 0.0153 | -0.108 | 0.206 |
| | | 2 | 0.0484 | -0.111 | |
| | 3 | 2 | -0.095 | 0.218 | |
| | | 4 | -0.0885 | | |
| | 5 | 4 | 0.587 | | |
| $s_{1/2}d_{5/2}$ | 2 | 2 | 0.0203 | -0.328 | |
| | 3 | 2 | -0.0322 | 0.518 | |
| $p_{1/2}d_{3/2}$ | 1 | 1 | -0.0833 | 0.226 | |
| | 2 | 1 | 0.0289 | -0.0783 | |
| | | 3 | 0.718 | | |
| $d_{3/2}d_{5/2}$ | 1 | 0 | 0.0232 | -0.163 | 0.313 |
| | | 2 | -0.0639 | 0.146 | |
| | 2 | 2 | -0.121 | 0.277 | |
| | 3 | 2 | -0.0730 | 0.167 | |
| | | 4 | 0.231 | | |
| | 4 | 4 | 0.587 | | |

TABLE I. (cont'd)

| Configuration | J | L | $G_{NL1J}$ N = 1 | N = 2 | N = 3 |
|---|---|---|---|---|---|
| $2s_{1/2}d_{3/2}$ | 1 | 2 | 0.0323 | -0.518 | |
| | 2 | 2 | -0.0250 | 0.410 | |
| $(d_{3/2})^2$ | 1 | 0 | -0.0082 | 0.0578 | -0.111 |
| | | 2 | -0.0904 | 0.207 | |
| | 3 | 2 | 0.0158 | -0.0362 | |
| | | 4 | 0.533 | | |

functions reveals that important differences are introduced by the additional configurations, even when they have small amplitudes. Thus, for example, the ground-state wave function has an amplitude 0.9666 for $(p_{1/2})^2$, but the sum of the absolute values of the other amplitudes is 0.48; this is a very important fact when coherent sums are relevant. [See Eqs. (1) and (2).] To illustrate, in Fig. 1 the L=0 part of the wave function for

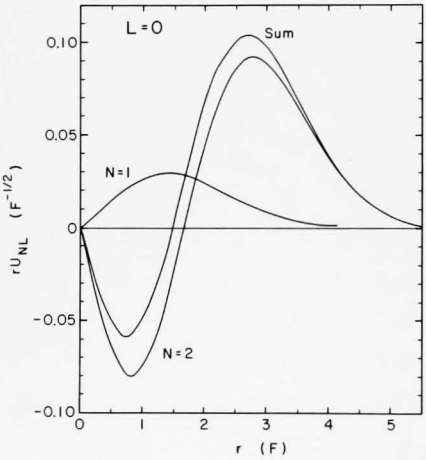


Fig. 1. The L=0 part of the wave function for the center-of-mass motion of two nucleons in the configuration $(p^2_{1/2})_{J=1}$ and having relative angular momentum zero. Its individual components weighted by the structure factors of Table I are also shown.

TABLE II. Structure factors for the configuration-mixed states of $N^{14}$ having isospin T=0.

| J | $E^a$ | L | $G_{NL1J}$ N = 1 | N = 2 | N = 3 |
|---|---|---|---|---|---|
| 1+ | 0 | 0 | 0.0423 | -0.152 | 0.0840 |
| | | 2 | -0.541 | -0.0986 | |
| | 6.34 | 0 | -0.0366 | 0.0360 | -0.560 |
| | | 2 | -0.0758 | -0.0094 | |
| | 9.92 | 0 | -0.0021 | 0.162 | -0.0959 |
| | | 2 | -0.0982 | 0.0627 | |
| | 12.24 | 0 | 0.0090 | -0.0645 | 0.0473 |
| | | 2 | -0.166 | 0.553 | |
| 1- | 4.9 | 1 | 0.0273 | 0.528 | |
| | 12.07 | 1 | 0.0871 | 0.165 | |
| 2+ | 9.45 | 2 | -0.0625 | 0.524 | |
| 2- | 4.83 | 1 | -0.133 | 0.362 | |
| | | 3 | 0.276 | | |
| | 7.89 | 1 | -0.0544 | 0.148 | |
| | | 3 | -0.679 | | |
| 3+ | 7.61 | 2 | 0.0803 | -0.582 | |
| | | 4 | 0.0141 | | |
| | 11.6 | 2 | -0.0807 | -0.0061 | |
| | | 4 | -0.0871 | | |

[a]The energies in MeV are the calculated ones of Ref. 8. They are close enough to the observed levels of the corresponding spin and parity that the information in this table can be easily associated with the correct level.

the center-of-mass motion of the configuration $(p^2_{1/2})_{J=1}$ is shown, together with the separate N components. Figure 2 shows the L=0 function for the full configuration-mixed wave function of the ground state, which contains 93% of $(p^2_{1/2})$. We draw attention to the smaller value of the functions in the interior and the increased concentration on the nuclear surface. This is a striking example of the coherent effect of the small components, especially important when one considers Fig. 3 where the L= 2 part of the wave functions is plotted. This function is less concentrated at large radius than the function of Fig. 1, and more concentrated there than that of Fig. 2.

After constructing the structure factors G, one can proceed in either of two ways. The first consists in doing a complete calculation by evaluating the transfer amplitudes $B^M_{NL}$ by the distorted-wave method and introducing the results into Eq. (1). The second is to try to extract from the experiments the implications of the varying intensities with which the levels are excited, without doing a complete calculation of the angular distributions. We pursue the latter course here. For that purpose the structure factors G must be further analyzed, because the N dependence of $B^M_{NL}$

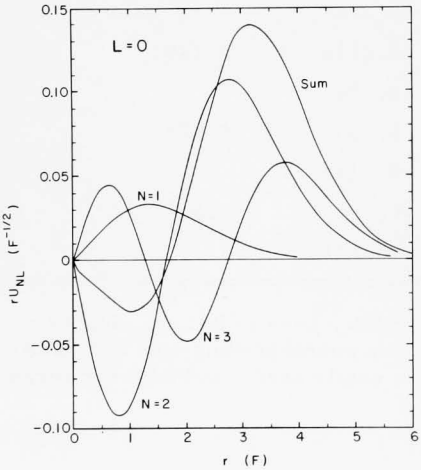


Fig. 2. The L=0 part of the wave function for the center-of-mass motion of two nucleons in the $J=1^+$, T=0 ground-state wave function of $N^{14}$ described in Ref. 8. Its individual components weighted by the structure factors of Table II are also shown.

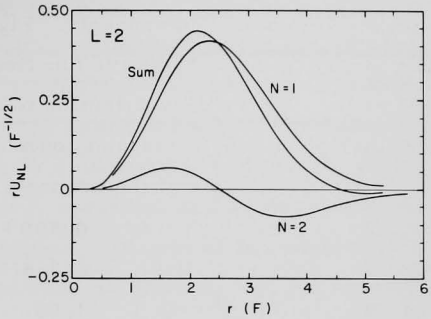


Fig. 3. The L=2 part of the wave function described in Fig. 2.

is strong, as a glance at the wave functions in, say, Fig. 2 suggests. The quantum number N refers to the number of nodes in the radial wave function describing the center-of-mass motion of the pair of nucleons that have been captured by the nucleus. By intuition, we can guess that this motion is usually more complicated than the motion of the individual nucleons. Table I shows, for example, that the center-of-mass motion of two nucleons in the 1d shell with L=0 requires functions of 0, 1, and 2 nodes (N = 1, 2, 3) to describe it. In the surface region and beyond, the sign of the functions of different N is given by $(-1)^{N-1}$ (according to the phase convention used by most authors). At the origin they all have the same sign. So, roughly speaking, if the $G_N$ have alternating signs, the wave function for the center-of-mass motion tends to be small in the interior and is peaked near the surface, while if the $G_N$ all have the same sign, the contrary holds.

For reactions in which the emitted particle is composite, we expect the surface region to be especially important. In this region the higher N components contribute more than the smaller ones. In the present case the approximate relative weights $W_N$ are shown in Table III. The strength of the L component in the cross section corresponding to a given level is then roughly given by

TABLE III. $W_{NL}$, the areas of the wave functions for the center-of-mass motion of the captured pair from r = 3 F outward.

| L | N = 1 | N = 2 | N = 3 |
|---|---|---|---|
| 0 | 0.150 | 0.672 | 1.13 |
| 1 | 0.315 | 0.972 | |
| 2 | 0.504 | 1.15 | |
| 3 | 0.768 | | |
| 4 | 1.00 | | |

$$S_{LSJ} = \left| \sum_N (-1)^N W_N G_{NLSJ} \right|^2. \tag{8}$$

In Fig. 4 we plot $(2J + 1)S_L$ for the T=0 levels of $N^{14}$. We would like to know how the transfer probabilities

$$P_L = \int \sum_M \left| B_L^M(\vec{k}_i, \vec{k}_f) \right|^2 d\Omega \tag{9}$$

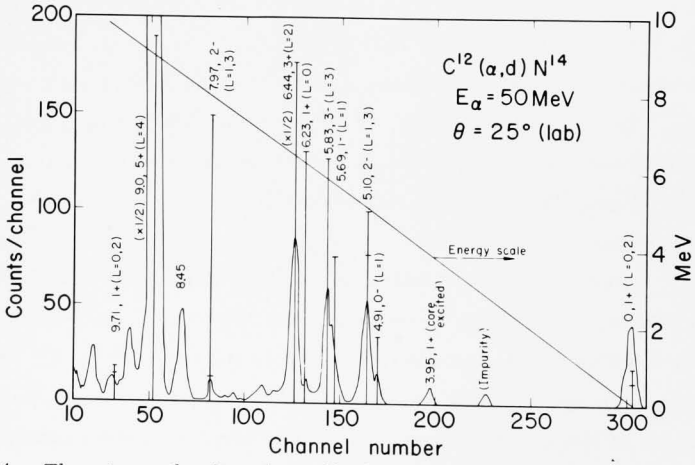


Fig. 4. The strengths $S_L$, described in the text, for the two-nucleon stripping reactions to levels in $N^{14}$ are shown by vertical lines. The observed spectrum of deuterons from $C^{12}(\alpha,d)N^{14}$ at $\theta = 25^\circ$, obtained by Harvey et al. (Ref. 7), is also shown.

behave as functions both of L and Q (kinetic energy increase). Then we would be able to say what intensities for the various levels are implied by the wave functions we have used to describe them, because the intensity is proportional to $\Sigma S_L P_L$. At the moment we do not have such information.[9] Thus we cannot make an unambiguous comparison with the experiments. Moreover the energy spectrum of outgoing deuterons has been measured only at several angles, and only at one angle with high resolution. With these reservations, we show $S_L$ and the observed energy spectrum at one angle in Fig. 4. For the very intense level at 9 MeV, $S_L$ is large, supporting the assignment[7] $(d^2_{5/2})_{J=5}$ used in calculating its strength. On the other hand the $1^+$ level at 6.23 MeV is very weakly excited while the calculated strength is large when compared with the ground state, where the opposite situation holds. The $2s^2_{1/2}$ configuration is mostly responsible for the large strength of the 6.23-MeV level. If subsequent calculations of $P_L$ support the relative intensities predicted for these two levels, then one would conclude that the ground state must have much more $2s^2_{1/2}$ mixed into it than True's calculation indicates. The experimenters find a level at 8.45 MeV which has not been fitted into True's scheme. On the other hand, the level at 7.97 MeV is very weak. This level was connected by True to his calculated $2^-$ state which has a large strength. Our results suggest that this state is really the one at 8.45 MeV, while the 7.97-MeV level probably has a core-excitation configuration as the dominant component.

A $4^+$ level, with calculated energy about 14 MeV, has a very large strength of about the magnitude of the strong level at 9 MeV. It is unfortunately beyond the range of the quoted experiments. Several $4^+$

---

[9] Distorted-wave calculations of $B^M_{NL}$ will be reported soon.

levels around 13 MeV have in fact been reported.[10] It will be interesting to see whether a strong transition is observed in the (α, d) reaction. Its observance would attach the $d_{3/2}d_{5/2}$ configuration as a strong component of the level. The nucleus is unstable against particle emission at such energies. However, the predicted state has angular momentum 4 and, according to its parentage, should decay to $C^{12}$ so that there is both a centrifugal and Coulomb barrier to retard its decay.

The existence of rather pure states at such high energy as the $5^+$ (9 MeV) and the precicted $4^+$ (~14 MeV) is surprising and interesting.

To summarize, we have shown how to extract from nuclear wave functions the information that is relevant to two-nucleon stripping reactions. The accuracy with which this information predicts the observed intensities reflects on the accuracy of the wave functions. While the nucleus we have analyzed is one which can be treated by the conventional (two-particle) shell model, the wave functions obtained by methods appropriate to more complicated situations can also be used to compute the overlap integrals β. The rest of the analysis would be the same as above.

---

[10] F. Ajzenberg-Selove and T. Lauritsen, Nucl. Phys. 11, 1 (1959).

# E-4. THE STUDY OF ($He^3$, n) REACTIONS*

G. U. Din, J. L. Weil, and G. C. Phillips

Rice University, Houston, Texas

Previous studies of ($He^3$, n) reactions have been characterized by studies of angular distributions at a few fixed bombarding energies. There are but a few ($He^3$, n) reactions[1] that have been investigated. The $C^{12}(He^3, n)O^{14}$ reaction[2] has been studied by a number of investigators from the threshold to 11 MeV bombarding energy. From a study of ($He^3$, n) reactions one might hope to obtain information on the reaction mechanism. It would be expected that both compound-nucleus formation and direct interaction may play substantial roles.

Six ($He^3$, n) reactions have been investigated at the Bonner Nuclear Laboratories. The nuclei bombarded with $He^3$ particles from the Van de Graaff accelerator were $Li^7$, $Be^9$, $B^{11}$, $C^{12}$, $C^{13}$, and $O^{18}$. Thin solid targets were used in all these experiments. $Li^7$, $Be^9$, and $B^{11}$ metals were evaporated onto tungsten backings. $C^{12}$ and $C^{13}$ targets were prepared by cracking methyl iodide onto hot tungsten backings.

---

*Supported in part by the U. S. Atomic Energy Commission.

[1] R. G. Johnson, L. F. Chase, Jr., and F. J. Vaughn, Proceedings of the Rutherford Jubilee International Conference (Heywood and Co., Ltd., London, 1962); J. L. Duggan, P. D. Miller, and R. F. Gabbard, Nucl. Phys. 46, 336 (1963).

[2] D. A. Bromley, E. Almquist, H. E. Gove, A. E. Litherland, E. P. Paul, and A. J. Ferguson, Phys. Rev. 105, 957 (1957); N. H. Gale, J. B. Garg, J. M. Calvert, and K. Ramavatram, Nucl. Phys. 20, 313 (1960); J. H. Towle and B. E. F. Macefield, Proc. Phys. Soc. (London) 77, 399 (1961); H. W. Fulbright, W. Parker, A. Ford, O. M. Bilaniuk, V. K. Deshpande, and J. W. Verha, University of Rochester Report NYO-10034 (Feb. 5, 1962); G. U. Din, H. M. Kuan, and T. W. Bonner, Proceedings of the Rutherford Jubilee International Conference (Heywood and Co., Ltd., London, 1962) and Nucl. Phys. (to be published).

For preparing the $O^{18}$ targets, tungsten blanks were heated in an atmosphere of 40% $O^{18}$ gas. The target thickness varied from 200 $\mu g/cm^2$ in the case of $O^{18}$ to 40 $\mu g/cm^2$ for $Li^7$. In the case of $Be^9$ and $O^{18}$, we studied the neutron groups leading to the first excited state and the ground state of the residual nuclei. For the remainder of the nuclei, the $(He^3, n)$ reactions were only investigated for the neutron groups leading to the ground state of the residual nuclei.

The neutron detector in the case of $C^{12}(He^3, n)O^{14}$ was a modified long counter. For the other five reactions a stilbene crystal was used as a proton recoil counter to detect the neutrons. Pulse-shape discrimination was employed to discriminate against the recording of gamma rays as well as beta-decay electrons in the crystal.

The $(He^3, n)$ reactions investigated have high positive Q values except for $C^{12}(He^3, n_0)O^{14}$ which has a Q value of -1.148 MeV. $O^{18}(He^3, n_0)Ne^{20}$ has the highest Q value (13.117 MeV). Because the Q values are generally large, the excitation energies in the compound nuclei vary from approximately 12 to 30 MeV, depending upon the target nucleus.

Figure 1 shows the differential cross section for the emission of neutrons at $0^o$ as a function of incident $He^3$ energy for the six target nuclei studied. The range of bombarding energy varied with the target studied but it was generally from 1.5 to 5.5 MeV. In the case of the $Li^7(He^3, n)B^9$ reaction, there is continuum from three-body-breakup neutrons. These neutrons are present for all energies below that of ground state. In the analysis of the data, it was not possible to subtract this background of neutrons from the monoenergetic group of neutrons.

Figures 2 and 3 show excitation curves through similar bombarding energy ranges for the same targets at $90^o$ and at backward angles.

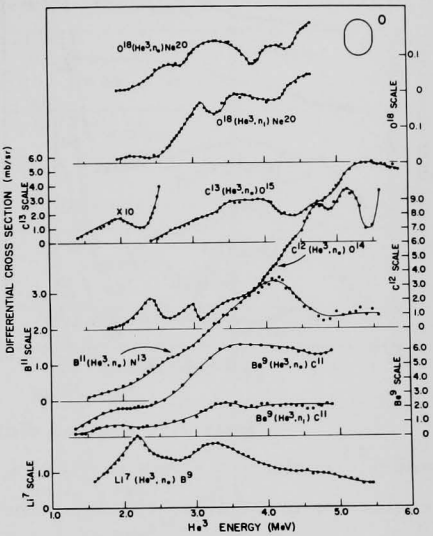


Fig. 1. Excitation curves for ($He^3$, n) reactions at $0^o$. Cross sections (lab) are in millibarns/steradian. The respective vertical scales are marked for various target nuclei.

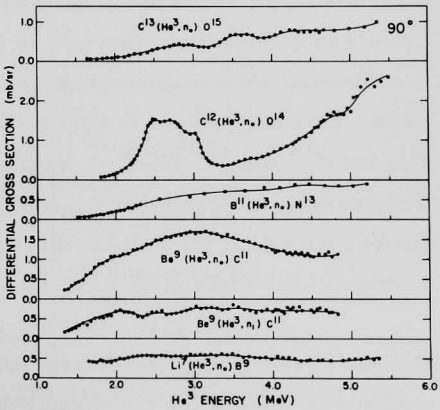


Fig. 2. Excitation curves for ($He^3$, n) reactions at $90^o$. Cross sections (lab) are in millibarns/steradian.

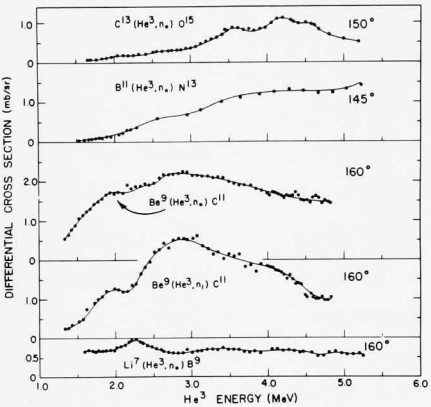


Fig. 3. Excitation curves at 160° for $Li^7(He^3, n_0)B^9$, $Be^9(He^3, n_1)C^{11}$, and $Be^9(He^3, n_0)C^{11}$; at 145° for $B^{11}(He^3, n_0)N^{13}$; and at 150° for $C^{13}(He^3, n_0)O^{15}$. Cross sections are in mb/sr (lab).

Sixty-five angular distributions for $Li^7$, $Be^9$, $B^{11}$, $C^{12}$, and $C^{13}$ nuclei are shown in Figs. 4, 5, and 6. Cross sections and angles are in the c.m. system. The solid lines are sums of Legendre polynomials fitted to the data. Most of the angular distributions were fitted for polynomials only up to $P_6$. A few at lower bombarding energies required no higher than $P_4$ to obtain reasonable agreement.

These angular distributions were taken at small energy intervals within the range of bombarding energy of $He^3$. Whenever there was a resonance structure in the yield curves at 0° the angular distributions were measured before the peak, at the peak, and after the peak. This can be seen in the case of $Li^7$, $C^{12}$, and $C^{13}$. It is noted that the $C^{12}$ and $C^{13}$ $(He^3, n)$ reactions indicate rapidly changing angular distributions in the neighborhood of the resonance. At the lower bombarding energies, the angular distributions frequently are isotropic and in other cases symmetric about 90°.

Total cross sections in millibarns for $Be^9$, $B^{11}$, $C^{12}$, and $C^{13}$ are shown in Fig. 7. Except for $C^{12}$, the total cross sections were obtained by integrating the angular distributions. These excitation curves rise smoothly with increasing energy after which they are

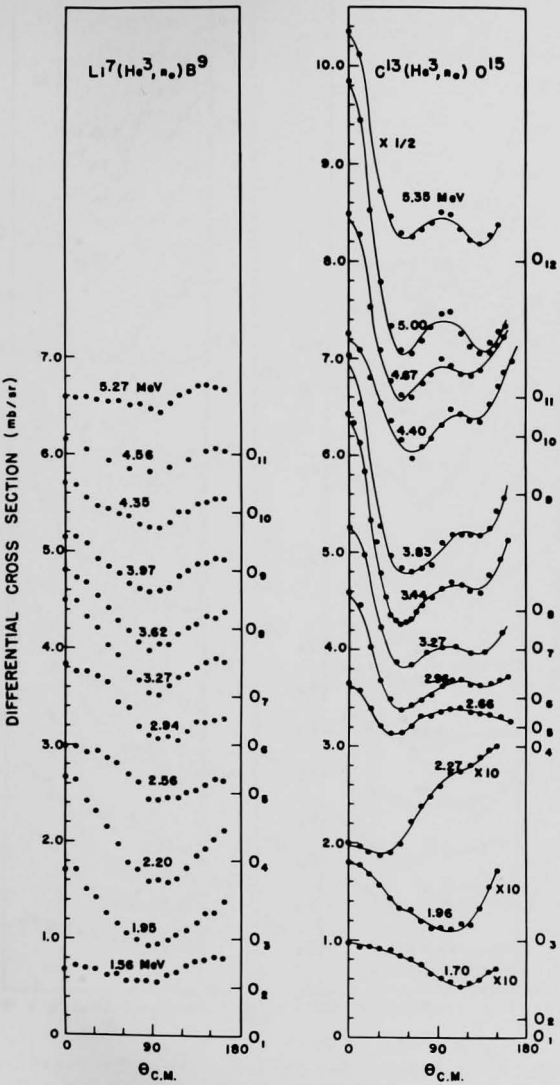


Fig. 4. Angular distributions for neutrons from the reactions $Li^7(He^3, n_0)B^9$ and $C^{13}(He^3, n_0)O^{15}$. Cross sections are in mb/sr in the center-of-mass system. The zeros on the right-hand scale represent, in ascending order, the positions of the zeros for the various curves. In order to obtain numbers from a particular curve, one must subtract from the left-hand scale the value of the zero for that curve.

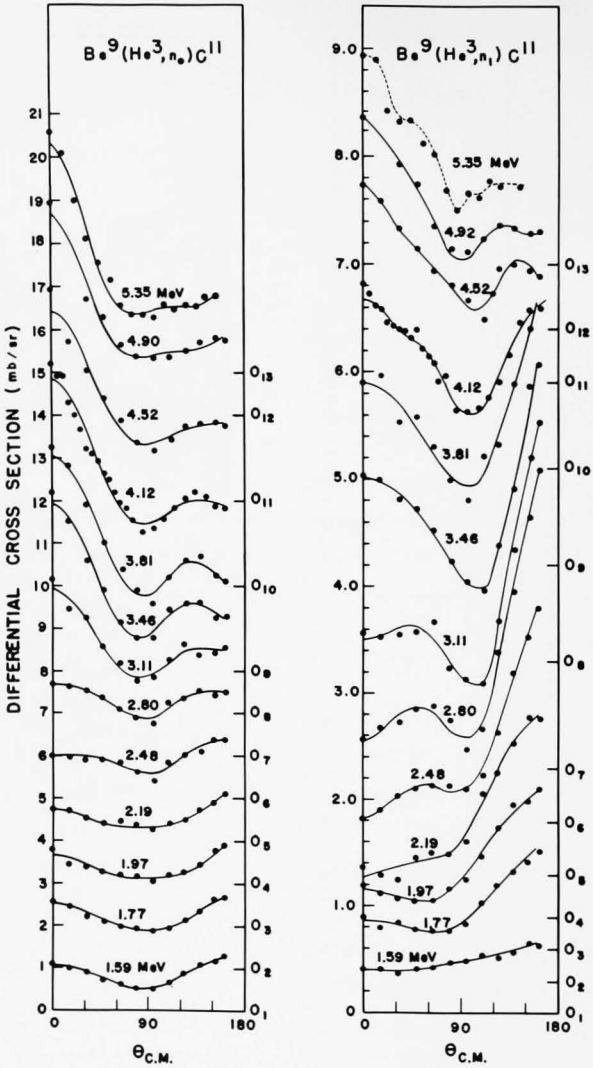


Fig. 5. Angular distributions for neutrons from the reactions $Be^9(He^3, n_1)C^{11}$ and $Be^9(He^3, n_0)C^{11}$. Cross sections are in mb/sr in the c.m. system. The zeros on the right-hand scale represent, in ascending order, the positions of the zeros for the various curves. In order to obtain a number from a particular curve, one must subtract from the left-hand scale the value of the zero for that curve.

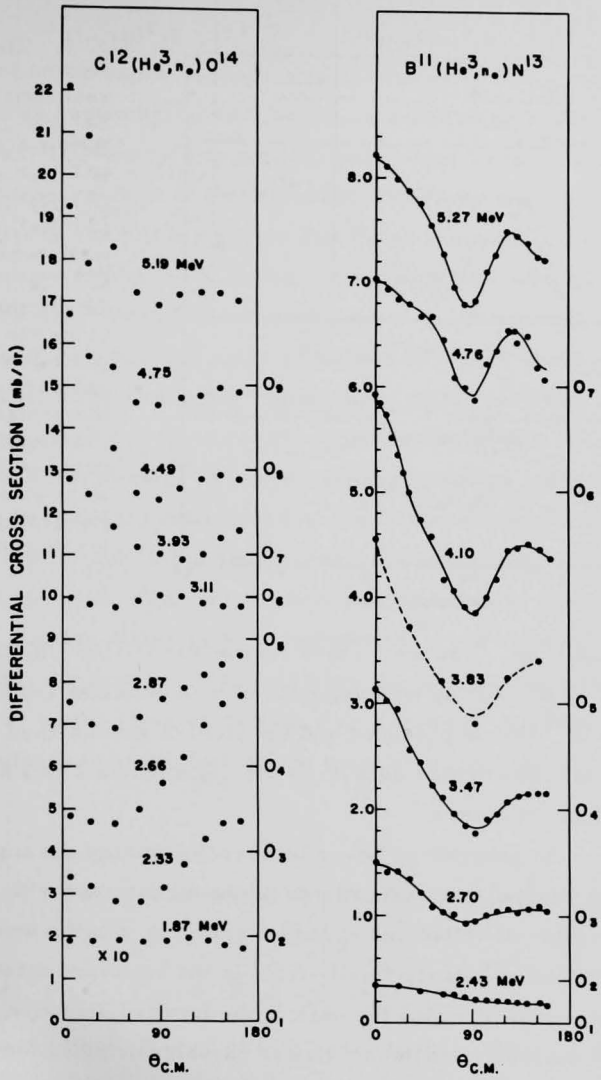


Fig. 6. Angular distributions for neutrons from the reactions $C^{12}(He^3, n_0)O^{14}$ and $B^{11}(He^3, n_0)N^{13}$. Cross sections are in mb/sr in the c.m. system. The zeros on the right-hand scale represent, in ascending order, the positions of the zeros for the various curves. In order to obtain a number from a particular curve, one must subtract from the left-hand scale the value of the zero for that curve.

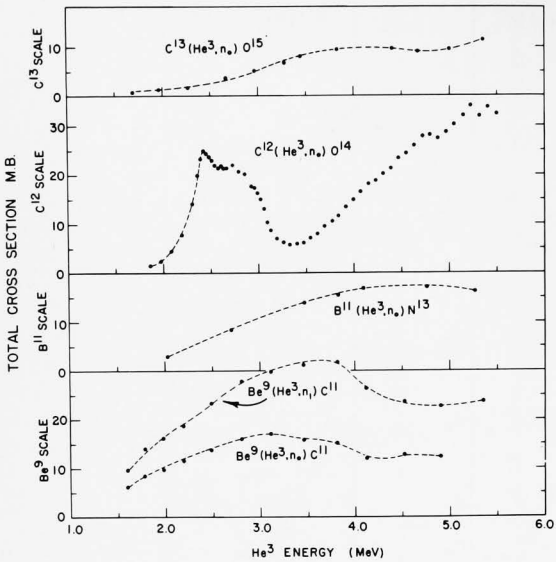


Fig. 7. The total cross section in mb for the reactions $Be^9(He^3, n_0)C^{11}$, $Be^9(He^3, n_1)C^{11}$, $B^{11}(He^3, n_0)N^{13}$, $C^{12}(He^3, n_0)O^{14}$, and $C^{13}(He^3, n_0)O^{15}$. The total cross section for $C^{12}(He^3, n_0)O^{14}$ was determined by measuring the yield of beta particles from the radioactive $O^{14}$. For the remainder of the reactions the total-cross-section points were obtained by integrating the angular distribution.

relatively constant. The total cross section for $C^{12}(He^3, n_0)O^{14}$ was determined by measuring both the yield of beta particles from the radioactive $O^{14}$ that is produced and the yield of gamma rays of 2.31 MeV which accompany this decay. In the region from 2 to 3 MeV there is a prominent resonance.

In general, at lower bombarding energy the angular distribution for $(He^3, n)$ reactions seems to change in shape with energy while the angular distributions at higher energies indicate strong forward peaking and relatively small yields in the backward direction. The bombarding energy at which the peak in the forward direction dominates varies from nucleus to nucleus. Newns'[3] double-stripping theory has been applied to some of these angular distributions. The curves in the forward direction at higher bombarding energies may be fitted, but in the backward direction the agreement is poor. For this reason no curves are shown in the figures.

---

[3] H. C. Newns, Proc. Phys. Soc. (London) 76, 489 (1960).

The rapid fluctuation (with energy) of the cross sections seems to be in contradiction to a direct-interaction mechanism. Nevertheless, the tendency to give stripping-type patterns (at some energies) seems to point in that direction. Perhaps the most reasonable interpretation is the following. (1) The broad resonant structure is indicative of a number (about 10) of broad, interfering resonant states whose lifetimes are very short. The fluctuations of cross section, at forward angles, is evidence of these states. (2) The lifetimes of the compound states are only a few times the transit times of the particles across nuclear dimensions and this lifetime is energy dependent because only a few states are interfering. When the energy is such a value (between resonances or at higher energies) that the lifetime is about as short as the transit times, then the forward peaks characteristic of direct interactions are manifest. This explanation seems to be a proper one for similar processes, such as states in $N^{14}$ studied by $C^{12} + d$[4] and $C^{13} + p$.[5] However, this explanation is incomplete; the data are apparently not accounted for by the ideas of Ericson[6] or Temmer[7] because of the pronounced tendency to show fluctuations most strongly only at forward angles.

---

[4] E. Kashy, R. R. Perry, and J. R. Risser, Phys. Rev. 117, 1289 (1960).

[5] T. Belote, Ph.D. Thesis, Rice University (1962).

[6] T. Ericson, Phys. Rev. Letters 5, 430 (1960); Phys. Letters 4, 258 (1963).

[7] G. M. Temmer (private communication).

# E-5. THE (p,t), (p,$He^3$), AND (p,α) REACTIONS ON $O^{16}$ INDUCED BY 43.7-MeV PROTONS

Joseph Cerny and Richard H. Pehl

Lawrence Radiation Laboratory and Department of Chemistry
University of California, Berkeley, California

Although investigation of the various two-nucleon transfer reactions has been increasing in recent years, little experimental work has been done on the (p,t) reaction and virtually none on (p,$He^3$) reactions. Such data permit a comparison of transitions to analog final states; in our case we can compare the $O^{16}$(p,t)$O^{14}$g.s. [$0^+$, T = 1] and $O^{16}$(p,$He^3$)$N^{14*}$ [2.31 MeV, $0^+$, T = 1] transitions. These reactions, as well as the (p,α) reaction, can give information on core-exctited states in the residual nuclei; conversely, information on the configurations of the final states may establish the reaction mechanism.

## Experimental

A beam of 43.7-MeV protons from the 88-in. cyclotron induced these reactions on a gas target. An improved particle identifier[1] fed by a semiconductor counter telescope identified the reaction products. Total-energy pulses were fed into a Nuclear Data analyzer which was appropriately gated so that the (p,t), (p,$He^3$), and (p,α) spectra were recorded simultaneously. Angles from $10^o$ to $70^o$ (lab) were observed.

---

[1] F. S. Goulding, Lawrence Radiation Laboratory, to be submitted to the Symposium on Scintillation and Semiconductor Counters, Washington, D. D., 26-28 February 1964.

Figures 1, 2, and 3 present $O^{16}(p,t)O^{14}$, $O^{16}(p,He^3)N^{14}$, and $O^{16}(p,\alpha)N^{13}$ spectra, respectively. The excitation of the various peaks is indicated.

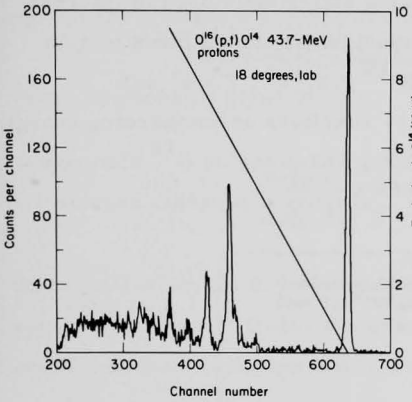


Fig. 1. Triton energy spectrum from the reaction $O^{16}(p,t)O^{14}$.

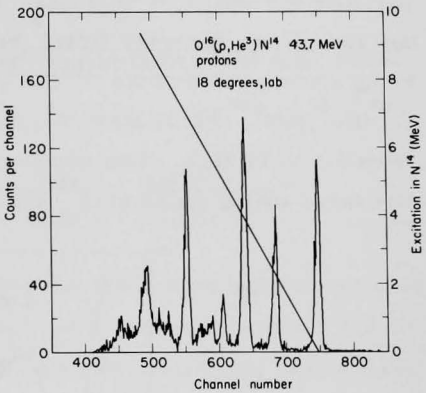


Fig. 2. $He^3$ energy spectrum from the reaction $O^{16}(p,He^3)N^{14}$.

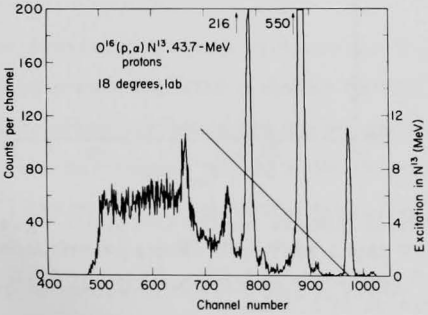


Fig. 3. $He^4$ energy spectrum from the reaction $O^{16}(p,\alpha)N^{13}$.

## Discussion

Angular distributions from isobaric final states. Comparisons of transitions to isobaric analog states have been of interest for some time, the most recent[2] two-nucleon stripping investigation being a comparison of the $C^{12}(He^3,n)O^{14}$ g.s. [$0^+$, T = 1] and $C^{12}(He^3,p)N^{14*}$ [2.31 MeV, $0^+$, T = 1] reactions at bombarding energies from 6.5 to 11 MeV. Two-nucleon pickup reactions on $O^{16}$ also populate these analog states of $O^{14}$ and $N^{14}$. Figure 4 presents angular

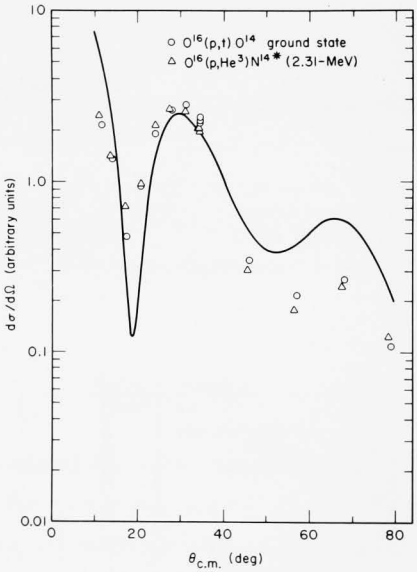


Fig. 4. Angular distributions for the $O^{16}(p,t)O^{14}$ g.s. [$0^+$, T = 1] and $O^{16}(p,He^3)N^{14*}$ [2.31 MeV, $0^+$, T = 1] transitions. The smooth line is an L=0 two-nucleon DWBA fit to the (p,t) transition at an interaction radius of 6.2 fm.

---

[2] H. W. Fulbright, W. Parker Alford, O. M. Bilaniuk, V. K. Deshpande, and J. W. Verba, Report NYO-10034, The University of Rochester.

distributions of the $O^{16}(p,t)O^{14}$ g.s. and $O^{16}(p,He^3)N^{14*}$ (2.31 MeV) reactions; the differential cross sections of the latter have been multiplied by two. Virtually identical angular distributions are observed except for a slight displacement in c.m. angle.

In the Born approximation, the ratio of the differential cross sections is given by

$$\frac{d\sigma(p,t)}{d\sigma(p,He^3)} = \frac{k(t)}{k(He^3)} \frac{|M(t)|^2}{|M(He^3)|^2} .$$

Since $k(t)/k(He^3) = 0.94$ for our case, the ratio of the matrix elements appears to be $\approx 2$. Under the assumptions of pure i-spin states for all nuclei involved in the transitions and an i-spin-conserving interaction, the theoretical ratio is

$$\frac{|M(t)|^2}{|M(He^3)|^2} = \left\{ \frac{C[t(p)T\ t(t);\ \tau(p),\ \tau(t) - \tau(p)]}{C[t(p)T\ t(He^3);\ \tau(p),\ \tau(He^3) - \tau(p)]} \right\}^2 = 2,$$

where T is the i-spin of the transferred pair. This is in agreement with our result.

If the differential cross sections for these reactions are plotted vs the momentum transfer q rather than the c.m. angle, the prediction of plane-wave stripping theory for an identical mechanism would be that the two curves should superimpose. When this is done, the $(p,He^3)$ reaction is displaced to larger values of q than the (p,t) reaction—the first maxima differ by about 7%. This would require the interaction radius of the two fits to differ such that $R(p,t) > R(p,He^3)$. To investigate further whether this result might imply a physically different nuclear region for the two pickup processes, a two-nucleon DWBA calculation was performed. Also

shown in Fig. 4 is a preliminary fit to the (p,t) data for a total angular momentum transfer L of zero; the same optical-model parameters will fit the $(p,He^3)$ data by a slight increase in R so that $R(p,t) \lesssim R(p,He^3)$. Hence some of the discrepancy which appears in the plane-wave analysis can be removed in a distorted-wave approach. Coulomb effects on the outgoing particles do not appear to be important; thus it is the energy dependence of the DWBA analysis which produces the improved agreement.

The DWBA fits to the above reactions and to the $O^{16}(p,He^3)N^{14}$ g.s. transition were calculated by use of a code written by Dr. N. K. Glendenning.[3] These two-nucleon-transfer calculations are based on a delta-function interaction at the "surface" and assume the two nucleons are transferred as a lump. Figure 5 presents an L=2 fit to the $O^{16}(p,He^3)N^{14}$ g.s. transition and also shows an L=2 fit to the $O^{16}(d,\alpha)N^{14}$ g.s. transition at 24 MeV calculated earlier.[4] No combination of different interaction radii or optical-model parameters indicates an appreciable admixture of L=0 is present in either of these ground-state transitions. This preference for L=2 over L=0 agrees with arguments based on the "momentum mismatch" occuring in these reactions and a coupling scheme developed by Glendenning[5] for two-nucleon-transfer reactions.

---

[3] N. K. Glendenning, Lawrence Radiation Laboratory (private communication).

[4] R. H. Pehl, "Studies in Nuclear Spectroscopy by Two-Nucleon Transfer Reactions" (Ph.D. Thesis), Lawrence Radiation Laboratory Report UCRL-10993, August 1963 (unpublished).

[5] N. K. Glendenning, Nucl. Phys. 29, 109 (1962).

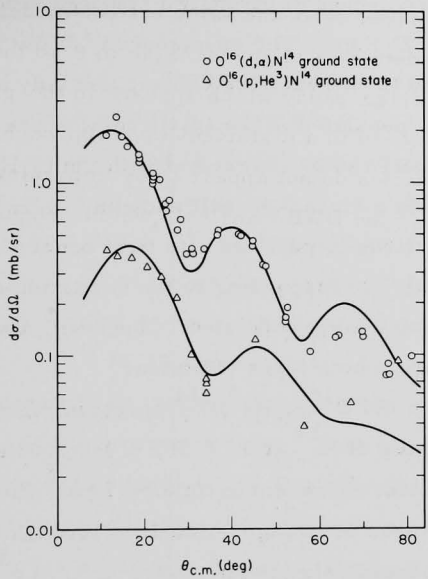


Fig. 5. Angular distributions for the $O^{16}(p,He^3)N^{14}$ g.s. transition (arbitrary units) and for the $O^{16}(d,\alpha)N^{14}$ g.s. transition(mb/sr). An L=2 DWBA fit is shown for the former at an interaction radius of 5.8 fm and for the latter at 6.0 fm. The optical-model parameters for these fits and for those of Fig. 4 were those listed in the following table.

| | V | W | a | b | $r_0$ | $r_1$ |
|---|---|---|---|---|---|---|
| p | -55 | -12 | 0.6 | 0.6 | 1.3 | 0 |
| $He^3$ | -60 | -20 | 0.5 | 0.5 | 1.3 | 1.2 |
| d | -56 | -12 | 0.65 | 0.55 | 1.20 | 0.75 |
| $\alpha$ | -35 | -7 | 0.45 | 0.60 | 1.30 | 1.20 |

Spectroscopy of Strongly Populated Final States and Nature of the Reaction Mechanism. The spectroscopy of the final states observed in these $(p,He^3)$ and $(p,\alpha)$ reactions can support only a pickup mechanism. Further, the states populated in the (p,t) reaction are consistent with a pickup mechanism and can be correlated with the $(p,He^3)$ results. Since $O^{16}$ is predominantly a closed-p-shell nucleus, we expect proton-induced pickup reactions to populate (to first order) states of configuration $1p^n$ and that any state corresponding to the excitation of a nucleon into the 1d,2s shell should be weakly populated. However, a knockout reaction could strongly populate both types of states.

From the $O^{16}(p,He^3)N^{14}$ spectrum shown in Fig. 2, it can be seen that states of $N^{14}$ at 0, 2.31, 3.95, 7.03, and about 9.15 MeV are strongly populated. A recent article by True[6] shows that these states are the only ones of configuration $1p^{10}$ through 9.4 MeV excitation and correspond, respectively, to $[p^2_{1/2}]_{1+,T=0}$, $[p^2_{1/2}]_{0+,T=1}$, $[p_{3/2}^{-1}p_{1/2}^{-1}]_{1+,T=0}$, $[p_{3/2}^{-1}p_{1/2}^{-1}]_{2+,T=0}$, and $[(s,d)+p_{3/2}^{-1}p_{1/2}^{-1}]_{2+,T=1}$. (The 10.42-MeV $2^+$, T=1 state of $N^{14}$ is thought to possess high admixtures of the same configurations as the 9.17-MeV state.) There are eight states in this energy region of configuration $1p^9 2s$ and $1p^9 1d$ and none are populated to an appreciable fraction of the $p^{10}$ states.

The previous discussion aids us in interpreting the (p,t) spectrum shown in Fig. 1. The energy scale has been normalized to the ground state of $O^{14}$ and to its established state at 7.5-MeV.[7] On

---

[6] W. W. True, Phys. Rev. 130, 1530 (1963).

[7] T. Lauritsen and F. Ajzenberg-Selove, "Energy Levels of Light Nuclei—May 1962," Nuclear Data Sheets, National Academy of Sciences - National Research Council, Washington, D. C.

this basis the other strongly populated state may be the known 6.30-MeV state. The transitions to both of these excited states show an L=2 pickup pattern while the g.s. shows the expected L=0. If we assume that these states correspond to $p^{10}$ states in $O^{14}$, their analog states in $N^{14}$ should occur near 9 and 10.5 MeV excitation. The only established $p^{10}$ states in this region of $N^{14}$ are the 9.17- and 10.42-MeV states discussed earlier; both are $2^+$, T = 1 and have an $[(s,d)+p_{3/2}^{-1}p_{1/2}^{-1}]$ configuration. The fact that both states have spin two agrees with our pickup analysis. A further comparison is possible in associating the $N^{14*}$(9.17 MeV) and $O^{14*}$(6.30 MeV) states. As was shown earlier, the (p,t) cross section to an isobaric-analog state appears to be twice the corresponding $(p,He^3)$ cross section. This ratio was calculated for these states at four angles (over which the individual differential cross sections decrease by about a factor of two) and was found to be 1.8 → 2.2, a further confirmation of this assignment. Hence the levels of $O^{14}$ at about 6.3 and 7.5 MeV excitation can be assigned as $2^+$, T=1 analog states of those in $N^{14}$ at 9.17 and 10.42 MeV, respectively.

We now wish to consider the final states populated in the $O^{16}(p,\alpha)N^{13}$ reaction, noting that the cluster-model picture of $O^{16}$ as four $\alpha$ particles makes this a favorable target for a knockout mechanism. Figure 3 indicates strongly populated states at 0, 3.5, 7.4, and 9.0 MeV excitation. A recent reinvestigation of $N^{13}$ indicates states of $p^9$ configuration at 0, 3.51, 7.42, 8.9, and 9.5 MeV[8]; these could be formed by either a pickup or a knockout mechanism. All other states below 9.5 MeV possess positive parity and are thought to correspond to an s or d nucleon coupled to the ground state or first excited state of

---

[8] F. C. Barker, Nucl. Phys. 45, 449, 467 (1963).

$C^{12}$. A knockout mechanism should also lead to population of the positive-parity states corresponding primarily to the $C^{12}$ g.s. plus an $s_{1/2}$, $d_{5/2}$, or $d_{3/2}$ nucleon (or $f_{7/2}$) which occur at 2.37, 3.56, and 8.08 MeV (and 10.36 MeV), respectively. Analysis of the angular distribution to the 3.5-MeV state(s) and comparison with the g.s. transition shows that it is primarily the 3.51-MeV level that is populated. Comparing our experimental results with these configurations, it is apparent that the lowest four states of $p^9$ configuration are strongly populated whereas none of the positive-parity states are appreciably formed.

# E-6. A STUDY OF THE NUCLEAR REACTIONS $Mg^{26}(p,t)Mg^{24}$ AND $Mg^{26}(He^4,He^6)Mg^{24}$†

M. E. Rickey,‡ H. E. Wegner, and K. W. Jones
Brookhaven National Laboratory, Upton, New York

and

B. M. Bardin, C. Hoot, and M. Kondo
University of Colorado, Boulder, Colorado

## I. Introduction

Many nuclear rearrangement collisions using very light nuclei are useful tools of nuclear spectroscopy. Single-neutron pickup may be observed by the (p,d), (d,t), and $(He^3,He^4)$ reactions. Comparisons of these reactions on the same targets are valuable since they provide critical tests of the reliability of spectroscopic information extracted from the data.

In the case of the two-neutron pickup reaction, only one reaction among those commonly studied is accessible, namely the (p,t) reaction. If $He^6$ is included in the family of reaction products, the $(He^4,He^6)$ analog reaction provides a supplementary means of studying the two-neutron pickup process.

## II. Experimental Procedure

The (p,t) measurements were made with 28-MeV protons from the University of Colorado variable-energy 52-in. sector-focused

†Work performed under the auspices of the U. S. Atomic Energy Commission.

‡On leave 1963-1964 from the University of Colorado.

cyclotron.[1] The ($He^4$, $He^6$) measurements were made with 40-MeV alpha particles from the Brookhaven 60-in. cyclotron.[2] The detectors were transmission-mounted surface-barrier counters.[3] Three detectors were used in each measurement: a thin $\Delta E$ detector, a stopping detector, and a veto counter to reject events associated with long-range particles. Coincident pulses were required in the first two detectors, and anticoincidence in the veto counter. The $\Delta E$ pulses were multiplied by E pulses formed by adding pulses from the $\Delta E$ and stopping detectors.[4] The product pulse was analyzed in a single-channel analyzer to select the particles of interest. Figure 1 shows the mass spectrum obtained for the $Mg^{26}(He^4, He^6)Mg^{24}$ reaction. The E pulses corresponding to the proper coincidence and mass-identification requirements were analyzed in a gated multichannel pulse-height analyzer.

## III. Results and Discussion

Figure 2 shows typical spectra at two angles for the ($He^4$, $He^6$) measurements. The large kinematic shift together with the 65-$\mu$ thickness of the $\Delta E$ detector severely limited the accessible range of excitation energy at large angles. The background and poor resolution at small angles lead to considerable uncertainty in the strength of small peaks. Figure 3 shows typical (p, t) spectra. The lower background is a consequence of a larger cross section and better resolution.

---

[1] D. A. Lind, J. J. Kraushaar, R. Smythe, and M. E. Rickey, Nucl. Instr. Methods 18, 19, 62 (1962).

[2] M. E. Rickey and H. E. Wegner, Bull. Am. Phys. Soc. 9, 78 (1964).

[3] Oak Ridge Technical Enterprises Corp., P. O. Box 485, Oak Ridge, Tennessee.

[4] G. L. Miller and V. Radeka, IEEE Trans. Nucl. Sci. (to be published).

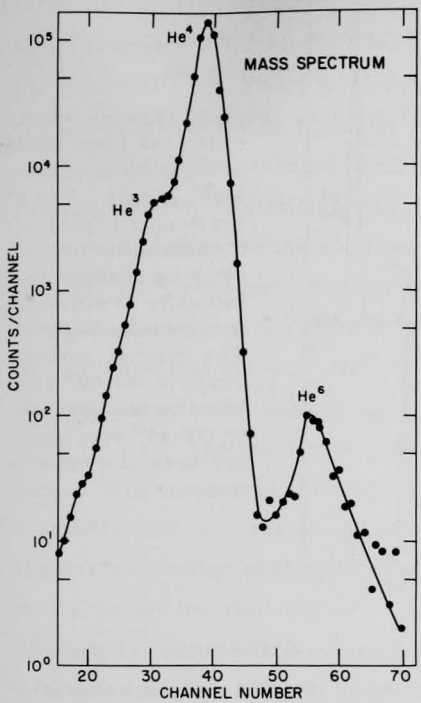


Fig. 1. Gated output from the multiplier circuit, showing the mass resolution. The $\Delta E$ and E counters are thick enough to stop the most energetic $He^6$ particles but only those $He^3$ and $He^4$ particles with less than 20—22 MeV. More penetrating particles are eliminated by an anticoincidence counter.

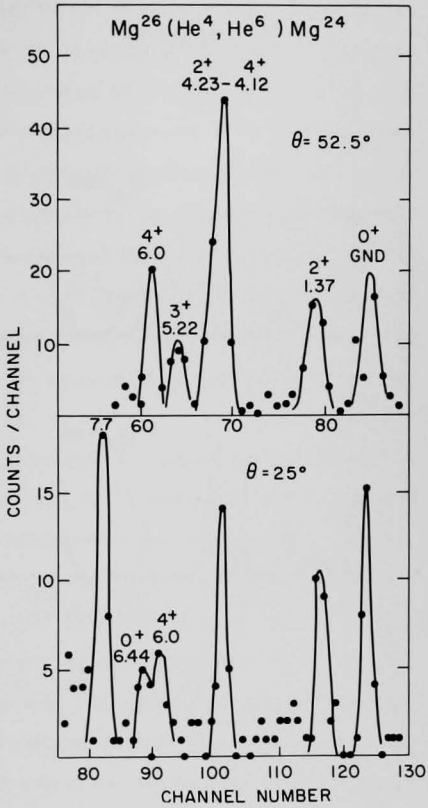


Fig. 2. Energy spectrum of $He^6$ particles from 40-MeV alpha particles incident on a $Mg^{26}$ target. The 52.5° spectrum shows the decreased background at back angles and the ($3^+$) 5.22-MeV state relatively strongly excited. The 25° spectrum shows the increased background at forward angles and the enhancement of the 6.44-MeV state which is not observed in the (p, t) measurements.

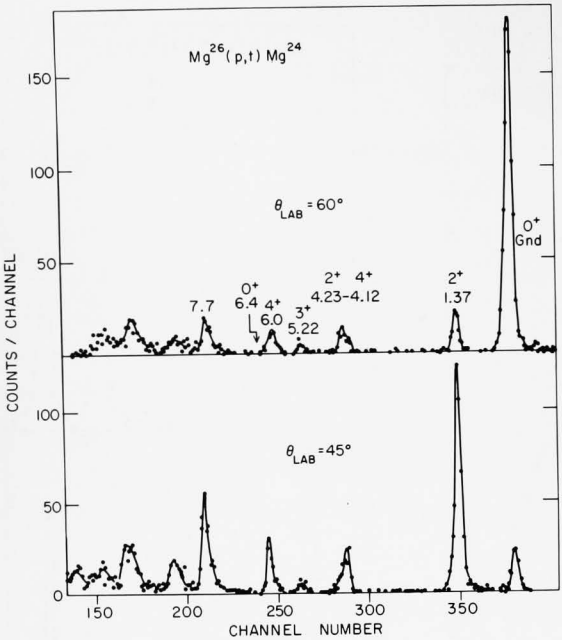


Fig. 3. Energy spectrum of tritons from 28-MeV protons incident on a $Mg^{26}$ target. The two scattering angles chosen show the striking changes in intensity of different groups with angle. The channel-number scale of the 60° spectrum is normalized to the 45° spectrum for ease of comparison.

A number of interesting features arise in the comparison of the spectra. The 25° ($He^4$, $He^6$) spectrum (Fig. 2) indicates that at this angle the 6.44-MeV $0^+$ state of $Mg^{24}$ is excited in this reaction. This level is also observed in the $C^{12}(O^{16}, He^4)Mg^{24}$ reaction.[5] It is not observed at any angles studied in the (p,t) measurements, nor is it prominent at larger angles in the ($He^4$, $He^6$) measurements. Better data are needed to show with certainty that the level is excited. However, if such data bear out these conclusions, then the ($He^4$, $He^6$) reaction mechanism for the excitation of this level must be different from that for the (p,t) reaction. On the other hand, a level at 7.7 MeV is strongly excited by both the (p,t) and ($He^4$, $He^6$) reactions; there are many $Mg^{24}$ levels in this region. Apparently one level, or a narrow band, has a

[5] S. Hinds, R. Middleton, and A. E. Litherland, Proc. Phys. Soc. (London) 77, 1210 (1961).

large two-neutron spectroscopic factor. The first T=1 level of $Mg^{24}$ is at approximately 9.5 MeV. This is the $4^+$ analog of the ground state of $Na^{24}$ (and $Al^{24}$).[6] There is no indication that this state is strongly excited by either the (p,t) or ($He^4$,$He^6$) reactions.

The strength of the (p,t) ground-state transition in comparison with the excitation of the other levels is quite apparent. This is in marked contrast to the relative strengths of the various transitions in the ($He^4$,$He^6$) reaction. Similar behavior of the (d,t) and ($He^3$,$He^4$) reactions is noted in the work of Blair and Wegner.[7] This is perhaps an indication that the ($He^4$,$He^6$) reaction accentuates higher $\ell$ transfers as conjectured in the case of ($He^3$,$He^4$).

The excitation of the 5.22-MeV $3^+$ unnatural parity state occurs with surprising strength in the ($He^4$,$He^6$) reaction. Clement[8] concludes that (p,t) reactions are approximately forbidden if the orbital angular momentum of the picked-up neutron pair is even and there is a parity change (or vice-versa). This selection rule is supported by the $C^{12}(t,p)C^{14}$ data of Jaffe et al.,[8] who find such transitions decreased by a factor of 5 to 15. The $3^+$ level in the $Mg^{26}(p,t)Mg^{24}$ is very weak compared with the ground state. It is only slightly diminished in the ($He^4$,$He^6$) measurements.

Bayman[9] has pointed out that this selection rule can be regarded as a consequence of the assumption that the two picked-up neutrons in the target are in a relative s state together with an assumption regarding

---

[6] P. M. Endt and C. Van der Lean, Nucl. Phys. 34, 51 (1962).

[7] A. G. Blair and H. E. Wegner, Phys. Rev. 127, 1245 (1962).

[8] C. F. Clement, Proceedings of the Conference on Direct Interactions and Nuclear Reaction Mechanisms, Padua, Italy, Sept. 3-8, 1962 (Gordon and Breach Science Publishers, New York, 1963), p. 457.

[9] B. F. Bayman (private conversation).

the interaction. If the angular momentum of the pair

$$\vec{L} = \vec{\ell}_1 + \vec{\ell}_2$$

is resolved into $\vec{\lambda}$, their relative angular momentum, and $\vec{\Lambda}$, the angular momentum of their center of mass relative to the nucleus, then

$$\vec{L} = \vec{\lambda} + \vec{\Lambda} \quad \text{and} \quad \Delta\pi = (-1)^{\lambda + \Lambda},$$

where $\Delta\pi$ is the change in parity. The parity of $\lambda$ is unchanged in the reaction if the interaction between the incident particle and the neutrons depends only on the separation of the systems. The assumption that $\lambda$ is even is then a consequence of the assumed spatial symmetry of the neutrons in the triton and $He^6$.

If we further assume that they are in a relative s state, the violation of the selection rule for either (p,t) or ($He^4$, $He^6$) follows if: (1) There is a $\lambda$=2 component in the wave function of the neutrons in the triton or $He^6$, in which case the $\lambda$=2 can couple to $\Lambda$ to form either even or odd L with the parity of $\Lambda$. (This is not inconsistent with a total orbital angular momentum of zero for the triton). (2) The interaction depends on spin or orbital angular momenta in addition to the position vector. (3) The reaction proceeds through compound-nucleus formation or multiple processes.

In spite of the large differences between ($He^4$, $He^6$) and (p,t) in the transitions to the ground state and 1.37-MeV state, the $3^+$ excitation is comparable in the two processes. This is probably fortuitous because of the great difference in distortion effects in the two reactions.

Figure 4 shows the angular distributions of the resolved groups up to 6 MeV excitation in $Mg^{24}$. The curves are of laboratory cross section as a function of laboratory angle. Theoretical fits to the

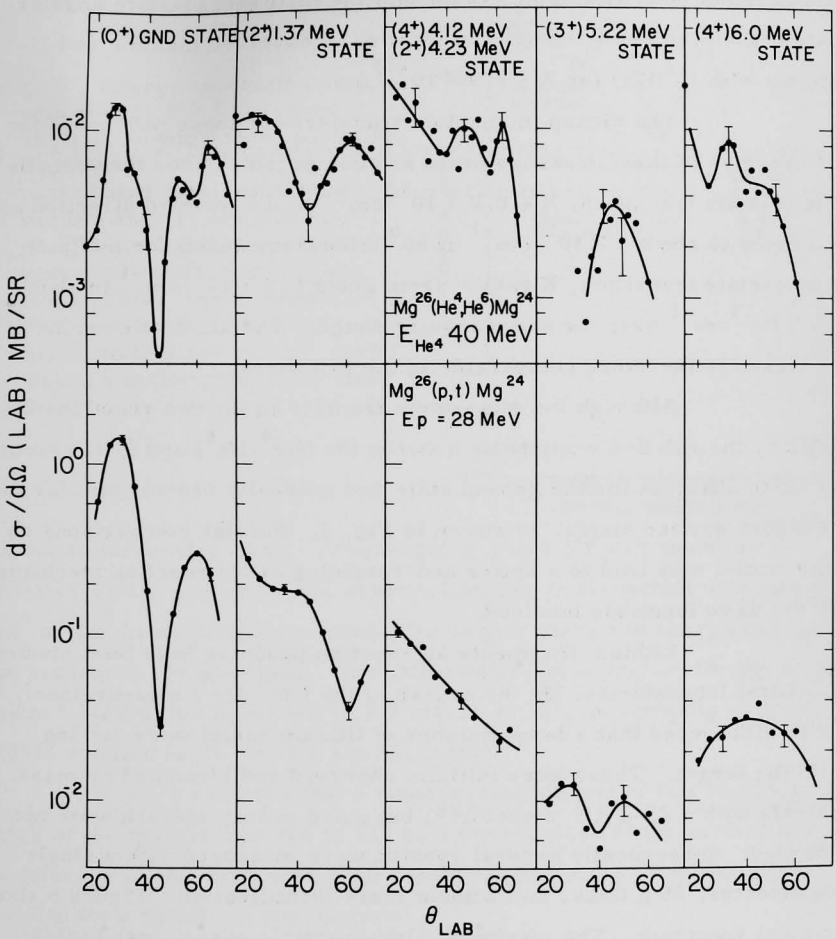


Fig. 4. Comparison of angular distributions of $He^6$ particles from the $Mg^{26}(He^4, He^6)Mg^{24}$ reaction and tritons from the $Mg^{26}(p,t)Mg^{24}$ reactions. The comparison shows that the (p,t) reaction excites the ground state and low-lying states much more strongly than the higher states, while the $(He^4, He^6)$ reaction excites all of the states approximately equally—but with 1/100 of the intensity in the case of the ground state.

data have not been attempted except that the (p,t) ground-state angular distribution was found to agree in location of observed maxima and minima with $j_0^2(KR)$ for $R = 5.9 \times 10^{-13}$ cm.

The pickup momentum transfers for these processes for the energies of these measurements are comparable. For the $(He^4, He^6)$ ground-state transition, $K \approx 0.2 \times 10^{13} cm^{-1}$ in the forward direction and increases to about $3 \times 10^{13} cm^{-1}$ at $80^\circ$ laboratory angle; for the (p,t) ground-state transition, K ranges from about $0.5 \times 10^{13} cm^{-1}$ to about $1.6 \times 10^{13} cm^{-1}$ over the same angular range. The kinematic region of the pickup is therefore comparable in the two cases.

Although the momentum transfer in the two reactions is similar, the relative excitations between the $(He^4, He^6)$ and (p,t) reactions are quite different for the ground state and gradually become similar for the higher excited states, as shown in Fig. 4. Similar comparisons on other nuclei may lead to a better understanding of the reaction mechanisms and the wave functions involved.

Lithium fragments as reaction products have been studied in several laboratories. In the course of the $(He^4, He^6)$ measurement, it was discovered that a large number of lithium nuclei were coming from the target. These were initially observed and identified by mass analysis with a 25-$\mu$ $\Delta E$ detector[10]; but gated energy spectra were not recorded. Subsequently several spectra were measured with a single thin detector, 65 $\mu$ thick, and without mass identification. Figure 5 shows a typical spectrum. The maximum alpha-particle energy loss in this detector is about 10 MeV and the $He^6$ fragments can lose at most about 10.8 MeV. It was not possible to identify the pronounced structure since mass identification was not used. The relatively poor energy resolution

---

[10] Thanks are due to W. M. Gibson for the loan of a planar etched $\Delta E$ counter 25 $\mu$ thick.

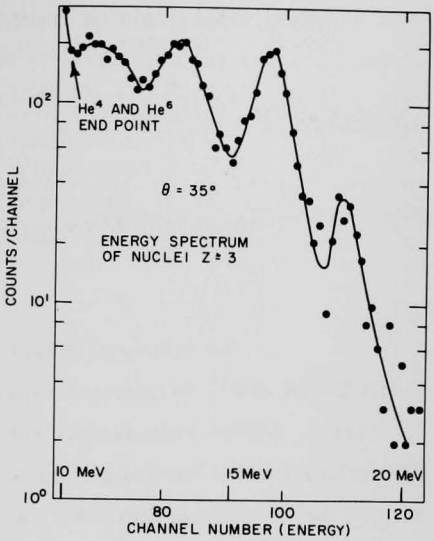


Fig. 5. Energy spectrum of nuclei with charge $Z \geqslant 3$ observed at $35^{\circ}$ with 40-MeV alpha particles incident on a $Mg^{26}$ target. The peaked structure persists at various angles, but it is impossible to determine which heavy nuclei or reactions are responsible. Other measurements with a thinner $\Delta E$ detector indicated that $Li^6$ and $Li^7$ nuclei played a major role in the total yield.

is due to target thickness. (The target is about 700 keV thick for 20-MeV $Li^6$.) The maximum observed energy is consistent with either $Li^6$ or $Li^7$ as an outgoing particle; but higher mass and charge can also be present in the spectrum. The differential cross section for the maximum 5 MeV of the spectrum is 3.5 mb/sr at $35^{\circ}$, an intensity ratio of 100/1 relative to $He^6$ in this energy region.

We believe that a considerable amount of this maximum 5 MeV of the spectrum is due to $Li^6$ as a consequence of the earlier mass studies. Further work with good resolution and mass identification is needed for a definitive comparison.

## Acknowledgments

The assistance and cooperation of C. P. Baker in providing the beam facility is appreciated.

# E-7. ANALYSIS OF THE $C^{13}(\alpha, n)O^{16}$ REACTION AT INTERMEDIATE ENERGIES

J. W. McRary and J. Y. Park
North Carolina State of the University of North Carolina, Raleigh

and

G. D. Thaxton and E. Merzbacher
University of North Carolina, Chapel Hill

The theory of direct nuclear knock-out reactions[1] is applied to the $C^{13}(\alpha, n)O^{16}$ reaction at α-particle energies of 12.8, 14.1, and 22.5 MeV. DWBA calculations are carried out using both a finite-range (Gaussian) and a zero-range interaction. Since optimum optical parameters for computing distorted waves are not available, we assumed nuclear optical potentials, including Coulomb and spin-orbit terms, which appeared reasonable in view of the existing scattering data. Both oscillator and square-well eigenfunctions have been examined as possible phenomenological solutions to the spectroscopic problem of neutron and α-particle wave functions. Reasonably good agreements with data are obtained for the shape and absolute magnitude of the differential cross sections. Theoretical polarizations are obtained, but no experimental data are available for comparison. Within the limitation of inexact optical parameters, it may be concluded that this reaction at these energies is proceeding predominantly via a knock-out process.

---

*Work supported in part by the U. S. Atomic Energy Commission.

[1] J. Y. Park, Progr. Theoret, Phys. (Kyoto) 30, 45 (1963).

# SESSION F

WEDNESDAY AFTERNOON

11 MARCH 1964

# F-1. DIRECT REACTION CONTRIBUTIONS TO FLUCTUATING REACTION CROSS SECTIONS*

G. M. Temmer, B. Teitelman, and F. G. Fender

Rutgers, The State University

We have analyzed excitation curves for a number of $(p, \alpha)$ reactions at various angles and energies, and to several residual states,[1] using the prescriptions of Ericson and Stephen.[2] At an excitation near 20 MeV and at 90°, the probability distribution of fluctuations about the local average cross sections are surprisingly well accounted for by the theory without direct-reaction amplitude (pure statistical regime). The strong dependence on the number of degrees of freedom N is clearly demonstrated between N = 2 and 72, using target nuclei between $N^{15}$ and $Co^{59}$. The sensitivity to the admixture of a nonfluctuating component has been computed for all N, using the theory of Stephen[2] and our Fortran program. Low-N reactions are preferable in deciding relative contributions of direct and compound-nucleus amplitudes. For $N^{15}$ we have data ranging from 20° to 160° so that we can follow the triton pickup contribution systematically, possibly throwing light on the question of heavy-particle stripping. The coherence energy $\Gamma$ at about 20 MeV is about 13 keV for $Ni^{60}$,

---

* Supported in part by the National Science Foundation.

[1] R. G. Davies, G. Roy, G. M. Temmer, and K. L. Warsh, published and unpublished results, Florida State University.

[2] T. Ericson, Phys. Letters 4, 258 (1963); R. O. Stephen (to be published).

and about 65 keV for $Si^{28}$. The roles of resolution, measurement interval, and the spectroscopic properties of the residual states involved will be discussed. Results of cross correlations between different channels will be available.

# F-2. MULTI-PARTICLE EXCITATIONS IN THE INTERMEDIATE COMPOUND STATE*

A. Lande and B. Block

Palmer Physical Laboratory, Princeton University

The following mechanism is offered as a description for the irregularly spaced peaks and valleys seen in scattering cross sections at several MeV.[1,2] These have been interpreted as fluctuations in the cross section by Ericson.[3]

An incident nucleon penetrates the single-particle well of the target nucleus at such an energy that it forms a virtual state. If it were not for the residual interaction between the incident nucleon and the target, the incident nucleon would live in this virtual state for a while and then leave the target, making a resonance peak in the cross section. However, when a two-body residual interaction exists, it may be de-excited from this level while exciting one of the target nucleons. (See Fig. 1.)

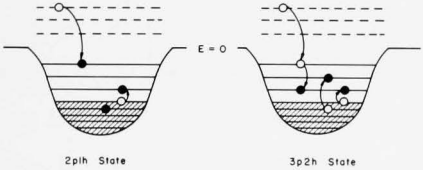


Fig. 1. Neutron (proton) incident at virtual level of neutron (proton) well. Shown are the type of 2p1h and succeeding 3p2h states made of neutrons (protons) only.

*This work was supported by the U.S. Atomic Energy Commission and the Higgins Scientific Trust Fund.

[1] B. Block and H. Feshbach, Ann. Phys. (N.Y.) 23, 47 (1963).

[2] A. K. Kerman, L. S. Rodberg, and J. E. Young, Phys. Rev. Letters 11, 422 (1963).

[3] T. Ericson, Ann. Phys. (N.Y.) 23, 390 (1963).

Such 2-particle, 1-hole states (denoted as 2p1h states), can, in general, arise from any virtual level. From these, the 3-particle, 2-hole states (denoted as 3p2h states) and more complex configurations may be reached in like manner. The occurrence of the 2p1h states will split the original virtual-state resonance into a series of narrower resonances.[1] This comes about in the following way. The set of 2p1h states are energy degenerate with respect to the incident virtual state. The residual interaction removes this degeneracy and produces splitting of the virtual-state resonance. Since these 2p1h states have definite phase relations among one another, they will show coherence effects.

In this note we will explore the systematics for the occurrence of 2p1h and 3p2h states for both incident neutrons and protons on sample even nuclei in the region $16 \leq A \leq 146$. It should be noted that the angular momentum of the incident nucleon inside the well is determined by the virtual level it occupies. Using conservation of angular momentum, parity, and energy (as discussed Ref. 1), the results for the systematics are broken into three categories: neutron-neutron, proton-proton, and neutron-proton interactions. It is assumed that the residual interactions are the same in all cases and may be represented by $L = 0-3$ multipole components. Green's neutron and proton levels were used.[4]

We examined two categories of 2p1h states but present only results for the former: the excited nucleons both end up in bound levels, or one of them ends up in a virtual level. The 2p1h states with at least one particle in a virtual level should be handled on a different basis from

---

[4] A. E. S. Green, Phys. Rev. 104, 1617 (1956).

the other case. A qualitative argument may be given for this. The lifetime of a 2p1h state with both particles bound is shorter than one with a particle in a virtual level by the lifetime of the virtual level. Similarly only 3p2h states in which all particles end up in bound levels have been considered.

Two representative tables are given. Table I shows the number of states reached through a given virtual level by way of the residual-interaction multipole components when incident neutrons (below 6 MeV) give rise to (2n - 1nh) and (3n - 2nh) states in the neutron well. Table II shows the number of states reached through a virtual level when incident protons give rise to (1p, 1n - 1nh) states followed by either a further (1n - 1nh) or (1p - 1ph) excitation. Similar results are found in the other cases.

The number of levels reached was determined for values of the energy uncertainty $\Delta_3 E$ for the (2p1h) states, $\Delta_3 E = 1.5$, 1, and 0.5 MeV. The energy uncertainty for the (3p2h) states was taken at $\Delta_5 E = 1.5$, 0.75, and 0.38 MeV with $\Delta_3 E = 1.5$ MeV and $\Delta_5 E = 1.5$ MeV for the other $\Delta_3 E$. As suggested by Feshbach, the energy width for the (3p2h) states may be quite different from (2p1h) width.

The qualitative behavior discussed below is independent of the energy uncertainties used, except that the total number of "degenerate" (2p1h) and (3p2h) states is cut down as the various $\Delta E$'s are made smaller.

## Incident Neutron on Neutron Well

There are two general features of this situation in the absence of a neutron-proton residual interaction. Excepting a few cases, 3p2h states do not occur below $A \approx 50$. They occur in appreciable numbers above about $A \approx 60$.

At a magic neutron number, there are no 3p2h states possible, even though they occur in large numbers for neighboring nuclei. (See Table I.) The case of an incident proton on a proton well with no proton-neutron residual interaction shows similar behavior.

Table I. Incident neutron in $2g_{9/2}$ virtual state. $\Delta_3 E = 1.5$ MeV, $\Delta_5 E = 1.5$ MeV. The symbols $L_3$ and $L_5$ refer to the multipole component of the residual potential used to excite respectively the 2p1h and 3p2h states; E(MeV) is the energy of the virtual state.

| | Z | N | A | $L_3=0$ | $L_3=1$ | $L_5=0$ | $L_5=1$ | $L_5=2$ | $L_3=2$ | $L_5=0$ | $L_5=1$ | $L_5=2$ | E(MeV) |
|---|---|---|---|---|---|---|---|---|---|---|---|---|---|
| Sn | 50 | 72 | 122 | 0 | 12 | 0 | 0 | 18 | 2 | 0 | 9 | 0 | 5.4 |
| Sn | 50 | 74 | 124 | 0 | 11 | 0 | 0 | 16 | 2 | 0 | 7 | 0 | 5.0 |
| Te | 52 | 74 | 126 | 0 | 11 | 0 | 0 | 17 | 2 | 0 | 7 | 0 | 4.8 |
| Te | 52 | 76 | 128 | 0 | 7 | 0 | 0 | 0 | 2 | 0 | 0 | 0 | 4.6 |
| Te | 52 | 78 | 130 | 0 | 8 | 0 | 0 | 13 | 2 | 0 | 0 | 2 | 4.3 |
| Xe | 54 | 78 | 132 | 0 | 9 | 0 | 0 | 15 | 2 | 0 | 0 | 2 | 4.1 |
| Xe | 54 | 80 | 134 | 0 | 14 | 0 | 0 | 35 | 2 | 0 | 0 | 2 | 3.8 |
| Ba | 56 | 80 | 136 | 0 | 16 | 0 | 0 | 38 | 2 | 0 | 0 | 2 | 3.5 |
| Ba | 56 | 82 | 138 | 0 | 17 | 0 | 0 | 0 | 2 | 0 | 0 | 0 | 3.1 |
| Ce | 58 | 82 | 140 | 0 | 17 | 0 | 0 | 0 | 2 | 0 | 0 | 0 | 2.9 |
| Ce | 58 | 84 | 142 | 0 | 17 | 0 | 0 | 32 | 2 | 0 | 0 | 2 | 2.6 |
| Nd | 60 | 84 | 144 | 0 | 17 | 0 | 0 | 32 | 2 | 0 | 0 | 2 | 2.4 |
| Nd | 60 | 86 | 146 | 0 | 18 | 0 | 0 | 43 | 2 | 0 | 0 | 2 | 2.2 |

## Incident Proton on Neutron Well

The general features of this situation where one allows a proton-neutron residual interaction are somewhat different from the above

cases. The major change is that there is no pronounced difference in the number of 3p2h states for magic proton numbers compared to neighboring nuclei.(See Table II.) This qualitative difference in the behavior at closed shells due to the neutron-proton interaction could provide a tool for examining it.

Table II. Incident proton in $2f_{7/2}$ virtual state. $\Delta_3 E = 1.5$ MeV, $\Delta_5 E = 1.5$ MeV. The symbols $L_3$ and $L_5$ refer to the multipole component of the residual potential used to excite respectively the 2p1h and 3p2h states; E(MeV) is the energy of the virtual state.

| | Z | N | A | $L_3=0$ | $L_3=1$ | $L_5=0$ | $L_5=1$ | $L_5=2$ | $L_3=2$ | $L_5=0$ | $L_5=1$ | $L_5=2$ | E(MeV) |
|---|---|---|---|---|---|---|---|---|---|---|---|---|---|
| Sn | 50 | 70 | 120 | 0 | 14 | 0 | 0 | 24 | 2 | 0 | 0 | 0 | 4.9 |
| Sn | 50 | 72 | 122 | 0 | 13 | 0 | 0 | 23 | 2 | 0 | 0 | 0 | 4.7 |
| Sn | 50 | 74 | 124 | 0 | 14 | 0 | 0 | 25 | 2 | 0 | 0 | 0 | 4.4 |
| Te | 52 | 74 | 126 | 0 | 15 | 0 | 0 | 49 | 2 | 0 | 0 | 1 | 4.3 |
| Te | 52 | 76 | 128 | 0 | 13 | 0 | 0 | 29 | 2 | 0 | 0 | 2 | 4.1 |
| Te | 52 | 78 | 130 | 0 | 11 | 0 | 0 | 31 | 2 | 0 | 0 | 3 | 3.8 |
| Xe | 54 | 78 | 132 | 0 | 12 | 0 | 0 | 31 | 2 | 0 | 0 | 3 | 3.7 |
| Xe | 54 | 80 | 134 | 0 | 13 | 0 | 0 | 41 | 2 | 0 | 0 | 3 | 3.4 |
| Ba | 56 | 80 | 136 | 0 | 13 | 0 | 0 | 43 | 2 | 0 | 0 | 3 | 3.3 |
| Ba | 56 | 82 | 138 | 0 | 12 | 0 | 0 | 13 | 2 | 0 | 0 | 1 | 3.0 |
| Ce | 58 | 82 | 140 | 0 | 9 | 0 | 0 | 3 | 2 | 0 | 0 | 1 | 3.2 |
| Ce | 58 | 84 | 142 | 0 | 9 | 8 | 0 | 12 | 2 | 2 | 0 | 3 | 2.5 |
| Nd | 60 | 84 | 144 | 0 | 9 | 9 | 0 | 21 | 2 | 2 | 0 | 4 | 2.6 |
| Nd | 60 | 86 | 146 | 0 | 9 | 9 | 0 | 18 | 2 | 2 | 0 | 3 | 2.1 |

The occurrence of 3p2h states for increasing A follows a similar pattern to the above neutron case. Finally, if a neutron is incident on a proton well, the results are similar to the case of an incident proton on neutron well.

The effect of shell structure can be seen in the tables through not only the selection of certain multipole components of the residual potential but also by modulation of the number of each type of state. The number of 2p1h states gives the degeneracy splitting of the virtual level. The effect of the 3p2h states on the 2p1h states is to change their strength. It is therefore necessary to know where the 3p2h states occur before one can estimate the width of the 2p1h "doorway states."

We may summarize by noting that states which require excitations over only one energy gap can be plentiful. When two such excitations are necessary, the number of 3p2h states is severely curtailed. The region of immediate experimental interest for a study of the neutron-proton interaction would therefore be at and near the doubly-magic nuclei.

This survey gives one some feeling for the complexity and systematics of the compound states that may be built out of particle-hole interactions. It also predicts regions where the "compound nucleus" is simple enough to lend itself to computation.

The authors wish to thank H. Feshbach for several enlightening conversations and for his continued interest.

# F-3. AN ESTIMATION OF PION NUCLEAR ELASTIC CHARGE-EXCHANGE SCATTERING*

R. K. Kerman and R. K. Logan

Laboratory for Nuclear Science, Massachusetts Institute of Technology

Cambridge, Massachusetts

With the advent of meson factories one will soon have large fluxes of charged pions with energies ranging from 40 to 500 MeV. These mesons make good nuclear probes since they interact strongly with the nucleus and yet do not form a compound state. Since the pions form an isotopic triplet state allowing both single and double charge-exchange scattering, new isobaric states can be investigated. In general, the nucleus which is formed in a $\pi^+$ to $\pi^-$ double charge exchange is proton rich and has not been studied (or even produced) before. Other interesting aspects of the pions is their predominant p-wave interaction with nucleons through the "3/2, 3/2" resonance, and the ability of the pion to be totally absorbed, dumping 140 MeV into the nucleus all at once.

Analyses of pion-nucleon scattering to date have all made use of an optical potential. The first was performed by Byfield et al.,[1] in which they fitted 62-MeV $\pi^-$-carbon elastic scattering with a potential of

* This work supported in part through funds provided by the Atomic Energy Commission contract number AT(30-1)-2098.

[1] H. Byfield et al., Phys. Rev. 86, 17 (1952).

the form $V = V_r + i V_1$. Watson et al.[2,3] showed how to calculate the pion-nuclear potential from basic $\pi$-N scattering results. Kisslinger[4] applied this work to low-energy scattering in which only S- and P-wave contributions of $\pi$-N scattering were considered. The P-wave term gave rise to a new term in the potential, viz.

$$\vec{\nabla} \cdot [\rho(r) \ \vec{\nabla} \psi(r)],$$

where $\rho(r)$ is the nuclear density and $\psi(r)$ is the pion wave function. Kisslinger obtained a fit to the $\pi^-$-carbon data using a Gaussian distribution for $\rho(r)$.

We wish to describe the elastic scattering of pions from nuclei using an optical potential similar to the one used by Kisslinger. We will extend his work, however, to include elastic charge-exchange scattering, where the nucleus is scattered to various states of a single isotopic multiplet. This is in contradistinction to inelastic charge exchange in which case the nucleus is scattered from one isotopic multiplet to another. Elastic charge-exchange scattering is, of course, not purely elastic since there is a difference in energy in the various charge states of an isobar due to Coulomb effects. For light nuclei the existence of isobars is well established. For heavier nuclei the concept of isobars might break down because the difference in Coulomb energy is becoming very large. However, there is evidence from (p, n) and ($He^3$, t) reactions[5,6]

---

[2] K. M. Watson, Phys. Rev. 89, 575 (1953).

[3] N. C. Francis and K. M. Watson, Phys. Rev. 92, 291 (1953).

[4] L. S. Kisslinger, Phys. Rev. 98, 761 (1955).

[5] J. D. Anderson and C. Wong, Phys. Rev. Letters 8, 442 (1962).

[6] A. G. Blair and H. E. Wegner, Phys. Rev. Letters 9, 168 (1962).

that isotopic spin may still be a useful concept in the heavy nuclei. The pion double charge exchange can be used to check this further, in particular to look for states which differ from the ground state by two units of isospin.

The optical-model potential is constructed by summing the $\pi$-N scattering amplitude $t_i$ of each nucleon in the nucleus, i.e.,

$$\langle k' | U | k \rangle = \sum_{i=1}^{N} \langle 0 | e^{i\vec{k}' \cdot \vec{r}} t_i \, e^{i\vec{k}' \cdot r} | 0 \rangle , \tag{2}$$

where $|0\rangle$ is the ground state of the nucleus and the $t_i$ are the $\pi$-N scattering amplitudes. The amplitude t is given by

$$t_i = A + C\,\hat{k} \cdot \hat{k}' + [B + D\hat{k} \cdot \hat{k}']\,\vec{\tau}_i \cdot \vec{t}, \tag{3}$$

where A, B, C, and D are functions of the S- and P-wave phase shifts and $\tau$ and t are isotopic-spin operators for the nucleon and pion, respectively. It is the $(\vec{\tau} \cdot \vec{t})$ terms that give rise to elastic charge-exchange scattering and have not been included before. It should be noted here that we are making use of the impulse approximation, which should not be unreasonable for pions with as little kinetic energy as 40 MeV. We neglect direct absorption of a pion by a nucleon and other higher order corrections to the optical potential. We were willing to make these approximations since our aim is an estimate of double charge exchange. Upon transforming the potential from momentum space to coordinate space and substitution for $t_i$ in Eq. (3), we obtain

$$U(r) = A\,\rho(r) + C\,\vec{\nabla} \cdot \left(\rho(r)\,\vec{\nabla}\right) + \frac{\vec{t} \cdot \vec{T}}{N} \left\{ B\rho_\tau(r) + D\,\vec{\nabla}\left(\rho_\tau(r)\,\vec{\nabla}\right) \right\},$$

where N is the total number of nucleons, T is the total isotopic spin and $\rho(r)$ and $\rho_\tau(r)$ are nucleon form factors. Note that the charge-exchange part of the potential is of the order of T/N times the nonexchange part. Although

$\rho(r)$ and $\rho_\tau(r)$ are not identical, we approximate both by the Fermi density distribution.

In a preliminary study we calculated the double charge-exchange cross section without including Coulomb corrections. Results are given in Table I. We are now in the process of including the Coulomb effects, which means adding a term $Ze^2/r$ to the potential and taking into account the difference in energy of the various charge states of an isobaric multiplet.

TABLE I. Double charge-exchange cross section in microbarns.

| T | N | T/N | E = 20 | E = 40 | E = 65 |
|---|---|---|---|---|---|
| 56 | 2 | 0.036 | 0.61 | 1.48 | 0.8 |
| 120 | 10 | 0.083 | 0.85 | 0.82 | 0.6 |
| 152 | 14 | 0.092 | 0.66 | 0.54 | 0.08 |
| 208 | 22 | 0.106 | 0.48 | 0.32 | 0.06 |

# F-4. EXCITATION OF $C^{12}$ BY HIGH-ENERGY PROTONS*

R. Haybron† and H. McManus‡

Michigan State University, East Lansing, Michigan

The inelastic scattering of high-energy (100 — 300 MeV) protons from $C^{12}$ has been studied by use of a distorted-wave impulse approximation. The detailed wave functions of V. Gillet[1] were used in an attempt to obtain quantitative agreement with experiment in the prediction of peak differential cross sections and proton polarization. Distorted waves were calculated with the Oak Ridge computer code "JULIE". Results will be shown.

---

*Work supported by the U. S. Atomic Energy Commission.

†On loan to the Oak Ridge National Laboratory.

‡Guggenheim Fellow, 1963-64 at NORDITA.

[1] V. Gillet, Thesis, Paris, 1962.

# F-5. THEORY OF INTERMEDIATE STRUCTURE*

J. E. Young

University of California, Los Alamos Scientific Laboratory

Los Alamos, New Mexico

The extension of the configuration-mixing shell model to continuum states has been suggested by Feshbach[1] and his collaborators. Physically, one expects to see the neutron strength function broken up owing to the presence of couplings into complicated shell-model configurations. These have been identified as the states of two particles and one hole (2p, 1h). Such states degenerate at the neutron bombarding energy couple into the optical-potential state.[2] The result of the energy-conserving transitions is to give rise to resonances in neutron-scattering cross sections. These are characterized as having the average parameters $\langle\Gamma\rangle \approx 150$ keV, $\langle D\rangle \approx 3$ MeV$^{-1}$.

Experimental confirmation of the qualitative picture is believed to be found in the total neutron elastic data of Foster and Glasgow.[3] There is also suggestive evidence for the intermediate structure behavior in

---

* Work done under the auspices of the U.S. Atomic Energy Commission.

[1] H. Feshbach, Ann. Phys. (N.Y.) 5, 357 (1958); 19, 287 (1962); B. Block and H. Feshbach, Ann. Phys. (N.Y.) 23, 47 (1963); C. M. Shakin, Ann. Phys. (N.Y.) 22, 373 (1963); R. H. Lemmer and C. M. Shakin (to be published).

[2] G. L. Shaw, Ann. Phys. (N.Y.) 22, 509 (1959).

[3] D. G. Foster, Jr., and D. W. Glasgow, Bull. Am. Phys. Soc. 7, 334 (1962); D. W. Glasgow and D. G. Foster, Jr., Bull. Am. Phys. Soc. 8, 321 (1963). We thank Dr. L. Cranberg for calling our attention to these results.

the neutron (total, differential, and polarization cross sections) data of Elwyn et al.[4]

A theoretical description which is capable of indicating why the (2p, 1h) states are singled out is to be found in the many-body formulation of elastic scattering. Essentially one computes the irreducible self energy $\Sigma_k(\omega)$ for a particle in a continuum state k with energy $\omega$. The formal method of obtaining $\Sigma$ is that of the Green's functions introduced by Martin and Schwinger.[5]

To see how the results come about, we shall require certain formal apparatus. Much of this is familiar or at least is readily available to the reader in other places. The presentation is therefore designed to be illustrative rather than exhaustive.

The single-particle propagator or Green's function G is defined as the time-ordered product of Heisenberg operators, taken in the N-particle ground state, i.e.,

$$G(1, 1') = -i \langle T\psi(1)\psi^+(1')\rangle \quad ; \qquad (1 = \hat{x}_1 t_1). \qquad (1)$$

This operator satisfies the equation of motion

$$G_0^{-1}(1, \overline{1}')\, G(\overline{1}', 2) = \delta(1-2) - iv(1, \overline{3})\, G_2(1\overline{3}, 2\overline{3}^+); \qquad (2)$$

$$G_0^{-1}(1, 1') = \left(i\frac{\partial}{\partial t} + \frac{\nabla^2}{2M}\right)_1 \delta(1-1'),\ v(1, 3) = \delta(t_1-t_3)\, v(|\hat{x}_1-\hat{x}_3|),$$

---

[4] A. J. Elwyn, J. E. Monahan, R. O. Lane, and A. Langsdorf, Jr. (to be published). We thank Dr. Elwyn for making these results available to us.

[5] P. C. Martin and J. Schwinger, Phys. Rev. 115, 1342 (1959).

where a matrix notation[6] is employed. Variables which carry bars are to be integrated over. The propagator $G_2$ is that for two particles, v is the given two-body interaction.

Equation (2) may be converted to an integro-differential equation in G by means of the statement

$$\Sigma \quad (1, \bar{2})\, G(\bar{2}, 1) = -iv(1, \bar{3})\, G_2(1\bar{3}, 1'\bar{3}^+). \tag{3}$$

This defines the operator for the irreducible self-energy $\Sigma$. Now Eq. (2) can be rewritten as an equation for the propagator inverse

$$G^{-1}(1, 1') = G_0^{-1}(1, 1') - \Sigma\,(1, 1'). \tag{4}$$

Given that there exists a single-particle biorthogonal basis set and that all processes are stationary in time, homogeneous in space, we can write

$$G(1, 2) \equiv G(1-2) = \Sigma\; |\tilde{\psi}_s(\hat{x}_1) > G_s(t_1 - t_2) < \psi_s(\hat{x}_2)|. \tag{5}$$

It is straight forward to then establish the Fourier-state relation

$$G_s^{-1}(\omega) = \omega - \omega_s - \Sigma_s\,(\omega) \tag{6}$$

which follows from (4). Equation (6) tells us where the poles of $G(\omega)$ occur. These poles locate the states $\omega_i$ describing the motion of a single particle (hole) which is added to (subtracted from) the ground-state system of N particles in the presence of interactions.

To discuss $\Sigma_s(\omega)$, we shall have to know $G_2$. The latter propagator is expressed in terms of the operator L for density-density correlations as

$$G_2(12, 1'2') = L(12, 1'2') + G(1, 1')G(2, 2'). \tag{7}$$

---

[6] G. Baym and L. P. Kadanoff, Phys. Rev. 124, 287 (1961).

Also, the Bethe-Salpeter equation in the lowest approximation to the 4-point vertex function gives $G_2$ as

$$G_2(12, 1'2') = G(1, 1')G(2, 2') - G(1, 2')G(2, 1')$$
$$+ iG(1, \overline{3})G(2, \overline{4})v(\overline{3}, \overline{4})G_2(\overline{34}, , 1'2'). \tag{8}$$

The definition of an interaction operator t as

$$t(12, \overline{34}) \left[ G(\overline{3}, 1')G(\overline{4}, 2') - G(\overline{3}, 2')G(\overline{4}, 1') \right] = v(1, 2)G(12, 1'2'), \tag{9}$$

together with Eq. (8), leads to the equation

$$t(12, 1'2') = v(1, 2)\, \delta\, (1-1')\delta\, (2-2')$$
$$+ iv(1, 2)G(1, \overline{3})G(2, \overline{4})\, t\, (\overline{34}, 1'2'). \tag{10}$$

Then, from Eqs. (3) and (9) we find that

$$\Sigma\, (1, 1') = -it(1\overline{2}, 1'\overline{3})G(\overline{2}, \overline{3}^+). \tag{11}$$

The formal solution summarized by Eq. (11) can be replaced by an alternative one generated from L. We sketch the main points of the derivation in an algebraic notation. First, a scalar external field $U(1, 1') = \lambda u(1, 1')$, coupled to the density at two points, is added to the many-body Hamiltonian. All propagators are then defined in the presence of U. Functional differentiations are carried out with respect to U and then $\lambda$ is set equal to zero. In particular, we quote the result

$$\frac{\delta}{\delta U(2,2\ )}\, G(1, 1';U) \Big|_{U=0} = L(12, 1'2'). \tag{12}$$

This, together with Eqs. (4), (11), and the Brueckner equivalent of (10), namely

$$t_B = v + ivG^+G^+t_B; \qquad (G^+\text{-particle propagator}), \tag{10'}$$

enables us to derive an integral equation for L. This equation, given in Ref. 6, takes the form

$$L(12, 1'2') = -G^{+}(1, 2')G^{-}(2, 1) + G^{+}G^{-}\,\Xi\, L; \tag{13}$$

$$\Xi = t_B + i\, t_B G^{-} G^{-} t_B; \qquad (G^{-}\text{-hole propagator}).$$

Equation (13) may be solved by the Fredholm method and the corresponding self-energy derived.[7] When one does this, $\Sigma$ is given as a power series in $t_B$. The first three orders of that expansion are shown in Figs. 1 and 2.

Intermediate structure depends largely upon states in the vicinity of the Fermi level. At the Fermi surface there is nearly complete symmetry between particles and holes. Equation (10') ignores this, referring as it does to particle interactions. Some of the symmetry is restored by Eq. (13). To do this as completely as possible, we define the J interaction of Shaw:

$$t_B L = J\, G^{+} G^{-}; \tag{14}$$

whereby

$$J = t_B + i\, t_B\, G^{+} G^{-}\, \Xi, \tag{15a}$$

$$J \approx t_B + i\, t_B\, G^{+} G^{-} t_B. \tag{15b}$$

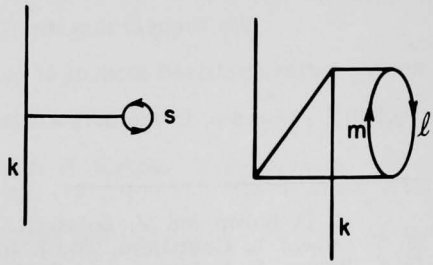


Fig. 1. The horizontal lines are Brueckner operators $t_B$. The two self-energy contributions $\Sigma_k(\omega)$ to the self-consistent single-particle energies $\omega = \omega_k$ are (a) Brueckner-Hartree-Fock, and (b) second-order rearrangement.

[7] J. E. Young (to be published).

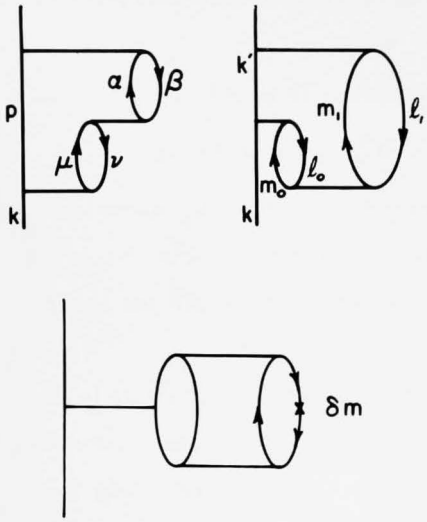


Fig. 2. The third-order diagrams which are to be treated in perturbation theory, i.e., calculated with the self-consistent $t_B$ of Fig. 1:(a) excitation of (p,h) pairs, (b) annihilation of (p,h) pair belonging to a vacuum fluctuation, (c) scattering from a vacuum fluctuation, or third-order rearrangement with mass renormalization $\delta m$ on hole lines.

In Eq. (15b) we ignore the hole-hole interactions.

The partial summation of Eq. (14) has two effects. Graphically, it introduces the third-order $\Sigma$ of Fig. 3. This is the resonant contribution producing intermediate structure. Physically, the diagonalization of J (diagonalization equals summation) among the particle-hole states means that $\psi_0(N)$ has these components present. This has been discussed by Brown and his collaborators.[8]

We suggest that the (2p1h) intermediate states of Fig. 3 are the antisymmetrized product of quasi-particle, $|s\rangle$ and (p, h, ), $|\psi_i(ph)\rangle$ , where $\psi_i$ is the diagonalization of J.

---

[8] G. E. Brown and M. Bolsterli, Phys. Rev. Letters 3, 472 (1959); G. E. Brown, L. Castillejo, and J. A. Evans, Nucl. Phys. 22, 1 (1961); G. E. Brown, J. A. Evans, and D. J. Thouless, Nucl. Phys. 24, 1 (1961).

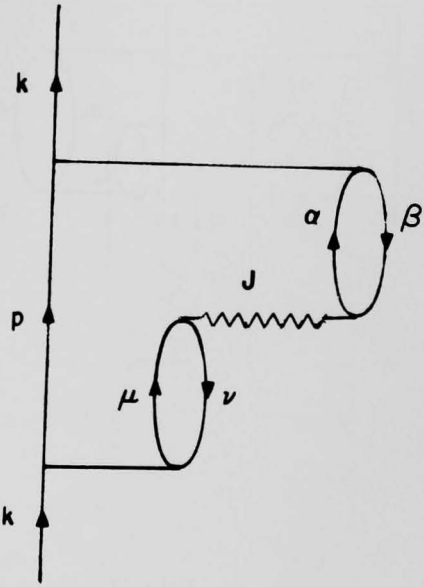


Fig. 3. The intermediate-structure diagram which replaces that of Fig. 2(a) and which is added to the $\Sigma_k(\omega)$ of Fig. 1 to produce the intermediate-structure resonance spectrum. Note that all (p,h) pairs are strongly coupled through the J interaction.

This representation extends that of the intermediate-coupling model proposed by Lane, Thomas, and Wigner.[9] Furthermore the (2p, 1h) states of Fig. 4, which lead to the usual imaginary part of the optical potential, do not contribute to intermediate structure. This is required by the Rodberg model[10] where a projection separates the two classes of (2p, 1h) states.

---

[9] A. M. Lane, R. G. Thomas, and E. P. Eigner, Phys. Rev. 98, 693 (1955).

[10] L. S. Rodberg, Phys. Rev. 124, 210 (1961).

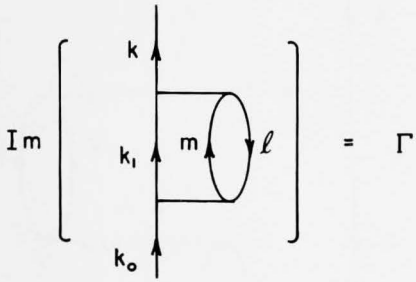


Fig. 4. The imaginary part W of the optical potential $\Gamma = 2W$ is determined by the uncoupled (i.e., independent) (2p, 1h) states degenerate at the energy $\omega = \omega_k$. These states do not contribute to intermediate structure; compare with Fig. 3.

ARGONNE NATIONAL LAB WEST
3 4444 00009114 0

grateful to Mr. Frank Gentille and his associates in the Argonne Graphic Arts Department for the rush job of printing and binding the volume, and especially to Mr. Joseph Fierce for his skill and care in preparing the plates for the figures.

# TABLE OF CONTENTS

iii

TABLE OF CONTENTS

iii

TABLE OF CONTENTS

iii

TABLE OF CONTENTS

iii

TABLE OF CONTENTS

iii

TABLE OF CONTENTS

iii

TABLE OF CONTENTS

iii

TABLE OF CONTENTS

iii

TABLE OF CONTENTS

iii

TABLE OF CONTENTS

iii

TABLE OF CONTENTS

iii

TABLE OF CONTENTS

iii

TABLE OF CONTENTS

iii

TABLE OF CONTENTS